CREATING GROWTH HORMONE RESISTANCE IN CELLS USING A HAMMERHEAD RIBOZYME APPROACH

A dissertation presented to

the faculty of

the College of Arts and Sciences of Ohio University

In partial fulfillment

of the requirements for the degree

Doctor of Philosophy

Edward Owen List

August 2001

This dissertation entitled

CREATING GROWTH HORMONE RESISTANCE IN CELLS

USING A HAMMERHEAD RIBOZYME APPROACH

BY

EDWARD O. LIST

has been approved for

the Department of Chemistry and Biochemistry

and the College of Arts and Sciences by

John J. Kopchick

Goll-Ohio Professor of Molecular Biology

Leslie A. Flemming

Dean, College of Arts and Sciences

LIST, EDWARD O. Ph.D. August 2001. Chemistry and Biochemistry

Creating Growth Hormone Resistance in Cells using a Hammerhead Ribozyme Approach. (298 pp.)

Director of Dissertation: **John J. Kopchick**

ABSTRACT

In an effort to create growth hormone (GH) resistance in mouse L cells and in mice, we have designed a ribozyme (RZ) directed against mouse GH receptor (GHR) mRNA. The ability of the RZ to specifically cleave GHR mRNA at the designated target site was verified by *in vitro* analysis. The ability of the RZ to cleave more than one substrate was also demonstrated *in vitro*.

We have established several stable mouse L-cell lines expressing different amounts of mouse GHR. A metallothionein driven "mini-gene" containing the mouse GHR cDNA with added introns flanking exon 8a allowing for the production of both GHR and GH binding protein (GHBP) was used to create the cell lines. GH binding assays followed by Scatchard analysis revealed GHR numbers per cell ranging from ~50,000 to ~240,000. Western blot analysis using an antibody against phosphorylated tyrosines demonstrated a correlation between GHR number and STAT-5 phosphorylation. A linear relationship existed between receptor number and GH stimulated STAT-5 activation up to ~150,000 GHRs per cell, with maximal activation occurring at ~300,000.

One of the GHR/BP cells lines that expressed ~170,000 GHRs per cell (E6 cells) was transfected with GHR-RZ coding DNA. Western blot analysis revealed a

~50% decrease in GHR abundance in RZ transfected cells. This decrease was confirmed by GH binding assays, which revealed the RZ transfected cells had ~81,000 GHRs per cell compared to ~170,000 without the RZ. This decrease in receptor levels was enough to greatly reduced E6 cell sensitivity to GH as shown by a decrease in GH-dependent STAT-5 activation, thus causing GH resistance in these cells.

The same GHR-RZ was used to establish several transgenic mouse lines. Analysis of growth revealed no significant change between transgenic mice containing the RZ "mini-gene" as compared to non-transgenic littermates. Western blot analysis of GHR levels in the liver samples revealed that the RZ-DNA positive transgenic mice had similar GHR levels to that of control mice. Therefore, the GHR-RZ was successful at creating GH resistance in cultured cells but not in mice.

Approved

Goll-Ohio Professor of Molecular Biology

ACKNOWLEDGMENTS

I would like to thank everyone who made it possible for me to achieve this level of education. Throughout my life I have had the privilege to interact with many individuals with great character, values, and philosophies. These individual have no doubt shaped my own philosophy on life. Starting at an early age my parents, Dan and Joyce created an environment conducive to learning and achievement through example and by accepting nothing less than excellence. This was no easy task as I was one of eight siblings and our entire family was supported by a single modest income. Nevertheless, every one of my brothers and sisters has become a successful individual with strong values and great character. So thank you mom and dad for all of you love and support.

I would also like to thank my brothers, John and Pat and sisters Chrissy, Theresa, Mary, Amy, and Dot for their love and support. Although we are all grown now and have families of our own, we still share a strong bond and support one another without reservation. I would like to thank my grandmother Marian Vordenberg, my great aunt Katherine Pence, and my late grandparents John and Dorothy List and for their unconditional love and support. I would like to thank all of the friends I have had throughout the years for their friendship and their unique points of view, most notably Charles Cox, Jack Klinger, Trent Patterson, and Michael Schroeder. Every one of the friends I have encountered has broadened my perspectives on life.

This accomplishment could also not have been achieved without the guidance of the many instructors I have had to privilege to study under. Beginning with the Forest Hills School District who took me as a rambunctious and uncooperative kid (to put it nicely) and shaped me into a college bound student (although still rambunctious and uncooperative). Although I feel that all of the instructors I had throughout grades 1-12 were excellent, one instructor stood apart from the rest, my honors biology instructor Mr. Cummings, who taught me not only what to learn but how to learn. In addition, the report he had me do on "recombinant DNA" may have had a more profound effect on my life than was initially intended. I would like to thank all of the faculty and staff of Ohio University, the Education Department, the Department of Biology, the Department of Chemistry, and the Molecular and Cellular Biology Program for providing me with a learning experience second to none. I would especially like to thank Dr. Joan Saffron for giving me the courage to achieve more than I thought possible through her encouragement.

I would like to thank all of the individuals associated with the Edison Biotechnology Institute, Lori Abdella, Deborah Buckley, Karen Coschigano, Allen Gattis, Amy Holland, Greg Hovanic, Bruce Kelder, Chris Lewis, Yunsheng Li, Maria Lozykowski, Terry Marovich, Pattie McCoy-Leib, Shigeru Okada, Markus Riders, Kelly Walker, David White, Linda Bellush, Joanne Knapp, Fred Woodly, Eric Johnson, Ed Stevens, Chris Schwirian, Jean Tong, Christopher Darrus, David Workman, Jerry Andry, Matt Martin, Sergio Ulloa, Gail Matheny, Eileen Workman, Wen Chen, Nian Chen, Paul Harding, Paul Wyle, Ahmet Arman, Xinzhong Wang

Yihua Zhou and Jennifer McGlone. Everybody with whom I have interacted with at EBI has helped me with this achievement.

I would like to thank my committee members Dr. Calvin James, Dr. Xiaozhuo Chen, Dr. Peter Coschigano, and my committee advisor Dr. John Kopchick for the contributions that they have made to my research my development as a scientist. I would especially like to thank my advisor Dr. John Kopchick who took me under his wing and allowed me to learn at the highest level. He has taught me much more than a phiolosphy of science but a philosophy of life, not only thought his words but through the way he has lived his own life and treated others.

Finally, I would like to give thanks and my love to my wife Stephanie and my son Gregory. I could not have attained this goal without their love, patience, and the sacrifices they have made. I dedicate this dissertation to you both and thank you from the bottom of my heart. I would also like to thank my wife's parents Greg and Phyllis Brown for the generosity, love and support they have given to Gregory, Stephanie and me without reservation.

TABLE OF CONTENTS

LIST OF TABLES

LIST OF FIGURES

ABBREVIATIONS

aa., amino acids
AGE, advance glycation end products
APRT, adenine phosphoribosyltransferase
ASBV, avocado sunblotch viroid
ATP, adenosine triphosphate
AVP, arginine vasopressin
b, bovine
βAPP, β–amyloid peptide precursor
β2M, β2-microglobulin
bp, base pair
BSA, bovine serum albumin
CAT, chloramphenicol acetyltransferase
CBC, cap-binding protein complex
CDC, center for disease control
cDNA, complementary DNA
CF, cleavage factor
CHO, Chinese hamster ovary cells
CMV, cytomegalovirus
CPSF, cleavage and polyadenylation specificity factor
cpm, counts per minute
Cst, cleavage stimulatory factor
CRH, corticotropin-releasing hormone
DAG, diacylglycerol
DMEM, Dulbecco's Modified Eagle's Medium
DMS0, dimethyl sulfoxide
DNA, deoxyribonucleic acid
dNTPs, deoxyribonucleoside triphosphate
DTT, dithiothreotol
E2, estradiol
E6 cells, mouse L cells transfected with a GHR/BP "mini-gene"
EDTA, ethylenediaminetetraacetic acid
EGF. epidermal growth factor
ERK, extracellular signal-regulated kinase
ES, embryonic stem cells
FGF, fibroblast growth factor
FSH, follicle-stimulating hormone
G4 18, geneticin
GAS, γ activated sequences
GDP, guanosine diphosphate

GH, growth hormone
GHBP, growth hormone serum binding protein
GHR, growth hormone receptor
GHR/BP, growth hormone receptor/binding protein gene
GHR/BP -/-, mice containing no functional GHR/BP alleles
GHR/BP +/-, mice containing only one functional GHR/BP allele
GHR/BP +/+, mice containing two functional GHR/BP alleles
GHRH, GH-releasing hormone
GK, glucokinase
Glut, glucose transporters
GRB2, growth factor receptor-bound protein *2*
GTP, guanosine triphosphate
h, human
HAT media, DMEM containing 10% Nu-serum, 50 ug/ml gentamicin, 15 ug/ml hypoxanthine, 1 ug/ml aminopterin and 5.15 ug/ml thymidine
HDV, hepatitis delta virus
hnRNA, heterogeneous nuclear RNA
HPRT, hypoxanthine phophoribosyl transferase
HSV, Herpes simplex virus
IGF, insulin-like growth factor
IL, interleukin
INFγ, interferon-γ
$1P_3$, inositol triphosphate
IRS, insulin receptor substrate
IVS, intervening sequence
JAK, Janus-associated kinase
kb, kilo base
Kd, dissociation constant
kDa, kilo Dalton
LH, luteinizing hormone
LHR, lactogenic hormone response element
LHRH, LH-releasing hormone
LIF, leukemia inhibitory factor
LTR, long terminal repeat
m, mouse
MAPK, mitogen activated protein kinase
MET, mouse metallothionein I promoter/enhancer
MLC, mouse L cells
MMTV, mouse mammary tumor virus
MODY, maturity-onset diabetes of the young
mRNA, messenger RNA
MSV, Moloney murine sarcoma virus
NCp7, nucleocapsid protein of HIV-1

neo, neomycin resistance gene
NLM, National Library of Medicine
nt(s), nucleotides
NUH, for nucleotide sequence where N is any base and X can be A, U, or C
NuS, Nu-serum I culture supplement
o, ovine
p, porcine
PABP, poly A binding protein
PAGE, polyacrylamide gel electrophoresis
PAN, poly A nuclease
PAP, poly A polymerase
PBS, phosphate buffered saline
PCR, polymerase chain reaction
PDGF, platelet-derived growth factor
P1 3-kinase, phosphatidylinositol 3-kinase-associated p85
Pit-1, pituitary transcription factor-1
PKC, protein kinase C
PL, placental lactogen
PLC, phospholipase C
pol, polymerase
Poly A, polyadenylation
PRL, prolactin
PRLR, prolactin receptor
ptRZ, tRNA-tethered ribozyme
PY20, anti-phosphotyrosine serum
r, rat
RAGE, receptor for
Ran, a small G protein
RanBP, Ran binding protein
RNA, ribonucleic acid
RPA, ribonuclease protection assay
RPI, Ribozyme Pharmaceuticals Inc.
RNase P, Ribonuclease
rRNA, ribosomal RNA
RSV, Rous sarcoma virus
RT, reverse transcription
RT-PCR, reverse transcriptase-polymerase chain reaction
sBYDV, satellite RNA of the barley yellow dwarf virus
SDS, sodium dodecyl sulphate
SH2, src-homology 2 domain
SH3, src-homology 3 domain
SIE, Sis-inducible element
SNMV, virusoid of solanum nodiflorum mottel virus

SOCS, suppressors of cytokine signaling
snoRNA, small nucleolar RNA
SnRNA, hnRNP A1 small nuclear RNA
ssDNA, single stranded DNA
sTobRV, satellite RNA of tobacco ringspot virus
STAT, signal transducers and activators of transcription
STZ, streptozotocin
SV-40, Simian virus-40
T, testosterone
T3, triiodothyronine
T4, thyroxine
TBS, tris buffered saline
TK, thymidine kinase
TRE, transcriptional regulatory element
TRH, thyrotropin-releasing hormone
tRNA, transfer RNA
VEGF, vascular endothelial growth factor
VLTSV, virusoid of Lucerne transient steak virus
vVTMoV, virusoid of velvet tobacco mottel virus

INTRODUCTION

Ribozymes

Ribozymes are RNA molecules that have the ability to catalyze a chemical reaction, they act as true enzymes and are aptly named ribonucleic acid/enzymes or ribozymes. Although ribozymes are mainly known for their RNA cleavage activity, they have been found to catalyze a variety of reactions such as: DNA cleavage (Raillard and Joyce, 1996), 3'-5' RNA ligation (Hager and Szostak, 1997), 5'-5' RNA ligation (Chapman and Szostak, 1995), 3'-5' RNA-DNA ligation (Tokumoto and Saigo, 1992), peptide bond formation (Zhang and Cech, 1997; Zhang and Cech, 1998), amide bond cleavage (Dai et al., 1995), and carbon-carbon bond formation (Tarasow et al., 1997). In addition, several DNA sequences have been described to have catalytic properties (Geyer and Sen, 1998; Li and Breaker, 1999; Sen and Geyer, 1998). RNA cleaving ribozymes are RNA molecules that anneal to specific sequences on themselves or other RNA molecules and catalyze a cleavage reaction. Because of their specificity, RNA cleaving ribozymes have become valuable tools for inhibiting gene expression.

The discovery of ribozymes

Ribozymes were discovered independently by Thomas Cech of the University of Colorado and Sidney Altman of Yale in 1982 and 1983, respectively. Cech observed that the ribosomal DNA found in *Tetrahymena*, a genus of ciliated protozoa, was interrupted by a 413 base pair intron-like sequence. He termed this segment of DNA an intervening sequence (IVS). The IVS was included in the precursor RNA

transcript, but not in the mature RNA. When incubated *in vitro* in a buffer containing a divalent cation and GTP in the absence of protein, the IVS was precisely spliced out and the exons were ligated. In 1981, Cech et al were able to isolate and purify the pre-rRNA that spliced out its IVS without the addition of protein (Cech et al., 1981). Even after they purified the RNA by SDS-phenol extraction, boiling in SDS, and extensive treatment with proteases, they were still concerned that a possible explanation for the observed splicing activity was that an unusually stable protein enzyme was tightly associated with the RNA. More importantly, a second explanation given by Cech was that the RNA molecule itself could have carried out the splicing reaction. In 1982, Cech and his colleagues performed an experiment in an effort to remove the possibility of a tightly associated protein catalyzing the splicing reaction (Kruger et al., 1982). They cloned a portion of the pre-rRNA into a plasmid transcription system containing an *E. coli* RNA polymerase promoter. The *in vitro* transcripts were purified by SDS-phenol extraction. When the transcripts were incubated in a solution containing 0.1 mM GTP, 10 mM $MgCl_2$, 100 mM $(NH_4)_2SO_4$, and 50 mM Tris-HCl (pH 7.5) self-splicing of the RNA was observed. By using *in vitro* transcripts Cech eliminated the possibility of a tightly associated cellular protein possessing catalytic activity and concluded that the splicing activity was intrinsic to the structure of the RNA. Importantly, he showed that protein enzymes are not required for these reactions.

Ribonuclease P (RNase P), the enzyme responsible for the maturation of the 5' termini of tRNA molecules, was known to have essential protein and RNA

components for activity *in vivo* and *in vitro* (Akaboshi et al., 1980; Gardiner and Pace, 1980; Kole et al., 1980; Stark et al., 1977). To determine if the RNA component of RNase P was responsible for the catalytic activity of the enzyme, two separate groups (Gardiner and Pace, 1980; Stark et al., 1977) assayed the RNA portion of RNase P in a buffer containing up to 10 mM of $MgCl_2$. Under these conditions, catalytic activity was not observed. In 1983, Altman et al revisited the attempt to attribute the catalytic activity of RNase P to the RNA portion of the enzyme citing the recent finding by Cech that *Tetrahymena* RNA can catalyze a self-splicing reaction (Guerrier-Takada et al., 1983). In their experiment, the isolated RNA portion of the enzyme was found to have cleavage activity at higher concentrations of $MgCl_2$ (60 mM). In addition, the RNA portion of the enzyme was also found to have catalytic activity at an $MgCl_2$ concentration of 10 mM in the presence of 1 mM spermidine (a small polyamine). These discoveries were significant because prior to 1982, it was thought that only proteins could act as enzymes and that RNAs were only passive carriers of genetic information. In 1989, Cech and Altman were recognized for their accomplishment by being awarded the Nobel Prize in chemistry. Ironically, if either Stark in 1977 or Gardiner and Pace in 1980 used a higher concentration of magnesium in their experiments, they could have been the first to discover catalytic RNA instead of Cech and Altman.

The two ways ribozymes prevent translation

There are two basic ways that ribozymes prevent translation. The first and most noted is the ability of the ribozyme to catalyze the cleavage of the mRNA prior to its translation. Once an mRNA is cleaved, it is quickly degraded by 5'-3' and 3'-5' RNases (Sorrentino and Libonati, 1997). The unprotected 3' end of the 5' cleavage product as well as the unprotected 5' end of the 3' cleavage product are each rendered labile due to the absence of the 5' cap structure and poly adenylation sequence, respectively (Beelman and Parker, 1995; Jacobson and Peltz, 1996; Ross, 1996). For cellular mRNAs, a mechanism called the de-adenylation-dependent decay of mRNAs requires the shortening of the poly (A) tail as the first step (Beelman and Parker, 1995; Jacobson and Peltz, 1996; Wilson and Brewer, 1999). A ribonuclease called poly (A) nuclease (PAN) degrades the poly (A) tail 3'-5' in the absence of poly (A) binding proteins (PABP). Therefore the PABPs serve to protect the mRNA from the action of PAN. PABPs are spaced approximately 25 bases apart and require a minimum of 12 adenosines. The PABPs eventually fall off or are removed over time and allow PAN to shorten the poly (A) tail. Once the tail reaches a length of approximately 25 adenosines (a length that is thought to coincide with the loss of the final PABP) the 5' cap structure is removed by a pyrophosphotase. This demonstrates an association between the termini of the mRNA. Once the 5' cap structure is removed, 5'-3' exonucleases quickly dispose of the decapitated message. Another mechanism, called the de-adenylation-independent decay of cellular mRNAs, involves endonucleolytic cleavage followed by 5'-3' and 3'-5' exonucleolytic degradation of the fragments

(Beelman and Parker, 1995; Jacobson and Peltz, 1996; Ross, 1996; Wilson and Brewer, 1999). It is proposed that all polyadenylated mRNAs are susceptible to the de-adenylation-dependent decay and that the de-adenylation-independent pathway is more specific to individual mRNAs, thus overall decay will depend on a particular RNA's susceptibility to both these pathways (Beelman and Parker, 1995).

The second method in which ribozymes prevent translation is by an antisense effect. This effect is achieved by physically blocking the ribosomal assembly from continuing translation at the point of ribozyme attachment to the mRNA (Forsdyke, 1995; Robinson-Benion and Holt, 1995; Scanlon et al., 1995). The theory of using complementary oligonucleotides to prevent translation was proposed in 1967 (according to Scanlon et al, it was in 1995 with no citation given for their statement) and first demonstrated to work in 1978 with the inhibition of Rous sarcoma virus expression *in vitro* (Zamecnik and Stephenson, 1978). Prior to the use of ribozymes for reducing gene expression "knockdowns", antisense RNAs were used for the very same purpose and are still used today (Anazodo et al., 1995; Delihas et al., 1997; Shen et al., 1997; Strickland et al., 1988; Ueno et al., 1997). The percentage of ribozyme catalysis versus antisense will always vary depending on the individual ribozyme. Such factors as the length of the antisense arms, the G/C content of the antisense arms, the region of mRNA targeted, and cellular molecules that interact with the specific ribozyme designed can influence the antisense effect of a ribozyme. There have been several reports in which the catalytic activity was reported separately from the antisense activity of the ribozyme studied. By comparing a catalytically inactive

ribozyme with that of an active one, Giannini et al reported that their 2'-O-allyl modified ribozyme containing arms of 8 and 9 bases was 2 fold more potent in decreasing cellular Ki-ras mRNA levels (Giannini et al., 1999). Using stable cells expressing luciferase, Bramlage et al reported ribozymes targeted against the luciferase mRNA in HeLa cells was primarily due to the antisense effect because catalytically inactive ribozymes demonstrated a similar decrease in luciferase activity (~50%) (Bramlage et al., 1999). In addition to physically blocking the ribosomal assembly, it has also been suggested that the antisense effect may occur within the nucleus blocking early steps of mRNA processing. This results in the prevention of mRNA transport out of the nucleus (Cornelissen, 1989; Kim and Wold, 1985). These examples all end with the same result, decreased gene expression. Regardless of which effect is causing the decrease in translation, if the goal of the experiment is to "knockdown" gene expression, the argument of which activity is preventing translation becomes purely academic.

The origin of life

The discovery of catalytic RNA not only allowed for the creation of ribozymes as "tools" for molecular biologists, it has helped fuel a long-standing argument regarding the participation of RNA in the origin of life. In 1968 Francis Crick and Leslie Orgel, each admittedly inspired by a symposium in London on the origins of life (Orgel and Crick, 1993), wrote independent manuscripts on ideas discussed on the topic (Crick, 1968; Orgel, 1968). In their manuscripts, they both recognized that a

major obstacle to understanding the evolution of life was solving the "chicken and the egg" problem in that the synthesis of nucleic acids requires protein and protein synthesis requires the presence of nucleic acids. Each came to the same conclusion that this problem could be solved if nucleic acids acted as catalysts early in the evolution of life. In addition, they also predicted that RNA may have acted as a ribonuclease and that the first ribosomes could have been composed of RNA only. Fourteen years after the publication of their manuscripts, catalytic RNAs were indeed discovered (Kruger et al., 1982), and the "RNA-world" hypothesis was born (Gilbert, 1986; Joyce, 1989; Lahav, 1993; Szathmary, 1997; Waldrop, 1992). The hypothesis indicates that RNA preceded the existence of both DNA and protein synthesis, in that genetic information was stored in RNA and biological chemical reactions catalyzed by RNA in the absence of protein enzymes. Eventually RNA was replaced by more efficient protein enzymes and the more stable nucleic acid DNA, leaving RNA as an intermediate between the two. Recent findings such as an RNA dependent RNA polymerase ribozyme that can transcribe templates up to 6 nucleotides with high fidelity, in which extension by nucleotides complementary to the template were 1000 times more efficient than mismatched nucleotides have strengthened the argument for an "RNA-world" (Ekland and Bartel, 1996). The discovery of self-replicating small circular RNA molecules called viroids (Diener, 1971) also substantiate the hypothesis. Diener goes as far as to suggest that viroids and satellite RNAs are "living fossils" of pre-cellular life (Diener, 1989). Although a preponderance of evidence has been discovered for the possibility of such a world existing, no direct evidence has been

discovered to prove such an existence in our early evolution, and the possibility of such an archaeological find seems unlikely due to the fragile nature of RNA.

Hammerhead ribozymes were designed by nature

Naturally occurring ribozymes are found in a variety of RNAs including ribonuclease P (Akaboshi et al., 1980; Gardiner and Pace, 1980; Guerrier-Takada et al., 1983; Hardt et al., 1995; Schon, 1999; Stark et al., 1977), group I introns (Cech et al., 1981; Golden et al., 1998; Herschlag and Cech, 1990; Kruger et al., 1982; McSwiggen and Cech, 1989; Olive et al., 1995; Rajagopal et al., 1989; Tanner and Cech, 1997; Wang et al., 1993a), group II introns (Jacquier and Michel, 1987; Qin and Pyle, 1999; Saldanha et al., 1993; Zimmerly et al., 1995a; Zimmerly et al., 1995b), hepatitis delta virus (HDV) (Chowrira et al., 1994; Kawakami et al., 1996; Matysiak et al., 1999; Westhof and Michel, 1998), several species within the *Schistosome* (blood flukes) family (Ferbeyre et al., 1998), viroids, virusoids, and satellite RNAs (Buzayan et al., 1986a; Buzayan et al., 1986b; Diener, 1989; Forster and Symons, 1987; Haseloff and Gerlach, 1988; Henco et al., 1977; Hutchins et al., 1986; Mei et al., 1989). The last three of this group (viroids, virusoids, and satellite RNAs) have proven to be instrumental in the evolution of the hammerhead ribozyme. Viroids are small circular single stranded RNA molecules found in plants that are able to self-replicate (Forster and Symons, 1987). Similarly, virusoids and satellite RNAs are found in plants as circular single stranded RNAs, but they depend on the association of

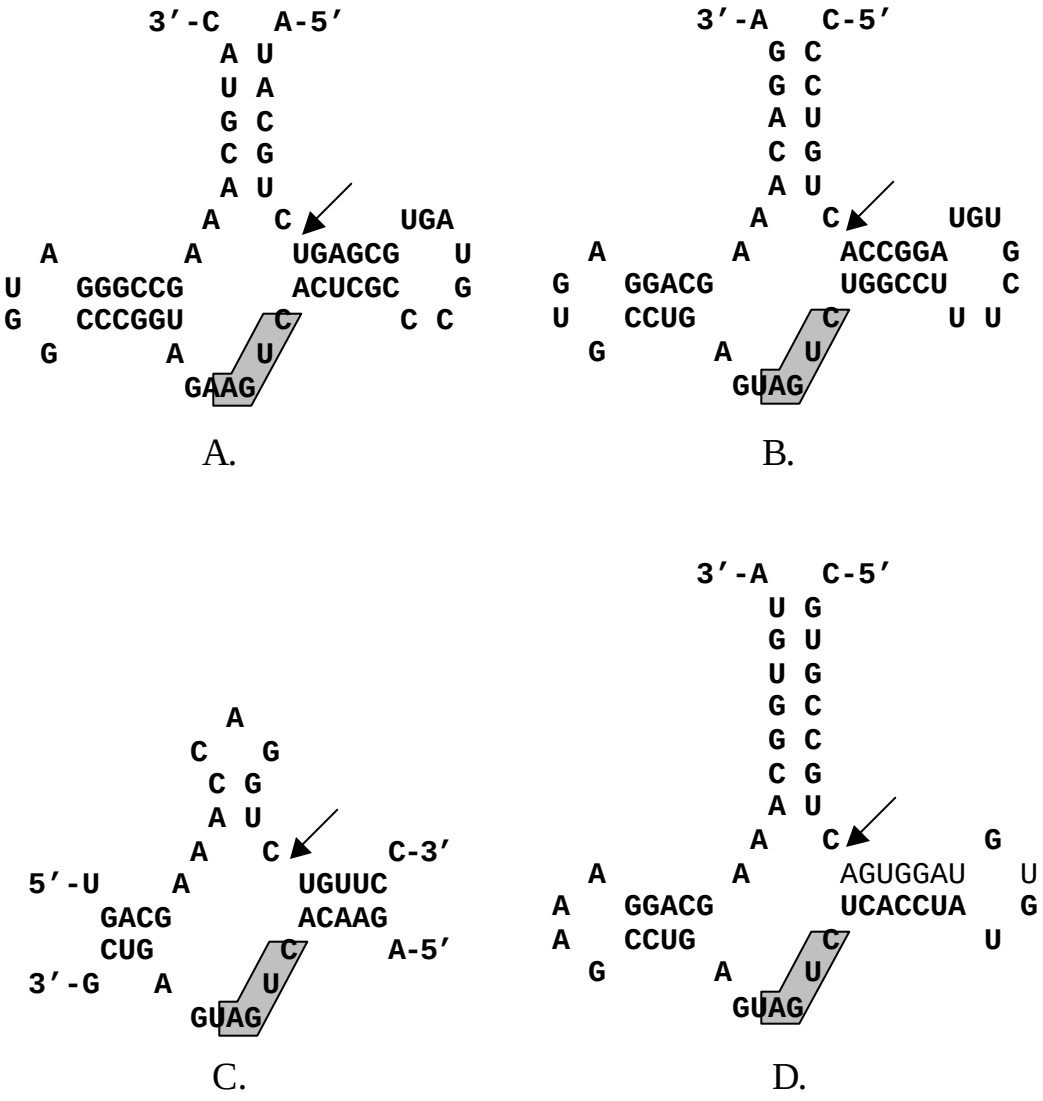

Figure 1. Sequences and secondary structures of natural hammerhead ribozymes found among viroids, virusoids and satellite RNAs. The CUGA (shaded boxes) sequence represents a conserved catalytic pocket essential for ribozyme cleavage activity. Cleavage occurs 3' of the cytosine in the GUC substrate strand as indicated by the arrows. The hammerhead structures of A. vLTSV-A, B. sTRSV, C. ASBV, and D. vVTMoV are represented (Forster and Symons, 1987).

a helper virus for replication. Satellite RNAs differ from virusoids in that virusoids are encapsulated by their helper virus, while satellite RNAs are not. In 1987, Forster and Symons showed that the avocado sunblotch viroid (ASBV) and the virusoid of Lucerne transient steak virus (vLTSV) undergo site-specific self-cleavage *in vitro* in the presence of magnesium. Structural analysis has demonstrated that these RNAs contain small catalytic RNA sequences that form a distinctive hammerhead secondary structure (see figure 1). Despite their size, these hammerhead structures are among the most efficient RNA catalysts. Further analysis has revealed that the hammerhead secondary structure is also present in the virusoid of velvet tobacco mottel virus (vVTMoV), the virusoid of solanum nodiflorum mottel virus (SNMV), and the satellite RNA of tobacco ringspot virus (sTobRV) (Forster and Symons, 1987).

Prelude to the hammerhead ribozyme

Based on the proposal of the Foster and Simons that the secondary structure forming the conserved hammerhead motif was the domain responsible for the self-cleavage activity in these plant pathogens, Uhlenbeck created the first *trans*-acting hammerhead ribozyme (Uhlenbeck, 1987). In his experiment, Uhlenbeck used *in vitro* transcription to produce a 19-nucleotide ribozyme and a 24-nucleotide substrate. Unlike the classic hammerhead ribozyme design used today, part of the secondary structure required for catalytic cleavage was present in the substrate oligonucleotide. Helix I was contained solely within the substrate RNA and helix II was not contained within the ribozyme strand, but rather as part of the 3' ribozyme annealing arm.

Nevertheless, when Uhlenbeck incubated the ribozyme and substrate RNAs in a Tris-buffered solution at pH-7.5 containing 18 mM $MgCl_2$, he observed cleavage of the substrate band with no decrease in the ribozyme band. Uhlenbeck also demonstrated the ability of his *trans*-acting ribozyme to turn over by demonstrating a 90% cleavage rate in substrate at a 21–fold molar excess in comparison to the ribozyme. He suggests that the significance of the *trans*-cleavage reaction could have potential biological significance in that RNA molecules containing the target sequence could be specifically selected for cleavage by the ribozyme construct.

Creating the first hammerhead ribozymes

Citing Uhlenback's 1987 experiment, Haseloff and Gerlach pointed out that the cleaved RNA contained conserved sequences required for secondary structure and subsequent cleavage. In addition, they found that Uhlenback's system was not appropriate for use as a general model for designing ribozymes with a wide range of sequence specificity (Haseloff and Gerlach, 1988). In an effort to create a general model for hammerhead ribozymes, Haseloff and Gerlach used the conserved hammerhead sequence from the self-cleaving domain of the (+) strand of the sTobRV to separate the enzyme and substrate activities. They designed a ribozyme in which all of the conserved sequence and secondary structure was present within the ribozyme strand and used an RNA substrate that contained no conserved sequence essential for cleavage. The ribozyme was targeted against three sites within a chloramphenicol acetyl-transferase (CAT) mRNA sequence. Each of the three ribozymes was shown to

cleave and produce fragments that were consistent with the predicted sites of cleavage. Haseloff and Gerlach's hammerhead ribozyme has become a model for the majority of ribozymes used in research and therapeutics today (see figure 2).

Hammerhead vs. hairpin and HDV ribozymes

HDV (Chowrira et al., 1994; Kawakami et al., 1996; Matysiak et al., 1999) and hairpin (Borneman et al., 1995; Cepero et al., 1998; Denman et al., 1994; MacKay et al., 1999; Ojwang et al., 1992; Yu et al., 1995; Yu et al., 1998) ribozymes have also been used to target specific mRNAs. The hairpin ribozyme functions efficiently in both cleavage and ligation reactions such that the extent of final cleavage is dependent on the rapid dissociation of product (Berzal-Herranz et al., 1992; Chowrira et al., 1993). If the dissociation of the cleaved RNA products is slowed, the probability of ligation is enhanced resulting in reduced cleavage. In addition, Denman has described cleavage using hairpin ribozymes as promiscuous and called for greater vigilance for those who might use them as a therapeutic agent (Denman, 1999). When the HDV and hairpin ribozymes are compared to hammerhead ribozymes, hammerhead ribozyme cleavage activity is least affected by the addition of flanking sequences added for stability in the cellular environment (Chowrira et al., 1994). The structures of the HDV and hairpin ribozymes required for substrate cleavage are more complex than that of the hammerhead ribozyme. Minimal sequences required for the hairpin and HDV ribozymes are 50 and 72 nucleotides, respectively with 4 helical formations necessary for each. Hammerhead ribozymes can cleave substrate RNA with less than

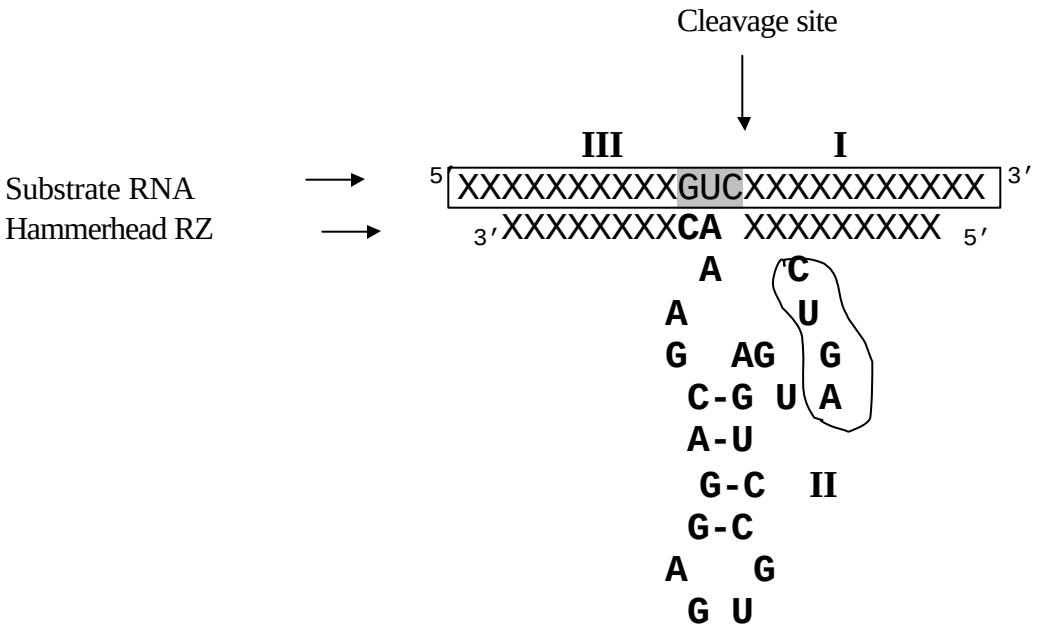

Figure 2. The classic Haseloff and Gerlach hammerhead ribozyme. The substrate RNA is represented by the top strand of Xs (boxed) with a GUC (shaded) target sequence in the center. Cleavage of the substrate RNA occurs after the cytosine as indicated by the arrow. The core hammerhead sequence (in bold print) is flanked by 5' and 3' arms that can be designed to anneal to any specific RNA sequence. The CUGA catalytic pocket (circled) contains several possible Mg^{2+} binding sites. Roman numerals I, II, and III represent the three helices that must form prior to substrate cleavage. Helix I and III form between the substrate RNA and the arms of the ribozyme, while helix II is intrinsic to the ribozyme (Haseloff and Gerlach, 1988).

30 nucleotides and require only 3 helical formations. It has been reported that hammerhead ribozymes can function in the absence of helix II by replacing the 12 ribonucleotide that make up the helix with only 4 ribonucleotides (McCall et al., 1992; Sakamoto et al., 1997). Although, the non-helix II containing ribozyme did show some activity, it was greatly reduced in comparison to the native helix II containing form. Moreover, McCall and her colleagues reported that the activity was restored to that of a helix II containing ribozyme when 4 deoxyribonucleotides are used instead of ribonucleotides, and that only 22 nucleotides are required for activity (McCall et al., 1992). It is the size and simplicity of the hammerhead ribozyme that has made it the ribozyme of choice for decreasing gene expression *in vivo*.

The hammerhead ribozyme cleavage reaction

Hammerhead ribozyme RNA cleavage reactions can be broken down into 3 steps, association, cleavage, and dissociation. The association of substrate RNA to ribozyme involves annealing of specific sequences from 5' and 3' arms of the ribozyme to complementary sequences in the target RNA. The helix formed between the 5' arm of the ribozyme and the substrate RNA is referred to as helix I, while the helix between the 3' arm and the substrate termed helix III. The formation of both helix I and helix III are necessary for subsequent cleavage. Ribozyme RNA cleavage also requires the presence of divalent metal ions (Allain and Varani, 1995; Koizumi and Ohtsuka, 1991; Menger et al., 1996; Orita et al., 1996; Peracchi et al., 1997; Pontius et al., 1997; Scott et al., 1995; Uchimaru et al., 1993). Crystal structure

analysis has revealed 5 potential magnesium-binding sites, one of which is associated with the catalytic pocket of the ribozyme (Scott et al., 1995). It is proposed that magnesium held in the CUGA catalytic pocket ionizes the 2'-hydroxyl by removing a proton at the cleavage site (the 2'-OH of cytosine in the GUC target sequence). The exposed oxygen then acts as a nucleophile to attack the adjacent phosphate. A transitional state with a penta-coordinated phosphate is formed. The pro-R oxygen of the phosphate is stabilized by magnesium in the transitional state. It is not known if the same magnesium, which removed the proton from the 2'-hydroxyl or a second magnesium binds the pro-R oxygen to stabilize the intermediate penta-coordinated phosphate. The reaction generates 5'-hydroxyl and 2', 3'-cyclic phosphate termini at the cleavage site. The cleaved substrates are slowly and independently released by the "breathing" of hydrogen bonds in helix I and III.

The proposed mechanism of hammerhead ribozyme cleavage

The reaction mechanism by which hammerhead ribozymes cleavage occurs (see figure 3) was first proposed to occur by an S_N2 in-line attack transesterfication reaction by van Tol and his colleagues in 1990 (van Tol et al., 1990). In their experiment, synthetic oligonucleotides representing the sequence of the satellite RNA of the tobacco ringspot virus (sTobRV) possessing full processing activity and specific ^{35}S-labeled phosphophorothioate diesters in the pro-R configuration. Following the autocatalytic cleavage of the oligonucleotide, thin layer chromatography was used to separate the endo- and exo-isomers of the cleaved products. Only the endo-isomer

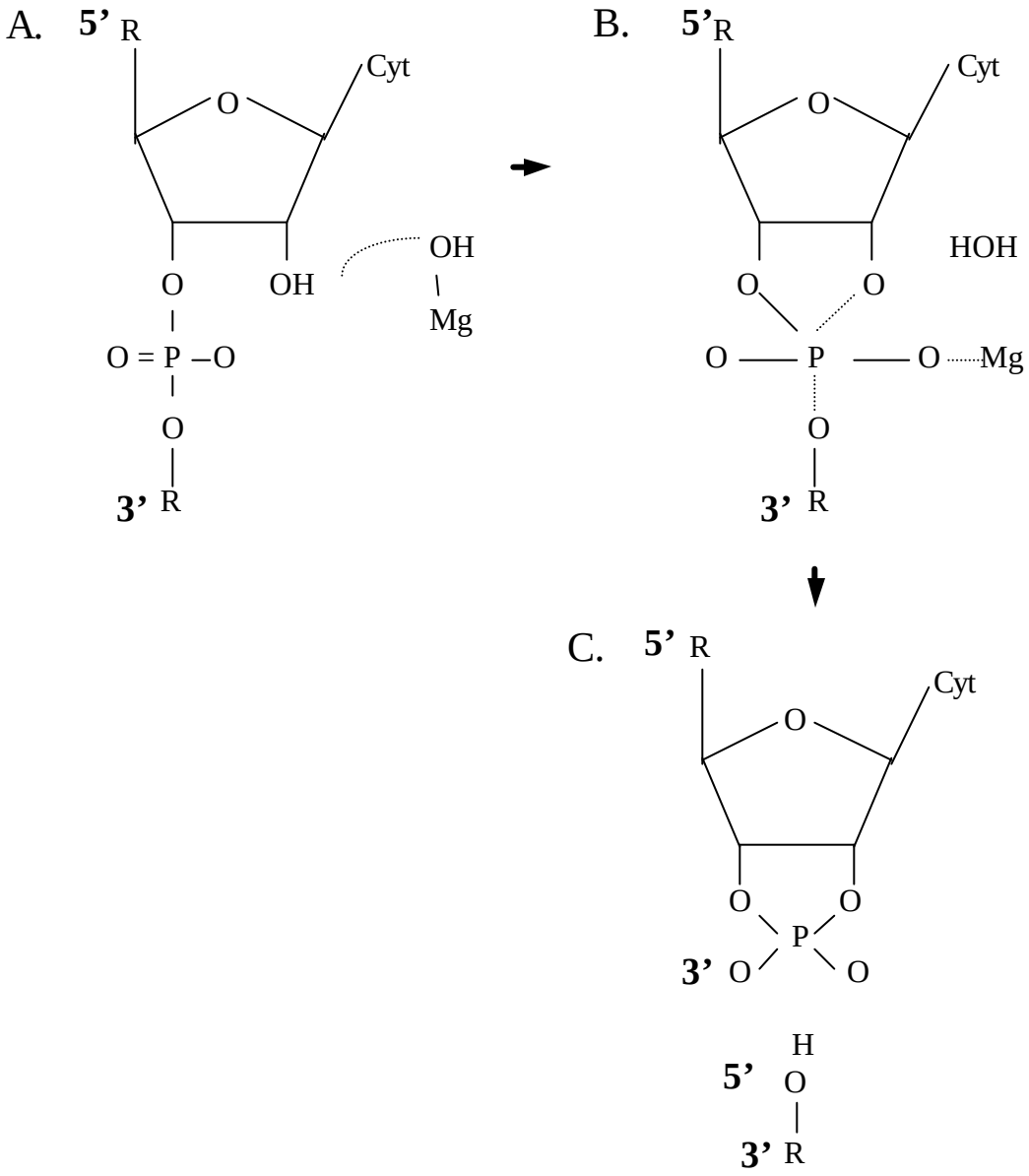

Figure 3. The basic mechanism of ribozyme cleavage. The S_N2 in-line attack transesterfication reaction proposed for ribozyme cleavage (van Tol et al., 1990) was later proven with the elucidation of the structural intermediate (Murray et al., 1998). A. The magnesium (in the form of magnesium hydroxide) removes a proton from the 2'-OH of cytosine in the GUC target. B. The exposed oxygen acts as a nucleophile to attack the adjacent phosphate. A transitional state with a pentacoordinated phosphate is formed with a magnesium ion stabilizing the intermediate. C. The reaction generates 5'-OH and 2',3'-cyclic phosphate termini.

was found, indicating that the ^{35}S-labled phosphate was inverted in the product. Van Tol and his colleagues stated that: "this result is consistent with an in-line attack of the 2'-hydroxyl group in an S_N2 transesterfication reaction". They also suggested that trans acting ribozymes based on the hammerhead motif of the sTobRV should follow the same mechanism. This result was in agreement with similar studies performed a year later (Koizumi and Ohtsuka, 1991; Slim and Gait, 1991). In addition, an earlier study performed by McSwiggen and Cech, who in 1989 suggested that the *Tetrahymena* ribozyme reaction mechanism also proceeded by an in line, S_N2 transesterfication reaction (McSwiggen and Cech, 1989). Although it was generally accepted that the in-line attack S_N2 transesterfication reaction was indeed the mechanism by which hammerhead ribozyme cleavage occurred, actual structural data was needed to confirm this assumption.

Finding the structural proof for the in-line attack mechanism

In attempting to solve the reaction mechanism of hammerhead ribozyme cleavage by crystal structural analysis, it was necessary to slow down or stop the cleavage reaction so that structural data could be obtained from the transition-state of the ribozyme/substrate complex. In 1996 William Scott from Cambridge England was the first to crystallize and trap an all RNA hammerhead ribozyme/substrate intermediate (Scott et al., 1996). Prior to this, two research groups used modified substrates to prevent substrate cleavage in an attempt to trap the intermediate. The first group used a hammerhead ribozyme with a DNA, instead of an RNA substrate

(Pley et al., 1994). The second group used an all RNA hammerhead ribozyme and an RNA substrate with a single 2'-methoxyl modification, replacing the 2'-OH at the active site (Scott et al., 1995). Although the structures obtained by these experiments agreed with one another, skepticism remained due to the modifications of the substrates. In an effort to circumvent this concern, Scott et al prepared crystals of an unmodified RNA hammerhead ribozyme, both in the presence and the absence of magnesium ions. The crystals were stabilized in a 20% glycerol, 1.8 M $LiSO_4$ buffer at various pH's and flash frozen in liquid propane at 100°K. The crystallized ribozymes were able to cleave, suggesting that the fold in the crystal structure of the ribozyme/substrate complex was correct. The crystal structure Scott obtained from the unmodified hammerhead ribozyme at lower pH (5 and 6), agreed with the previous structures obtained with modified substrates. All of which indicate that the scissile phosphodiester bond (the bond that will be cleaved) and the 2'-OH nucleophile were on the wrong side of the phosphate atom for an in-line attack mechanism to occur. Since it was still believed that the in-line attack mechanism was the mechanism for ribozyme cleavage, Scott and his colleagues assumed that a conformational change from this observed intermediate must take place prior to cleavage. They referred to this low pH structure as a "ground state" structure of a ribozyme/substrate intermediate. At a higher pH (8.5), Scott observed a conformational change that was not previously observed. He found that a new hydrogen bond forms between the furanose oxygen of the C17 (the cleavage site nucleotide on the substrate strand) and the 2'-OH of the U16 (the U adjacent to the cleavage site C). He also found three new

potential Mg^{2+} binding sites one of which was coordinated directly next to the pro-R oxygen of the cleavage site phosphate adjacent to the scissile bond. The second structure was described by Scott to be a flash frozen "early" conformational intermediate that exists only for a short amount of time prior to cleavage. This new "early" conformation was more compatible with the in-line attack mechanism but still required more of a conformational change. In an effort to elucidate the theoretical "later intermediate" required for in-line attack, Scott, Murray and colleagues (Murray et al., 1998) replaced the ribose leaving group of an RNA hammerhead ribozyme with a tallo-5'-C-methyl-ribose. (Scott now had his own lab at Indiana University and James Murray was a member of his group) Since the attacking 2'-OH nucleophile was left intact and only the leaving group was altered, it was thought that the final point of the reaction would be trapped in a "kinetic bottleneck". To confirm that the addition of the methyl group to the substrate RNA did not interfere with the formation of either the "ground state" or "early" intermediates, both structures were crystallized and were found to be indistinguishable from those previously described. The "later" intermediate that Murray and Scott were seeking was finally found by using this "kinetic bottleneck" method of trapping the intermediates. In this structure, Murrey et al describe the following: "A 60-degree rotation in C17 (cleavage site C) causing it to stack upon A6 (A in the CUGA catalytic pocket of the ribozyme). The furanose oxygen of A1.1 (the nucleotide 3' of the of the cleavage site C in the substrate strand) now associates with the base of C17. The scissile phosphate is pulled away from its helical position by movement of the cleavage site base, C17." These major

conformational changes described for this "later" intermediate were indeed consistent with the positioning necessary for an in-line attack mechanism to occur and the theory was finally proven with the elucidation of this structural intermediate.

Designing a hammerhead ribozyme

The design of an efficient hammerhead ribozyme for decreasing gene expression requires several considerations. To begin with, an appropriate target sequence must be selected. The target sequence can contain the nucleotides NUH, where N is any base and H can be A, U, or C. The triplet sequence GUC has been shown to have the highest cleavage potential and is discussed in greater detail later in the text (Shimayama et al., 1995). The accessibility of the target sequence is also important. Target sequences that are hidden in long stretches of double stranded helices present in mRNAs are less accessible to the antisense arms of the ribozyme than if the target sequences are located on a single stranded loop region of mRNA (Sioud, 1997). The numbers of bases present in the antisense arms effects the specificity and turnover rate of the ribozyme. Longer antisense arms decrease the turnover rate, while increasing the specificity of the ribozyme to its designated target RNA. A greater G/C content also decreases the turnover rate because of the relative number of hydrogen bonds compared to A/U (three and two, respectively). It has been reported that ribozymes require only three nucleotides in helix I (Tabler et al., 1994), and that the optimal Kcat/Km at 37°C is achieved *in vitro* when helix I and III are a combined length of 12 nucleotides (Bertrand and Rossi, 1994). The consequence of

using a ribozyme that only recognizes 12 bases of a target mRNA would be an increase in non-specific mRNA cleavage. According to Alberts and his colleagues, there are an estimated 20,000 different mRNA species in a typical mammalian cell with an average length of 2000 bases (Alberts, 1994). If this estimation holds true, the sequence complexity would be ~$4x10^7$. For a ribozyme to recognize a unique sequence, at least 13 bases are needed to produce a complexity of ~$7x10^7$ or (4^{13}). Contrary to conventional thinking, Herschlag argues that increasing the number of base pairs does not necessarily increase specificity for a ribozyme (Herschlag, 1991). He contends that adding more bases ultimately reduces specificity, as cleavage occurs essentially every time the target RNA or a mismatched RNA binds the ribozyme. The greatest specificity could be expected with an A/U rich sequence. This is due to the weaker base pairing as compared to that of G/C allows recognition to be spread over a larger number of bases, as opposed to the strong binding of G/C. In addition, an A rich sequence is favored over a U rich sequence due to the non-intended formation of U•G wobble pairs (Herschlag, 1991).

Promiscuous cleavage

When ribozymes are designed for potential use as therapeutic agents, it is essential that specificity be conserved to avoid any non-specific cleavage of mRNAs, even at the expense of turnover efficiency of the ribozyme. An example of "promiscuous cleavage" of mRNA other than the intended target mRNA has been

reported by Denman (Denman, 1999). Previously, Denman and his colleagues used a hammerhead and a hairpin ribozyme targeted to the β–amyloid peptide precursor (βAPP) mRNA (Denman et al., 1994). They demonstrated an ~80% decrease in βAPP mRNA using either ribozyme in COS-7 cell lines. Five years later, in an effort to determine the specificity of his ribozymes, Denman found that in cells containing the hairpin ribozyme, rat ribosomal L19 message was also cleaved. He described the cleavage using hairpin ribozymes as promiscuous and called for greater vigilance for those who might use them as a therapeutic agent (Denman, 1999).

Predicting the secondary structure of mRNA using computational analysis

When targeting a ribozyme to a particular mRNA it is important that the targeted sequence on the substrate RNA be accessible to the antisense arms of the ribozyme. Several methods have been employed to determine the secondary structure of mRNA including: using random sequences placed into adenovirus-mediated expression cassettes (Lieber et al., 1997; Lieber and Strauss, 1995), probing target RNAs with oligodeoxynucleotides to identify RNase H accessible sites (Frank and Goodchild, 1997; Scherr and Rossi, 1998), and the use of computer-aided calculations for predicting RNA secondary structures (Denman, 1993; James and Cowe, 1997; Sczakiel and Tabler, 1997). Of the thee methods mentioned, the first and second use random sequences and endonuclease probing which are extremely labor intensive techniques and in the time it takes to perform these methods, actual ribozymes

themselves could have been used as probes to determine optimal cleavage sites. Only the use of computer predicted RNA secondary structures can be carried out in less than 10 minutes. The energy minimization algorithm by Zuker et al has been shown to predict RNA structures of 400 bases with 80% accuracy (Zuker et al., 1991). The percent accuracy increases as the size of the RNA decreases due to the smaller number of possible structures, and conversely, the larger the RNA predicted, the less accurate the prediction becomes. Nevertheless, even a 10% accurately predicted RNA is better than randomly choosing target sites within a given mRNA.

In vitro analysis of ribozyme cleavage

While a correlation between the test tube and cell culture activity of a ribozyme is questionable (Crisell et al., 1993), *In vitro* cleavage reactions between ribozymes and their target RNAs are commonly used prior to the introduction of ribozymes *in vivo*. Determining catalytic activity is often used in studies involving ribozymes such as selecting the most catalytic ribozyme from a population of ribozymes directed against a specific gene transcript (Chen et al., 1998; L'Huillier et al., 1992; Scherr et al., 1997) or viral RNA (Gavin and Gupta, 1997; Heidenreich and Eckstein, 1992; Lieber et al., 1996).

There are several methods for quantifying *in vitro* ribozyme cleavage activity against a specific RNA target. These methods can be divided into two categories; those that use radiolabeled substrate and those that do not. In general, radiolabeled methods involve the incorporation of radiolabeled nucleotides with or without

unlabeled nucleotide into a target molecule using a T7 or SP6 *in vitro* RNA synthesis reaction. Following ribozyme cleavage, the products and uncleaved substrate RNAs are separated on a denaturing polyacrylamide gel. After gel separation, the radiolabeled RNA bands can then be visualized by placing the gel under a phosphorimager screen (Chen et al., 1998; Scherr et al., 1997) or placed with autoradiographic film (Gavin and Gupta, 1997; Heidenreich and Eckstein, 1992; Lieber et al., 1996). Images obtained from both the phosphorimager and autoradiograph are then scanned and quantified using densitometry software that calculates amounts of RNA by the pixel density of the image. There are several limitations that should be considered when densitometry is used for quantifying RNA. First, the image being scanned must be clear with well-defined bands representing the RNA. Second, the background must not only be low, but uniform because the bands representing the RNA are usually compared to a section of background. Third, the amount of RNA to be quantified is limited to the detection ability of the imaging system. This is important because, when densitometry is used for determining ribozyme kinetic constants such as K_m and V_{max}, a "standard" assay for determining these constants involves maintaining a constant ribozyme concentration while varying the amount of substrate RNA. The range of substrate concentration is limited as to the ability of the imaging system to separate pixel densities that can be easily overwhelmed for the most intense bands especially if the sensitivity is adjusted to detect the lower concentration bands. For the BIO RAD Gel Doc 1000, the dynamic range (according to the specifications provided by the company) is linear to 1.5 orders

of magnitude. This limited substrate range is problematic because the smaller the range of substrate concentration, the larger the resulting error for determining kinetic constants.

An alternative method for quantifying gel separated radiolabeled cleavage products and substrates uses scintillation counting instead of densitometry scanning (DeYoung et al., 1997; L'Huillier et al., 1992; Ruffner et al., 1990). This method involves using an exposed autoradiograph superimposed on the original gel. Using the autoradiograph as a guide, the regions of the gel corresponding to substrate and product RNAs are physically excised from the gel and placed into individual vials with scintillation cocktail. The amount of RNA present in each band is then quantified using a scintillation counter. The use of scintillation counting for quantifying RNA avoids some of the limitations of densitometry analysis; most importantly the range of detection is increased.

The non-radiolabeled methods for quantifying ribozyme cleavage activity generally involve staining gel separated substrate and cleavage product RNA. The stained RNA bands are then scanned and quantified using densitometry. Agarose gels can be used for separation followed by ethidium bromide staining and visualization under an ultraviolet light source (Du et al., 1996; Lieber et al., 1996). This method is seldom used for quantification due to its poor sensitivity and resolution. A more sensitive alternative to ethidium bromide staining for RNA detection is silver staining (Du et al., 1996; Palfner et al., 1995), where as little as 15 ng of RNA can be detected in the presence of 7 M urea. In addition, Palfner et al (Palfner et al., 1995) describes a

modified silver staining protocol from Allen et al (Allen et al., 1989) that results in a significant reduction in background staining. Without the modifications, Palfner reports that silver staining according to Allen is not suitable for densitometry analysis due to a high background. The use of other stains such as aziridine (Matsuhisa et al., 1994) and streptavidin-Nanogold-silver staining (Hauser-Kronberger, 1998) have also been described for detection of RNA. In addition, the visualization of RNA without staining by short-wave UV epi-illumination has also been described (Mukhopadhyay and Roth, 1994).

A new method for quantifying ribozyme cleavage activity involving scintillation counting of silver stained radiolabeled RNA substrate was developed by combining the non-radioactive method of silver staining RNA for visualization followed by excision and scintillation counting of the stained RNA bands (List, 1994). Silver staining polyacrylamide gels prior to scintillation counting not only allowed for direct visualization of RNA, but also allowed for a direct comparison of densitometry scanning of the silver stained gels to that of scintillation counting of the same silver stained RNA. The RNA bands from the silver stained gels were quantified by densitometry scanning prior to quantification by scintillation counting using the same silver stained gel. The % volume of pixels scanned (for the densitometry method), and number of scintillation counts (for the scintillation method) for the uncleaved substrate bands in the presence of ribozyme were compared to the negative control RNA at each substrate concentration to determine the amount of ribozyme cleavage. Using these data, double-reciprocal plots were constructed for both methods of

quantification. The r^2 values of the best-fit lines from each plot was used for comparing the accuracy of each method. In the comparison, the r^2 values were significantly greater when scintillation counting was used. These results were not surprising considering the low dynamic range (linear to 1.5 orders of magnitude according to specifications from the manufacturer) of the imaging system BIO RAD Gel Doc 1000 system (BIO RAD, Hercules, CA, USA) compared to the dynamic range of scintillation counting (approximately 6 orders of magnitude) based on the manufactures specification of the LS 6500 liquid scintillation system (Beckman Coulter). For enzymatic assays, a large dynamic range is desired. In addition, when performing an enzymatic assay in which the enzyme is held at a fixed concentration and the substrate concentration is varied, the likelihood that error will occur in determining kinetic constants decreases as the range of substrate concentration increases. Improvements in imaging technology are allowing for much greater dynamic ranges for densitometry analysis, which may eventually provide equivalent capabilities to that of scintillation counting. However, in laboratories where this technology is not available, the method of quantifying radiolabeled RNA by scintillation counting appears to be a preferred method.

The NUH rule

Substrate RNAs as targets for hammerhead ribozyme cleavage usually contain a GUC triplet sequence with cleavage occurring 3' of the cytosine. Other triplet sequences have been reported which allow for substrate cleavage, but usually at a

significantly decreased catalytic efficiency (Shimayama et al., 1995). This is not unexpected when one considers that the majority of naturally occurring hammerhead ribozymes utilize the same GUC triplet sequence for self cleavage found in the following: the satellite RNA of the tobacco ringspot virus (sTobRV) (Buzayan et al., 1986b), the positive strand of the (vLTSV) (Forster and Symons, 1987), the violet tobacco motel virus (vVTMoV), both the positive and negative strands of the avocado sunblotch viroid (ASBV) (Hutchins et al., 1986), and the newt satellite-2 RNA (Epstein and Gall, 1987). And as with many things in life, there are exceptions to the GUC rule. The negative strand of the (vLTSV) uses a GUA triplet target sequence for cleavage (Forster and Symons, 1987) and the satellite RNA of the barley yellow dwarf virus (sBYDV) uses an AUA triplet target sequence. With the advent of engineered *trans*-acting hammerhead ribozymes, several studies have been performed *in vitro* to determine the most efficient target site sequence for hammerhead ribozyme cleavage (Koizumi et al., 1988; Nakamaye and Eckstein, 1994; Perriman et al., 1992; Ruffner et al., 1990; Shimayama et al., 1995; Zoumadakis and Tabler, 1995). Although it was generally agreed that the sequence GUC was among the most efficient in each of the studies, there were inconsistencies with regards to the efficiencies of other triplet sequences. For example, Perriman reported that when AUC was used as a target sequence, virtually no cleavage occurred. This was in stark contrast to the observations of Zoumadakis, in which the AUC target was cleaved at the highest efficiency of all the sequences tested, even higher than that of GUC. Zoumadakis and Ruffner each reported that the target sequence CUC had low cleavage efficiency, less

than 10 percent in comparison to that of GUC, while Koizumi and Perriman each observed efficiencies nearly equal to that of GUC. Similar discrepancies were reported for other triplet sequences. The combined results of these experiments lead to the general acceptance of the NUH rule, in which N stands for any base and H stands for any base except for G (Shimayama et al., 1995). Shimayama and others originally used the designation X for any base except for G. More recently H is being used to designate any base except for G (Junn and Kang, 1996). In general, the NUH rule states that any target RNA containing an NUH sequence can potentially be cleaved by a ribozyme. It is important to note that the NUH rule does not mention the efficiencies of the various triplet sequences, and considerable doubt still remained about the relative efficiencies. A possible reason for the inconsistencies may be due to the limitations of the early cleavage assays. The catalytic efficiencies of ribozyme cleavage were not reported as separate kinetic data such as K_m and K_{cat} values, but rather by comparing the percentage of substrate cleavage containing a given triplet sequence to the percent cleavage of the GUC triplet. In 1995 Shimayama et al performed a comprehensive study in which all of the 12 possible NUH cleavage sites were compared and their kinetic values compared. In their study, Shimayama et al reported the K_m of each target sequence as well as the K_{cat}. From these data, the true catalytic efficiencies (K_{cat}/K_m) were reported. The Kcat of the GUC sequence was the second highest value at 4.0 min-1 with AUC being the highest value at 4.4 min^{-1}. The K_m of the GUC sequence was the lowest value at 20 nM, while the Km of the AUC was the highest of the 12 sequences at 700 nM. When the catalytic efficiencies were

reported as K_{cat}/K_m, the GUC sequence was the highest value of the 12 sequences at 200 nM^{-1} min^{-1}. The sequences with the second and third highest values were CUC (38 nM^{-1} min^{-1}) and UUC (16 nM^{-1} min^{-1}). While the AUC sequence had the highest K_{cat} value, the low K_m gave this target a low catalytic efficiency of 6.3 nM^{-1} min^{-1}. The catalytic efficiencies reported by Shimayama et al are generally considered to be the most accurate representation of possible NUH sequences, but they are not considered absolute (Shimayama et al., 1995). A major reason for this doubt is that a comparison based solely on K_{cat}/K_m is problematic in ribozyme kinetics (Zoumadakis and Tabler, 1995). These values are believed to be influenced by the surrounding substrate nucleotides as well as the particular nucleotides in the ribozyme arms that make up helix I and III. In addition, variations in reaction conditions such as pH, Mg^{2+} availability, temperature, and various ribozyme inhibitors and enhancers can alter kinetic constants. Because the GUC sequence consistently demonstrated high if not the highest catalytic efficiency in each of the studies involved, it is by far the most common target site used for hammerhead ribozyme cleavage. Hairpin ribozymes target sights have also been studied. They do not follow the NUH rule. The optimal sequence for hairpin ribozyme cleavage has been defined as RYNGUC (R represents A or G, Y represents C or U, and N can be any base) with cleavage occurring between the N and the G (Yu et al., 1998).

Enhancers and inhibitors of ribozyme activity

It is important to note that *in vitro* reports of ribozyme activity are not always representative of a ribozyme activity in cultured cells or animals. Crisell and his colleagues reported a direct example of this (Crisell et al., 1993). They performed two separate experiments to determine the activity of 11 different hammerhead ribozymes directed against the *tat* RNA from HIV-1. In the first experiment, they used *in vitro* analysis to compare the relative cleavage activities of each ribozyme. In a separate experiment, Crisell et al analyzed the efficiencies of each ribozyme within cells that were infected with HIV-1. They observed the inhibition of HIV by a ribozyme that did not show efficient catalytic activity *in vitro*. In addition, ribozymes that showed high efficiency *in vitro* failed to inhibit HIV growth in cells. Crisell postulated that protein interactions with the ribozyme RNA enhanced the ability of the ribozyme that showed poor *in vitro* activity, allowing it to be a more efficient catalyst. Crisell contended, "Current *in vitro* assays of ribozyme activity are not helpful in predicting activity in the cell".

Ribozyme activity can be enhanced or inhibited by associating with several types of molecules. RNA binding proteins such as nucleocapsid protein of HIV-1 (NCp7) and hnRNP A1 enhance the turnover rate of ribozymes by accelerating the attainment of the thermodynamically most stable species throughout the ribozyme catalytic cycle (Bertrand and Rossi, 1994; Herschlag et al., 1994; Tsuchihashi et al., 1993). In addition, NCp7 has been shown to resolve a misfolded ribozyme-substrate RNA complex that is otherwise long lived (Herschlag et al., 1994). Certain

aminoglycoside antibiotics can inhibit the activity of ribozymes. Neomycin B, kanamycin, 5-epi-sisomicin, and tobramycin have been shown to decrease the activity of ribozyme cleavage (Earnshaw and Gait, 1998; Hermann and Westhof, 1998; Llano-Sotelo and Chow, 1999). Crystallography analysis has revealed structural complementarities between the charged amino groups on aminoglycosides and the metal binding sites within the catalytic pocket of hammerhead ribozymes (Hermann and Westhof, 1998). This indicates the aminoglycoside antibiotics actually compete with magnesium for the metal binding sites within the catalytic domain. In contrast, viomycin has been shown to enhance the interactions between RNA molecules, increasing the cleavage activity of ribozymes (Olive et al., 1995). Unlike aminoglycoside antibiotics, viomycin is a basic cyclic peptide antibiotic of the tuberactinomycin group. In his experiment, Olive reported that in the presence of viomycin, the required magnesium concentration was decreased by one order of magnitude. Competition assays using the metal ion terbium (III) (Tb (III)) and magnesium has demonstrated that Tb (III) inhibited hammerhead ribozyme cleavage by competing with magnesium (Feig et al., 1998). Oligonucleotide facilitators have also been shown to enhance or inhibit ribozyme activity (Jankowsky and Schwenzer, 1996; Jankowsky and Schwenzer, 1998). When short oligonucleotides directed to the substrate RNA immediately 5' and 3' of helix I and III formation were added to ribozyme cleavage reactions involving substrates of different lengths, it was shown that the presence of the facilitators enhanced ribozyme cleavage. It is proposed that the facilitators accelerate the association of the ribozyme and substrate by coaxial

helix stacking. The effect of the facilitators may also cause a conformational change in the substrate RNA increasing accessibility to ribozyme binding. In addition, the effect was more pronounced when facilitators were used with longer substrates (Jankowsky and Schwenzer, 1996).

Protecting ribozymes in the cell

Ribozymes designed for use in cell culture or *in vivo* must be protected from cellular RNase degradation. If a ribozyme is expressed endogenously (incorporation into the genome of cells or transgenic animals), it should contain the same components that protect endogenous mRNA from exonucleases such as a 5' untranslated region with a 5' cap and a 3' untranslated region, which contains a polyadenylated tail. In addition to protecting ribozymes from exonucleases, it has been shown that UA and CA dinucleotide sequences are target sites for endonuclease cleavage and should be avoided if possible (Qiu et al., 1998). Qiu and his colleagues demonstrated using primer extension analysis that in cellular extracts ribozymes were cleaved at these dinucleotide sequences. Removal of these sequences made the ribozymes as well as mRNAs more stable. Finally, the addition of extra UA and CA sequences to ribozymes resulted in shorter half-lives.

If a ribozyme is delivered exogenously (injection or lipofectin association), chemical modifications can dramatically increase the stability of ribozymes. RNases utilize the ribose 2'-hydroxyl group to cleave the phosphodiester bond of RNAs, therefore, RNase degradation can be avoided by its removal (Taylor et al., 1992). 2'-

alkoxy, 2'-fluoro, and 2'-amino functional groups can also be added to the ribose to avoid degradation (Desjardins et al., 1996; Goodchild, 1992; Heidenreich and Eckstein, 1992; Paolella et al., 1992). In addition, degradation from 3'-exonucleases other than RNases can be inhibited by creating an internucleotide linkage such as a 5'-5' or a 3'-3' phosphate diester (Ortigao et al., 1992).

mRNA processing of Pol II transcripts

Eucaryotic mRNAs are produced as larger pre-mRNAs by RNA polymerase II (pol II) in the nucleus. In eukaryotes, there are three major processing events involved in the formation of mature mRNA: The addition of a 5'-cap, splicing of exons, and the addition of a polyadenylation tail to the 3'-end. All of these processes are thought to occur co-transcriptionally. In addition, protein complexes involved in each process are thought to play an important role by influencing the other processes. Several pol II transcribed RNAs do not follow some of these processing events such as histone mRNA, small nuclear RNA (snRNA), small nucleolar RNA (snoRNA), and heterogeneous nuclear RNA (hnRNA). Although snRNA, snoRNA and hnRNA are pol II transcribed RNAs, they are not considered mRNA because they do not serve as "messengers" for translation.

5'-end mRNA processing

In eukaryotes, all pol II transcribed RNAs are capped at the 5'-end of the mRNA (Lewis and Izaurralde, 1997). The cap structure is an inverted 7-methyl

guanosine linked by a 5'-5' triphosphate to the first nucleotide. This reaction is carried out by an enzyme with two distinct enzymatic activities, the capping enzyme and a second enzyme called RNA (guanine-7)-methyltransferase. First, the capping enzyme uses an RNA 5'-triphosphatase activity to remove the last phosphate from the 5'-terminal triphosphate. Second, the capping enzyme then uses a guanylyltransferase activity to transfer GMP to the newly formed 5'-diphosphate. Finally the cap is methylated by RNA (guanine-7)-methyltransferase resulting in a 7-methyl-guananine cap. The monomethylated form of the cap is called the cap 0 form. Further methylation has been observed in higher eukaryotes (Banerjee, 1980). Methylation at the 2'-O position of the second ribose ring produces a cap structure referred to as cap 1. Methylation at the 2'-O position of the third ribose ring produces the cap 2 structure. It is thought that the presence of the extra methyl groups in the cap structures may increase the resistance of mRNAs to RNase degradation (Bouloy et al., 1980). The 5'-cap is bound by a complex of proteins called the cap-binding protein complex (CBC). This complex is involved in pre-mRNA splicing (Izaurralde et al., 1994), cleavage and polyadenylation of the mRNA 3'end (Cooke and Alwine, 1996; Minvielle-Sabastia and Keller, 1999; Wahle and Ruegsegger, 1999), and nuclear export of the mature mRNA to the cytoplasm (Adam, 1999; Izaurralde and Mattaj, 1992; Minvielle-Sabastia and Keller, 1999; Wahle and Ruegsegger, 1999).

3'-end mRNA processing

In eukaryotes, all pre-mRNAs are cleaved by an endonuclease the identity of which is still unknown (Wahle and Ruegsegger, 1999). Although a 30-kDa subunit of the cleavage and polyadenylation specificity factor (CPSF) that binds the polyadenylation signal (AAUAAA) as well as the polyadenylation cleavage site has been implicated (Bai and Tolias, 1996), previous experiments suggest that this subunit may not be essential for cleavage (Gilmartin et al., 1995; Murthy and Manley, 1992). It is known that a complex of factors is involved in the cleavage process. These factors include: CPSF, cleavage stimulatory factor (CstF), cleavage factor I (CF-I), cleavage factor II (CF-II), and poly A polymerase (PAP). Following cleavage of the 3' end, all mRNAs (except for histone mRNAs) are polyadenylated by the enzyme poly A polymerase (PAP). The polyadenylation reaction also involves a complex of factors that includes: PAP, CPSF, and poly A binding protein II (PABP-II). 5'-cleavage fragments lacking poly A tails are not detectable in crude cell extracts or reconstituted reactions suggesting that both the cleavage and poly adenylation reactions are tightly coupled (Wahle and Ruegsegger, 1999). The poly A tail is essential for stabilizing the mRNA and increasing its half-life in the cytoplasm. Removal of the poly A tail has been shown to be a first, and rate-limiting step in mRNA degradation (Beelman and Parker, 1995). The poly A tail is also implicated in the transport of mRNAs from the nucleus to the cytoplasm, which may be due to its association with the 5'-cap complex (Eckner et al., 1991; Huang and Carmichael, 1996; Minvielle-Sabastia and Keller, 1999).

How mRNA reaches the cytoplasm

As previously mentioned the CBC that associates with the 5' cap also influences splicing and 3' processing of the pre-mRNA. After the mRNA is processed in the nucleus, the CBC remains associated at the 5' cap of the mature mRNA. The proteins involved in 3' end processing are also thought to remain bound, with CPSF attached to the AAUAAA poly addition signal, PAP at the poly adenylation site, and multiple PAPBP II's attached to the poly A tract. The association of all of the aforementioned proteins and complexes are then thought to help direct transport of the mature mRNA to the cytoplasm (Minvielle-Sabastia and Keller, 1999). Growing knowledge of the factors associated with mRNA during nuclear transport has lead to an early understanding of how mRNA reaches the cytoplasm. In a model proposed by Lewis and Izaurralde (Lewis and Izaurralde, 1997), a protein called importin-α associates with the CBC/mRNA in the nucleus and directs transport through the nuclear pore complex. Once in the cytoplasm, importin-β associates with the mRNA/CBC/ importin-α complex causing the release of the mRNA with subsequent recycling of the CBC/importin-α/importin-β complex back into the nucleus. More recently, the importins have been placed into a family of transporter proteins called the karyopherins, with additional transport proteins such as exportins included (Adam, 1999; Gamblin and Smerdon, 1999). In addition, a small G protein named Ran, is thought to mediate the karyopherin transport mechanism. In a model proposed by Adam the nuclear transport cycle is driven by Ran (Adam, 1999). In the nucleus, the

GTP form of Ran binds to exportins and its cargo (mRNA/CBC in the case of mRNA export). The entire complex is transported through a nuclear pore into the cytoplasm, where the GTP is hydrolyzed to GDP by the GTPase RanGAP, which is attached to the cytoplasmic fibrils of the nuclear pore by Ran binding proteins 1 and 2 (RanBP1 & 2) (Hillig et al., 1999). This causes a conformational change resulting in the release of the mRNA with recycling of the GDP-Ran complex back into the nucleus. Once in the nucleus, the GDP associated with Ran is exchanged for GTP by the guanine nucleotide exchange factor RCC1. RCC1 is located within the nucleus in association with chromatin (Renault et al., 1998).

RNA compartmentalization

As with any enzyme catalyzed reaction the substrate must be in close proximity to the enzyme for catalysis to occur. It is therefore important to consider the sub-cellular localization of mRNAs and RZs. We know from basic cellular metabolism that mRNAs are transcribed in the nucleus, are transported to the cytoplasm, and eventually end up at ribosomes for translation. A growing body of evidence suggests that RNA transport is more orchestrated than previously thought and that certain mRNAs are transported to distinct sub-cellular compartments (Oleynikov and Singer, 1998). *Cis*-acting elements located in the 3'-untranslated regions (UTR) of certain mRNAs have been shown to bind RNA binding proteins for transport (Ferrandon et al., 1994; Macdonald and Kerr, 1997; Munro et al., 1999). It is proposed that these proteins either bind directly to actin or tubulin for transport, or are

part of a complex of interchangeable proteins that can recognize either actin or tubulin for transport (Oleynikov and Singer, 1998).

Perhaps the most understood example of mRNA compartmentalization is seen *Drosophila*. In *Drosophila* oocytes, bicoid RNA is localized to the anterior, while oskar RNA is localized posteriorly. These RNAs give rise to proteins that direct formation of the head (anterior) and abdomen (posterior). The protein of the gene *staufen* is involved in the transport of both *bicoid* and *oskar* mRNAs to their respective sub-cellular domains. *Staufen* protein contains an RNA binding domain, that recognizes a *cis*-element in the 3'-UTR of these mRNAs and has been shown to associate with microtubules and to be transported in a microtubule-dependent manner (Ferrandon et al., 1994; St Johnston et al., 1991). *Prospero* mRNA, which is required for proper mitosis in *Drosophila*, has been shown to be transported via actin filament associated proteins, therefore, both actin and microtubule mechanisms of RNA transport exist (Jan and Jan, 1998).

While reports of this type of compartmentalization had been limited to developing cells of *Drosophila* (Ding et al., 1993; Ferrandon et al., 1994; Macdonald and Kerr, 1997), *Xenopus* (Cote et al., 1999; Elisha et al., 1995), and budding yeast (Jansen et al., 1996; Sil and Herskowitz, 1996), discoveries in differentiated cells such as neurons (Baka et al., 1996; Landry and Hokfelt, 1998) and fibroblasts (Ross et al., 1997) suggests that RNA compartmentalization plays a key role in conveying asymmetry to cells. Recently, an 11-nucleotide *cis*-element (A2RE) of the myelin basic protein mRNA has been shown to be the binding site of heterogeneous

ribonuclear protein (hnRNP) A2 (Munro et al., 1999). hnRNP A2 is involved in mRNA splicing and has been shown to mediate transport of RNA in oligodendrocytes. The abundance of hnRNP A2 in the cytoplasm of brain cells suggests that this protein may be involved in the transport of a wide variety of messages that contain similar response elements. While relatively few mRNAs have directly been shown to exhibit such sophisticated mechanisms for cellular localization, it is possible that all mRNAs contain some version of these mechanisms and may prove to be an important consideration for RZ design. Moreover, if *cis*-acting motifs are eventually described for all mRNAs, then the inclusion of these *cis*-acting motifs into the 3'-UTR of RZs could prove to be crucial for optimizing RZ/substrate-RNA interactions.

Polymerase III / tRNA-tethered ribozymes

RNA polymerase III (pol III) transcribes large amounts of small RNAs such as tRNAs and small nuclear RNAs that are highly abundant in all cells. The use of tRNA derived promoters to improve the transcription of recombinant RNAs have been reported with >100 fold increases in accumulation of transcripts compared to pol II systems (Thompson et al., 1995). Due to the high expression levels of pol III driven transcripts, ribozyme constructs tethered to tRNAs have been successfully used to drive ribozyme expression (Koseki et al., 1999; Kuwabara et al., 1999; Kuwabara et al., 1998; Thompson et al., 1995). Ribozyme/tRNA tethered transcripts have several advantages over pol II transcribed ribozymes, they are produced at much higher levels (Thompson et al., 1995), tRNA structures are highly stable (Traboni et al., 1984), and

they are small, and therefore more mobile catalysts. In addition, they are produced in all cells thereby removing the pol II concern of whether a promoter is active in a given tissue. All tRNAs contain A and B box promoter elements coded within the mature tRNA transcription sequence, and a poly T tract for termination of transcription (Wolin and Matera, 1999). To avoid 3' end processing of tRNAs, which would cleave the tethered ribozyme sequence, the last seven bases of the mature tRNA-Val can be removed without effecting transcription (Koseki et al., 1999). This was first demonstrated in 1984 by deletion experiments of methionine tRNA 3' sequences in a cell-free system and in cells (Adeniyi-Jones et al., 1984). Adeniyi-Jones also demonstrated that termination relied only on the presence of the poly T tract regardless of position. By moving the poly T tract further downstream, sequences greater than 1000 bases could be transcribed leading Adeniyi-Jones to suggest the potential use of tRNA leaders as promoters for recombinant RNAs (Adeniyi-Jones et al., 1984). As with mRNAs, tRNAs have also been demonstrated to use the exportin/RanGTP system for transport from the nucleus to the cytoplasm. A specific exportin, exportin (tRNA) has been identified (Arts et al., 1998). It has been shown that, in addition to blocking 3' processing by deleting the last 11 bases of the mature tRNA-Met, the export of the tRNA to the cytoplasm was inhibited and accumulated in the nucleus (Bertrand et al., 1997). This suggested that 3' processing was important for tRNA export from the nucleus. In contrast, the altered 3' seven based of the tRNA-Val construct reported by Koseki et al has been used with at least 12 separate ribozymes, all of which were found in the cytoplasm after transcription suggesting that this

sequence is not involved in exportin/RanGTP binding (Koseki et al., 1999). The efficiency of the tRNA-Val/ribozyme tethered system developed by Koseki et al is demonstrated in cells stably transfected with the tRNA-Val/ribozyme by a 97% decrease in targeted U5 HIV RNA gene product and a ~99% inhibition of HIV replication in HIV challenged cells.

Ribozymes as "tools" for molecular biology

Ribozymes have been successfully used to decrease the expression of a specific gene for and tested as potential therapeutic agents for a variety of conditions, the majority of which are gene products involved in cancer and viral infections. Leukemic processes due to the presence of a new gene product such as *bcr-abl*, and H-ras, are favorite targets for ribozymes because the RNA products of the *bcr-abl* fusion gene and activated H-ras are not found in normal cells and have been successfully decreased in cells (Funato et al., 1994; Ohta et al., 1996b; Snyder et al., 1993). Ribozymes have also successfully been used to reduce the over expression of other genes implicated in cancer processes such as *c-fos* (Ohta et al., 1996a; Scanlon et al., 1991), telomerase activity (Kanazawa et al., 1996; Yokoyama et al., 1998), tumor necrosis factor (Sioud et al., 1992) reversal of multi-drug resistance (MDR1) in tumor cells (Kobayashi et al., 1994), abrogation of lung metastasis by reduction of integrin α6 subunit expression (Yamamoto et al., 1996), and inhibition of matrix metalloproteinase 9 expression blocking mastasis in rat sarcomas (Hua and Muschel, 1996).

Pathogenic viruses are also major targets for ribozyme therapy. Ribozymes have been used to successfully decrease viral infection in cells challenged with the particular virus such as: human papillomavirus (Chen et al., 1995), sendai virus (Gavin and Gupta, 1997), hepatitis C (Lieber et al., 1996; Welch et al., 1998), mumps virus (Albuquerque-Silva et al., 1999), and HIV-1 (Brower et al., 1998; Chen et al., 1992; Crisell et al., 1993; Gervaix et al., 1997; Michienzi et al., 1996; Ojwang et al., 1992; Rowe, 1996; Sun et al., 1994; Weerasinghe et al., 1991; Wong-Staal et al., 1998; Zhou et al., 1996). One of the first successful attempts at creating resistance to HIV in cells was performed by Weerasinghe and his colleagues in 1991. Weerasinghe transfected several anti HIV-1 ribozymes (differing only by the promoter used to drive ribozyme transcription) into a human CD4 lymphocyte-derived cell line (Weerasinghe et al., 1991). Although several of the promoters used were able to delay the onset of HIV infection when challenged with the virus, only cells containing a ribozyme under the control of a *tat*-inducible promoter were able to resist HIV infection. According to Weerasinghe, the reason that a *tat*-inducible promoter was used was because the HIV protein *tat* had been shown to be a positive regulator of HIV gene expression (Rosen and Pavlakis, 1990). The use of a *tat*-inducible promoter not only upregulated the ribozyme at a crucial time of infection, it also competed with HIV for the *tat* protein resulting in less *tat* for HIV induction. In 1995, Sun and his colleagues designed two ribozymes directed against the *tat* gene of HIV. The first ribozyme (RZ1) was targeted to a 5' splicing region of the *tat* gene with a target sequence of GUCA in the strain HIV-1SF2. A single base mutation in a separate strain HIV-1IIIB gave a target

sequence GUCG and was used to determine the effect of a helix I mismatch on this particular ribozyme. The second ribozyme (RZ2) was targeted to the translation initiation sequence of the *tat* gene, which was conserved in both strains of HIV and used as a control. Both ribozymes were transfected into a human CD4 T cell line. When challenged with each of the two strains of HIV, RZ1 was only able to efficiently cleave the *tat* RNA of HIV-1SF2 and not HIV-1IIIB. RZ2 was able to efficiently cleave the *tat* RNA from both strains. In addition, RZ1 containing cells were significantly protected from HIV-1SF2 infection but not from HIV-1IIIB infection. RZ2 successfully inhibited infection from both strains of HIV. Sun concluded that the resistance given to the cells containing ribozymes targeted against tat was due to their catalytic activities and not the antisense effect because a single mismatch following the GUC target sequence would only significantly interfere with catalysis and not ribozyme recognition (Sun et al., 1995).

Other examples of successful reduction in gene expression using ribozymes are indicated below: (1) the inhibition of fatty acid synthesis (30-70%) in 30A5 preadipocyte cells stably transfected with a ribozyme directed against acetyl-CoA carboxylase (Ha and Kim, 1994). (2) An (~80%) decrease in β–amyloid peptide (βAPP) mRNA in COS-7 cells stably transfected with either a hammerhead or hairpin ribozyme directed against βAPP. (3) A similar decrease in βAPP was observed at the protein level as observed by western blot analysis of cell extracts (Denman et al 1994). (4) A (~40%) decrease in IGF-II mRNA levels of prostate cancer cells expressing a

double hammerhead ribozyme resulting in a prolonged doubling time from 28.3 hrs. to 42.5 hrs (Xu et al., 1999). (5) A ribozyme targeted against the G protein γ7 subunit expressed in human HEK 293 cells demonstrated a (~40%) reduction in mRNA levels with an (~85%) decrease in protein levels of the γ7 subunit. This decrease was enough to effectively reduce cAMP accumulation in response to isoproterinol (a potent β–adrenergic receptor agonist) stimulation by (~30%) in cells containing the ribozyme. Therefore the use of a ribozyme was instrumental in suggesting a role for the γ7 subunit in transducing the signal from the β–adrenergic receptor to adenylylcyclase (Wang et al., 1997; Wang et al., 1999b).

In 1998, Hsuji and his colleagues expressed a ribozyme directed against the receptor for advance glycation end products (RAGE) in an effort to decrease the effects of AGEs on diabetic nephropathy (Tsuji et al., 1998). AGEs are glycosylated proteins that are commonly produce in diabetics due to the high blood sugar environment. AGEs increase the synthesis of type IV collagen in glomeruli resulting in nephropathy common to diabetic patients. In the experiment, a mesangial cell line was established from the glomeruli of mice. This cell line was transfected with a self-processing ribozyme in which a central hammerhead ribozyme tethered to a tRNA structure was flanked by two hammerhead ribozymes that cleaved *cis* regions resulting in the liberation of the single hammerhead ribozyme tethered to the tRNA. The promoter used in this construct was a hybrid promoter system designated SRα that was created by a separate lab in 1988 (Takebe et al., 1988). This promoter system

consisted of the SV 40 promoter and part of the long terminal repeat of human T-cell leukemia virus type-1. The SRα promoter system demonstrated a 10-20 fold increase in expression when compared to the SV 40 promoter in several cell types. *In vitro* analysis demonstrated the ability of the ribozyme to self-cleave into the core ribozyme/tRNA unit and to catalyze the cleavage of RAGE at the appropriate site. RT-PCR was used to detect ribozyme expression in transfected mesangial cells. RNase protection assays and RT-PCR demonstrated a "decrease" in RAGE mRNA levels (no quantification of RAGE mRNA levels was reported). Next ribozyme transfected cells and control cells were exposed to AGE-bovine serum albumin (BSA) or non AGE-BSA to examine the induction of type IV collagen. AGE-BSA treatment in non-ribozyme containing cells increased the levels of type IV collagen 1.86±0.30 fold compared to control cells. In contrast, the ribozyme containing cells exhibited no increase in type IV collagen (1.00±0.07) when treated with AGE-BSA in comparison with BSA treated ribozyme-containing cells. Tsuji concluded that RAGE might be involved in the development of diabetic nephropathy and that ribozymes directed against RAGE could regulate the progression of the disease.

Ribozymes expressed in transgenic animals

To date, there are only a few reports in the literature in which a ribozyme has been stably expressed in transgenic animals as a transgene. In 1993 the first two cases of ribozymes expressed in transgenic animals were reported (Heinrich et al., 1993;

Zhao and Pick, 1993). *Drosophila* was used as the animal in each case and the genes targeted were each decreased to the point where phenotypic changes were observed. Zhao and Pick targeted the *fushi tarazu* gene product (*ftz*), a gene that is involved in the seven-stripe patterning and plays a role in neurogenesis during larval development. Both of these stages are controlled temporally by the expression of the *ftz* at critical times during development. By using the *drosophila* heat shock protein promoter (*hsp70*) to drive transcription of a hammerhead ribozyme in an inducible manner, Zhao and Pick were able to interrupt both developmental processes individually. The disruption of the seven-stripe patterning was achieved by giving transgenic embryos two short heat pulses at two and two and half-hours after egg laying (AEL). Similarly, three heat pulses were used between four and a half and five and a half hours AEL resulting in the absence of neural tube formation.

Heinrich and Tabler in 1993 expressed a ribozyme directed against the primary white gene transcript in *drosophila*. Once again a phenotypic change was observed by the reduction of eye pigmentation. *In vitro* analysis was used to demonstrate that the target mRNA was catalytically cleaved by the ribozyme at the target sequence.

In 1994, the first transgenic mammal expressing a ribozyme was reported by Efrat and his colleagues (Efrat et al., 1994). In an effort to create an animal model for maturity-onset diabetes of the young (MODY), a form of type II non-insulin dependent diabetes, Efrat constructed a hammerhead ribozyme directed against glucokinase (GK) mRNA, transcription of which was driven by the rat insulin II gene promoter/enhancer. The construct also contained an intron element between the

promoter and the ribozyme, and a simian virus 40 (SV 40) late polyadenylation signal sequence at the 3' end. The plasmid containing the ribozyme construct was used to create transgenic lines of mice *via* pro-nuclear microinjection of fertilized oocytes. RT-PCR was used to confirm the expression in β–cells of the pancreas by the presence of band corresponding to a correctly spliced ribozyme. Mice from two separate lines containing the ribozyme demonstrated a 70% decrease in islet GK activity. In addition, glucose stimulated insulin release was impaired, while both plasma glucose and plasma insulin levels were reported to be normal. Efrat concluded that the mice containing the GK ribozyme are likely to be predisposed to develop type II diabetes.

Larson and his colleagues produced the second transgenic mouse containing a ribozyme in 1994 (Larsson et al., 1994). In their experiment, three ribozymes directed against different regions of β2-microglobulin (β2M) mRNA were tested in NIH-3T3 mouse cells prior to expression in mice in order to determine the most efficient catalyst. The ribozymes each contained the immediate early gene enhancer/promoter region from cytomegalovirus (CMV) to drive transcription. No intron sequence was incorporated into the construct and a second *cis* cleaving ribozyme was added to the 3' end instead of a polyadenylation signal. Following analysis in cell culture, the third ribozyme (RZ-c) demonstrated the highest catalytic efficiency with an 80% reduction in β2M mRNA. This ribozyme was then used to create transgenic lines of mice *via* pro-nuclear microinjection. Seven founders were obtained. RZ-c was not detectable by Northern blot analysis, or by RNase protection assay. A band corresponding to the

correct size was observed by using RT-PCR. Although the authors contend that this was proof of RZ-c expression, the absence of an intronic sequence in their construct makes it highly possible that the band seen represents PCR amplification of the DNA gene sequence of the ribozyme and not expressed ribozyme RNA. The difficulty they encountered trying to detect ribozyme RNA may have been due to the absence of a 3' poly (A) tail, resulting in rapid degradation by nucleases. Nevertheless, Larsson reported that Northern blot analysis of total RNA from lung tissue of individual transgenic mice demonstrated a 22-94% decrease in β2M mRNA levels. Larsson could not explain the great variation observed from mouse to mouse, but suggested that the CMV transcriptional regulatory element used in his construct could have been affected by "trans-acting effects from known or unknown viral pathogens in our animal colony". Less dramatic decreases were also reported in spleen and kidney samples. No phenotype beyond β2M mRNA levels was reported.

In 1995 Heinrich and Tabler published a follow up to their 1993 experiment in which they expressed a ribozyme directed against the primary white gene transcript in transgenic *drosophila*. In this report, Heinrich and Tabler use the same *hsp 70* promoter Zhao and Pick used in their transgenic drosophila to drive expression of their white gene ribozyme (Heinrich et al., 1995). Heinrich and Tabler found that the concentration of their ribozyme was proportional to the copy number and the suppressive effect of their ribozyme was dependent on ribozyme concentration.

In 1996, a double transgenic mouse was used to express a ribozyme directed against bovine α–lactalbumin mRNA (L'Huillier et al., 1996). The double transgenic mice were obtained by crossing a mouse transgenic for the bovine α–lactalbumin gene with a mouse transgenic for a ribozyme against this gene transcript. This hammerhead ribozyme construct contained a mouse mammary tumor virus long terminal repeat (MMTV-LTR) to drive transcription, an SV 40 intron, and an SV 40 poly (A) signal. This ribozyme was predicted to be 1150 bases after transcription and splicing, not including polyadenylation. The large size of this ribozyme was due to the large 5' (transcription initiation was ~268 bases upstream of the ribozyme) and 3' (the poly (A) cleavage site was ~822 bases downstream of the ribozyme) untranslated regions. The ribozyme sequence itself contained only two 12-nucleotide arms and the standard 22 bases that make up the hammerhead structure. The computer program *mfold* was used to select the target sequence for this ribozyme based on predicted secondary structures. Transgenic mice were first made by pro-nuclear microinjection as with the previously mentioned transgenic mice. But unlike the other transgenic mice, this was the first ribozyme in a transgenic animal to be detected by Northern blot analysis. All other ribozymes were detected by RT-PCR. A possible reason for this may be due to its large size. Northern blot analysis of bovine α–lactalbumin in mammary gland tissue was reduced 22, 42, and 50 % in three separate lines compared to non-ribozyme containing littermates. Similar decreases were reported in the levels of protein. It was also pointed out that the levels of endogenous mouse α–lactalbumin were unaffected

by the presence of the ribozyme, and even though the GUC target sequence was conserved across both species, 6 out of the 24 nucleotides that form helices I and III with the ribozyme were not conserved.

In an attempt to directly compare the effectiveness of antisense RNA, ribozymes, and multi-ribozymes, Sokol et al produced transgenic mouse lines containing one of the three constructs directed against bacterial chloramphenicol acetyltransferase (CAT) gene transcripts present in another transgenic mouse line (Sokol et al., 1998). All of the anti-CAT constructs contained the same bovine α-s1-casein promoter/enhancer element, and the small t intron and poly (A) addition signal derived from SV 40. Once again double transgenic mice were obtained by breeding positive animals. CAT protein levels were compared in lactating double-hemizygous transgenic female mice. Mice containing the antisense construct demonstrated a 90% decrease in CAT protein levels. This was very close to mice containing the ribozyme construct that demonstrated an 87% decrease. Surprisingly, the multizyme exhibited the lowest decrease in CAT protein levels at 67%. Sokol concluded that the incorporation of multiple ribozymes does not enhance effectiveness in his system.

Clinical trials involving ribozymes

Currently, there are at least two separate ribozymes being used in human clinical trials. The first of which is a hammerhead ribozyme directed against the vascular endothelial growth factor (VEGF) receptor. VEGF is a cytokine that is involved in normal vascular growth, but is also implicated in several pathological

conditions including proliferative retinopathy and solid tumor growth and metastasis. Elevated expression of VEGF leads to neovascularization, which provides oxygen and nourishment to tumor cells allowing for tumor growth and metastasis. Ribozyme Pharmaceuticals Inc. (RPI) and Chiron corporation have formed a joint effort to decrease the ability of VEGF to signal by producing a hammerhead ribozyme directed against the VEGF receptor mRNA. The therapeutic was given the name ANGIOZYME^{TM}. Dr. Nassim Usman of RPI has reported, "The ribozyme compound was able to completely inhibit metastases in a clinically relevant colorectal cancer model. In addition, ANGIOZYME^{TM} was shown to halt tumor growth and metastases in a Lewis Lung Maurine model." According to a recent press release (July 14, 1999), RPI announced the successful completion of Phase Ia and Ib human clinical trials of ANGIOZYME^{TM}. "The Phase Ia trial demonstrated excellent tolerability of low single doses of ANGIOZYME^{TM} administered either intravenously or subcutaneously to healthy volunteers. The subsequent Phase Ib trial, performed with cancer patients, extended to higher doses of ANGIOZYME^{TM} up to 300 mg/m^2 to help define the appropriate dosing for future Phase II and III trials." Unlike most anti-cancer drugs, no clinically significant side effects were observed. Pharmacokinetic data demonstrated that ANGIOZYME^{TM} was detectable at levels greater than those predicted for an anti-angiogenic effect up to 24 hours following subcutaneous injection. The next round of clinical studies was said to begin six to nine months fom the July 14, 1999 press release date, and will involve multiple dose schedules to study the effects of continuous administration of ANGIOZYME^{TM}.

The second ribozyme currently in Phase II clinical trials is an anti-HIV double ribozyme packaged in a retroviral vector. Once again RPI was the sponsoring company. The purpose of this Phase II trial is "to assess the safety and feasibility of administering peripheral blood progenitor cells (PBPC) transduced with retroviral vectors encoding an anti-HIV double ribozyme to HIV + patients undergoing intensive chemotherapy and stem cell transplantation for non-Hodgkin's lymphoma. To determine if these genetically modified PBPC can engraft, differentiate, and circulate in the blood of transplanted recipients." According to the Food and Drug Administration the cells themselves that are transduced with the ribozyme containing retrovirus are considered the "drug" for the study. The preceding information about this Phase II trial was obtained from the AIDS Clinical Trials Information website (www.actis.org). This website is sponsored by the FDA, the Center of Disease Control and Prevention (CDC), and the National Library of Medicine (NLM). In the methods described at the RPI website (www.rpi.com), patients will have bone marrow samples taken daily following injections of G-CSF to stimulate stem cell collection, with as many as six collections if necessary. The stem cells will be divided into two groups. The first will function as a negative control and remain unchanged. The second will be transduced with the ribozyme containing retrovirus. Patients will then undergo seven days of intense chemotherapy followed by infusion of the treated or untreated stem cells back into the patients. According to the RPI website, the Phase I safety study in five healthy HIV infected individuals encountered no serious events, with no deaths or withdrawals.

GROWTH HORMONE

The Pituitary

In 1886, the French neurologist Pierre Marie pioneered pituitary endocrinology with his observations that patients with acromegaly exhibited enlarged pituitaries. This led Pierre to suggest that the pituitary was involved in the progression of this disease spurring an interest in pituitary research. The origins of the word pituitary, a combination of the Latin word for mucus (*pituita*) and the Greek word to spit (*ptuo*), come from the original belief that nasal mucus was produced in the pituitary (Wilson and Foster, 1998).

The pituitary forms in the human embryo at about the third month of gestation under the control of several genes, the most studied being pituitary transcription factor-1 (Pit-1). Pit-1 has been shown to regulate the differentiation of three of the five hormone releasing cell types in the pituitary; somatotrophs, lactotrophs, and thyrotrophs (de la Hoya et al., 1998). Somatotroph cells that produce growth hormone (GH) are detectable as early as the third month of gestation while the final hormone secreting cells to develop in the anterior pituitary are the lactotroph cells, which appear at five months of gestation. The weight of the pituitary at birth is about 0.1g and grows to an adult weight of 0.6g. Pituitaries in women tend to increase in weight during pregnancy due to the increase in hormone production (Scheithauer et al., 1990). The pituitary is divided into two distinct lobes, the anterior and posterior lobes. The anterior lobe accounts for 80% of the pituitary and is further divided into the pars distalis, pars intermedia, and pars tuberalis. The pars distalis is the region of the

anterior pituitary in which all five hormone-secreting cell types reside. The posterior pituitary stores the osmoregulatory hormones vasopressin, antidiuretic hormone (ADH) and oxytocin that are produced in the hypothalamus and releases them into the blood stream.

A common theme for anterior pituitary hormones

All hormones produced in the anterior pituitary are released into the bloodstream in a pulsatile manner. Furthermore, all hormones produced in the anterior pituitary are regulated by corresponding hormones produced in the hypothalamus (see table 1). These hypothalamic regulatory hormones are transported *via* portal veins that run from the hypothalamus to the anterior pituitary where they bind to specific receptors on the individual cell types and either stimulate or repress pituitary hormone production. Most if not all hormones produced in the anterior pituitary exhibit a feedback control mechanism (see table 1). Hormones that are secreted by target tissues of the pituitary hormones negatively regulate the production of that hormone. The only anterior pituitary hormone in which a feedback control mechanism has not been discovered is prolactin (Wilson and Foster, 1998).

Table 1. Relationship between hypothalamic, pituitary, and target tissue secretion (taken directly from Wilson JD and Foster DW 1998 textbook et al 1998 p252).

Hypothalamic hormone	Pituitary hormone	Target gland	Feedback hormone
TRH	Thyrotropin	thyroid	T3 & T4
LHRH	LH	gonad	E2 & T
	FSH	gonad	Inhibin, E2 & T
Somatostatin	GH	multiple	IGF-1
GHRH	GH	multiple	IGF-1
Dopamine	Prolactin	breast	?
CRH	Corticotropin	adrenal	Cortisol
AVP	Corticotropin	adrenal	Cortisol

AVP, arginine vasopressin; CRH, corticotropin-releasing hormone; E2, estradiol; FSH, follicle-stimulating hormone; GHRH, GH-releasing hormone; IGF-1, insulin-like growth factor-1; LH, luteinizing hormone; LHRH, LH-releasing hormone; T, testosterone; T3, triiodothyronine; T4, thyroxine; TRH, thyrotropin-releasing hormone.

Growth Hormone

Growth hormone (GH) is a 22-kDa protein secreted form anterior pituitary into the bloodstream where it acts on a variety of target tissues by binding to a specific membrane bound receptor, GH receptor (GHR). GH belongs to the prolactin-GH family, which includes GH, prolactin, and placental lactogen. All three members of this family share amino acid identities and are proposed to originate from a single ancestral gene (Niall et al., 1971). The structural organization of each gene is similar, all with five coding exons and four introns (Barsh et al., 1983; Cooke et al., 1981). In humans, the majority of pituitary GH is found as a 191 amino acid single chain polypeptide with two intramolecular disulfide bonds. A 20 kDa alternatively spliced form of GH makes up less than 10% of pituitary GH (Cooke et al., 1988; DeNoto et al., 1981). A non-pituitary form of GH is secreted by the placenta during pregnancy and is termed GH variant. GH variant shares an 84% amino acid identity with the 22-kDa pituitary GH with two disulfide bonds in the same position (Frankenne et al., 1988; Frankenne et al., 1987).

GH signaling

Circulating GH binds to two GHRs on the cell surface (Cunningham et al., 1991) resulting in a conformational change in the structure of the receptors (Mellado et al., 1997). The change in conformation results in the activation of the tyrosine kinase JAK-2 (see figure 4). JAK-2 is a ~120 kDa tyrosine kinase that was first

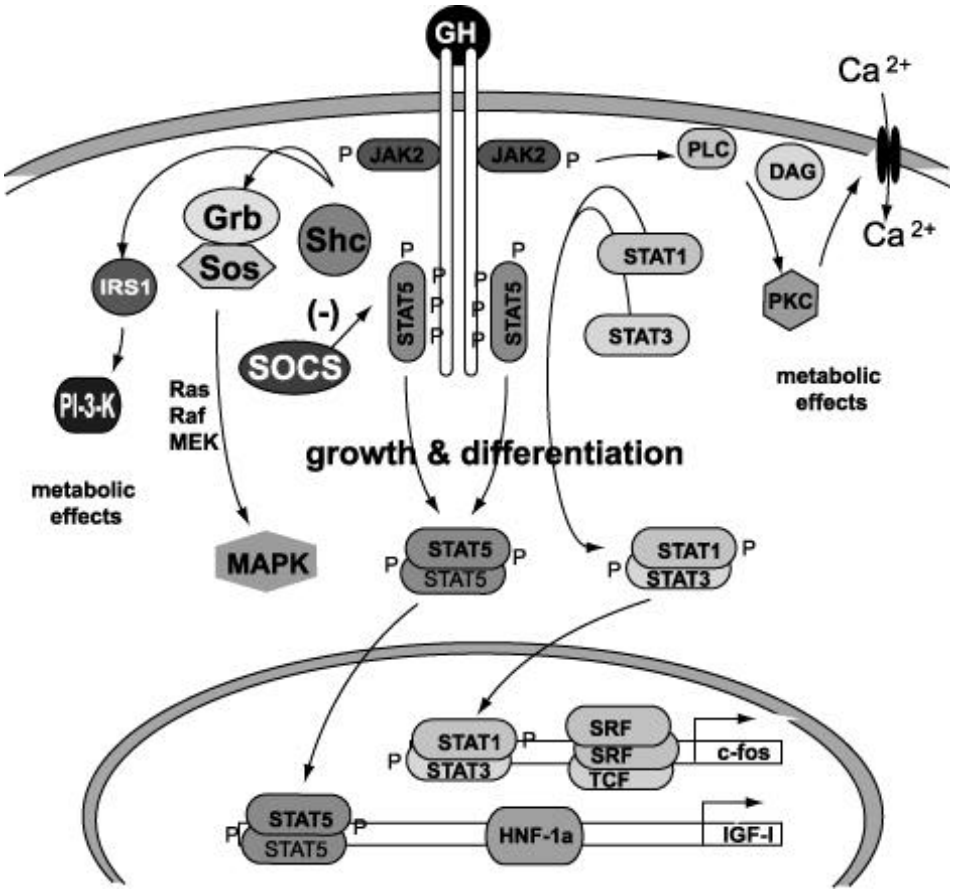

Figure 4. Several pathways involved in growth hormone signal transduction (Carter-Su and Smit, 1998).

described to be present in GHR preparations by Wang et al in 1993 and was shown to associate with the GHR by Argetsinger et al that same year (Argetsinger et al., 1993; Wang et al., 1993c). Following tyrosine phosphorylation of JAK-2 and the GHR, signal transducers and activators of transcription (STAT) 1, 3, 5a, & 5b have been shown to be tyrosine phosphorylated in response to GH treatment (Campbell et al., 1995; Gronowski and Rotwein, 1994; Gronowski et al., 1995; Meyer et al., 1994; Wang et al., 1994; Wood et al., 1995). All STAT proteins contain Src homology (SH) 2 & 3 domains, are activated by tyrosine phosphorylation, and form homo or hetero dimers that are transported to the nucleus and regulate transcription by binding to specific DNA sequences. STATs 1 and 3 have been shown to bind the Sis-inducible element (SIE) in the *c-fos* promoter in response to GH treatment. STAT-5 a and b can each bind to γ activated sequences (GAS)-like elements in the serine protease inhibitor 2.1 promoter as well as the β-casein promoter. STAT-5 binding motifs have been described on the GHR by GHR deletion and mutational experiments demonstrating that STAT-5 a & b bind directly to the GHR (Smit et al., 1996; VanderKuur et al., 1995b; Wang et al., 1996; Wang et al., 1995; Xu et al., 1996). Although activation of STATs 1 & 3 have been observed in response to GH, no direct association of these STATs with the GHR has been observed. The STAT-1 binding motif identified on interferon-γ (INFγ) and leukemia inhibitory factor (LIF) receptors, as well as the STAT-3 binding motif identified on LIF receptors are not present on the GHR

suggesting that STATs 1 & 3 are activated by GH without associating with the GHR (Gerhartz et al., 1996; Greenlund et al., 1994; Stahl et al., 1995).

JAK-2 has also been shown to activate the MAP kinase pathway, which is implicated in cellular growth and differentiation. Prior to the discovery in 1993 that JAK-2 associates with and acts as the major kinase of GHR, three separate groups reported that ERKs 1 & 2 were activated in response to GH treatment (Anderson, 1992; Campbell et al., 1992; Harding et al., 1995; Winston and Bertics, 1992). It is thought that the MAP kinase cascade is initiated by the association SHC at specific SH2 domains to phosphorylated tyrosines on the GHR. SHC, now phosphorylated by JAK-2 associates with SH2 domain containing Grb2. Grb2 is complexed with SOS, a guanine nucleotide exchange factor that activates Ras, a membrane bound GTP binding protein. The serine/threonine kinase, Raf is activated by Ras which then activates the tyrosine/serine/threonine kinase MEK. MEK then activates ERK 1 and 2 (Cobb and Goldsmith, 1995; VanderKuur et al., 1995a; Vanderkuur et al., 1997).

A third GH signaling pathway was discovered by Argetsinger et al in 1995 (Argetsinger et al., 1995; Argetsinger et al., 1996). Argetsinger observed tyrosine phosphorylation of insulin receptor substrate (IRS) 1 and 2 in 3T3-F442A fibroblasts in response to GH treatment. IRS-1 and –2 are 160-180 kDa mobile adapter proteins originally identified as signaling molecules for insulin. The discovery of IRS involvement in GH signaling could account for earlier observations that GH can induce an insulin-like effect on fat and carbohydrate metabolism (Davidson, 1987). This was demonstrated by a transient increase in glucose transporters (Glut1 and

Glut4) to the plasma membrane of adipocytes effectively increasing glucose transport in response to GH treatment (Carter-Su et al., 1988; Tanner et al., 1992). Phosphorylated tyrosines on IRS molecules are responsible for association and activation of a number of signaling molecules including the regulatory subunit of PI3 kinase (p85), SH2 domain-containing tyrosine phosphatase (SHP2), and the Src kinases (fyn, Nck, & Grb). In addition to GH stimulation of SHP2 *via* association with IRS molecules, an isoform of the tyrosine phosphatase SHP2, SH2-Bβ was identified by Rui et al in 1997 to associate with JAK2, and not with IRS molecules (Rui et al., 1997). The function of SH2-Bβ is currently unknown, but being a phosphatase, it is probably involved in the negative regulation of JAK2 signaling events.

More recently, potential negative regulators of GH signaling have been identified. Moutoussamy et al reported that Grb10 interacts with both GHR and JAK2 in response to GH treatment and down regulates some GH signaling pathways independent of STAT-5 (Moutoussamy et al., 1998). A newly found family of proteins called suppressors of cytokine signaling (SOCS) have been identified and have been shown act negatively on the signal transduction of cytokines. Seven members of this family have been identified and include SOCS 1-7 (Bjorbaek et al., 1998; Endo et al., 1997; Naka et al., 1997; Narazaki et al., 1998; Starr and Hilton, 1998; Starr et al., 1998; Starr et al., 1997; Yoshimura et al., 1995). SOCS-1, -2, & -3 have been shown to affect GH signaling (Favre et al., 1999). Favre and her colleagues used human kidney fibroblast 293 cells co-transfected with a set amount of monkey

GHR containing plasmid and set amount of a luciferase reporter gene fusion carrying six copies of the lactogenic hormone response element (LHRE). LHRE is a response element of the β–casein promoter that is activated in response to GH treatment via STAT-5. In addition, these cells were co-transfected with increasing amounts of either SOCS-1, -2, or –3 containing plasmids. Favre reported that cells transfected with SOCS-1 or –3 inhibited the transcriptional activation of the reporter gene in a dose dependant manner. Cells transfected with SOCS-2 also demonstrated a decrease in transcription at low concentrations but at higher SOCS-2 concentrations an increase in luciferase activity was observed. In addition, Favre reported that when SOCS-2 was co-expressed with SOCS-1 or SOCS-3, SOCS-2 was able to block the inhibitory effect of SOCS-1 on GH signaling. Apparently this effect was specific for SOCS-1, as SOCS-2 was unable to block the inhibitory effects of SOCS-3. Referring to the interaction of SOCS-1 and –2, Favre suggested that the mechanisms of inhibition of SOCS-1 and –3 are different and that a major role of SOCS-2 might be to restore the sensitivity of cells to GH following the initial inhibitory effects of other SOCS molecules. In support of Favre's proposed role for SOCS-2, she referred to a report by Adams et al in 1998 that showed that SOCS-1 and –3 were expressed earlier than SOCS-2 in response to GH treatment (Adams et al., 1998).

The GH receptor

The GHR belongs to the cytokine family of receptors, all of which are all single membrane spanning with or without tyrosine kinase activity in their

intracellular domains. Members of the cytokine family of receptors share homology mainly in the extracellular portion of the receptors including a cytokine receptor homology (CRH) region, four conserved cysteine residues, fibronectin type III, modules, and a WSXWS motif (Wells and de Vos, 1996). In the cytoplasmic domain three conserved regions are common to most cytokine receptors. They are termed box 1, 2, and 3 with respect to their amino to carboxyl position. Box 1 is located approximately 10 amino acid residues from the transmembrane domain, and boxes 2 and 3 being more carboxyl, respectively. The use of truncated GHRs demonstrated that only first 54 residues of the cytoplasmic domain, which contains box 1 are sufficient for mitogenesis (Colosi et al., 1993). This region, as well as others in the cytoplasmic domain of the GHR is discussed in more detail later in the text. The GHR has been found in most tissues examined at some level with the highest levels being present in liver, kidney, and fat (Silva et al., 1999). The GHR was first cloned in 1987 by Leung et al from rabbit and human liver (Leung et al., 1987). This was soon followed by cloning of GHR from mouse (Smith et al., 1989), rat (Mathews et al., 1989), bovine (Hauser et al., 1990), sheep (Adams et al., 1990), and pig (Cioffi et al., 1990). The mature GHRs are approximately 620 amino acid residues with an ~24 amino acid single membrane spanning region separating an ~246 amino acid extracellular domain and an ~350 amino acid cytoplasmic domain. The extracellular domains are glycosylated and responsible for ligand binding of the GH. In all species studies, the gene encoding the GHR also encodes the GH binding protein. In mice, the gene that codes for GHR/BP is made up of 11 coding exons with two major 5'

untranslated regions (UTR) designated L1 and L2. The majority of GHR and BP transcripts expressed in tissues contain the L2 5'-UTR, which is encoded by a single exon approximately 27 kb 5' of exon 2. High expressed levels of L1 5'-UTR containing transcripts are found only in the livers of pregnant mice (Moffat et al., 1999). Two exons (4B and 8A) found in mice that are not present in the human GHR/BP gene. Moffrat and his colleagues used reverse transcriptase-polymerase chain reaction (RT-PCR) on mouse liver, kidney, mammary gland, and skeletal muscle, and rat liver to determine the extent of exon 4B inclusion. In all mouse tissues studied, exon 4B was included. Exon 4B was not present in the rat liver sample (the only tissue Moffrat examined in rat), making 4B apparently constitutively included and unique to mice (see table 2).

GH binding protein

In all species studied that contain GHR, a circulating GH binding protein (GHBP) with an amino acid sequence corresponding to the extracellular domain of the GHR has been found. Although it has been shown that the GHR and GHBP are encoded by a single gene in all species examined, the methods by which the two proteins are generated differ. In rodents, the receptor and binding protein are generated by alternative splicing of exon 8A (see figure 5). More specifically, when exon 7 splices to exon 8 excluding exon 8A (located between exon 7 and exon 8), the GHR transcript is generated with poly adenosine (A) addition signal and translational stop codon located in exon 10. When exon 7 splices to exon 8A, the GHBP transcript

Table 2. Amino acid sequence alignment of the exon 4B region within the GHR from various species (Moffat JG et al 1999).

	Exon 4	Exon 4B	Exon 5
Mouse	PGSIQLYYAKR	ESQRQAAR	IAHEWTQEWKECPDY
Rat	PGSIQLYYARR		IAHEWTPEWKECPDY
Human	LGPIQLFYTRR		NTQEWTQEWKECPDY
Pig	PGSIQLFYIRR		STQEWTQEWKECPDY
Rabbit	PGSVQLFYIRR		NTQEWTQEWKECPDY
Bovine	PGSVQMFYIRR		DIQEWKECPDY
Sheep	PGSVQMFYIRR		DIQEWKECPDY

Note: Exon 4B is apparently unique to mouse, and is found in all mouse tissues studied (Moffat JG et al 1999).

is generated with a poly A addition signal and translational stop codon contained within exon 8A (Baumbach et al., 1989; Edens et al., 1994; Zhou et al., 1994). In non-rodent species, the generation of GHBP results from proteolytic cleavage of the GHR (Sotiropoulos et al., 1993; Trivedi and Daughaday, 1988). Trivedi also reported that in humans, the majority of GHBP generated by proteolytic cleavage occurs with membrane bound GHR. The location of cleavage in other species and the enzyme responsible for cleaving the GHR are still unknown. Curiously, there is one report by Martini et al in which both proteolytic cleavage and alternative splicing were observed in monkey (Martini et al., 1997). This redundancy observed in the production GHBP in the monkey, the evolution of at least two distinct methods for generating GHBP, and the presence of GHBP in all species studied containing GH all suggest a critical role for GHBP in regulating the actions of GH. Theories ranging from GHBP increasing the actions of GH by binding serum GH and effectively prolonging its half-life due to decreased renal clearance because of the increase in size of the complex, to GHBP decreasing the actions of GH by competing with the GHR, remain unproven. Current work by Kopchick et al (unpublished work in progress) in which the GHBP is selectively "knocked out" in mice by homologous recombination, and work by Workman et al (unpublished work in progress) in which mouse GHBP containing an epitope tag will be over expressed in mice, may provide the answers about GHBP function.

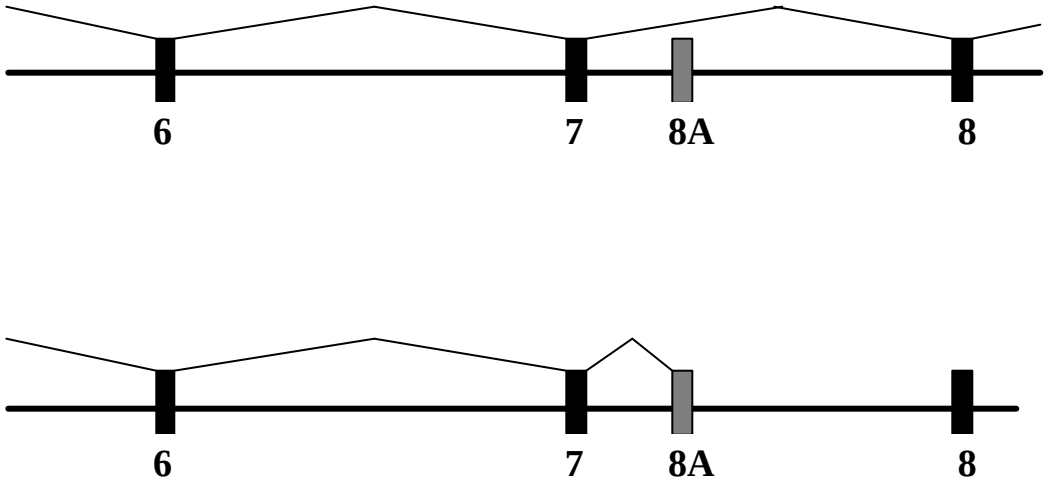

Figure 5. Alternative splicing of exon 8A in rodents pre-mRNA GHR/BP transcripts determines whether GHR or GHBP is expressed. Splicing that involves exon 8A exclusion (top) results in the production GHR mature transcripts. Splicing that involves exon 8A inclusion (bottom) results in the production of GHBP mature transcripts. Exon 8A contains its own poly A addition signal and translational stop codon. (Edens et al 1994).

Discovering regions of the GHR important for association of signaling molecules

The growth hormone receptor (GHR), like other members of the cytokine family of receptors, lacks intrinsic kinase activity and must therefore rely on the association of proteins with kinase activity. For the GHR, that protein is Janus kinase-2 (JAK-2). Although 4 members of the JAK family have been identified, only JAK-2 has been shown to associate with GHR and affect GH signaling (Argetsinger et al., 1993). Argetsinger and his colleagues (1993) first demonstrated that JAK-2 could form a complex with GHR in response to GH treatment. He performed immunoprecipitation with anti-GHR antibody on GH treated and untreated fibroblasts followed by an anti-JAK-2 immunoblot. The JAK-2 was able to co-precipitate demonstrating for the first time that JAK-2 associated with GHR. In addition, Argetsinger demonstrated that JAK-2 functioned as a GH dependent tyrosine kinase when he showed that JAK-2 immuno-complexes incubated with γ-^{32}P ATP incorporated phosphate onto tyrosine residues of JAK-2 and GHR in response to GH treatment.

To further define the association of JAK-2 with GHR, Vanderkuur and his colleagues have identified a region on the cytoplasmic domain of the GHR between amino acids 297 - 311 that is required for the association of JAK-2 and GH dependent JAK-2 tyrosine phosphorylation (VanderKuur et al., 1994). Vanderkuur used a series of truncated GHRs, a GHR with amino acids 297 - 311 deleted, and a GHR with prolines 300, 301, 303, and 305 changed to alanines to determine the region of JAK-2 association. After transfecting the altered receptors into Chinese hamster ovary

(CHO) cells, cell lysates were immunoprecipitated with a GHR antibody followed by an immunoblot using a JAK-2 antibody. The results showed that the GHR truncation at amino acid 294, the GHR with a deletion of amino acids 297 - 311, and the GHR with mutated prolines at 300, 301, 303, and 305 were all unable to associate with JAK-2. GH dependent JAK-2 tyrosine phosphorylation was also lost in response to these same mutations, demonstrated by an anti-JAK-2 immunoprecipitation followed by western blot analysis with an anti-phosphotyrosine antibody.

In 1994 Wang and his colleagues discovered a second protein that associated with the GHR in response to GH (Wang et al., 1994). In his experiment, Wang transfected porcine GHR (pGHR) cDNA into mouse L-cells (MLC). He then treated these cells with or without GH. After western blot analysis using an anti-phosphotyrosine antibody, only MLCs treated with GH demonstrated the presence of a 95 kDa protein that was tyrosine phosphorylated. Wang also demonstrated that human, bovine, mouse, and rat GH were able to induce tyrosine phosphorylation of the 95 kDa protein, while IL-2, EGF, FGF, PDGF, INS, and IGF-1 could not. Wang termed the protein pp95.

In an unsuccessful effort to identify pp95, Xu and his colleagues performed a series of immunoprecipitations and western blot analyses using anti-STAT-1, -3, and 4 antibodies (Xu et al., 1995). Anti-GHR antibody was also used in case the protein was actually a fragment of the GHR. None of the suspected proteins were shown to be present. Up until 1995, the only protein shown to associate with the GHR was the previously mentioned JAK-2. Since JAKs have been shown to activate signal

transducers and activators of transcription (STATs), it was logical for Xu and his colleagues to try to identify the unknown protein using STAT antibodies. Unfortunately they didn't use all STAT antibodies because it wouldn't be until 1996 that Xu identified pp95 as STAT-5 using a STAT-5 antibody and three other groups also identified STAT-5 as a GH responsive signaling molecule (Chow et al., 1996; Ram et al., 1996; Silva et al., 1996; Xu et al., 1996).

In 1996, two important discoveries were made by Xu and his colleagues (Xu et al., 1996). First, Xu identified pp95 as STAT-5, and second, he showed that STAT-5 associated directly with GHR in a GH dependent manner. Prior to this point, no STATs had been shown to associate with GHR. To demonstrate that pp95 was actually STAT-5, Xu performed immunoprecipitations with an anti-STAT-5 antibody followed by immunoblotting with either anti-STAT-5 or anti-phosphotyrosine on MLC transfected with pGHR and treated with or without GH. Not only did STAT-5 migrate at the predicted 95 kDa mass, it was also tyrosine phosphorylated in GH treated preps. To demonstrate the association of STAT-5 with GHR, Xu performed immunoprecipitations using anti-GHR antibody followed by immunoblotting with anti-STAT-5 or anti-phosphotyrosine. For both immunoblots, a 95-kDa protein was co-precipitated.

Now that it was known that STAT-5 associates with GHR in response to GH, a logical step would be to identify the region on the GHR to which STAT-5 associates. Conveniently, this work had already begun prior to the identification of the unknown pp95 as STAT-5 by Wang and his colleagues (Wang et al., 1995). In 1995 Wang and

his colleagues identified a region of the GHR on the cytoplasmic domain between amino acids 476 -516 that was necessary for tyrosine phosphorylation of pp95. Using a series of truncated GHRs transfected into MLCs, he performed western blot analysis using anti-phosphotyrosine on GH or non-GH treated cells. In his results, only wild type, and the GHRs truncated at residue 588 and 516 were able to induce tyrosine phosphorylation of pp95. The GHRs truncated at residue 476 or shorter were unable to induce tyrosine phosphorylation of pp95.

In 1996, in an effort to further elucidate the interactions of STAT-5 with GHR, Wang and his colleagues performed a comprehensive analysis of the individual tyrosines on the cytoplasmic domain of GHR involved in STAT-5 association (Wang et al., 1996). In his experiment, Wang individually changed each tyrosine to phenylalanine using oligonucleotide directed mutagenesis of the pGHR cDNA. He also additively changed the tyrosines starting from the carboxyl-terminal of the GHR and proceeding in the amino terminal direction until all the tyrosines were changed to phenylalanine. And starting with the receptor completely void of tyrosines, he sequentially replaced each individual tyrosine. All together Wang had 22 individual GHR mutant clones for this experiment. Each clone was then transfected into MLCs. The expression of each was verified by northern analysis and their ability to bind GH was verified by binding assays. STAT-5 phosphorylation assays were performed using cells treated with or without GH followed by western blot analysis using a phosphotyrosine antibody. Wang's results indicated that the presence of a single

tyrosine at position 487, 534, 566, or 627 alone was able to allow GH induces STAT-5 phosphorylation.

The same set of mutated receptors were analyzed by Hansen and his colleagues for their ability to induce a CAT reporter construct containing a spi 2.1 promoter sequence which contains a STAT-5 binding element (Hansen et al., 1996). Once again, the presence of an individual tyrosine at position 534, 566, or 627 was sufficient for CAT activation in this experiment. Curiously, tyrosine 485, which was shown to allow STAT-5 tyrosine phosphorylation by Wang did not induce CAT activity for Hansen. This suggests that tyrosine 485 can somehow allow STAT-5 tyrosine phosphorylation without STAT-5 activation. This may be due to the inhibition of STAT-5 dimerization, a process that is required for STAT-5 translocation to the nucleus.

GH stimulated activation of JAK/STAT signaling has been shown to deactivate approximately one hour after the removal of GH (Hackett et al., 1997). The SH-2 domain containing protein tyrosine phosphotase-1 (SHP-1) is thought to act as the molecule responsible for the deactivation of GH stimulated JAK/STAT activation. SHP-1 has been shown to down regulate interferon JAK/STAT signaling (David et al., 1995). A region in the cytoplasmic domain of human GHR between residues 520 - 540 has been demonstrated to play an important role in the deactivation of GH stimulated JAK/STAT signaling (Hackett et al., 1997). In his experiments, Hackett used a series of truncated GHRs to demonstrate that full length GHR and GHR

truncated at residue 540 exhibited normal deactivation of both GH induced STAT complex, and rapid dephosphorylation of JAK-2. GHRs truncated at residue 521 and shorter did not demonstrate either deactivation of GH induced STAT complex or dephosphorylation of JAK-2. Hackett also reported that SHP-1 co-immunoprecipitated with the GHR only in the absence of GH and upon GH treatment, the association was lost. In contrast to this, Ram and Waxman concluded that SHP-1 was not able to associate with GHR either in the presence or absence of GH (Ram and Waxman, 1997). In addition, Ram and Waxman demonstrated that SHP-1 was able to associate with STAT-5 in the nuclei of GH treated cells. Although the results of Hackett et al and Ram and Waxman contrast one another, they both suggest a role of SHP-1 in the deactivation of GH activated JAK/STAT signaling.

Regulation of GH

As previously mentioned, GH is produced in the anterior pituitary under the control of two hypothalamic hormones, somatostatin and GH releasing hormone (GHRH) (see figure 6). GHRH has been shown to increases pituitary GH by upregulating transcription of GH mRNA, and stimulate secretion by a Ca^{2+} dependent mechanism leading to the accumulation of cAMP (Barinaga et al., 1983; Holl et al., 1988). In contrast, somatostatin appears to have no transcriptional regulatory activity, only regulating the timing and amplitude of GH pulsatile release by lowering levels of cAMP and intracellular Ca^{2+} (Holl et al., 1988). The stimulatory effect of GHRH is blocked by somatostatin (Wehrenberg et al., 1983). In addition to the neuronal "open

loop" regulatory system of the hypothalamus, GH is also negatively regulated by two "closed loop" systems. GH itself has been shown to stimulate somatostatin release from the hypothalamus in a short closed loop system (Abe et al., 1983; Berelowitz et al., 1981a). In a long closed loop system, IGF-1 has been shown to both stimulate somatostatin release form the hypothalamus and act directly on the pituitary by inhibiting the effects of GHRH (Abe et al., 1983; Berelowitz et al., 1981b).

GH releasing peptides (GHRPs) are a group of artificial compounds that cause the release of GH from the pituitary in all species tested (Seoane et al., 2000). The identification of a natural occurring receptor GH secretagogue-receptor (GHS-R) to these synthetic peptides led researchers to hypothesize that an unknown natural ligand existed and that the GHRP were mimics of this natural ligand (Howard et al., 1996; McKee et al., 1997). Three years after the initial cloning of GHS-R the natural ligand was discovered by Kojima and colleagues (Kojima et al., 1999). Kojima named this new peptide "Ghrelin" based on the Proto-Indo-European word "ghre" which means to grow. The purified peptide consists of 28 amino acids. Serine 3 in the peptide is O-n-actanoylated, a post-translational modification that is required for activity (Muccioli et al., 2001). Ghrelin is produced mainly in the stomach with lower levels of expression detected in other tissues such as kidney and hypothalamus (Kojima et al., 1999; Mori et al., 2000; Nakazato et al., 2001). Ghrelin has been reported to increase *in vitro* GH secretion as well as *in vivo* plasma GH levels in rats and humans (Kojima et al., 1999; Peino et al., 2000) by binding to GHS-R in the hypothalamus and pituitary (Muccioli et al., 2001). In addition to stimulating GH secretion, recent

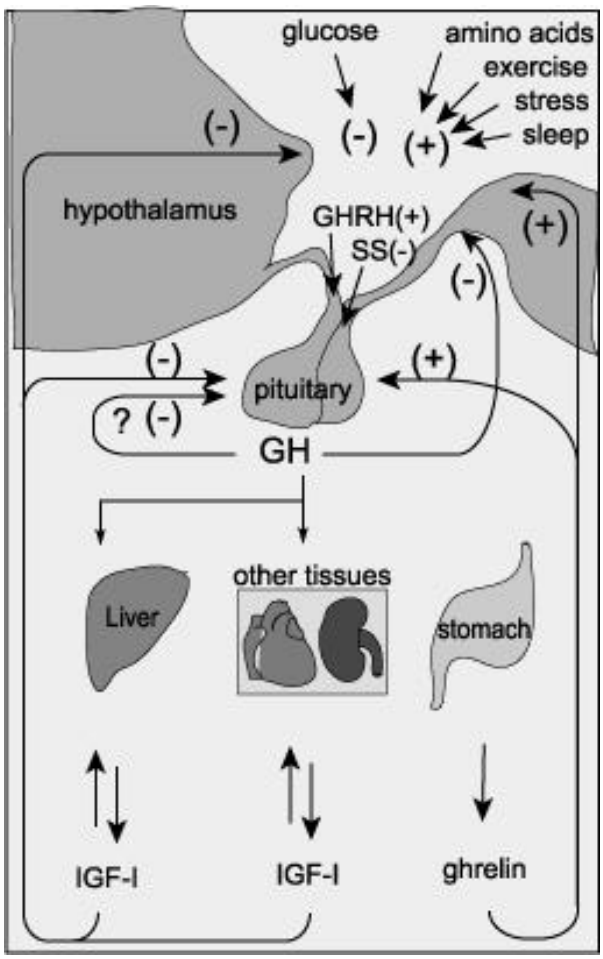

Figure 6. Factors regulating the production growth hormone (Harris, 1996).

studies suggest that ghrelin is a mediator of feeding response. Ghrelin injections stimulate feeding and weight gain in rats, and ghrelin is negatively regulated by leptin (Asakawa et al., 2001; Nakazato et al., 2001).

Affects of pulsatile GH release

Studies in rats and mice have demonstrated that the pulsatile release of GH plays an important role in the effects of GH. Administrating GH results in increased linear growth and weight gain, IGF-1 mRNA levels in skeletal muscle, and serum IGF-1 levels to a greater extent than continuous administration (Clark et al., 1985; Isgaard et al., 1988; Maiter et al., 1988). In addition, intermittent administration of GH in rat liver activates STAT-5 followed by nuclear translocation, an event that did not occur with continuous administration of GH (Waxman et al., 1995). In a separate experiment, Ram from Waxman's lab demonstrated that STATs 1 & 3 were activated independent of intermittent GH administration and confirmed that only STAT-5 required intermittent administration of GH for activation in rat liver cells (Ram et al., 1996). Furthermore, Gebert from Waxman's lab has demonstrated that it is the STAT-5b isoform that is responsive to the pulsatile release of GH. Gilbert et al propose that phosphatases in the nucleus play an important role in inactivating STAT-5b causing it to move back to the cytoplasm to prepare for another round of activation by the next pulse of GH (Gebert et al., 1997).

GH action *in vitro*

GH affects the metabolism of most tissues in the body such as bone, muscle, fat, liver, kidney, heart, intestine, lung, pancreas, lymphocyte, testes, ovaries, and breast, all of which express GHR (Silva et al., 1999). Multiple studies have been performed in which GH is administered to isolated tissues *in vitro*. Results include: increased RNA synthesis, plasma protein synthesis and IGF-1 release in liver (Griffin and Miller, 1974; Jefferson and Korner, 1967; McConaghey and Sledge, 1970), increased amino acid transport and incorporation in rat heart (Hjalmarson et al., 1969), increased lipolysis and amino acid incorporation in rat adipocytes (Fain et al., 1965; Goodman, 1968), increased DNA synthesis and sulfate incorporation in rabbit and rat chondrocytes (Madsen et al., 1985), increased mitosis in rat lymphocyte, human leukemic lymphoblasts and human erythrogenic precursor cells (Desai et al., 1973; Golde et al., 1977; Whitfield et al., 1971). The effect of GH has been shown to differ depending on cell type. For instance, in mouse pre-adipocyte 3T3F442A cell lines, it has been shown that the signaling molecules JAK-2, STATs 1, 3 & 5, IRS-1, PI-3 kinase, SHC, Grb-2, and kinases involved in the MAP kinase pathway are activated in response to GH treatment (Carter-Su et al., 1996). In the human lymphoma cell line IM-9 STATs 1 & 3, and the MAP kinase pathway are not activated even though these signaling molecules were found to be present in the cells and activated by other substances such as interferon-γ (INFγ) and the phorbol ester TPA (Silva et al., 1996; Silva et al., 1994). In addition, STATs 1 & 3, IRS-1, and SHC are not activated by GH in rat liver and skeletal muscle. Only JAK-2 and STAT-5 were shown to be

activated in these cells following GH treatment (Chow et al., 1996). Although the mechanisms are not clearly understood, it appears that the specific pathway activated in response to GH may depend on the specific cell type.

GH action *in vivo*

GH is so named for its most obvious action, that of longitudinal growth. The absence of GH during puberty results in dwarfism, while an overabundance of GH in subjects with active growth plates leads to gigantism. Metabolic effects of GH other than growth have been established for close to 70 years. In 1934, Lee and Schaffer demonstrated that administration of crude GH extracts from the pituitary of bovine increased protein mass while reducing fat mass in rats (Lee and Schaffer, 1934). GH replacement therapy in hypopituitary dwarf patients began in the late 1950's with the use of GH harvested form human cadaver pituitaries (Beck et al., 1957). The first account of increased linear growth in pituitary dwarf children due to GH replacement therapy was reported by Raben in 1958 (Raben, 1959). Initially non-primate GH was used and found to be inactive in humans (Raben, 1958). Replenishing hGH to physiological levels in GH deficient children enhances nitrogen balance, decreases urea production, reduces carbohydrate utilization and redistributes body fat (Frohman et al., 1967). Continuous administration of GH to produce serum concentrations of 6-10 ug/L in patients with diabetes mellitus causes lipolysis and ketosis. This effect is not observed in normal individuals when administered similar concentrations of GH (Gerich et al., 1976). Continuous administration of GH producing serum

concentrations of 10-50 ug/L in normal individuals results in insulin resistance without changes in blood glucose, lipids, or ketone bodies. Prolonged administration of GH in normal individuals results in fasting hyperglycemia, hyperinsulinemia, and increased fatty acid concentrations (Metcalfe et al., 1981).

Retinoic acid, an important regulator of embryonic development, has been shown to increase expression of GH mRNA in rat embryos (Umesono et al., 1988). The GHR has been detected as early as day 12 in the rat embryos (Garcia-Aragon et al., 1992) and has been shown to respond to retinoic acid in embryonic stem cells (Ohlsson et al., 1993b). Ohlsson and his colleagues demonstrated that in cultured embryonic stem cells treatment with retinoic acid increased GHR mRNA levels over 100 fold. In contrast, Mathews and his colleagues reported that GHR is barely detectable in fetal tissues (Mathews et al., 1989). Nevertheless, the presence of both GH and GHR in embryos and their responsiveness to retinoic acid suggest the GHR might play an important role in embryonic development.

GHR/BP gene disrupted mice

GHR/BP gene disrupted mice were created in our lab in 1997 via homologous recombination (Zhou et al., 1997). Phenotypic differences in weight and body size were noticeable at 3 weeks of age, and continued throughout the lifespan of the mice. These differences were observed most dramatically between homozygous gene-disrupted (-/-) and wild type (+/+) mice. While both male and female (+/-) mice tend to be smaller than their (+/+) littermates, no significant difference has been published

to date. The only reported physiological difference between the GHR/BP +/- and +/+ mice to date is a significant difference in GHR levels as determined by GH binding assays (Zhou et al., 1997). Although the actual levels were not reported (only a statement that the difference was significant), interpretation of the accompanying graph suggests that male +/- mice exhibit ~50% GH binding compared to +/+ males, while female +/- mice exhibit ~75% GH binding compared to +/+ females. A GHR western from the same report also demonstrated a non-quantified decrease in GHR levels for the heterozygous mice as compared to wild type. No other significant physiological differences have been reported for the GHR/BP +/- mice as compared to +/+ littermates. The GHR/BP -/- mice appear to mimic the human genetic disease, Laron Syndrome (humans with a mutation altering GHR function) (Kopchick and Laron, 1999). The most notable similarities include severely depressed serum IGF-I levels, delayed and retarded growth, delayed sexual maturity, and elevated serum GH levels with a complete inability to utilize GH. These mice therefore serve as a valuable animal model for this condition by allowing research to be performed on the mice instead of humans. Moreover, these mice have served as valuable tools for elucidating the physiological effects of GH. Several studies have been performed to study the effects of GH in development, metabolic control, and longevity.

When GHR/BP -/- male mice were mated with +/+ females only a 53% pregnancy rate was observed compared to 88% for control +/+ male matings (Chandrashekar et al., 1999). No significant difference was observed in litter size or in the number of pups born dead. Serum IGF-I levels were undetectable in young adult

male GHR/BP -/- mice, while serum prolactin levels were significantly increased. No significant difference observed in circulating luteinizing hormone (LH) or testosterone levels between GHR/BP -/- and +/+ males. However, an attenuated increase in serum LH levels following treatment with gonadotropin releasing hormone (GnRH), was observed in the GHR/BP -/- mice. Testosterone release was also significantly decreased in testes isolated from GHR/BP -/- mice. A decrease in LH-stimulated testosterone release in testes from the GHR/BP -/- animals is likely due to a decrease in the number of LH receptors, as GH administration has been shown to increase LH receptor number in the testes of hypophysectomized rats (Zipf et al., 1978). Therefore, GH plays a role in testicular function both within the pituitary, by altering the effect of GnRH on LH secretion, and within the testis, by effecting LH-stimulated testosterone release (Chandrashekar et al., 1999).

Female reproduction is also altered in the GHR/BP -/- mice (Danilovich et al., 1999). The time of first vaginal opening in the GHR/BP -/- females is significantly delayed. In addition, pregnant GHR/BP -/- females have significantly increased placental weights, while fetal weights are reduced regardless of fetal genotype possibly due to the low IGF-I and/or insulin levels seen in the GHR/BP -/- animals (Danilovich et al., 1999). Litter sizes and newborn body weights are also significantly reduced in GHR/BP -/- females.

Bone growth and remodeling is altered GHR/BP -/- mice (Sims et al., 2000; Sjögren et al., 2000). Disproportionate bone growth was observed when the lengths of femur, tibia and crown-rump were analyzed in relation to one another. Both

femur/tibia and femur/crown-rump GHR/BP -/- growth ratios expressed as a percentage of +/+ bone growth were significantly different. Femur growth was decreased to a greater extent in the GHR/BP -/- animals than tibia or crown-rump growth. This is suggested to result from the particular developmental stage at which each bone was formed (Sjögren et al., 2000). Femur growth is reported to occur later than tibia growth in mouse skeletal development (Windahl et al., 1999). In addition, GH-dependent growth occurs mainly after birth (Garcia-Aragon et al., 1992; Ohlsson et al., 1993a; Zhou et al., 1997). Therefore, femur growth would be more sensitive to GH action than tibia growth. GH's involvement in bone remodeling is also evident in that bone mineral content is significantly decreased in the GHR/BP -/- mice (Sjögren et al., 2000). In addition, GHR expression has been detected in osteoblasts and chondrocytes further supporting GH importance in bone metabolism (Nilsson et al., 1995; Werther et al., 1990). GH's involvement in bone growth and remodeling from appears to be through GH-stimulated IGF-I production (Sims et al., 2000). GHR/BP -/- mice receiving compensatory IGF-I treatment exhibited near normal bone growth and bone turnover during remodeling as compared to control mice. These data suggest that most of the GH action that influences bone growth and remodeling occurs indirectly .

When organ weights are compared to body weight in GHR/BP -/- mice, the kidney, spleen, heart, and testes are decreased proportionally. Curiously, a significant decrease in liver weight as well as a significant increase in brain weight relative to body weight has been reported (Sjögren et al., 2000). These observations indicate that

GH plays and more important role in liver growth and a less important role in brain growth compared to the other organs. When brain weights are compared without considering the body weight of the animal, no significant difference between GHR/BP -/- and +/+ mice is observed. In addition, mice over-expressing GH have a decreased brain weight relative to body weight (Shea et al., 1987). Therefore, it appears that GH has little effect on brain growth.

GHR/BP -/- mice also exhibit a hypersensitivity to insulin (Coschigano et al., 1999; Dominici et al., 2000). Fasting insulin and fasting blood glucose levels are significantly decreased in the GHR/BP -/- mice. Moreover, glucose tolerance is decreased, while insulin sensitivity is increased in the GHR/BP -/- mice (Coschigano et al., 1999). It has been suggested that the impaired glucose tolerance in the GHR/BP -/- mice is probably not due to reduced sensitivity of the tissue to insulin but rather to an inability of the pancreatic ß–cells to cope with increased glucose loads resulting from the diminished insulin requirement in the GHR/BP -/- mice (Dominici et al., 2000). The increased sensitivity to insulin appears to result from increased insulin receptor (IR) levels as well as an increase in insulin-stimulated IR activation (increased insulin-stimulated tyrosine phosphorylation) in the GHR/BP -/- (Dominici et al., 2000).

Lifespan of the GHR/BP -/- mice is significantly increased compared to +/+ mice as well as +/- mice. Male GHR/BP -/- mice are reported to live an average 975±106 days as compared to +/+ male littermate controls 629±72 days (Coschigano et al., 2000). Female GHR/BP -/- mice averaged 1031±41 days compared to 749±41

days for +/+ female littermate controls. In agreement, GH deficient mice also have longer average lifespans (Bartke et al., 1998; Brown-Borg et al., 1999). Therefore it appears that the lack of GH activity leads to an increased lifespan. Whether the GHR/BP -/- mice actually age slower or live longer due to a prolonged senescence is not known, although the delay in first vaginal opening (Danilovich et al., 1999) and the delay of first conception observed in female GHR/BP -/- mice (Zhou et al., 1997) points to a decreased rate of development. Another theory suggests that a decreased exposure to insulin can play an important role in the extension of life (Parr, 1996; Parr, 1997).

GHR/BP -/- mice are protected from diabetic nephropathy (Bellush et al., 2000). In an experiment performed by our laboratory, pancreatic ß–cells were destroyed with streptozotocin (STZ) treatment to induce diabetes in GHR/BP -/- and +/+ mice. Blood glucose was increased ~4-fold as compared to vehicle-treated control animals. Analysis of kidney weights from the +/+ mice revealed a significant increase in the diabetic mice when compared to non-diabetic mice. In contrast, kidney weights from diabetic and non-diabetic GHR/BP -/- mice, did not change. Furthermore, gomerular volume and the ratio of mesangial area/total glomerular surface area (an indicator of renal hypertrophy) were unchanged in GHR/BP -/- mice, while a significant increase occurred in diabetic +/+ animals. Renal histology showed that only the +/+ diabetic mice exhibited glomerular lesions, while the GHR/BP -/- glomeruli were similar in histology to the non-diabetic mice. The presence of glomerular lesions and increase in mesangial area indicated that glomerulosclerosis

occurred in the +/+ mice when diabetes was induced with STZ, while kidneys from the GHR/BP -/- mice were protected from STZ-induced diabetic damage. These results suggest that GH plays a crucial role in the progression of glomerulosclerosis.

HYPOTHESIS AND GOALS

The general goal of this project is to create GH resistance in cultured cells and in transgenic mice using a ribozyme approach. Hence, the following specific goals outlines below were undertaken in an effort to test the hypothesis that ***the stable integration of DNA encoding a hammerhead ribozyme targeted to the GHR mRNA into cultured cells and mice will cause resistance to GH.***

I. To design and construct a hammerhead ribozyme targeted to the mouse GHR-mRNA with the goals of:
   a. Analyzing the potential target sites from sequence data of mGHR
   b. Designing a ribozyme based on nucleotide sequences flanking the selected target site
   c. Cloning the ribozyme into a mammalian expression vector

II. To test the ribozyme *in vitro* for activity and specificity by:
   a. Creating DNA templates for *in vitro* transcription
   b. *In vitro* transcribing the ribozyme and GHR RNA
   c. Performing ribozyme cleavage assays
   d. Confirming the presence of cleavage products

III. To create a stable cell line that expresses detectable levels of GHR through:
   a. Stable transfection of the GHR/BP 'mini-gene" into mouse L Cells
   b. Verifying stable integration of the DNA
   c. Determining the level of GHR expression in isolated clones
   d. Determining the level of GH stimulated STAT-5 activation in the isolated clones

e. Determining the relationship between receptor number and STAT-5 activation

IV. To test the ribozyme in cultured cells by:

a. Stable transfection of ribozyme DNA into mouse cells expressing GHR

b. Verifying stable integration of the DNA

c. Determining the level of GHR expression in ribozyme transfected clones

d. Determining if a decrease in GHR sufficient to create GH resistance in the form of decreased GH stimulated STAT-5 activation

V. To test the ribozyme in transgenic mice:

a. Establishing transgenic mice via microinjection of ribozyme DNA

b. Verifying stable integration of the DNA

c. Determining the level of GHR expression in transgenic mice

d. Determining if a decrease in weight occurs in the transgenic mice

VI. To cross RZ transgenic mice to GHR +/- mice:

a. Verifying genotype

b. Determining the level of GHR expression in transgenic mice

c. Determining if a decrease in weight occurs in the transgenic mice

MATERIALS AND METHODS

MATERIALS

The plasmids pMTK-bGH-C, pMet-IG-mGHR, pMet-mGHR/BP, pMet-STAT5A-flag, pMSV-Δ29, pCMV-bGH-B, pGB2/B, pGB1/H, and pGB/HR-7/8 were obtained from Dr. John Kopchick (Ohio University, Athens, OH). The plasmid pNTL, containing the LoxP-TK/neo used in the cloning of pBPKO/99, was obtained as a gift from Dr. Allen Bradley (Baylor College of Medicine, Houston, TX). The plasmid pUC19dt, used for all tRNA-tethered ribozyme constructions, was obtained as a gift from Dr. Kazunari Taira (University of Tsukuba, Tsukuba Science City, Japan). Oligonucleotides were purchased from Sigma-Genosys Fisher (The Woodlands, TX). All modifying enzymes, including restriction enzymes were acquired from New England Biolabs (Beverly, MA) or Promega (Madison, WI). Elutip-dTM columns were purchased from Schleicher and Scheull (Keene, NH). Large-scale plasmid preparation kits were purchased from QIAGEN (Valencia, CA). Sequencing reagents including Klenow were purchased in a kit from Amersham (Arlington Hts, IL). ^{32}P for sequencing and *in vitro* transcription reactions was purchased from DuPont NEN Research Products (Boston, MA). *In vitro* transcription was performed using MEGAscript™ and Megashortscript™ kits purchased from Ambion (Austin, TX). All gel electrophoresis apparati were purchased from BioRad (Hercules, CA). A LS 6500 liquid scintillation system purchased from Beckman Coulter (Fullerton, CA) was used for all scintillation counting. Ready Safe™ liquid scintillation cocktail and Poly-Q™ vials were also purchased from Beckman Coulter. Mouse L cells were obtained from ATCC (Rockville, MD). LipofectAMINE, DMEM, and other cell culture reagents

and media components were purchased from Life Technologies Gibco BRL (Rockville, MD). C57 black/6 mice were purchased from Jackson Laboratory (Maine, USA). All other chemicals including those used for silver staining were purchased from Fischer Scientific (Pittsburgh, PA) or Sigma Chemical (St. Louis, MO).

METHODS

Selection of the ribozyme target site

The full-length cDNA sequence of the mouse GHR (see figures 7 & 8) was used to identify GTC triplet sequences as potential targets for ribozyme cleavage (Moffat et al., 1999). From the GTC potential target sequences, twelve base pair helices flanking the cytosine of the GTC target were identified. These helices, representing helix I and III of a hammerhead ribozyme/target RNA interaction, were analyzed using criteria outlined in figures 9 & 10, reported in the literature to be important for ribozyme design. A general rating scheme was created based on the following: The greater the number of adenosines (#As) present in the ribozyme arms the better (Herschlag, 1991). Multiple repeats of a single nucleotide (m-Ns) is discouraged in primer prediction programs such as GeneWorks™. The strong binding associated with high (GC) content favors non-specific association with short stretches of sequence and is discouraged (Herschlag, 1991). Ribozymes have been shown to degrade at a higher rate when UA and CA dinucleotides are present. These sites are specific targets for an unidentified endoribonuclease (Qiu et al., 1998). Using these criteria, the second GTC following the translational start site in exon 2 was selected as the target site for ribozyme cleavage. The classic 22-nucleotide hammerhead ribozyme core sequence was used for the catalytic core of the ribozyme.

Exon1: tgacaacccacgagctgccaagcaggcgcagccatgggaagaggaggcg**GTC**tagggagcggcgg
cactggcagaggcggctgctacagcggcggtggtggcgacggctgttactgaaccccggcagccgcggggatcccgg
gctgg**GTC**cacgcggcctgaggcctcggctccagcagcccccaagcggacacgaacccgcgttct**GTC**tcccga
ggcgaaactccgag

Exon2: GTCtcaggtatggatctttGTCagGTCttcttaaccttggcactggca**GTC**accagcagcacattt
tctggaagtgagg

Exon 3: ctacaccagctactcttggcaaagcttccccagttctgcaaagaatcaatccaagcctggggacaa

Exon 4: gttcttctggaaagcctcgattcaccaagt**GTC**gttcccctgaactggagacattttcatgctactggacaa
aggagataatcctgatttaaagaccccaggatctattcagctgtactatgctaaaag

Exon 4B: ggaaagccaacgacaagctgcaag

Exon 5: aattgctcatgaatggacccaggaatggaaagaatgccctgattat**GTC**tctgctggaaaaaacagctgtt
acttcaactcatcatatacctccatttggataccctactgcatcaagctaactacaaatggtgatttgctggaccaaaaatgtttc
actgttgacgaaatag

Exon 6: tgcaacctgatccacccattggcctcaactggactttactaaacattagtttgaccgggattcgtggagacatc
caagtgagttggcaaccaccacccaatgcagatgttctgaagggatggataattctggagtatgaaattcagtacaaagaag
taaatgaatcaaaatggaaagtg

Exon 7: atgggccctatatggttaacatact**GTC**cagtgtactcattgagaatggataaagaacatgaagtgcgggtg
agatccagacaacggagctttgaaaagtacagcgagttcagcgaa**GTC**ctccgtgtaatatttcctcagacgaacatattg
gaagcatgtgaagaag

Exon 8A: gaaccaa**GTC**caattctcagcacccacatcaagagattgacaaccacctgtatcaccagcttcagagga
tccgccatcctagccttgtgggcacctgcattcatatgcacatacatgcatacgcataattcaaaataataaaa

Exon 8: atatccagtttccatggttcttaattattatctttggaatatttggagtagcagtgatgctatttgtagttatattttcaa
agcagcaaag

Exon 9: gattaagatgctgattttacccccca**GTC**ccagttccaaagattaaagggattgatccagatcttctcaag

Figure 7. cDNA sequence of exons 1 through 9 of mouse GHR. Potential GTC hammerhead ribozyme target sequences are represented in bold print. The translational start codon (atg) in exon 2 is boxed (Moffat et al., 1999).

Exon 10: ggagggaagttggaggaggtgaacaccatcttaggcattcatgataactacaaacccgacttctacaatgat
gattcctgg**GTC**gagttcattgagctagatattgatgaagcagatgtggatgagaagactgaagg**GTC**tgacacagac
agacttctaagcaatgatcatgagaaatcagctggtatccttggagcaaaggatgatgattctgggcgtaccagctgttacga
ccctgacattttggatactgatttccataccagtgacatgtgtgatggtaccttgaagtttgctca**GTC**acagaagttaaatat
ggaagctgatctcttgtgccttgatcagaagaatctgaagaacttgccttatgatgcttcccttggctctctgcatccctccatta
cccagacagtagaagaaaacaagccacagccacttttgagcagcgaaactgaggcaacccaccaactcgcctctacacc
gatgagtaatcccacatcactggcaaacattgacttttatgcccaagtaagcgacattacaccagcaggtggtgat**GTC**ct
ttccccaggccaaaagattaaggcagggatagcccaaggcaatacccagcgggaggtggccacgccctgccaagaaaa
ttacagcatgaacagtgcctacttttgtga**GTC**agatgccaaaaaatgcatcgctgtggccc**GTC**gcatggaagccac
GTCttgtataaaaccaagctttaaccaagaggacatttacatcaccacagaaagccttaccactactgcccagat**GTC**t
gagacagcagatattgctccagatgctgagat**GTC**t**GTC**ccagactacaccacggttcacaccgtgca**GTC**tcca
aggggccttatactcaacgcaactgctttgcctttgcctgacaaaaagaattttccctcctcgtgtggttatgtgagcacagacc
aactgaacaaaatcatgcagtagcctttcctatctttaaatggcaagggaaaggctgggcacaaacgcttaaaccaaaactat
gttttaaatctgtgttgggagagcatgagagtggatatggattctaaaatacttttctggaaat**GTC**aaaatatcaataagtg
gaaaatcaagaattcgtaatcagataaatgctcccattgtgaattataaatattttaatgaatt**GTC**tttaagactgtatagtgg
cagtgatt**GTC**tgtactgtgg**GTC**ttaattttgtgatactaagcattaaatagctacgtttttatgtatgtagatcatgcttttg
gaaaaagcaaaacaatcaggtggcttttgcagttcaggaaattgaatgcagattatagcacaggctgatttttttttctttttaa
ataactgggaactaaaactctaggtgagaaggtaaaactagnttggatatgcaaaacatttatttgacatnaaattgataaag
atatttttaataatttacactttaagcatgagkmctttataatatgctacacacatattgtagttcagaacaatccatctnaggatgt
agcagctacagtgtaaagagggnttcatgttttg**GTC**aatgaacgtaaagaaaaccaaacaagttagatttttacaaagcc
cttttataacttccaaaacttcttaactctaaaaat**GTC**taataacctgcattattagaaaaaaacattttaaatttgtaaacgaat
atttttttaattttgaaaactttatttttttttaatgttgaatcaacgtatcatacaccaaacagtaaacagaaattataataatggaag
aagtgctttcttcgacaaatttccattcaagccacacagctacatgtaagagaagtagaagtgatgtggtgtgattggctagga
tgcagaagagcttcaggaatacaagaagtgagagcccaaggattgggaggaggggctctcacatctccacagtgca**G**
TCt**GTC**aaacccagcttggtttttatagtattctaagaattattgtgtacaaggaaaa**GTC**tcacatgtatgaaatccagt
atccagatggggtaaagttagcagataataggataggaaattaaagacctagatctagnactagtggacttttttcacagaca
gnacacaaatttttaattcagggagaagggacagaataaatgacttcccactcacaaagcacaactcagaagtaattaaaca
ggtaacagaaaccttgccatcaaacctttgataagatgtattttaagtagtaagcagtatttcaatgcttnttacttaccctcccag
gacaaccgatctcaaataagggagataaggtagataaaaatcacttttgattctgtaataacataaacatagttctttgggttag
cacccccccaaaaaaaaatttatgggagaaagaggactctcagctgactgaagaatacatntnatttaaatatttttttagatgc
ctgaaactttaaaattacctttaagttttaatggattaccattttgccaagacctttgtggggaaacaagcttaatgtttagtgatttt
gaaatctctttcatgcaggagagacagtgaaaatctagccttgggtgtttaaggttcgccttgttactttgtaatagattttaataa
gtttttctgctactttgctgctatggtttctccaatggctacatgatttagttcatatgaagtatcatcaacttagaatctattcagctt
aaagatgtgtgttttgatgaactatcttaccatttcaccataggctgaccacgtttctatagccaaaaatagctaaatacctcaat
cagttccagaat**GTC**atttttggtactttgctggccacacaagccgttattcaccgtttaactagttgtgttctgca**GTC**tat
atttaactttctttat**GTC**tgtggatttttcccttcaaagttcaataaa

Figure 8. cDNA sequence of exon 10 of mouse GHR. Potential GTC hammerhead ribozyme target sequences are represented in bold print. The translational stop codon (tag) is boxed (Moffat et al., 1999).

		#As	m-Ns	GC	CA/UA
Exon 2:	atggatctttGTCaggtcttcttaa uaccuagaaaca uccagaagaauu	**11**	**3**	**8**	3
	tctttgtcagGTCttcttaaccttg** agaaacagucca aagaauuggaac	**12**	**3**	**9**	**2**
	ggcactggcaGTCaccagcagcaca ccgugaccguca uggucgucgugu	*2*	**1**	12	**1***
Exon 4:	ttcaccaagtGTCgttcccctgaac aagugguucaca caaggggacuug	**7**	4	12	3
Exon 5:	ccctgattatGTCtctgctggaaaa gggacuaauaca agacgaccuuuu	**8**	4/3	**10**	3
Exon 7:	ttaacatactGTCcagtgtactcat aauuguaugaca gucacaugugua	**8**	**1**	**8**	*5*
	gttcagcgaaGTCctccgtgtaata caagucgauuca gaggcacauuau	6	**1**	**11**	*5*
Exon 8a:	aaggaaccaaGTCcaattctcagca uuccuugguuca guuaagagucgu	**10**	**1**	**10**	**2**
Exon 9:	tttacccccaGTCccagttccaaag aaaugggggguca ggucaagguuuc	6	*5/3*	**7**	**2**

Figure 9. Potential ribozyme target sites from exons 2-9 with corresponding antisense arms that represent helices I and III of ribozyme-GHR mRNA recognition. The numbers to the right of the sequences represent criteria reported to be important for ribozyme design. The greater the number of adenosines (#As) present in the ribozyme arms the better (Herschlag, 1991). Multiple repeats of a single nucleotide (m-Ns) is discouraged in primer prediction programs such as GeneWorks™. The strong binding associated with high (GC) content favors non-specific association with short stretches of sequence and is discouraged (Herschlag, 1991). Ribozymes have been shown to degrade at a higher rate when UA and CA dinucleotides or present. These sites are specific targets for an unidentified endoribonuclease (Qiu et al., 1998). **Target site selected for ribozyme design.
Key: **(bold underlined = optimal; bold = good;** regular text = indifferent; *italic = sub optimal*)

		#As	m-Ns	GCCA/UA	
Exon 10:	tgattcctggGTCgagttcattgag acuaaggaccca cucaaguaacuc	**9**	**1t**	**11**	*4*
	agactgaaggGTCtgacacagacag ucugacuuccca acugugucuguc	*3*	**1t**	12	**1**
	agtttgctcaGTCacagaagttaaa ucaaacgaguca ugucuucaauuu	**7**	**2t**	**8**	3
	aggtggtgatGTCctttccccaggc uccaccacuaca gaaagggguccg	**7**	1q1t	14	*4*
	acttttgtgaGTCagatgccaaaaa ugaaaacacuca ucuacgguuuuu	**7**	*1P1q*	**8**	3
	gctgtggcccGTCgcatggaagcca cgacaccgggca cguaccuucggu	4	**1t**	*16*	3
	tggaagccacGTCttgtataaaacc accuucggugca aacauauuuugg	6	1q	**10**	3
	ctgcccagatGTCtgagacagcaga gacgggucuaca acucugucgucu	4	**1t**	13	**2**
	atgctgagatGTCtgtcccagacta uacgacucuaca acagggucugau	**7**	**1t**	**11**	*4*

Figure 10. The first 9 Potential ribozyme target sites from exons 10 with corresponding antisense arms that represent helices I and III of ribozyme-GHR mRNA recognition. The numbers to the right of the sequences represent criteria reported to be important for ribozyme design. The greater the number of adenosines (#As) present in the ribozyme arms the better (Herschlag, 1991). Multiple repeats of a single nucleotide (m-Ns) is discouraged in primer prediction programs such as GeneWorks™. The strong binding associated with high (GC) content favors non-specific association with short stretches of sequence and is discouraged (Herschlag, 1991). Ribozymes have been shown to degrade at a higher rate when UA and CA dinucleotides or present. These sites are specific targets for an unidentified endoribonuclease (Qiu et al., 1998). Key: **(bold underlined = optimal; bold = good;** regular text = indifferent; *italic = sub optimal*)

GHR-RZ plasmid construction

Plasmid DNA manipulations were performed using standard cloning techniques (Maniatis et al., 1982). The plasmid pMet-IG-mGHR containing the ampicillin resistance gene, a bovine growth hormone poly adenylation signal sequence, and a mouse metallothionine-I transcriptional regulatory element was used as an expression vector for the GHR ribozyme (see figure 11). The plasmid was prepared for ligation by digestion with *Xba*I and *Xbo*I. The fragments were separated for 2 hours at 100 volts by electrophoresis on a 1% agarose gel in TAE buffer (25mM tris-Acitate pH 8.0, 10 mM sodium acetate, 1 mM EDTA). DNA bands were visualized under ultraviolet light in the presence of ethidium bromide and the ~4100 bp band corresponding to the pMet-IG-mGHR expression vector alone (minus the mGHR cDNA) was removed using a scalpel. The fragment was placed into dialysis tubing containing TAE. The DNA was extracted from the agarose by electrophoresis for 1 hour at 80 volts and purified using Elutip-d^{TM} (Schleicher & Schuell Inc., Keene, NH) ion exchange columns equilibrated with a low salt buffer (0.2 M NaCl, 20 mM Tris-HCl pH 7.5, 1 mM EDTA). The column was washed once with 5 ml of the low salt buffer. The DNA was eluted from the column with 500 ul of a high salt buffer (1 M NaCl, 20 mM Tris-HCl pH 7.5, 1 mM EDTA). The DNA was then precipitated with 2 volumes of 100% ethanol at 4°C for one hour. The precipitated DNA was pelleted by centrifugation for 10 minutes at 16,000 x g. The DNA pellet was washed once with ~1 ml of 70% ethanol followed by desiccation in a Speed-vac centrifuge. The DNA was resusended in deionized H_2O. The ribozyme DNA insert for ligation

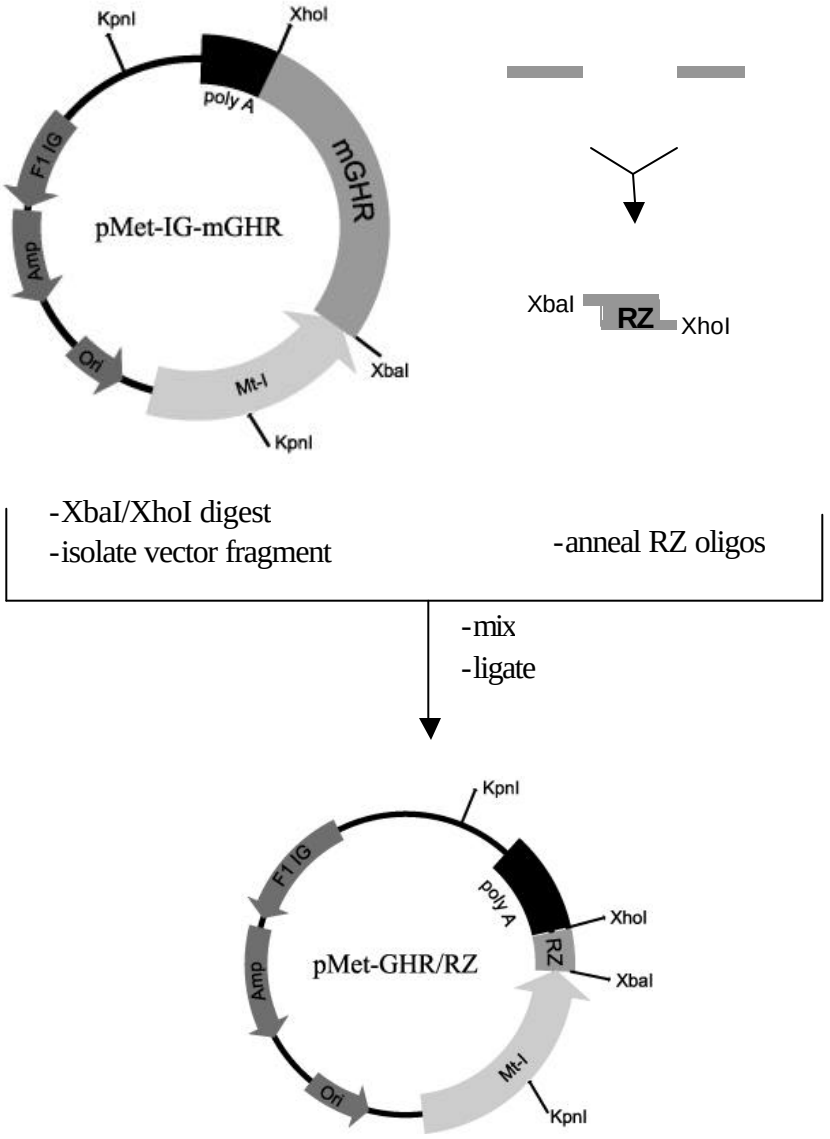

Figure 11. The Construction of pMet-GHR-RZ. The plasmid pMet-IG-mGHR containing the ampicillin resistance gene, a bovine growth hormone poly adenylation signal sequence, and a mouse metallothionine-I transcriptional regulatory element was used as an expression vector for the GHR ribozyme. The plasmid was prepared for ligation by digestion at unique *Xba*I and *Xbo*I sites. Oligonucleotides encoding the sense and antisense sequences of the GHR-RZ were annealed with overlapping *Xba*I and *Xbo*I sites at the 5' and 3' ends, respectively.

was prepared by annealing 10 ug of 52 nucleotide long sense, and 10 ug of 52 nucleotide long antisense oligonucleotides in T4 DNA ligase buffer from Promega (30 mM Tris-HCl pH 7.8, 10 mM $MgCl_2$, 10 mM DTT, 10 mM ATP) in a total volume of 60 ul. The reaction mixture was heated to 98°C and slowly cooled to 25°C over a period of 1 hour (when annealed, the ribozyme oligonucleotide DNAs were designed to have *Xba*I / *Xbo*I overhangs at the 5' and 3' ends, respectively). 1 ul of the ribozyme annealing reaction was removed and added to a ligation reaction containing 100 ng of the ~4100 bp pMet-IG-mGHR expression vector cleaved at the *Xba*I and *Xbo*I. The ligations were performed according to the manufactures instructions (Promega; Madison, WI). To the ribozyme and vector DNAs, 1 ul T4 DNA ligase, 1 ul of T4 DNA ligase buffer and H_2O to a final volume of 10 ul was added. The ligation reaction was incubated 14°C for 16 hours. Following the ligation reaction the reaction was diluted with 32 ul of TE (10 mM Tris-HCl pH 8.0, 1 mM EDTA).

Bacterial transformations

Transformations were performed according to the manufactures instructions (Gibco BRL; Gaithersburg, MD). 1 ul of the diluted ligation reaction mixture was added to 20 ul of *E. coli* DH5α strain pretreated with calcium chloride. The cells were incubated on ice for 30 minutes followed by a brief heat shock at 42°C for 45 seconds. 80 ul of SOC medium (2% Tryptone, 0.5% yeast extract, 10 mM NaCl, 2.5 mM KCl, 10 mM $MgSO_4$) was added to each transformation reaction tube followed by

incubation at 37°C for 1 hour. The cells were then spread on LB agar plates (10 g tryptone, 5 g yeast extract, 10 g NaCl, 15 g Bacto-agar, H_2O to 1 L) containing 50 ug/ml ampicillin and incubated over night at 37°C.

Small-scale plasmid preparations

Following the overnight incubation of plated transformed cells, individual bacterial colonies were transferred to individual tubes containing 5 ml of LB media with 50ug/ml ampicillin and incubated at 37°C overnight. Plasmid DNA was then isolated by the alkaline lysis method as described (Maniatis et al., 1982). 1.5 ml cultures were transferred to 1.5 ml Eppendorf tubes, centrifuged at 16,000 x g for 30 seconds and the resulting supernatant was aspirated and discarded. The pelleted cells were resuspended in 100 ul of lysis buffer (25 mM Tris-HCl pH 8.0, 10 mM EDTA, 50 mM glucose) and incubated for 5 minutes at room temperature. The cells were lysed by the addition of 200 ul 0.2 N NaOH + 1% SDS. Following lysis, the samples were neutralized with 150ul cold KOAc buffer (60 ml 5 M KOAc, 1.5 ml glacial acetic acid, 28.5 ml H_2O, pH 4.8) for 5 minutes on ice. The samples were centrifuged for 5 minutes at 16,000 x g. The supernatant was then transferred to new Eppendorf tubes. An equal volume of a 1:1 mixture of phenol/chloroform was added followed by mixing by brief vortex and centrifugation for 2 minutes at 16,000 x g. The supernatant was then transferred to new Eppendorf tubes in which the DNA was precipitated by the addition of 2 volumes of ethanol, vortexing and centrifugation. The pelleted DNA

was washed with 70% ethanol, dried and resuspended in 50 ul TE containing 20 mg/ml RNase A.

Screening clones / sequencing

Initial screening for plasmids containing the ribozyme insert was performed using the restriction endonuclease *Kpn*I on plasmid DNA isolated from small-scale plasmid preparations. The digested plasmid fragments were resolved on a 0.8% agarose gel at 100 volts for 30 minutes. The sequences of the plasmids containing the ribozymes were confirmed by dideoxy chain termination method according to the manufactures instructions (Amersham; Arlington Hts, IL). 2 ug of each plasmid were denatured in a solution of 0.2 N sodium hydroxide for 5 minutes at 80°C. The solution was neutralized with sodium acetate. The plasmid DNAs were then precipitated with ethanol, washed and dried in a vacuum desiccator. An oligonucleotide primer (designed to begin at the 5' CAP sequence of the metallothionine promoter and direct DNA extension in a 3' direction towards ribozyme sequences) was combined with the denatured DNAs and annealed by heating to 65°C for 2 minutes and then slowly cooling to 30°C. T7 DNA polymerase, all four dNTPs, sequenase buffer, and a-^{32}P labeled dATP were added and the mixture was incubated for 3 minutes at 25°C. Four equal aliquots of the mixture were added to four tubes containing the didioxynucleotides of G, A, T, and C and incubated for 5 minutes at 37°C. The reaction was stopped with the addition of formamide and heated

for 2 minutes at 95°C. The reaction mixtures were separated on a 6% polyacrylamide gel containing 8M urea. The gel was fixed in a solution of 10% methanol and 10% acetic acid, dried, and exposed to film overnight.

Large-scale plasmid preparations

To isolate a large amount of plasmid DNA, bacteria positive for the plasmid containing the ribozyme were added to 100 ml of LB media containing 50 ug/ml ampicillin and incubated at 37°C overnight on an orbital shaker set at 180 rpm. 20 ml of the cell growth were added to 500 ml of LB media containing ampicillin and incubated at 37°C. For all pBR322 based plasmids (pMet-IG-mGHR, pMet-mGHR/BP, pMTK-bGH-c, pGHR-RZ, and pBPRZ) 170 ug/ml chloramphenicol was added to growing cultures to increase plasmid copy number and reduce the amount of chromosomal DNA in the plasmid preparations. Following the growth of overnight bacterial cultures, plasmid DNA was isolated using QIAGEN Plasmid Maxi Kits according to manufacturers instructions (QIAGEN; Valencia, CA). Bacterial cells were pelleted by centrifugation for 15 minutes at 6000 x g at 4°C. After discarding the supernatant the cells were resuspended in 10 ml buffer P1 (50 mM Tris-HCl pH 8.0, 10 mM EDTA; 10 ug/ml RNase A) by vortexing. To lyse the cells, 10 ml of buffer P2 (200 mM NaOH, 1% SDS) was added, mixed by inverting the tubes 5 times and incubated at room temperature for 5 minutes. The mixture was then neutralized with 10 ml of buffer P3 (3.0 M potassium acetate pH 5.5). The lysate was then

transferred to a QIAfilter cartridge (for filtering out cellular debris) where it was incubated at room temperature for 10 minutes. During the incubation, a QIAGEN-tip anion exchange column was equilibrated with 10 ml buffer QBT (750 mM NaCl, 50 mM MOPS pH 7.0, 15% isopropanol, 0.15% Triton X-100). After the 10 minutes incubation, the lysate in the QIAfilter cartridge was filtered into the equilibrated QIAGEN-tip column and allowed to gravity flow though the column. The column was then washed 2 times with 30 ml of buffer QC (1.0 M NaCl, 50 mM MOPS pH 7.0, 15% isopropanol). The plasmid DNA was then eluted from the column with 15 ml of buffer QF (1.25 M NaCl, 50 mM Tris-HCl pH 8.5, 15% isopropanol). The DNA was precipitated by the addition of 0.7 volumes (10.5 ml) isopropanol and centrifugation at 15,000 x g for 30 minutes at 4°C. The DNA pellet was washed with 70% ethanol air-dried and resuspended in TE.

***In vitro* transcription.**

Large-scale synthesis of substrate and ribozyme RNAs were performed using T7-MEGAscript and T7-MEGAshortscript kits, respectively (Ambion; Austin, TX) according to the manufacture's protocol. The template DNAs used for the production of ribozyme transcripts were synthesized by PCR (see figure 12). A 5' primer directed to the CAP sequence of the metallothionine promoter was designed with a 23 base T7 promoter sequence appended at the 5' end. Amplification of the target DNA yielded PCR products, which contain the T7 promoter upstream of the ribozyme sequences. The PCR product was purified by phenol/chloroform extraction, ethanol precipitation,

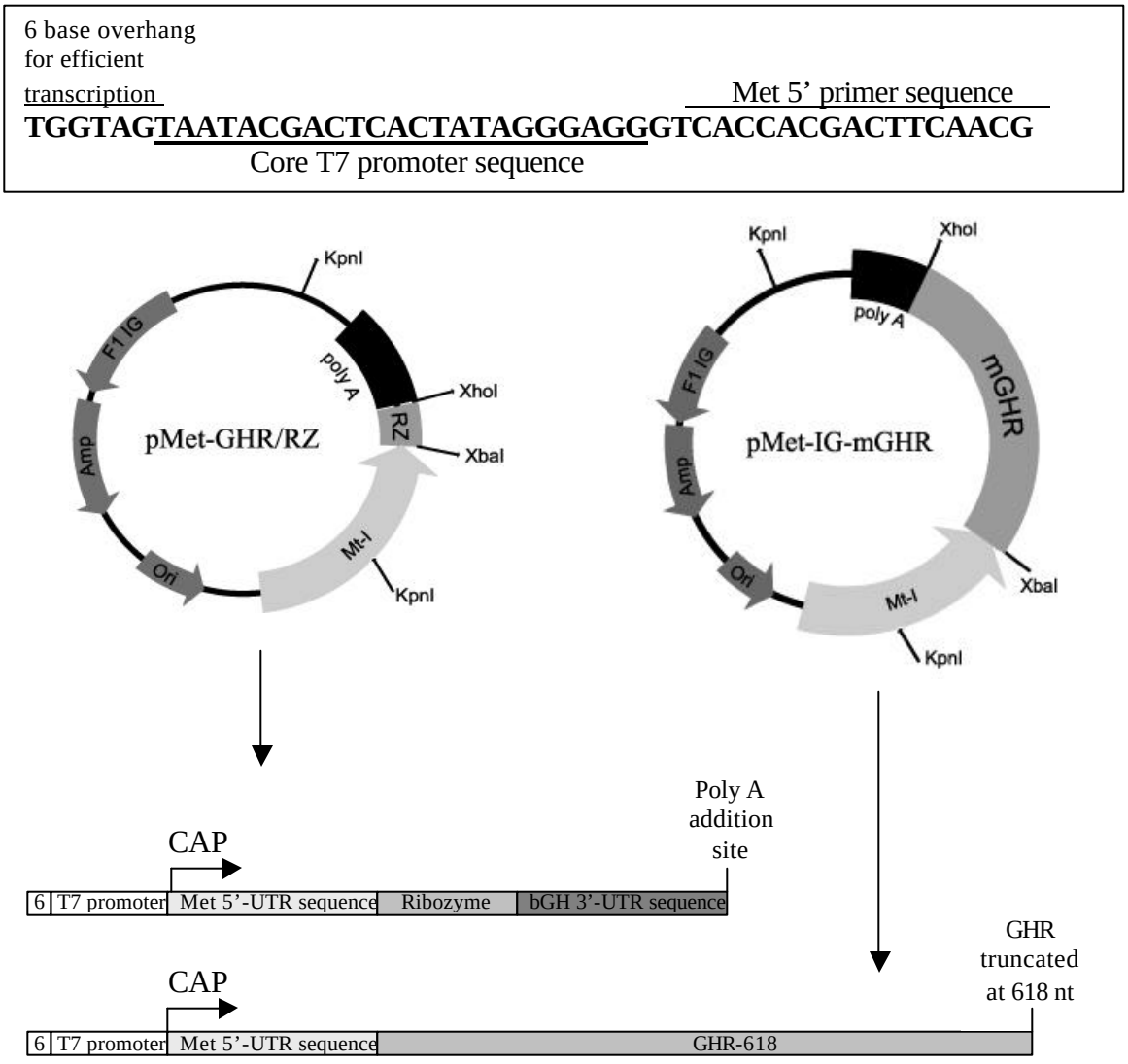

Figure 12. DNA templates for *in vitro* transcription were generated by PCR. A 5' primer (boxed sequence at top) directed to the CAP sequence of the metallothionine promoter was designed with a 23 base T7 promoter sequence appended at the 5' ends. Amplification of the target DNA yielded PCR products that contained the T7 promoter upstream of the ribozyme sequences (bottom). This allowed for the production of a PCR product that, when transcribed *in vitro* by T7 DNA polymerase run off transcription, would produce RNA similar in size to the predicted RZ-mRNA transcribed *in vivo* (with the exception of mRNA processing events).

ethanol wash, vacuum desiccation, and resuspended in RNase free water supplied by the T7-MEGAscript kit. In vitro transcription was performed according to T7-MEGAscript kit manufacture's instructions (see figure 13) 5 ul of a 200 ng/ul purified solution of DNA containing the T7 core promoter sequence were added to the following mixture: 2 ul 10 x transcription buffer, 2 ul ATP solution (75 mM), 2 ul CTP solution (75 mM), 2 ul GTP solution (75 mM), 2 ul UTP solution (75 mM), 2 ul T7 MEGAshortscript enzyme mix, and 2 ul RNase-free deionized water for a final volume of 20 ul. For RNA used in single turnover reactions for determining kinetic constants, 1 ul ^{32}P-labeled UTP (10 mM) was added to the reaction (DuPont NEN Research Products, Boston, MA). The contents were mixed by gentle vortexing followed by a brief microcentrifuge spin to collect all the reaction mixture at the bottom of the tube. The reaction was incubated for 4 hours at 37°C. Incubation was stopped by the addition of 10 ul of RNase-free deionized water and 30 ul of lithium chloride precipitation solution. The RNA was then mixed thoroughly, chilled for 30 minutes at -20°C, and centrifuged for 15 minutes at maximum speed. The supernatant solution was carefully removed by aspiration with a small glass pipette. The RNA was then washed with 70% ethanol and the supernatant once again removed with a glass pipette. The RNA was then dried with vacuum desiccation.

Ribozyme Cleavage Assays

The concentrations of ribozyme and substrate RNA's were determined by spectophotometry and the molarities calculated. 1.5 ml RNase-free microfuge tubes

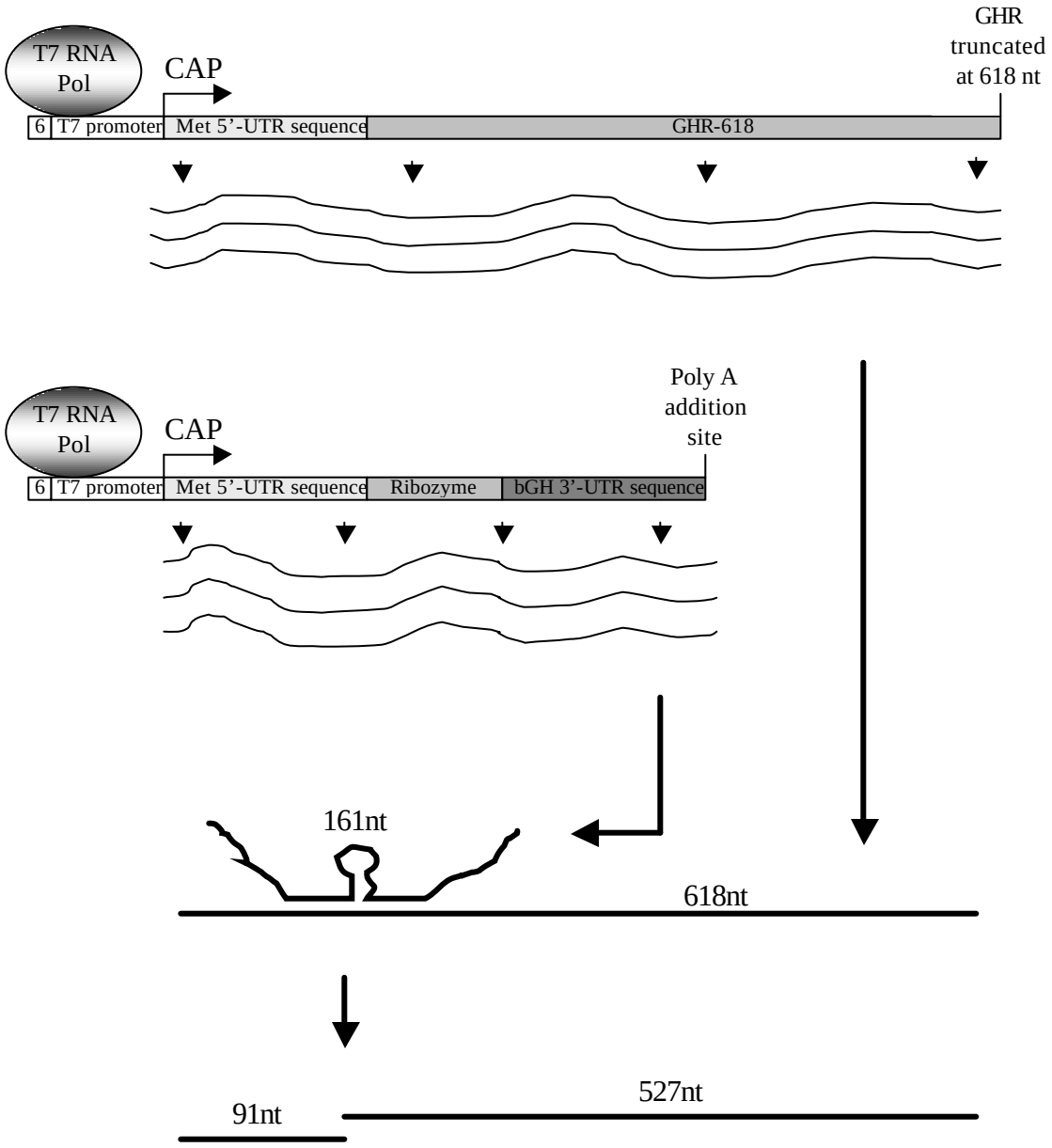

Figure 13. ***In vitro*** **transcription using PCR generated DNA templates.** T7 RNA polymerase *in vitro* transcription reactions performed using PCR generated DNA templastes containing T7 core promoters designed into the 5'-primers. The RNAs were quantified and combined to verify cleavage activity of the GHR-RZ. The RZ was predicted to anneal to a target site 91 nts into the truncated GHR-substrate RNA (618 nt). Following cleavage catalyzed by the RZ, a 91 nt 5' cleavage product and a 527 nt 3' cleavage product were predicted.

were placed on ice and the ribozyme and substrate RNA's were added to a "standard" reaction mixture of 50 mM Tris-Cl pH 7.5, 50 mM NaCl, and 10 mM $MgCl_2$. The "standard" reaction mixture was based on conditions most commonly used in reported ribozyme cleavage assays (RCAs). These conditions were confirmed by performing RCAs in which each of parameters were altered individually. Multiple turnover reactions were incubated at 37°C for various amounts of time by removing 20 ul aliquots at specific time intervals. Varying concentrations of substrate RNA's were incubated with a fixed ribozyme concentration to determine the cleavage activity of individual ribozymes *in vitro*. Single turnover reactions were incubation at 59°C for 15 minutes. All reactions were stopped by the addition of stop solution that contained 95% formamide, 20 mM EDTA, 0.05% bromophenol blue and 0.05% cyanocyanol and placed on dry ice. The reactions were heated for 2 minutes at 95°C and ice quenched to discourage RNA/RNA intermolecular binding prior to resolving via gel electrophoresis. RNA's from the individual reactions were resolved on 6% polyacrylamide gels in 8 M urea.

Silver Staining, Image Analysis and Scintillation Counting

Polyacrylamide gels containing the resolved RNA from the ribozyme cleavage reactions were silver stained according to Palfner *et al* (Palfner et al., 1995). Gels were incubated in a 1% solution of HNO^3 for 15 minutes followed by a 15-minute incubation in a solution of 0.2% silver nitrate. The gels were rinsed with deionized

H_2O and placed in a developing solution (30 g/L Na_2CO_3, 0.5 ml/L 37% formaldehyde, 2 mg/L sodium thiosulfate) until RNA bands were visible (approximately 20 minutes). The gels were fixed with 10% acetic acid for 10 minutes and dried between a piece of 3M filter paper and a clear cellophane sheet for 1 hour on a heated gel dryer. Image analysis was performed on the dried gels using the BIO RAD Gel Doc 1000 system and molecular analyst software (BIO RAD, Hercules, CA, USA). Following image analysis, the silver stained RNA bands were excised from the gel and placed into Poly-Q™ vials with Ready Safe™ liquid scintillation cocktail (Beckman, Arlington Hts, IL). An LS 6500 liquid scintillation system (Beckman) was used for scintillation counting.

Generating stable mouse L cells expressing mouse GHR

Mouse L cells (subcutaneous connective fibroblasts) negative for both thymidine kinase (TK) and adenine phoshoribosyltransferase (APRT) were stably transfected using the Ca_2PO_4 method previously described (Wigler 1977, Wold 1979, Pellicer 1980, Roberts 1982, Kelder 1994). Approximately $1x10^6$ cells in culture medium (DMEM containing 10% serum and 50 ug/ml gentamicin sulfate) were passed to 100 mm culture dishes and incubated for 18 hours at 37°C. 3 ug of pMet-GHR/BP (see figure 14), 30 ng of pDλAT3, 15 ug of L cell DNA and 60 ul 2 M $CaCl_2$ was mixed in deionized H_2O to a volume of 500 ul. The DNA mixture was then added to an equal volume (500 ul) of 2x HEPES buffered saline (21 mM n-2-hydroxyethylpiperazine-n'-2-ethanesulfonic acid (HEPES), 137 mM NaCl, 5 mM

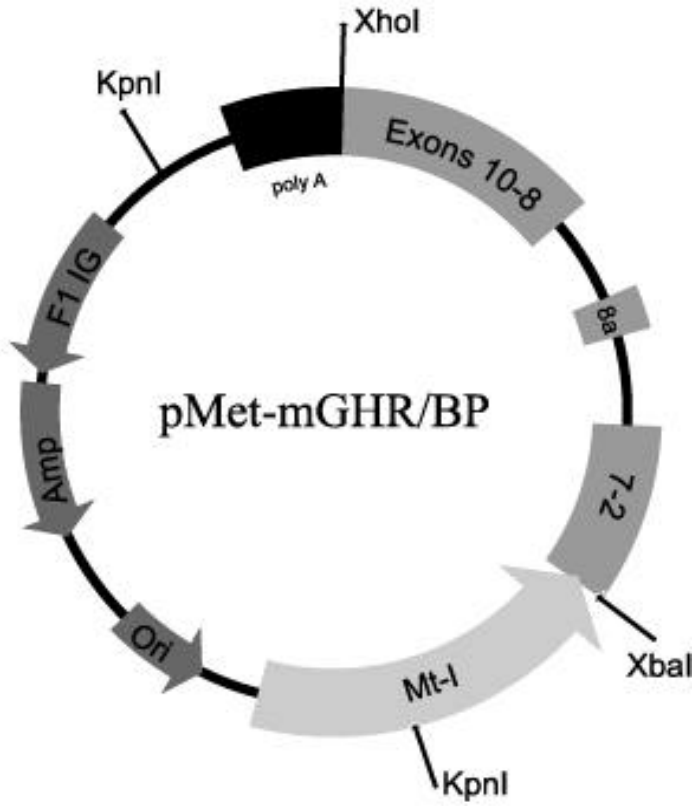

Figure 14. The mouse GHR/BP expression vector pMet-mGHR/BP was used to create stable mouse L cells that express both GHR and GHBP. The plasmid contained the ampicillin resistance gene, a bovine growth hormone poly adenylation signal sequence, and a mouse metallothionine-I transcriptional regulatory element. The GHR"mini-gene" contained mGHR cDNA plus genomic sequence from the 3' end of exon 7 to the 5' end of exon 8. The inclusion of intervening sequences flanking exon 8a allowed for expression of both the GHR and GHBP alternatively spliced gene products.

KCl, 0.7 mM Na_2PO_4, 6 mM glucose) containing 10 ul 70 mM phosphate pH 6.9 and incubated for 15 minutes at room temperature. The combined mixture was added to the L cells and incubated at 37°C for 5 hours. Following the incubation, the transfection media was removed and the cells were incubated with 10 ml HEPES buffered saline containing 5% dimethyl sulfoxide for 90 seconds. The cells were then washed twice with DMEM followed by the addition of 10 ml culture medium (DMEM containing 10% serum and 50 ug/ml gentamicin sulfate). 24 hours after the transfection, the cells were passed to 150 cm^2 flasks and APRT+ cells were selected in culture medium containing 4 ug/ml azaserine and 15 ug/ml adenine. Once the surviving cells had expanded to approximately 70 % confluence in the 150 cm^2 flasks, TK+ cells were selected using HAT media (culture media containing 15 ug/ml hypoxanthine, 1 ug/ml aminopterin and 5.15 ug/ml thymidine). HAT media was also used for maintaining the cells following selection at 37°C in a humidified atmosphere of 5% CO_2. From the surviving pools of cells, individual clones were isolated by passing cells into 96-well plates at a concentration of 0.5 cells/well. Wells containing single cells were identified under a dissecting microscope. Following expansion of the individual clones, colonies were transferred to individual 25 cm^2 flasks by stirring the bottom of the wells with a pipette tip and removing the medium. HAT medium was added back to the wells of the 96-well plate to allow the cells left over from pipetting to expand for PCR analysis.

PCR on GHR/BP transfected cells

PCR was performed on 15 stable cell lines to verify the presence of the transfected GHR/BP DNA. Medium was removed from cell colonies growing in 96-well plates. 190 ul of PCR lysis buffer (10 mM Tris-HCl pH 8.0, 50 mM KCl, 0.45% NP-40, 0.45% Tween-20) with 10 ul of a 20 mg/ml stock solution of Proteinase K (20 mg/ml Proteinase K, 40% glycerol, suspended in PCR lysis buffer) was added back to each well containing the desired cell colonies. The plates were then incubated over night at 55°C. The resulting cell lysates were then transferred from individual wells to 1.5 ml Eppendorf tubes. 4 ul of cell lysate was added to 26 ul of a PCR "master mix" cocktail containing (3 ul 10 x PCR reaction buffer (500 mM KCl, 100 mM Tris-HCl pH 9.0, 1% Triton X-100), 1.8 ul 25 mM $MgCl_2$, 2.4 ul of an equal mixture of all 4 dNTPs each at 2.5 mM in the mixture, 0.375 ul 20 uM of the 5' primer **GTCACCACGACTTCAACGTCC** (directed to the transcriptional start site in the mouse metallothionein-I transcriptional regulatory element), 0.375 ul 20 uM of the 3' primer **CTACAAATAGCATGACTGCTAGTCC** (618 bases 3'of the mouse GHR cDNA translational start site), 17.65 ul H20, 0.15 ul 5 u/ul Taq DNA polymerase) per sample. The reactions were heated 2 minutes at 94°C, cycled 30 times from 94°C for 20 seconds to 58°C for 20 seconds to 72°C for 20 seconds, and held at 4°C until removal from the thermocycler. 10 ul of the each PCR reaction was loaded onto a 0.8% agarose gel and resolved for 30 minutes at 100 volts.

Screening cells for functional GHR expression

The stably transfected GHR/BP DNA positive L cells as well as double transfected GHR-RZ cells were screened for GHR expression using GHR binding assays as described by Emtner et al 1990. In 6-well tissue culture plates monolayers of the stable cells were propagated to 100% confluence (~$1x10^6$ cells/well). The cells were depleted in serum free DMEM medium for 2 hours at 37°C. Cells were then washed 3 times in 1x PBS containing 0.1% bovine serum albumin (BSA). 160,000 cpm of ^{125}I-hGH at a concentration 1 nM in 2 ml of 1x PBS with 0.1% BSA was added to each well with or without 100 nM non-radioactive bGH. The cells were incubated for 2 hours at room temperature on a slow orbital shaker. Following incubation, the cells were washed twice with 1x PBS + 0.1% BSA. The addition of 1 ml of 0.1 N NaOH + 1% SDS to each well, followed by 5 minutes of fast shaking on a orbital shaker was performed to lyse the cells. Cell lysates were then transferred to vials containing 10 ml Ready Safe^{TM} liquid scintillation cocktail (Beckman Coulter) and the number of counts was measured using a LS 6500 liquid scintillation system purchased from (Fullerton, CA). The evaluation of relative GHR expression for each stable cell line was based on the mean value of at least two experiments. Each experiment was carried out in triplicate. The sixth GHR/BP cell line, which had a medium level of GHR expression (as compared to all 15 cell lines screened by GHR binding assays), was selected for subsequent study and referred to as “E6” cells.

Stable transfection of E6 cells with a GHR-RZ

E6 cells, which express GHR (Mouse L cells stably transfected with GHR/BP DNA), were used for GHR-RZ transfections. GHR-RZ transfections were performed according to the general procedure for stable transfection of adherent cells with LipofectAMINE^{TM} outlined by the manufacturer's protocol (Gibco BRL). E6 cells were maintained in HAT medium at 37°C in a humidified atmosphere of 5% CO_2. Cells were cultured in a 150cm^2 flask to a confluence of approximately 50% (~3X10^{7}cells). 1 ml of solution A (20 ug pMet-GHR-RZ, 200 ng pRSV-neo, DMEM to a total volume of 1 ml) and 1 ml of solution B (600 ul LipofectAMINE^{TM}, DMEM to a total volume of 1 ml) were prepared in polystyrene tubes. The two solutions were mixed gently and incubated for 30 minutes at room temperature. The cells were washed 1x with DMEM. 10 ml HT media without serum (DMEM with only 15 ug/ml hypoxanthine, and 5.15 ug/ml thymidine added) was added to each flask. Following the 30-minute incubation, the A/B mixture, was gently added to the flask. 5 hours after the start of the transfection, 10 ml of HT media with 20 % serum was added to the flask and incubated for 19 hours. Following the 19-hour incubation, the transfection medium was removed and fresh HAT medium was added back to the cells. 72 hours after the start of the transfection, the cells were cultured in neomycin selection medium (HAT medium with 0.5675 mg/ml Geneticin, a neomycin analog purchased from Gibco BRL). Following one week of selection in the HAT medium with 0.5675 mg/ml Geneticin, the surviving cells were maintained in HAT medium with 0.28375 mg/ml Geneticin. From the surviving pools of cells, individual clones

were isolated by passing cells into 96-well plates at a concentration of 0.5 cells/well. Wells containing single cells were identified under a dissecting microscope. Following expansion of the individual clones, colonies were transferred to individual 25 cm^2 flasks by stirring the bottom of the wells with a pipette tip and pipetting off the medium. HAT medium was added back to the wells of the 96-well plate to allow the cells left over from pipetting to expand for PCR analysis.

PCR screening of GHR-RZ transfected E6 cells

PCR was performed on 10 stable cell lines to verify the presence of the transfected GHR-RZ DNA. The method of screening was similar to method described earlier for PCR screening of GHR/BP transfected cells with the following exception: While the same 5' primer **GTCACCACGACTTCAACGTCC** (directed to the transcriptional start site in the mouse metallothionein-I transcriptional regulatory element) was used, a different 3' primer was used for detecting the RZ "mini-gene". The 3' primer, **CTACAAATAGCATGACTGCTAGTCC** (directed to the poly adenylation signal sequence located in the bovine GH exon-4, 3' of the RZ sequence) was used in the reactions.

Preparation of RNA from cultured cells

RNAs from cultured cells were prepared based on procedures outlined in current protocols in molecular biology for the preparation of cytoplasmic RNA by from tissue culture cells (Gilman, 1997). Cells were grown to confluence in 75 cm^2

flasks (~$6x10^7$ cells). Medium was removed from the flasks and cells were washed 3 times with ice chilled 1x PBS. 10 ml of ice chilled 1x PBS was added to each flask. The cells were then scraped from the bottom of the flasks and transferred to 15 ml conical tubes pre-chilled on ice. The tubes were centrifuged at 300 x g for 5 minutes and media discarded. The cells were lysed by mixing with 375 ul of lysis buffer B (50 mM Tris-HCl, pH 8.0, 100 mM NaCl, 5 mM $MgCl_2$, 0.5% NP-40) and incubating for 5 minutes on ice. The lysates were then centrifuged for 2 minutes at 15,000xg at 4°C. The supernatant was removed to new tubes containing 4 ul of 20% SDS. The samples were mixed by vortexing. The samples were then incubated in 2.5 ul of 20 mg/ml proteinase K for 15 minutes at 37°C. 400 ul of 1:1 phenol/chloroform was added to the samples, mixed by vortexing, and centrifuged for 10 minutes at 15,000 xg. The aqueous layers were removed to new tubes where a second phenol/chloroform extraction was performed. Aqueous layers from the second extraction were removed to new tubes. 40 ul of 3 M NaOAc pH 5.2 and 1 ml of 100% ethanol was added to each sample, mixed by inverting ~10 times, and incubated over night at -20°C. The following day the samples were centrifuged 15,000 xg for 15 minutes at 4°C. The pelleted RNAs were rinsed with 1 ml 75% ethanol/25% 0.1 M NaOAc and dried in a speed-vac vacuum desiccator.

Removal of DNA from RNA samples

RNA samples were treated with RNase free DNase I to remove any contaminating DNA according to procedures outlined in current protocols in molecular biology (Gilman, 1997). RNA samples were resuspended in 50 ul TE. 50 ul of a DNase I cocktail (10 ul 100 mM MgCl2/10 mM DTT, 0.2 ul of 2.5 mg/ml RNase-free DNase I, 0.1 ul of 50 U/ul placental ribonuclease inhibitor, 39.7 ul TE) was added to each sample and incubated for 15 minutes at 37°C. The DNase digestion was stopped by the addition of 25 ul DNase stop mix (50 mM EDTA, 1.5 M NaOAc, 1% SDS). 125 ul of 1:1 phenol/chloroform was added to the samples, mixed by vortexing, and centrifuged for 10 minutes at 15,000 xg. The aqueous layers were removed to new tubes where a chloroform extraction was performed. Supernatant from the second extraction was removed to new tubes. 325 ul of 100% ethanol was added to each sample, mixed by inverting vortexing, and incubated over night at -20°C. The following day the samples were centrifuged 15,000xg for 15 minutes at 4°C. The pelleted RNAs were rinsed with 1 ml 75% ethanol/25% 0.1 M NaOAc and dried in a speed-vac vacuum desiccator.

Northern blot analysis

Northern analyses were preformed based on procedures outlined in current protocols in molecular biology (Gilman, 1997). Gel electrophoresis equipment and the Pyrex transfer dish were soaked in 0.1 M NaOH for 1 hour and rinsed with

distilled water prior to use. In RNase free microcentrifuge tubes 10 ug of RNA was prepared in a denaturing cocktail (25 ul deionized formamide, 9 ul 37% (w/v) formaldehyde, 5 ul 5x MOPS pH 7.0, deionized H_20 to a final volume of 50 ul). The samples were gently mixed and incubated for 15 minutes at 55°C. Following the incubation, the samples were placed on ice and 10 ul of formaldehyde loading buffer (1 mM EDTA, pH 8.0, 0.25% (w/v) bromophenol blue, 0.25% (w/v) xylene cyanol, 50% glycerol) was added. The samples were then loaded into wells of a 1% agarose gel and resolved for 1 hour at 100 volts. The gel was stained in an RNase free glass dish with 0.5 M ammonium acetate and 0.5 ug/ml ethidium bromide for ~30 minutes and photographed next to a ruler using a ultraviolet transilluminator. A GeneScreen-Plus nylon hybridization transfer membrane was cut to size and pre-soaked in deionized H_20 for 15 minutes. The gel was placed in a dish and washed 2 times ~15 minutes with deionized H_20 for to remove formamide. The gel was then incubated for 30 minutes in 0.05 M NaOH/1.5 M NaCl followed by an incubation in 0.5 M Tris-HCl pH 7.4/1.5 M NaCl for 20 minutes. A final incubation in 20x SSC for 45 minutes was performed prior to the transfer.

Transfer was set up using these materials sandwiched from bottom to top in an RNase free glass dish filled ~1 cm deep with 20x SSC: upside-down gel tray, 3 strips of Whatman 3 MM paper cut to overhang on two ends, gel containing the RNA, nylon hybridization transfer membrane cut to the same size as the gel, 5 sheets of Whatman 3 MM paper cut to the same size as the gel, a ~1 inch stack of paper towels cut to the same size as the gel, and a glass plate on top. The RNA was transferred overnight.

The membrane was removed, rinsed with 2x SSC and placed (still wet) under a ultraviolet closslinking light source for 1 minute.

The membrane was incubated in a rotating hybridization oven at 42°C for 2 hour in 20 ml hybridization solution (5x SSPE, 50% deionized formamide, 5x Denhardt's solution, 4 ml 5 M NaCl, 10% dextran sulfate, 1% SDS). A ^{32}P labeled probe directed to the extracellular domain of the GHR/BP (exons 2-7) was prepared using a random primed DNA labeling kit purchased from Roche Diagnostics (Mannheim, Germany). After the initial 2 hour pre-hybridization incubation, 20 ul of probe (~0.01ug at $\geq 1x10^9$ cpm/ug) was boiled with 200 ul of salmon sperm DNA (10 mg/ml) for 10 minutes and added to the hybridization solution. The membrane was then incubated with hybridization solution containing the ribozyme probe over night at 42°C. The following day the hybridization solution was removed and the membrane was washed 2 times for 15 minutes each in 2x SSPE at room temperature followed by two 30 minute washes in 2x SSPE + 2% SDS at 65°C. A final wash in 0.1x SSPE for 15 minutes was performed at room temperature. The membrane was air-dried on 3MM filter paper for approximately 5 minutes to remove excess liquid and placed in an autoradiograph cassette with film.

Isolation of DNA for slot blot analysis

DNA slot blot analysis was performed on cells stably transfected with GHR/BP DNA and cells stably transfected with GHR-RZ. In addition, all transgenic

mouse lines were verified by DNA slot blot analysis. For mice, approximately 1 cm (~200-400 mg of tissue) was removed from the tip of the tail using sterile scissors. For cultured cells, approximately $1x10^7$ cells were harvested from 25 cm^2 flasks. The tissue was placed into 1.5 ml Eppendorf tubes with 500 ul SSTE (100 mM NaCl, 1% SDS, 50 mM Tris-HCl pH 8.0, 15 mM EDTA pH 8.0) containing 400 ug proteinase K and incubated over night at 55°C. The following day, 20 ul of 10 mg/ml RNase A was added to each tube and incubated at 37°C for 1 hour. 500 ul of a 1:1 mixture of phenol/chloroform was then added, mixed by rotating at room temperature for 5 minutes, and centrifuged at 16,000xg for 10 minutes. The upper aqueous phase was then transferred to new tubes. 20 ul of 5 M NaCl followed by 500 ul of 4°C isopropanol were added. The samples were mixed by vortexing approximately 5 seconds and centrifuged at 16,000xg for 10 minutes. The liquid was then removed from the tubes and the DNA pellets were washed with 70% ethanol and dried in a speed-vac. The DNA was resuspended in 500 ul deionized H_20. The concentration of each sample was determined by spectrophotometry.

DNA slot blot analysis

For each sample, 10 ug of DNA was suspended in a volume of 180 ul. 20 ul of 3 M NaOH was added and the samples were incubated at 65°C for 1 hour to denature the DNA. The samples were then neutralized by the addition of 200 ul 2 M NH_4OAc, mixed by vortexing, and placed on ice. The samples were then loaded into

wells of a manifold II slot-blot system purchased from Schleicher & Schuell (Keene, NH). A vacuum was applied to the apparatus drawing the samples onto a GeneScreen-Plus nylon hybridization transfer membrane (NEN life sciences products; Boston MA) pre-soaked in 10x SSC (87.65 g NaCl, 44.1 g sodium citrate, H_20 to 1 L pH 7.0). 5 minutes after all the samples had passed through the wells the membrane containing the DNA samples was removed from the apparatus and air-dried over night. The membrane was incubated in a rotating hybridization oven at 42°C for 1 hour in 20 ml hybridization solution (10 ml deionized formamide, 4 ml 5 M NaCl, 4 ml 50% dextran sulfate, 2 ml 10% SDS). A ^{32}P labeled probe directed to the 5' untranslated portion of the metallothionein-I transcriptional regulatory element was prepared using a random primed DNA labeling kit purchased from Roche Diagnostics (Mannheim, Germany). After the initial 1 hour pre-hybridization incubation, 20 ul of probe (~0.01ug at $\geq 1x10^9$ cpm/ug) was boiled with 500 ul of salmon sperm DNA (10 mg/ml) for 10 minutes and added to the hybridization solution. The membrane was then incubated with hybridization solution containing the metallothionein-I probe over night at 42°C. The following day the hybridization solution was removed and the membrane was washed for 5 minutes in 2x SSC at 56°C followed by a 30 minute wash in 2x SSC + 0.1% SDS at 56°C. The membrane was air-dried for approximately 15 minutes and placed in a autoradiograph cassette with film.

Preparing cell lysates from cell culture for western blot analysis

Cells were cultured in 75 cm^2 flasks to a confluence near 100%. Medium was removed from the flasks and 10 ml of ice-chilled 1x PBS was added. The cells were then scraped from the bottom of the flasks and transferred to 15 ml conical tubes pre-chilled on ice. The tubes were centrifuged at 1000 x g for 3 minutes and media discarded. The cells were resuspended in 1 ml of UBI lysis buffer (20 mM Tris-HCl pH 7.4, 10 mM EDTA, 100 mM NaCl, 1% NP-40, 10 ug/ml PMSF, 1 ug/ml Aprotinin, 1 ug/ml leupeptin, 1 mM Na-Vanadate). DNA in the cell lysates was sheered by passing the lysates through a 22 gauge needle ~10 times. The lysates were then transferred to pre-chilled 1.5 ml Eppendorf tubes and incubated on ice for 20 minutes. The lysates were then centrifuged at 16,000x g for 20 min at 4°C. The supernatant was removed and stored in 50 ul aliquots at -80°C.

Determining cell lysate protein concentrations (Bradford assay)

Protein concentrations of the cell lysates were determined by using Bradford assays as previously described (Bradford, 1976). 5 ul of cell lysate were diluted with 795 ul of H_2O in semi-micro 1.5 ml disposable polystyrene cuvettes (Bio-Rad; Hercules, CA). Bovine serum albumin (BSA) standards were prepared with set concentrations as controls. 200 ul of protein assay dye reagent purchased from Bio-Rad was added to the diluted samples and mixed by inverting the cuvettes 10 times. The samples were incubated at room temperature for 10 minutes. Following

incubation, the optical density was measured at a wavelength of 595 nm and the concentrations were determined based on comparisons to the BSA standards.

SDS-PAGE for western analysis

Samples were diluted to equal protein concentrations with H_2O and 3x SDS-PAGE sample buffer (0.15M Tris base pH 7.4, 10% SDS, β-mercaptoethanol, 20 mg bromophenol blue) and heated in a boiling water bath for 5 minutes. Protein II systems purchased from Bio-Rad were used for casting polyacrylamide gels, resolving protein, and transferring protein from the polyacrylamide gels to nitrocellulose membranes. 500 ug of total protein / sample was loaded into wells on a 7.5% SDS-PAGE gel. The proteins were resolved for 2 hours at a constant 150 volts. The polyacrylamide gel was removed from the resolving apparatus and placed in transfer buffer for 10 minutes (25 mM Tris base, 192 mM glycine, 20% methanol, 0.1% SDS, 0.5 mM sodium orthovanadate). A Hybond ECL nitrocellulose membrane (Amersham Pharmacia Biotech; Buckinghamshire, England) was cut to size, placed in H_2O for 5 minutes, and then placed in transfer buffer for 5 minutes. The polyacrylamide gel and nitrocellulose membrane were then placed together and proteins were transferred from the gel to the membrane at 70 volts for 1 hour. Following the transfer, the membrane was then placed directly into an appropriate blocking solution.

Coomassie staining

Following electrophoresis of proteins, some gels were stained using Coomassie Brilliant Blue instead of being transferred to nitrocellulose membranes. The gel was placed in Coomassie Brilliant Blue Stain (0.25G Coomassie Brilliant Blue, 90 ml 1:1 v/v Methanol:water, 10 ml of glacial acetic acid). Gels were stained overnight at room temperature with slight agitation. The following day, the gel was then placed in de-staining solution (1:1 v/v Methanol:water and 10% acetic acid) and incubated at room temperature with slight agitation. The de-staining solution was replaced with fresh solution periodically, until no stain was visible in the portions of gel containing no resolved proteins. Images of the de-stained gel were then scanned in using a Duoscan T1200 transparency scanner purchased from AGFA (Mortsel, Belgium).

Immunoblotting with GHR antiserum

Immunoblots were performed using a modified protocol based on methods previously described (Cataldo, 2001). Initially attempts using the original protocol did not allow sufficient separation of the GHR specific band from non-specific bands. Tissues collected from GHR -/- mice were used to verify the identity of the GHR specific band. Therefore, the following protocol was created as the result of ~20 GHR western blots altering individual steps.

Immediately following gel transfer, the nitrocellulose membrane was incubated in a 6% milk blocking solution (6% non-fat powdered milk, 1x TBS pH 7.6, 0.05 % tween-20) for 1 hour at room temperature with constant agitation. The membrane was

then incubated in 6% milk blocking solution containing GHR antiserum diluted 1:5,000 overnight at 4^{o}C with constant agitation. The GHR antibody (clone #181, a monoclonal antibody produced in rabbit and is directed to the intracellular domain of the mouse GHR) was obtained as a gift from Dr. Frank Talamantes (Professor of Biology at the University of California, Santa Cruz). The following day, the membrane was washed 4 times for 5 minutes with 1x TBS containing 0.05% tween-20. The membrane was then incubated in 6% milk blocking solution containing goat anti-rabbit IgG horseradish peroxidase conjugated secondary antibody (Boehringer Mannheim; Indianapolis, IN) diluted 1:5,000 at room temperature for one hour with constant agitation. The membrane was washed 4 times for 5 minutes with 1x TBS containing 0.05% Tween-20. The membrane was then incubated in ECL Western Blotting Detection Reagent (Amersham Pharmacia Biotech) for 1 minute at room temperature. The membrane was then removed from the ECL reagent, covered with clear plastic wrap (still wet with ECL reagent), and placed into an autoradiograph cassette with film.

Treatment of cells for analysis of STAT-5 activation

To determine GH induced STAT-5 activation (phosphorylation) in cultured cells, cell lines stably transfected with GHR/BP DNA, and GHR/BP stable cells transfected with GHR-RZ DNA were treated with GH and analyzed by western blot analysis using an anti-phosphotyrosine antibody as previously described (Wang et al 1993). Cells cultures at approximately 80% confluence in 75cm^2 flasks were depleted

in serum free medium for 2 hours. Following cell depletion, 500 ng/ml bGH was added to the flasks. The cells were incubated for 10 minutes in the GH containing medium at 37°C. Following the incubation, the flasks were immediately placed on ice where the media was removed and 10 ml iced 1x PBS was added. The cells were scraped from the flask bottom, transferred to 15 ml conical tubes, and centrifuged at 1000x g for 3 minutes at 4°C. The supernatant was removed and 1 ml of ice-chilled UBI lysis buffer was added. DNA in the cell lysates was sheered by passing the lysates through a 22 gauge needle ~10 times. The lysates were then transferred to pre-chilled 1.5 ml Eppendorf tubes, incubated on ice for 20 minutes, and centrifuged at 16,000x g for 20 min at 4°C. The supernatant was removed and stored in 50 ul aliquots at -80°C.

Immunoblotting with anti-phosphotyrosine antiserum

Immediately following gel transfer, the nitrocellulose membrane was washed briefly in rinsing buffer (10mM Tris-HCl pH 7.4, 75mM NaCl, 0.1% Tween-20, and 1mM EDTA) and then incubated overnight at 4°C with constant agitation in rinsing buffer containing 4% Bovine Serum Albumin. The following day, the membrane was washed 4 times for 5 minutes five minutes with rinsing buffer. The membrane was then incubated for one hour at room temperature with constant agitation in rinsing buffer containing a 1:10,000 dilution of horseradish conjugated anti-phosphotyrosine antibody (clone PY20) purchased from ICN pharmaceuticals (Costa Mesa, CA). The membrane was washed 3 times for five minutes with rinsing buffer. The membrane

was then incubated in ECL Western Blotting Detection Reagent (Amersham Pharmacia Biotech) for 1 minute at room temperature. The membrane was then removed from the ECL reagent, covered with clear plastic wrap (still wet with ECL reagent), and placed into an autoradiograph cassette with film.

Protein extraction from Mouse Tissues

Mice were weighed then sacrificed by cervical dislocation. Liver and kidneys were removed from the animals and each tissue was weighed. Samples not immediately used were wrapped in aluminum foil, frozen immediately by placing in liquid nitrogen, and stored at –80^{o}C. Tissues were then placed in 50 ml conical tubes with UBI lysis buffer and homogenized using a polytron homogenizer purchased from Brinkman (Westbury, NY). 1 ml of lysis buffer was added per 0.3 grams of liver. 1 mL of lysis buffer was added per 0.15 grams of kidney. The homogenized samples were incubated on ice for 20 minutes and centrifuged at 16,000x g for 20 minutes at 4^{o}C. The supernatant was then stored in 100 ul aliquots at –80^{o}C.

Preparation of GHR-RZ DNA for microinjection

41.2 ul of 0.485 ug/ul pMet-GHR-RZ (20 ug) was digested with 120 units *KpnI* (Promega) in 1x Promega buffer J (10 mM Tris-HCl pH 7.5, 7 mM $MgCl_2$, 50 mM KCl, 1 mM DDT) in a total volume of 200 ul. The reaction was incubated for 4 hours at 37^{o}C. Following the incubation, the reaction was resolved on a 0.8% agarose gel in 1x TAE buffer for 30 minutes at 80 volts. The gel was resolved in the absence

of ethidium bromide to avoid intercalation of the dye into DNA used to create transgenic mice. To locate the proper DNA band within the gel, 10 ul of the 200 ul reaction was loaded into a small well outside the preparative well containing the remaining 180 ul of the reaction. The side of the gel containing the resolved reaction that was loaded into the small well was removed with a scalpel and placed into a solution of 1x TAE containing ethidium bromide. After approximately 20 minutes, the gel section was "pieced" back together in it original position with the large portion of the gel and placed on a ultraviolet light trans-illuminator. Using the visible bands in the ethidium stained section of gel, a section of the unstained gel corresponding to the ~900 base pair DNA fragment was excised. The gel section was placed into dialysis tubing containing TAE. The DNA was extracted from the agarose by electrophoresis for 1 hour at 80 volts and purified using Elutip-d^{TM} (Schleicher & Schuell Inc., Keene, NH) ion exchange columns equilibrated with a low salt buffer (0.2 M NaCl, 20 mM Tris-HCl pH 7.5, 1 mM EDTA). The column was washed once with 5 ml of the low salt buffer. The DNA was eluted from the column with 500 ul of a high salt buffer (1 M NaCl, 20 mM Tris-HCl pH 7.5, 1 mM EDTA). The DNA was then precipitated with 2 volumes of 100% ethanol at 4°C for one hour. The precipitated DNA was pelleted by centrifugation for 10 minutes at 16,000 x g. The DNA pellet was washed once with ~1 ml of 70% ethanol followed by desiccation in a Speed-vac centrifuge. The DNA was resuspended in microinjection buffer (1 mM Tris-HCl pH 8.0, 0.1 mM EDTA) to a concentration of 4 ng DNA per ul buffer. The DNA was then microinjected into the male pro-nuclei of pre-zygotic fertilized eggs by

the animal technical staff at the Edison Biotechnology Institute, Athens OH (Lacy et al., 1994).

RESULTS

Creating the RZ expression vector

After careful analysis of the GHR sequence, the third GTC sequence within exon two was selected as a RZ target. The GHR-RZ targeted to sequence located in exon 2 was cloned into the mammalian expression plasmid pMet-IG-mGHR at unique *Xba*I/*Xbo*I restriction sites. The resulting plasmid, pMet-GHR-RZ, utilized the mouse metallothionein-I (Met-I) transcriptional regulatory element (TRE) for constitutively high levels of RZ expression and which also can be up-regulated in mouse cells and in mice with Zinc treatment. A bovine GH (bGH) polyadenylation (PA) signal was present at the 3' end of the RZ for transcription termination. Restriction endonuclease digestion with *Kpn*I revealed 9 clones (10, 16, 20, 22, 37-39, 41, & 43) with the proper predicted sized fragments (~3851 bp and ~922 bp) as seen in figure 15 (also see figure 6 for plasmid map). DNA sequencing results (see figure 15) confirmed that clone 37 and clone 41 had the proper integration of RZ-DNA into the expression plasmid. Although sequencing was performed on all 9 potentially positive clones, only sequencing data from clones 37 and 41 were clear enough to confirm proper cloning had occurred.

Creating DNA templates for T7 run-off transcription

RZ-DNA templates for *in vitro* transcription were produced by PCR amplification. The incorporation of a core T7 promoter sequence into the design of the 5' primer allowed the PCR product to serve as a template for run-off transcription by T7 DNA polymerase. The beginning and ending of PCR amplification for the RZ

A.

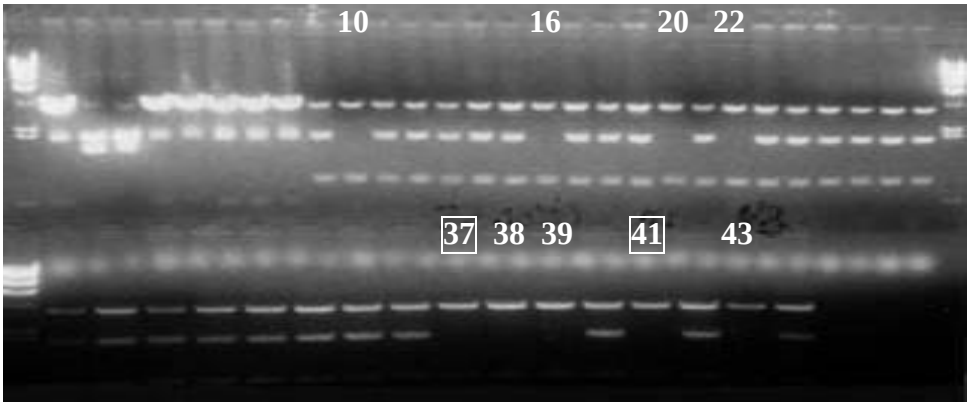

B.

AAACCGCCTG CTGGGTGCAA ACCCTTTGCG CCCGACTGTC

CAP

CAACGACTAT AAAGAGGGCA GGCTGTCCTC TAAGCGTCAC

CACGACTTCA AGCTTCTGAG TACCTTCTCC TCACTTACTC

XbaI

CGTAGCTCCA GCTTCACCAG ATCTAGACAA GGTTAAGAAC

XhoI

TGATGAGTCC GTGAGGACGA AACCTGACAA AGACTCGAGC

Poly A

TGTCCTTTCC TAATAAAATG AGGAAATTGC ATCGCATTGT

CTGAGTAGGT GTCATTCTAT TCTGGGGGGT GGGGTGGGGC

AGGACAGCAA GGGGGAGGAT TGGGAA

Figure 15. Screening pMet-GHR-RZ clones. A. Restriction endonuclease digestion with *Kpn*I revealed 9 clones (10, 16, 20, 22, 37-39, 41, & 43) with the proper predicted sized fragments (~3851 bp and ~922 bp). B. DNA sequencing results confirmed that clone #37 and clone #41 had the proper integration of RZ-DNA into the expression plasmid. Sequence obtained from the other clones was either incorrect or not clear enough for confirmation. The 161 nucleotides of shaded sequence represent the entire predicted ribozyme transcript. The light shaded sequences represent 5' and 3' UTR regions, while the dark shaded sequence represents the core ribozyme with the 12 nt 5' and 3' arms boxed. The transcriptional start and poly A addition sites are indicated by an arrow and a line, respectively. The *Xba*I and *Xbo*I restriction sites used for cloning were preserved as indicated with brackets.

DNA template was at the Met-I transcriptional start site and bGH poly A addition site, respectively. This allowed for the production of a PCR product that, when transcribed *in vitro* by T7 DNA polymerase run off transcription, would produce RNA similar in size to the predicted RZ-mRNA transcribed *in vivo* (with the exception of 5' an 3' end processing). That is, the *in vitro* transcribed RNAs were designed to begin and end at the predicted *in vivo* transcscriptional start and stop sites.

GHR-DNA templates for *in vitro* transcription were produced using the same strategy, initially. The same T7-Met 5' start site primer was used as the 5'-primer, and initially, the same bGH-PA addition site 3'-primer was used to produce a PCR generated GHR-DNA template designed to yield a full length GHR run off transcript. Production of RNA from the full-length GHR-DNA templates (~2.1 kb) proved to be troublesome. Low yields of PCR generated full length DNA template, low yields of *in vitro* transcribed GHR-RNA, and difficulty in resolving full length GHR-RNA on polyacrylamide gels led to the re-design of the 3'-primer used to create the GHR-DNA template. The second 3'-primer was designed to produce a truncated (618 bp) GHR-DNA template. As before, the same T7-Met 5' start site primer was used as the 5'-primer, while the redesigned (618-GHR) 3'-primer was used to generate PCR amplified GHR DNA templates. Both RZ and truncated GHR DNA templates generated by PCR were then used for *in vitro* transcription reactions. RNAs were purified and concentrations were determined by spectrophotometry. From the RNA concentrations and the known size of RZ and truncated GHR RNAs, the molarities of each RNA solution were calculated.

Ribozyme cleavage assays

Ribozyme cleavage assays (RCA) were performed using RNA purified from *in vit*ro transcription reactions. The RNA products of the RCAs were resolved on 1% agarose gels and stained with ethidium bromide. Visualization under ultraviolet light revealed that this method was not sufficient, as the cleavage products were not visible as distinct bands. Therefore, denaturing PAGE gels using 8 M urea were used to resolve the RNAs. Initially the resolved PAGE gels were also stained with ethidium bromide for visualization of RNA. Again, this method proved to be insufficient for visualization of RNA. The final method that allowed for successful visualization of resolved RCAs involved silver staining. Again, denaturing PAGE gels were used with 8 M urea. Following electrophoresis, the polyacrylamide gels were silver stained and dried. Initially, direct visualization and densitometry scanning of the silver stained RNA bands was used for analysis of RNA cleavage. The data obtained from densitometry scanning proved to be insufficient for quantification of RZ cleavage activity when kinetic constants were determined as large r^2 values from double reciprocal plots were observed using this method. Therefore, the method that was adopted for quantification of RZ cleavage in single turnover RCAs was a duel method of silver staining and quantification of ^{32}P labeled GHR substrate RNA by scintillation counting.

Five RCAs were performed using the method outlined in the methods section at various RZ to GHR substrate RNA concentrations (1:10, 1:5, 1:1, 5:1, and 10:1). In each of the reactions, cleavage products were observed (see figure 16). This

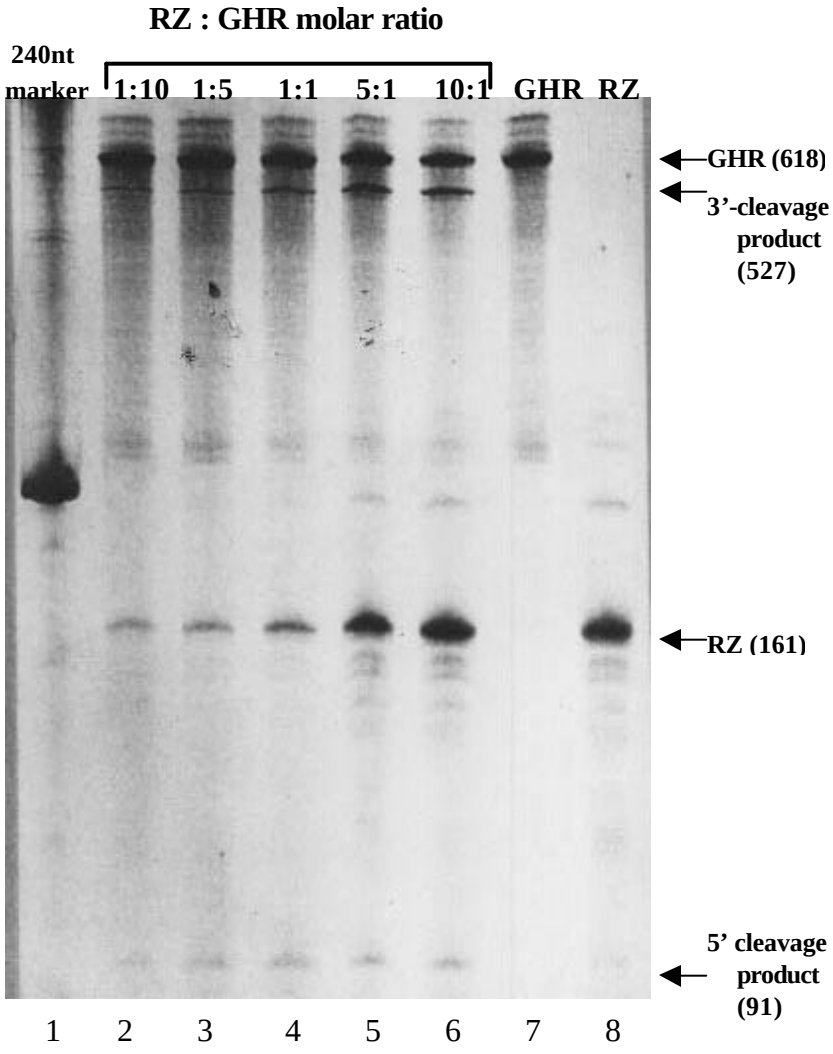

Figure 16. RCAs of GHR-RZ and GHR substrate RNAs at various molar ratios. Lane 1 contained a 240 nt RNA marker. Lanes 2-6 contained the reactions of five different RCAs at various molar ratios ranging from 1:10 to 10:1 RZ:GHR. Control lanes 7 and 8 contained truncated GHR substrate RNA alone and RZ RNA alone, respectively. The arrows indicate the location of the resolved RNAs.

demonstrated that the RZ was active. In addition, in each of the five reactions, cleavage occurred at the designed target site within the truncated GHR RNA. This was evident in that the cleavage products were as predicted with ~91 nt long 5', and ~527 nt long 3' apparent in each of the reactions. The amount of cleavage also increased in the reactions as the concentration of RZ was increased, suggesting the RZ as the agent catalyzing specific cleavage in the each of the reactions. Control GHR-substrate RNA incubated in the absence of RZ had no sign of cleavage at any specific region further identifying the RZ as an active and specific endonuclease. Thus, the ribozyme did in fact cleave GHR-RNA.

Approximate optimal conditions for RZ cleavage were determined by performing several RCAs in which the concentrations of NaCl and $MgCl_2$ were varied as well as pH, and temperature. Each of these variables was altered individually while the other effectors of RZ performance were held constant. The first parameter to be altered was NaCl (see figure 17). Five RCAs were set up varying only the concentration of NaCl (0, 10, 50, 100, 500 mM), while holding constant pH, temperature, and the concentrations of $MgCl_2$, RZ, and GHR-RNA. Analysis of RZ cleavage activity in the various concentrations of NaCl revealed no discernable difference in cleavage between each of the five RCAs, even in the absence of NaCl. Since the cleavage activities in the five reactions containing 0, 10, 50, 100, and 500 mM NaCl were indistinguishable, and 50 mM NaCl is most commonly used in the literature, there appeared to be no reason to stray from the standard 50 mM NaCl in future RCAs.

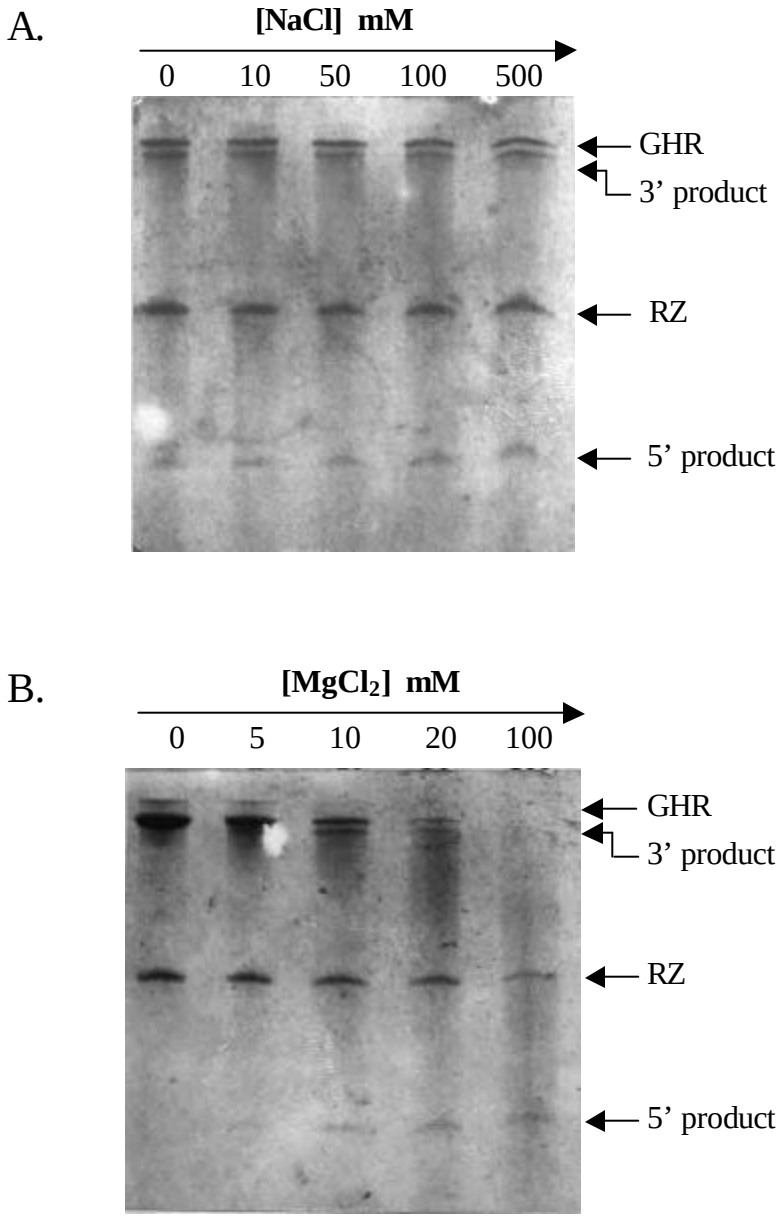

Figure 17. Determining approximate optimal concentrations of NaCl and $MgCl_2$ for GHR-RZ *in vitro* cleavage. All reactions were incubated at 50°C for 20 minutes at pH 7.5 at a 5:1 molar ratio of RZ to substrate. A. Five RCAs were set up using set reaction conditions with varying NaCl concentrations (0, 10, 50, 100, 500 mM). B. Five RCAs using varying concentrations of $MgCl_2$ (0, 5, 10, 20, 100 mM).

The second parameter to be altered was $MgCl_2$. Five RCAs were set up using various $MgCl_2$ concentrations (0, 5, 10, 20, 100 mM). Analysis of RZ cleavage activity revealed that a $MgCl_2$ concentration of 10 mM was sufficient for near optimal RZ cleavage. No cleavage was observed in the absence of $MgCl_2$ and only negligible cleavage was observed at 5 mM $MgCl_2$. While Mg^{2+} is a cofactor in RZ catalysis 10 mM $MgCl_2$ proved to be optimum for cleavage. Moreover, at 20 mM $MgCl_2$ indiscriminate RNA cleavage occurred as evident by smearing on the silver stain. The indiscriminate RNA cleavage occurred to a much greater extent at 100 mM $MgCl_2$. Minimal smearing was observed at 10 mM $MgCl_2$, only slightly more than in the absence of $MgCl_2$ or at 5 mM.

The third parameter to be altered was pH (see figure 18). Five RCAs were set up using various pHs (7.1, 7.3, 7.5, 7.7, and 7.9). Analysis of RZ cleavage activity revealed an optimal pH at pH 7.5, which is commonly used RZ *in vitro* cleavage reactions. Therefore, the standard pH of 7.5 was used in future RCAs. Less cleavage was detected at pH 7.3 while only slight cleavage was detected at pH 7.1. While the amount of cleavage was similar between pH 7.5 and 7.7, at pH of 7.7, most of the RNA was degraded into a non-distinguishable fragments, which appeared on the silver stained gel as a smear. The RNA was almost completely degraded at pH 7.9 as no bands or smear was visible in the silver stained gel.

The final parameter to be altered was temperature (see figure 19). Eight RCAs were set up using various temperatures (0, 37, 42, 47, 52, 57, 62, 67°C) and standard

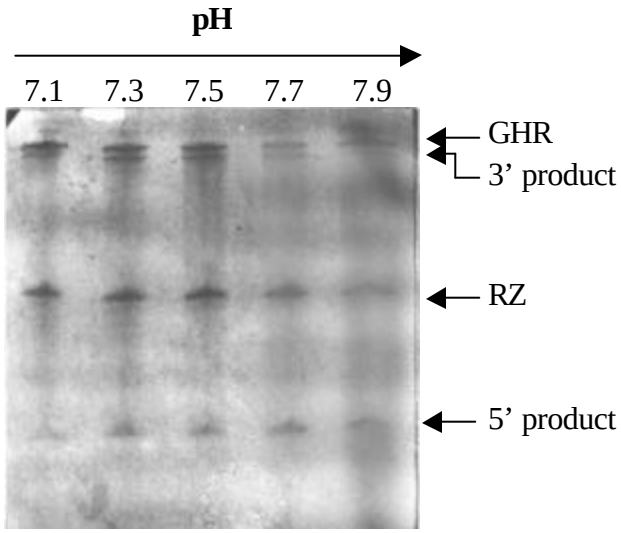

Figure 18. Determining approximate optimal pH for GHR-RZ *in vitro* cleavage. All reactions were incubated at 50°C for 20 minutes in 10 mM $MgCl_2$ and 50 mM NaCl at a 5:1 molar ratio of RZ to substrate. B. Five RCAs using varying pH varying by 0.2 units (7.1, 7.3, 7.5, 7.7, 7.9).

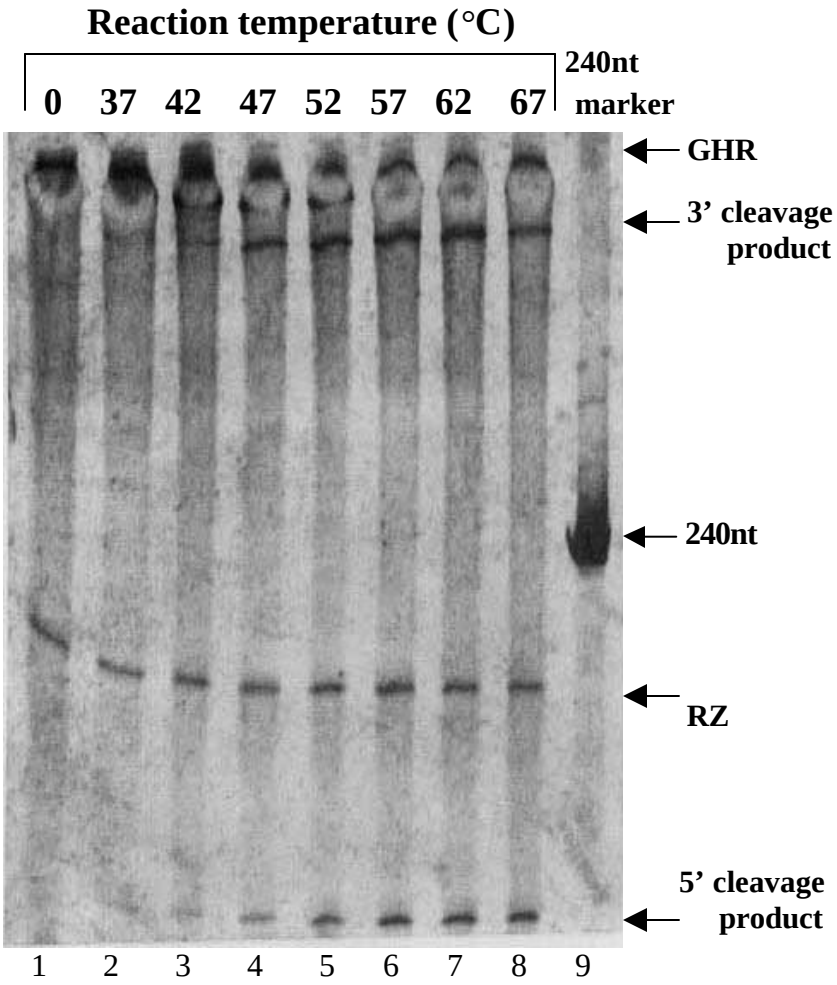

Figure 19. Determining approximate optimal temperature for GHR-RZ *in vitro* cleavage. All reactions were incubated for 20 minutes in 10 mM $MgCl_2$ and 50 mM NaCl, pH 7.5 at a 1:5 molar ratio of RZ to substrate. Eight RCAs were set up using set reaction conditions with temperatures varying by 5°C (0, 37, 42, 47, 52, 57, 62, 67). Maximal cleavage was observed at 57°C (lane 6) and 62°C (lanes 7).

reaction conditions (50 mM Tris-Cl pH 7.5, 50 mM NaCl, and 10 mM $MgCl_2$). A 1:5 ratio of RZ to GHR-substrate RNA was used in these eight RCAs, respectively. The reaction designated 0°C was incubated on ice and was therefore most likely slightly greater than the given temperature. Nevertheless, the RCA incubated on ice revealed no detectable cleavage. Analysis of cleavage at the various temperatures revealed a temperature dependent increase from 0°C to 57°C with similar maximal cleavage occurring at 57°C and 62°C. A slight bias for maximal cleavage occurred at 57°C therefore, the optimal temperature of the GHR-RZ for *in vitro* cleavage was designated 59°C. Although the optimal *in vitro* temperature is 22°C higher than that of the 37°C *in vivo* environment of cultured cells and mice, the presence of many extraneous factors such as RNA binding proteins *in vivo* makes predictions of RZ arm length and GC content difficult. It is important to note *in vitro* results do not always correlate with RZ activity *in vivo* (Crisell et al., 1993) and that *in vitro* optimization experiments were performed for the purpose of obtaining conditions for determining kinetic data from the RZ.

To determine if the GHR-RZ has the ability to turnover (cleave more than one substrate RNA), a timed RCA were performed (see figure 20). The timed RCA was set up as indicated in the methods section under multiple turnover conditions. The RZ to GHR-substrate RNA ratio was set at 1:20, respectively. At set time points, 20 ul aliquots were removed from the RCA and immediately frozen on dry ice in stop solution. When the last the reaction was completed, the 20 ul samples from the

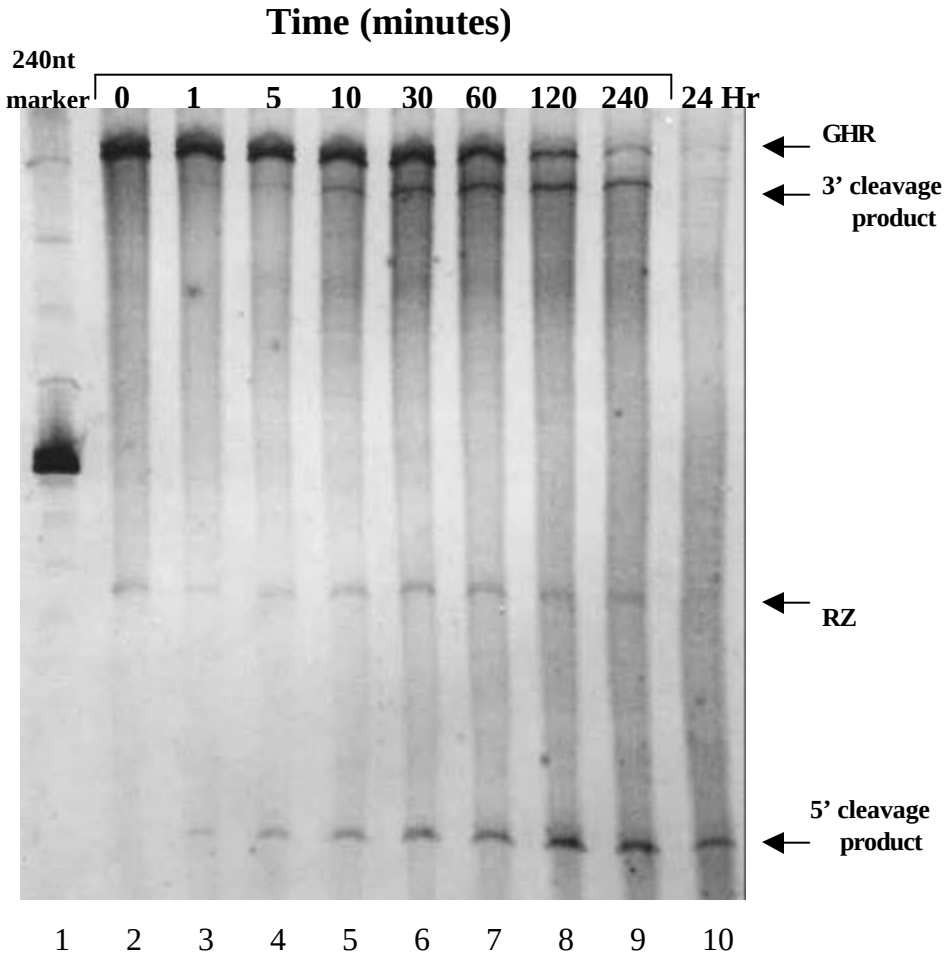

Figure 20. Timed RCA performed at 37°C using a RZ to GHR-substrate RNA ratio at 1:20, respectively. At set time points, 20 ul aliquots were removed from the RCA and immediately frozen on dry ice in stop solution. When the last the reaction was completed, the 20 ul samples from the various time points were resolved and silver stained. Greater than 5% cleavage was achieved within the first 30 minutes of incubation (lane 6). Approximately half the substrate was cleaved after two hours of incubation (lane 8). At four hours of incubation approximately 70% of the substrate RNA was cleaved (lane 9).

various time points were resolved and silver stained. Analysis of the silver stained RCA image revealed that the GHR-RZ was able to turnover. For turnover to exist in a reaction with 20 fold less RZ, greater than 5% cleavage must occur. This was achieved within the first 30 minutes of incubation. Approximately half the substrate was cleaved after two hours of incubation. At four hours of incubation approximately 70% of the substrate RNA was cleaved. The 24 hour incubation exhibited a high degree of non-specific RNA degradation as neither the substrate band nor the larger 3' cleavage product band were visible in the silver stained gel. Curiously, the 5' cleavage product appeared to be more resistant to RNase degradation in the reactions. In the 24-hour reaction, the uncleaved substrate, 3'-cleavage product, and RZ RNAs were all nearly degraded, while a significant amount of the 5'-cleavage product was still intact.

Establishing GHR expressing mouse L-cells

In an effort to create a mouse cell line that expresses detectable levels of GHR, the pMet-GHR/BP plasmid was stably transfected into mouse L-cells (see figure 21). After selection in HAT media, 15 individual clones were expanded. The cells were tested for stable integration of the pMet-GHR/BP DNA by PCR. Two separate sets of primers were used for the PCR screening. Of the 15 transfected cell lines, all were DNA positive for the pMet-GHR/BP as indicated by PCR amplification. GH binding assays were performed to determine the relative levels of GHR expression in the 15 clones (see table 3). While no specific binding was observed in non-transfected mouse L-cells, all of the DNA positive stable cell lines exhibited specific binding of ^{125}I-labled hGH. The number of counts measured ranged from a low of ~650 cpm, to a high of ~3,800 cpm. The stably transfected cell line that demonstrated a moderate amount of GHR expression level (~1334 cpm) relative to the 14 other clones was selected for use in GHR-RZ cell culture analysis. This cell line was expanded from the pMet-GHR/BP stably transfected clone #6 and will be referred to as E6 cells.

Establishing stable cell lines with the GHR-RZ

The E6 cell line (previously transfected with a GHR/BP "mini-gene") was used for stable transfection of the GHR-RZ. E6 cells were maintained in HAT media. The pMet-GHR-RZ plasmid was co-transfected with the plasmid pRSV-NEO. Pools of transfected cells were selected for neomycin resistance in HAT media containing 400 ug/ul G-418 (a neomycin analog). Surviving cells were maintained in HAT media

A.

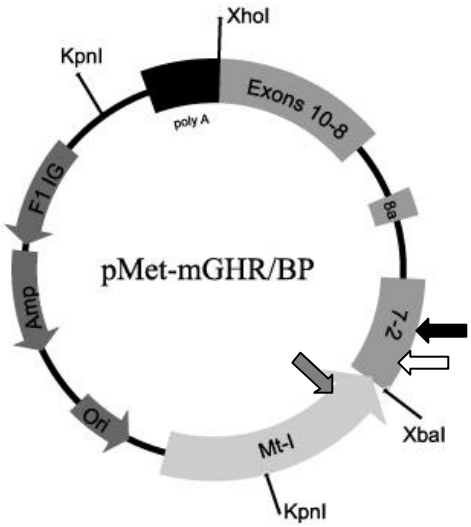

B.

Figure 21. PCR screening of stable L cells transfected with a GHR/BP "mini-gene". Two separate sets of primers were used for the PCR screening. A. Both sets of reactions utilized a 5'-primer directed -65 bases into the metallothionein UTR (striped arrow pointing to the position of the plasmid). The 3'-primers for the first and second set of reactions were directed positions 438 bases (black arrow) and 212 bases (white arrow) into the GHR/BP mini-gene, respectively. B. All 15 clones were PCR positive for the mini-gene. Lanes +C contained pMet-GHR/BP plasmid and served as a positive control, while non-transfected L cell lysate served as a negative control (-C).

Table 3. Relative GHR expression in L cells stably transfected with a mouse GHR/BP "mini-gene": Rank assigned by Specific binding of ^{125}I-labled hGH.

Rank	Clone #	Specific Binding (c.p.m.)
1	15	3799
2	1	3281
3	2	1576
4	14	1415
5	6 (E6)	1334
6	11	1116
7	12	1036
8	10	895
9	3	894
10	7	864
11	13	775
12	8	735
13	9	715
14	5	680
15	4	643
16	L cell (-C)	0

In 6-well tissue culture plates monolayers of the stable cells were propagated to ~1x10^6 cells/well. 160,000 cpm of ^{125}I-hGH at a concentration 1 nM in 2 ml of 1x PBS with 0.1% BSA was added to each well with or without 100 nM non-radioactive bGH. The cells were incubated for 2 hours at room temperature. The cells were lyses by the addition of 1 ml of 0.1 N NaOH + 1% SDS to each well. Cell lysates were then transferred to vials and the number of counts was measured. The evaluation of relative GHR expression for each stable cell line was based on the mean value of two experiments. The sixth GHR/BP cell line (shaded), which had an intermediate level of GHR expression (as compared to all 15 cell lines screened by GHR binding assays), was chosen for subsequent study and referred to as "E6" cells.

containing 200 ug/ul G-418 and isolated in 96-well plates. 10 cell lines, expanded from the individual clones, were analyzed for incorporation of the GHR-RZ "mini-gene" by PCR (see figure 22). Of the 10 cell lines analyzed, all were DNA positive for the GHR-RZ as indicated by PCR amplification.

GHR binding assays on RZ transfected cells

GHR binding assays were performed to determine the relative levels of GHR in the 10 clones (see table 4). The parental E6 cell line was used as a positive control. The specific binding observed in the stable RZ transfected cells was divided by the specific binding of the non-RZ transfected E6 cells to determine the amount of GHR decreased in these cells. Eight out of ten of the RZ-DNA positive stable cell lines exhibited a decrease in specific binding of ^{125}I-labled hGH ranging from 25% to a 52% decrease as compared to E6 cells. The fifth clone 6-5, which exhibited the greatest decrease in GHR expression (52% decrease), was used in for further study. Clone 6-4, which exhibited the second greatest decrease in GHR expression (44% decrease) was also used in some of these studies.

Northern blot analysis of RZ transfected cells

Northern blot analysis was performed on total RNA isolated from GHR/BP transfected E6 cells and RZ transfected 6-5 cells (see figure 23). RNA isolated from non-transfected L cells was used as a control. A probe designed against sequence in

A.

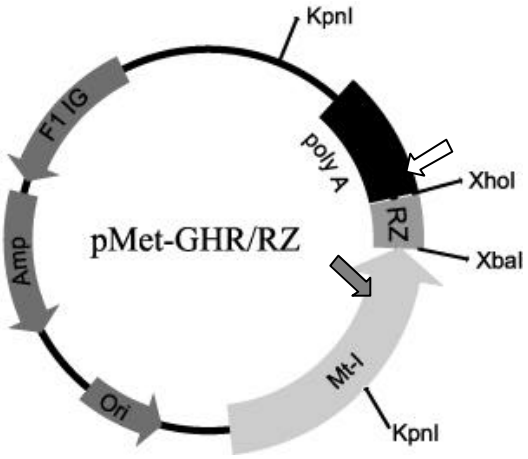

B.

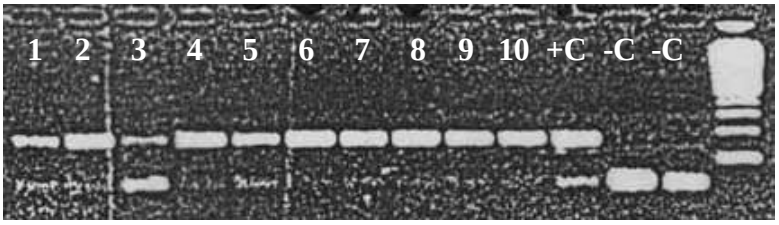

Figure 22. PCR screening of E6 cells stably transfected with the GHR-RZ. (A) A 5'-primer directed to the metallothionein transcriptional start site (striped arrow) and a 3'-primer directed to the bGH poly A addition site (white arrow) were used to produce a predicted 161 bp PCR product. (B) All 10 clones selected were PCR positive for the GHR-RZ DNA. Lanes 11, 12 and 13 served as controls with pMet-GHR-RZ plasmid in the positive control reaction (+C), non-transfected L cell lysate and no cell lysate added in the negative control reactions, respectively (-C).

Table 4. Relative GHR expression in E6 cells stably transfected with the GHR-RZ: Rank assigned by (specific binding of RZ transfected clone / specific binding in parent E6 cells).

Rank	Clone #	Specific Binding (% of E6)
	E6 (+C)	100
1*	6-5*	47.9*
2	6-4	55.6
3	6-8	64.6
4	6-1	66.3
5	6-3	71.5
6	6-7	73.5
7	6-6	83.0
8	6-2	88.3
9	6-9	98.1
10	6-10	102
11	L cell (-C)	0

In 6-well tissue culture plates monolayers of the stable cells were propagated to ~$1x10^6$ cells/well. 160,000 cpm of ^{125}I-hGH at a concentration 1 nM in 2 ml of 1x PBS with 0.1% BSA was added to each well with or without 100 nM non-radioactive bGH. The cells were incubated for 2 hours at room temperature. The cells were lyses by the addition of 1 ml of 0.1 N NaOH + 1% SDS to each well. Cell lysates were then transferred to vials and the number of counts was measured using a scintillation counter. The evaluation of relative GHR expression for each stable cell line was based on the mean value of two experiments. *The clone 6-5, exhibited the greatest decrease in GHR expression and was used in for further study. Clone 6-4 which exhibited the second greatest decrease in GHR expression was also used in some of these studies.

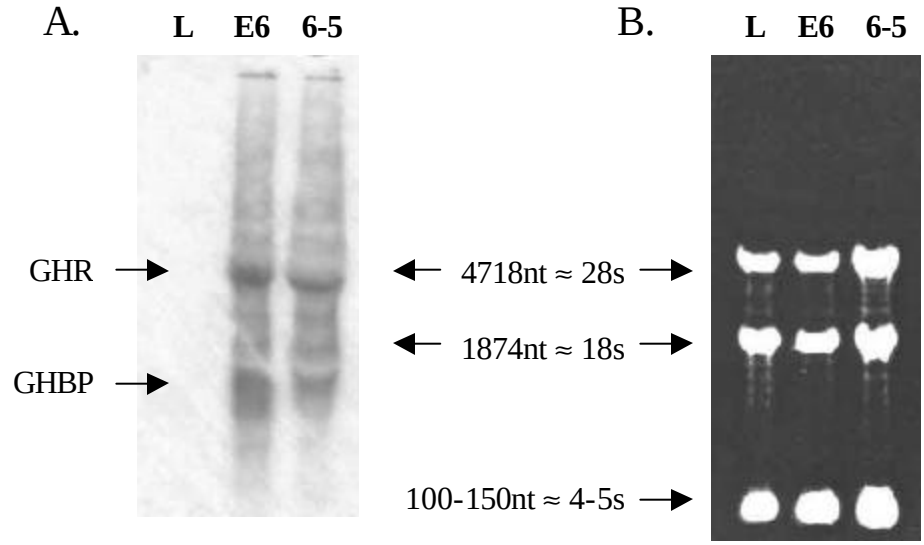

Figure 23. Analysis of GHR and GHBP transcripts from E6 cells stably transfected with the GHR-RZ. Northern blot analysis was performed on total RNA isolated from non-transfected L cells (lane 1), GHR/BP transfected E6 cells (lane 2), and RZ transfected E6 cells (lane 3). A. A probe designed against sequence in the GHR/BP cDNA from exons 2-7 so that it recognized both the GHR and GHBP transcripts. No transcripts were detected in negative control L cell preparations. B. Ethidium bromide staining of the agarose gel prior to RNA transfer served as control for RNA size and the amount of RNA loaded per well. 28s, 18s, and 5s ribosomal subunits are indicated.

the GHR/BP cDNA from exon 2-7 so that it recognized both the GHR and GHBP transcripts was used. A greater quantity of both GHR and BHBP transcripts was detected in E6 cells not transfected with the RZ than 6-5 cells that were RZ transfected. No transcripts were detected in negative control L cell preparations. The decrease in GHR and GHBP transcripts observed from RZ transfected 6-5 cells was most likely more dramatic when the amount of total RNA present in each lane was considered. Ethidium bromide staining of the agarose gel prior to RNA transfer revealed that approximately twice the amount of total RNA isolated from clone 6-5 was present compared to E6 RNA.

Western blot analysis of GHR-RZ transfected cells

To further verify the decreased GHR levels in the RZ transfected cell lines 6-4 and 6-5, western blot analysis using an anti-GHR monoclonal antibody was performed (see figure 24). Cell lysates were isolated from approximately $1x10^7$ cells for each clone. The concentration of protein in the lysates was determined using Bradford assays and equalized prior to western analysis. Three bands were visible on the western blot with sizes of 110 kDa, 66 kDa and 46 kDa. The top 110 kDa bands, which are the predicted size of the GHR, were used for densitometry measurements. In agreement with results from the GH binding assays, the amount of GHR detected in western blot for clones 6-4 and 6-5 were approximately 50% that of the positive control E6 cells. No GHR was detected for the non-transfected mouse L-cells. The presence of the 66 kDa and 46 kDa bands were likely alternatively processed versions

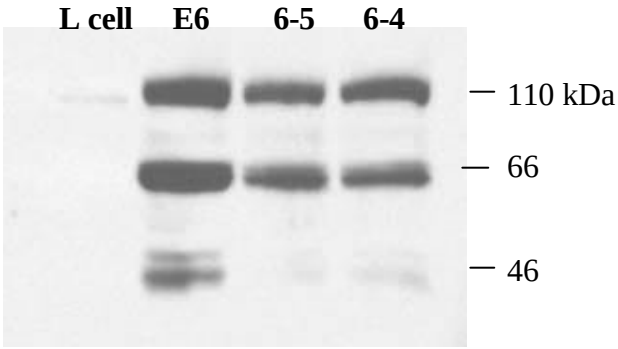

Figure 24. Western blot analysis of protein isolated from cultured cells. Western blot analysis was performed on total cell lysates isolated from non-transfected L cells (lane 1), GHR/BP transfected E6 cells (lane 2), and RZ transfected E6 cells clones 6-5 and 6-4 (lane 3 and 4, respectively). A monoclonal antibody designed against sequence in the cytoplasmic region of the GHR so that it recognized only the GHR gene product. No GHR was detected in negative control L cell preparations. Molecular weights of the bands in kilo Daltons (kDa) are marked.

of the GHR or cleaved portions of the cytoplasmic region. These bands were most likely fragments of the GHR as the lane containing L cell control lysates did not have the three bands or any other bands.

Decreased GH stimulated STAT-5 tyrosine phosphorylation in RZ transfected cells

The effect of decreased GHR levels (in RZ transfected clones 6-4 and 6-5) on GH induced signaling was analyzed by measuring the amount of STAT-5 tyrosine phosphorylation in response to GH treatment. Western blot analysis using an anti-phosphotyrosine (PY-20) polyclonal antibody was performed (see figure 25). Approximately $1x10^7$ cells for each clone were treated with 500 ng/ml bGH for 10 minutes prior to harvesting cell lysates. Non-treated cells were also harvested to serve as negative controls for each clones analyzed. The concentration of protein in the lysates was determined and equalized prior to western analysis. Analysis of the PY-20 immunoblot revealed a predominate band, which migrated to an area at the proper size for STAT-5 (~95 kDa), was present only in the GH treated E6 cells. Only slight bands at this size were visible in GH treated clone 6-4 and 6-5, suggesting that GH induced STAT-5 activation was severely decreased in these GHR-RZ positive cells lines.

Decreased GHBP levels in RZ transfected cells

The amount of GHBP produced in clones 6-4 and 6-5 was also measured. Using 75 cm^2 flasks, cells were allowed to grow to 100% confluence (approximately

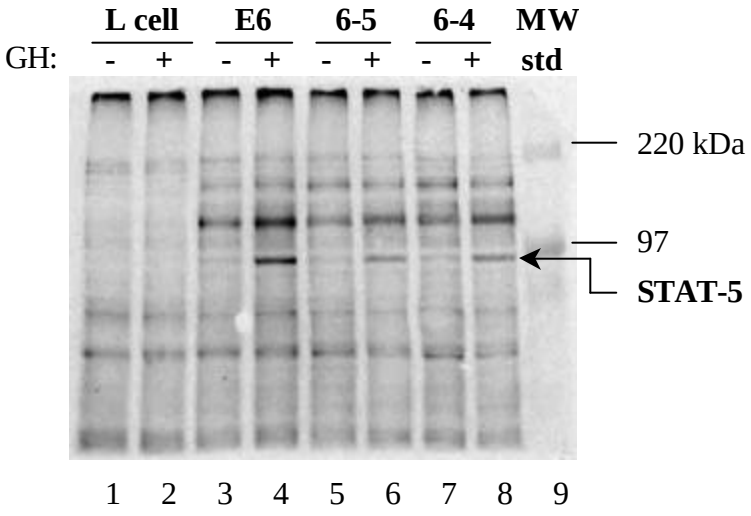

Figure 25. Decreased GH stimulated STAT-5 tyrosine phosphorylation in RZ transfected E6 cells. Western blot analysis using an anti-phosphotyrosine (PY-20) polyclonal antibody was performed on total cell lysates isolated from non-transfected L cells (lanes 1 and 2), GHR/BP transfected E6 cells (lanes 3 and 4), and RZ transfected E6 cells clones 6-5 and 6-4 (lanes 5 and 6) and (lanes 7 and 8), respectively. Approximately $1x10^7$ cells for each clone were treated with 500 ng/ml bGH for 10 minutes prior to harvesting cell lysates (lanes 2, 4, 6, and 8). Non-treated cells were also harvested to serve as negative controls for each clones analyzed (lanes 1, 3, 5, and 7). A molecular weight standard indicating 97 kDa and 220 kDa is marked (lane 9). The concentration of protein in the lysates was determined and equalized prior to western analysis. Bands from the molecular weight standard are marked in kilo Daltons (kDa). The bands migrating at 95 kDa (marked in bold) have been shown previously to be STAT-5 (Chow et al., 1996; Ram et al., 1996; Silva et al., 1996; Wang et al., 1994; Xu et al., 1996; Xu et al., 1995).

$9x10^7$ cells). Upon reaching confluence, the cells were washed and covered with 15 ml DMEM without serum. The media were collected after 24 hours of incubation and filtered using 0.45 um vacuum filters and placed on dry ice. The samples were then sent to Dr. Gerhard Baumann at Northwestern University where GHBP levels were determined using GH affinity columns. The levels of GHBP from clone 6-4 and 6-5were 32% and 38% decreased, respectively, as compared to the parental E6 cells. No GHBP was detected in the non-transfected L-cell control medium.

Determining GHR levels required for STAT-5 activation in mouse L-cells

Mouse L-cells, were used to establish stable cell lines that express various levels of GHR. The pMet-GHR/BP plasmid was stably transfected into mouse L-cells as described earlier in this text. Initial screening of the 15 clones to determine the relative levels of GHR expression was performed using competitive GH binding assays. While no specific binding was observed in non-transfected mouse L-cells, all of the DNA positive stable cell lines exhibited specific binding of ^{125}I-labled hGH. The number of counts measured in the stable cell lines exhibited a range of ~6 fold from the lowest to highest GHR expressing cells. Based on data from the initial GH binding assays, 6 of the GHR transfected stable cell lines representing a variety of GHR expression were selected for further study. DNA slot blot analysis using a probe directed to the metallothionein-I transcriptional regulatory element was used to screen the cell lines for DNA copy number. GH binding assays using a set concentration of ^{125}I-GH and varying concentrations of competing non-labeled GH were performed to

determine the number of GHRs per cell for each of the cell lines. In addition to the binding assays, the number of cells per well were counted using duplicate plates seeded with the same concentration of cells as used in plates for binding analysis. Using Scatchard plots and cell number (determined using a hemocytometer), the cell surface receptor numbers were determined for each cell line. The results showed that the number of GHRs per cell ranged from 50,000 to 240,000 in the GHR transfected cell lines (see table 5). One of the cell lines (clone #6), exhibiting 170,000 GHRs per cell, was stably transfected with a GHR-RZ. GHR levels in one of the GHR-RZ clones was determined to be 81,000 GHR per cell, a decrease of ~48%. This decrease was sufficient to lower the number of GHRs per cell to levels similar to receptor levels found in the GHR transfected clone #8 which expressed 80,000 GHRs per cell. Therefore two cell lines containing similar levels of GHR were established using two different methods, GHR transfection and GHR + RZ transfection.

Comparison of DNA copy number and GHR expression revealed a trend in that the three highest copy number cell lines (containing ~30-70 copies of the GHR/BP "minigene") had the highest levels of expression (110,000-240,000 GHRs/cell) while lower copy number cell lines (~5-10 copies) exhibited lower levels of expression (50,000-80,000 GHRs/cell)(see Table 6). This trend was not absolute in that certain cell lines with greater copy numbers of GHR DNA demonstrated lower levels of GHR expression compared to cell lines with lower copy numbers. The main example of this is seen in cell line #10, which had more than twice the copies of

Table 5. GHR number per cell was determined for several of the cell lines stably transfected with a GHR/BP "mini-gene" and for clone 6-5, which was also transfected with a GHR-RZ.

Clone #	GHR number /cell	STAT-5 activation (band intensity)
L cell	2000	0.33
12	50,000	5.82
4	57,000	7.86
8	80,000	11.37
6-5	81,000	11.73
10	110,000	18.73
6	170,000	22.20
15	240,000	22.96

In 12-well tissue culture plates monolayers of the stable GHR/BP cells were propagated to confluence. 80,000 cpm of ^{125}I-hGH at a concentration 1 nM in 1 ml of 1x PBS with 0.1% BSA was added to each well with or without non-radioactive bGH. 8 different concentration of bGH were used to compete with the ^{125}I-hGH. In addition to the binding assays, the number of cells per well were counted using duplicate plates seeded with the same concentration of cells as used in plates for binding analysis. Using Scatchard analysis and cell number, the cell surface receptor numbers were determined for each cell line. The evaluation of relative GHR expression for each stable cell line was based on the mean value of three experiments. E6 cells with and without RZ are reported (shaded). Densitometry scanning data from PY-20 western is reported in the last column for comparison.

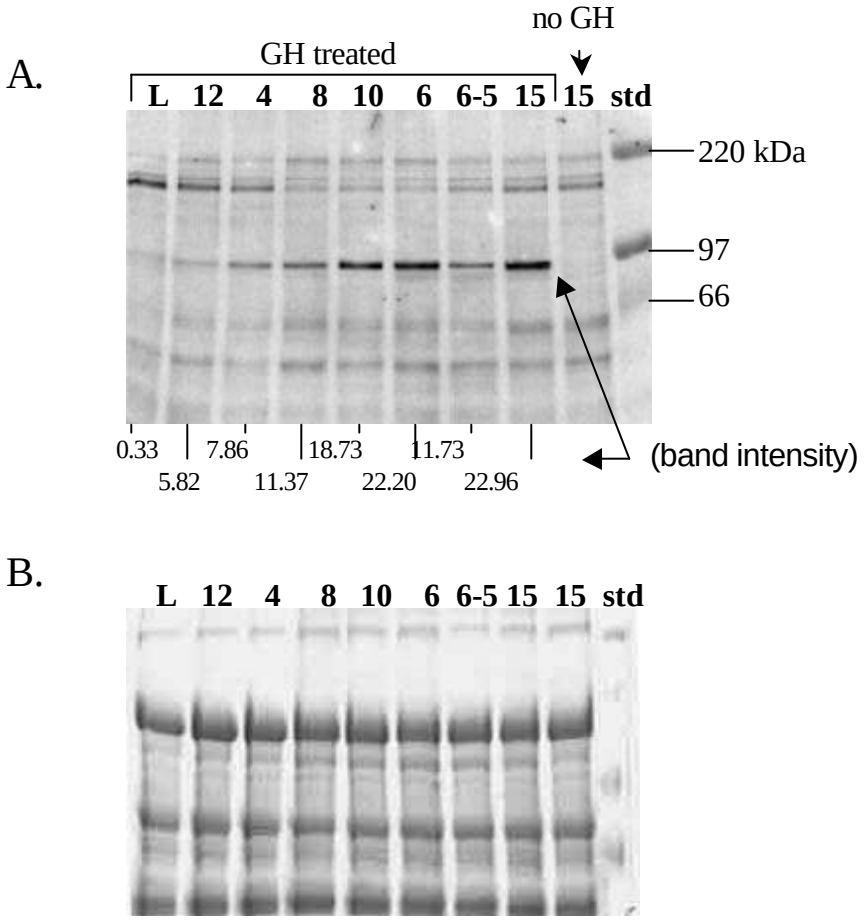

Figure 26. GH stimulated STAT-5 tyrosine phosphorylation in stable cells expressing various levels of GHR. A. Western blot analysis using an anti-phosphotyrosine (PY-20) polyclonal serum was performed on total cell lysates isolated from non-transfected L cells (lanes 1), GHR/BP transfected cells (lanes 2-9), and RZ transfected E6 cells, clone 6-5 (lane 7). Cells were treated with 500 ng/ml bGH for 10 minutes prior to harvesting cell lysates (lanes 1-8). GH treated L cells (lane 1) and non-treated clone #15 cells (lane 9) were included as controls. The concentration of protein in the lysates was determined and equalized prior to western analysis. STAT-5 band intensities were measured by densitometry scanning and are reported at the bottom of the gel. Two gels were resolved using at the same time using similar conditions. B. Of the two gels, one was stained with coomassie blue to further demonstrate equal amounts of protein were loaded for each clone.

Table 6. A comparison of GHR/BP "mini-gene" DNA incorporation to GHR expression level in transfected clones.

Clone #	GHR number /cell	Copies of GHR/BP mini-gene DNA*	
L cell	2000		0
12	50,000		~5
4	57,000		~10
8	80,000		~8
10	110,000		~70
6	170,000		~30
15	240,000		~40

*DNA slot blot analysis was performed on the stable cell lines to determine the relative amount of incorporated GHR/BP DNA. Approximate DNA copy numbers are indicated to the right of each DNA slot blot

GHR/BP "minigene" (~70 copies) as cell line #6 (~30 copies) but only expressed less GHRs/cell (110,000 for clone #10 and 170,000 for clone #6).

STAT-5 activation was also analyzed in the GHR/BP stable cell lines. Western blot analysis using an anti-phosphotyrosine (PY-20) polyclonal serum was performed (see figure 26). Approximately $1x10^7$ cells for each clone were treated with 500 ng/ml bGH for 10 minutes prior to harvesting cell lysates. Non-treated cells from clone #15 (the clone with the highest level of GHR expression) were also harvested to serve as a control. Non-transfected L-cells were also included to serve as a negative control. The concentration of protein in the lysates was determined and equalized prior to western analysis. In addition, duplicate gels were resolves and stained with coomassie blue to verify that equal concentration of cellular proteins were present from lane to lane. Analysis of the PY-20 immunoblot revealed a band, which migrated to an area at the proper size for STAT-5 (~95 kDa), that appeared with different intensities in lanes representing the cell lines with various levels of GHR expression. Only slight bands with the predicted size were visible in GH treated L-cell control and non-GH treated clone #15. Band intensities as determined by densitometry were compared to the levels of GHR expression for each done. When data from these two measurements were plotted (see figure 27), a linear increase was observed in STAT-5 activation as the number of GHR/cell increased up to ~110,GHR/cell. Maximum activation of STAT-5 was approached at ~240,000 GHR/cell as only a slight increase was observed between clone #6 with 170,000 GHR/cell and clone #15 with 240,000 GHR/cell. The relationship between GHR

GH stimulated STAT-5 tyrosine phosphorylation vs. GHR number in stable cells expressing various levels of GHR.

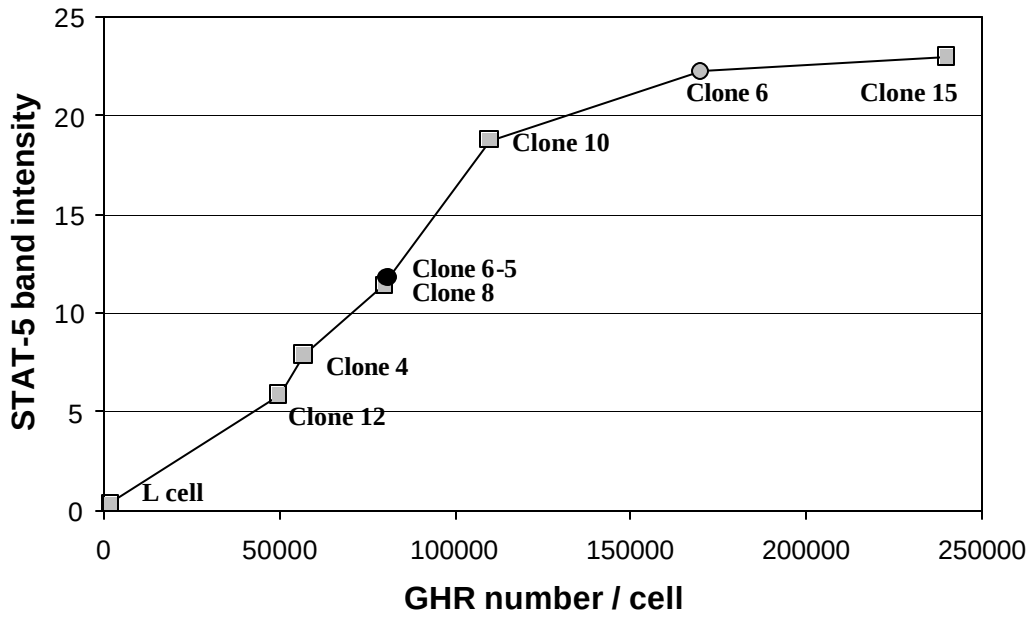

Figure 27. GH stimulated STAT-5 tyrosine phosphorylation vs. GHR number in stable cells expressing various levels of GHR. GH binding assays using a set concentration of ^{125}I-GH and various concentrations of competing non-labeled GH were performed to determine GHR specific binding for each cell line. Using Scatchard analysis and cell number, the number cell surface GHRs was determined for each cell line. STAT-5 activation as measured by PY-20 western blot analysis was plotted against GHR number per cell. Clone 6 (gray circle) and RZ transfected clone 6-5 (black circle) are represented by circles, while all other clones are represented by gray squares.

number and STAT-5 activation was strengthened by the observation that the level of STAT-5 activation in GHR-RZ transfected clone #6-5 with 81,000 GHR/cell (reduced from 170,000 GHR/cell in the parent clone #6) was similar to that of the GHR transfected clone #8 with 80,000 GHR/cell.

GHR-RZ transgenic mice

The pMet-GHR-RZ mammalian expression plasmid was used to generate GHR-RZ transgenic mice. The plasmid was digested with *KpnI* to generate an ~1 kb fragment and isolated without the use of ethidium bromide. The DNA was resuspended in microinjection buffer to a concentration of 4 ng DNA per ul buffer. The DNA was then microinjected into the male pro-nuclei of pre-zygotic fertilized eggs by the animal technical staff at the Edison Biotechnology Institute, Athens OH (Lacy et al., 1994). One hundred and twelve offspring were produced from the microinjection procedure. Transgenic mice were screened using PCR analysis (see figure 28) with 5' and 3' primers directed to the 5' metallothionein-I untranslated region and 3' bGH poly A region of the GHR-RZ "mini-gene", respectively. Of the 112 mice screened, only two females were DNA positive (mouse #76 and mouse #99). The RZ-DNA positive females were mated with non-transgenic males in an attempt to produce two lines of GHR-RZ transgenic mice. Thirteen attempts to produce offspring were unsuccessful. Observations of birthings during several of the later attempts revealed that both the transgenic females were killing their pups shortly after birth. In an effort to circumvent this problem, experienced foster female mice were housed with the transgenic females. No surviving pups were obtained from these breedings. The female transgenic mice cannibalize their own pups and the pups of the non-transgenic foster female mice. Final attempts to remove transgenic females immediately after giving birth also proved unsuccessful. Foster females were also observed cannibalizing the pups from the transgenic mice. After ~18 months of

A.

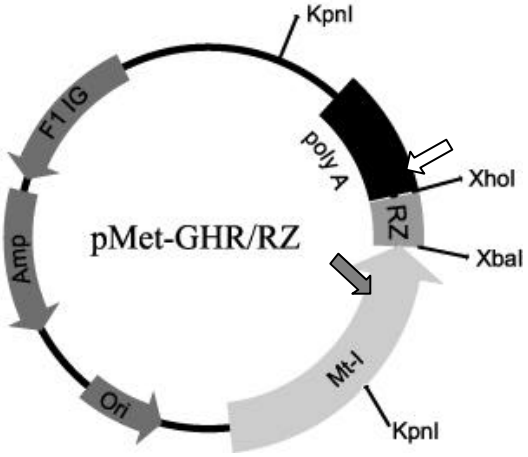

B.

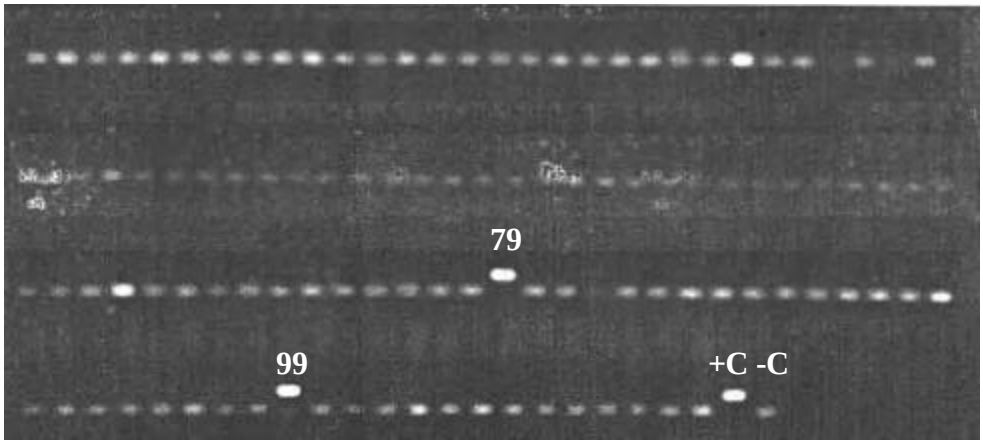

Figure 28. PCR screening of mouse tail DNA from the first set of founder mice microinjected with the GHR-RZ. A. A 5'-primer directed to the metallothionein transcriptional start site (striped arrow) and a 3'-primer directed to the bGH poly A addition site (white arrow) were used to produce a predicted 161 bp PCR product. B. Only two mice were PCR positive for the GHR-RZ DNA. The last two lanes in the bottom right corner contained the controls with pMet-GHR-RZ plasmid in the positive control reaction (+C), non-transgenic mouse tail DNA in the negative control reaction (-C), respectively.

breeding the two transgenic females no longer became pregnant and each female died at ~20 months of age.

Following unsuccessful attempts to continue GHR-RZ transgenic mouse lines, a second round of microinjections were performed using the same methods. One hundred and twenty seven offspring were produced from the microinjection procedure. DNA slot blot analysis using a probe directed to the metallothionein-I transcriptional regulatory element was used to screen the mice (see figure 29). Of the 127 mice screened, three were DNA positive (mouse #93-female, #113-male, and #126-female). Intensity of the blots as compared to copy number controls indicated that the number of GHR-RZ "mini-genes" integrated in the genome of the positive mice ranged from ~5 to ~30 copies (~5 copies for founder #93, ~5 copies for founder #126, and ~30 copies for founder #113). Transgenic founders were successfully mated with non-transgenic mice to expand the mouse lines. DNA slot bots were used to identify transgenic mice from each round of breeding. Due to problems breeding the lines 93 and 126, founder line 113 was expanded to a much grater extent. Once three generations of each mouse line were established, six animals (3 male and 3 female) from each of the three transgenic lines were sacrificed for analysis of GHR levels. Due to low copy numbers of the integrated RZ-DNA in founder lines 93 and 126, a distinction between homozygous and heterozygous animals could not be made. Therefore, a RZ-DNA positive genotype (which most likely included some homozygous mice as well as heterozygous animals) was used for designation of mice in founder lines 93 and 126. Both heterozygous and homozygous mice were used for

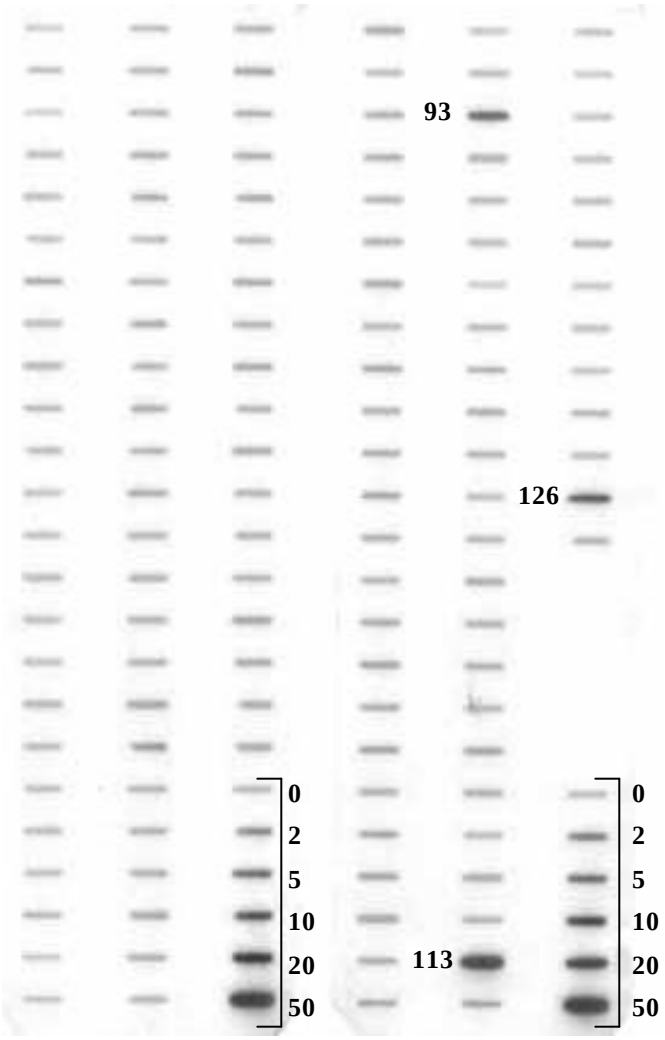

Figure 29. DNA slot blot analysis of mouse tail DNA from the second set of founder mice microinjected with the GHR-RZ. DNA slot blot analysis using a probe directed to the metallothionein-I transcriptional regulatory element was used to screen the mice. Of the 127 mice screened, three were DNA positive as indicated (mouse #93-female, #113-male, and #126-female). Intensity of the blots as compared to copy number controls indicated that the number of GHR-RZ "mini-genes" integrated in the genome of the positive mice ranged from ~5 to ~30 copies (~5 copies for founder #93, ~5 copies for founder #126, and ~30 copies for founder #113).

founder 113. The livers of sacrificed animals were used to perform GHR western blot analysis and those from GHR "knockout" mice served as controls for the GHR westerns. The GHR antibody (clone #181, a rabbit monoclonal antibody recognizing the intracellular domain of the mouse GHR) was used. Initial GHR westerns performed using a protocol previously described (Cataldo, 2001). While the presence of a GHR specific band was obtained using this procedure, it was not separate from the extraneous bands (see figure 30). These bands were determined not to be associated with GHR because they were also present in liver samples from the negative control GHR "knockout" mice, which do not express GHR. Modifications were made to the protocol, which eventually led to GHR westerns that allowed for separation of GHR from non-GHR proteins that were immunoreative to the GHR antibody. Using the modified protocol, western blot analysis was performed on liver samples from the three GHR-RZ founder lines. Analysis of band intensities from individual mice in the same genotype revealed inconsistencies. Conclusions about GHR levels in a given genotype were not attempted due to a large observed variability from individual mice in the same genotype (see figure 31). Therefore, in an effort to increase the number of animals from a given genotype observed by western blot analysis, 6 liver samples were pooled for each genotype analyzed (see figure 32). Analysis of immunoblots from three westerns revealed no change in GHR levels in transgenic mice from founder 93 and founder 126 when compared to non-transgenic littermate controls. Only a slight change in GHR levels was observed in transgenic mice from founder 113 when compared to controls. Due to the variability observed in

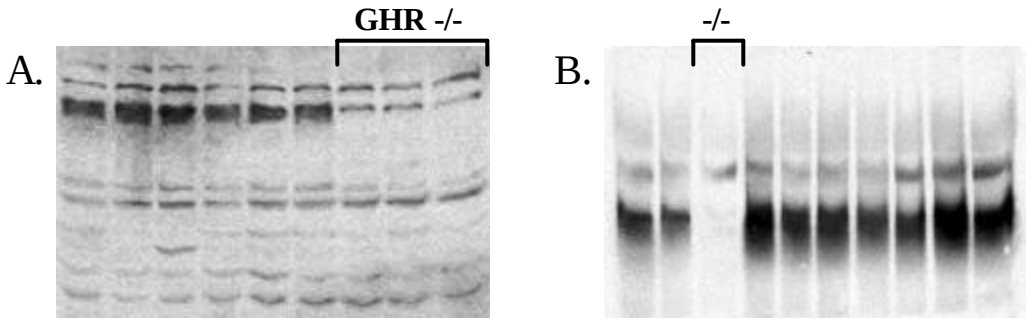

C.

Resolve 1 ½ Hrs @ 100 v	**Resolve 2 Hrs @ 150 v**
Transfer 1 Hr @ 70 v	
Block 1 Hr in 5% MTT (pH-7.4)	**6% MTT (pH-7.6)**
O/N @ 4°C in 5% MTT (pH-7.4)	**6% MTT (pH-7.6)**
w/ 1:5,000 Ab #181	
Wash 3 x 5 min with TT	**4 x 5 min**
1 Hr w/ goat a-rabbit in 5% MTT	**6% MTT**
Wash 4 x 5 min with TT	
ECL	

Figure 30. Modified western blot analysis on mouse liver samples using a GHR antibody. A. A GHR westerns performed using a protocol from Dr. Cataldo (Cataldo, 2001). The last 3 lanes contain liver samples from -/- GHR KO mice, which do not express the GHR, while lanes 1-6 contain liver samples from GHR +/- and +/+ mice, which express GHR. B. A GHR western performed using a modified protocol based on the protocol from Dr. Talamantes. Lane 3 contains pooled liver samples from 3 -/- GHR KO mice as indicated, while the other lanes contain liver samples from +/+, +/-, GHR-RZ positive and negative animals all of which express the GHR. C. The columns below the two immunoblots are a brief description of the initial protocols used for western blot analysis. The arrows indicate the modifications that were made with the old protocol to the left and the modification to the right of the corresponding arrow. The pH, NaCl and milk concentrations were altered individually in the MTT buffers (Milk, TBS-Tween) as well as the voltage and duration of resolving the SDS-PAGE gel to produce a more distinct GHR band.

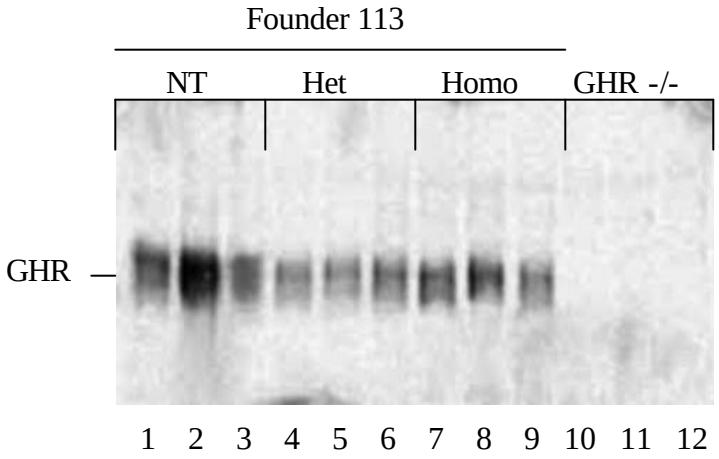

Figure 31. Western blot analysis on individual mouse liver samples using a GHR antibody. Lanes 1-9 contain individual liver samples from fourth generation offspring of RZ DNA-positive founder 113. Three non-transgenic littermates (lanes 1-3), three heterozygous GHR-RZ mice (lanes 4-6), and three homozygous GHR-RZ mice (lanes 7-9) were used. Liver samples from three individual GHR -/- animals were included as controls (lanes 10-12).

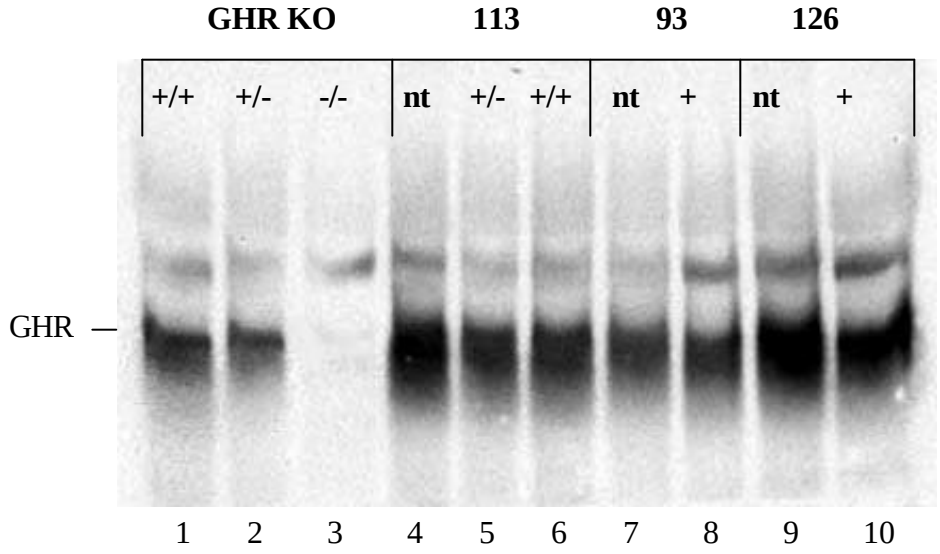

Figure 32. Western blot analysis on pooled mouse liver samples using a GHR antibody. All lanes contain pooled liver samples from 6 mice of the indicated genotype. Lanes 1-3 contain liver samples from the three genotypes of the GHR "knockout" mice as indicated. Lanes 4-6 contain liver samples from the three genotypes of the founder 113 GHR-RZ mice as indicated. Lanes 7 & 8 contain samples from non-transgenic littermates and RZ positive mice from founder 93, respectively. Lanes 9 & 10 contain samples from non-transgenic littermates and RZ positive mice from founder 126, respectively.

westerns performed on liver samples from individual mice it could not be concluded that a decrease in GHR had actually occurred in transgenic mice from founder 113. But, in the event that the observed slight decrease in GHR from the founder 113 mice was actually representative of a decrease in receptor levels, this line was further analyzed for decreased GHR levels.

Since it is known that heterozygous GHR (+/-) "knockout" mice have a decrease in GHR (only one functional allele), and that these animals do not appear to exhibit any observed phenotypic change as a consequence, the founder 113 GHR-RZ mice were crossed with heterozygous "knockout" mice to produce GHR-RZ transgenic mice that have only one functional GHR allele. The reasoning for this cross is to create an observable phenotypic change in the heterozygous GHR (+/-) "knockout" mice. If a decrease in GHR levels had occurred in the founder 113 line of mice, this cross could possibly decrease the levels of GHR in the heterozygous GHR +/- mice to levels sufficient for change into a phenotype. Additionally, half the animals obtained from these breedings were given drinking water with 25 mM $ZnSO_4$ in an effort to upregulate transcription of the metallothionein-I driven GHR-RZ "mini-gene".

One hundred thirty two (132) mice were obtained from breeding the founder 113 line of mice with heterozygous "knockout" mice. DNA slot blot analysis using a probe directed to the metallothionein-I transcriptional regulatory element was used to screen the mice for the presence of RZ-DNA (see figure 33). Of the 132 mice screened, 67 were DNA positive. PCR screening was used to determine the genotype

of the GHR heterozygous (+/-) and wild type (+/+) mice (see figure 34). Of the 132 mice screened, 63 were missing one allele while the other 69 mice had both functional GHR alleles. For PCR screening, the 5'-primer was directed to sequence located in exon 3. Two 3'-primers were used to distinguish between the wild type GHR/BP gene and the disrupted gene. The first 3'-primer was directed to sequence located in exon 4. This sequence was present in both wild type and gene-disrupted genes. The second 3'-primer was directed to a duplicated sequence located in the neomycin insert present only in disrupted genes. Wild type mice produced a single 390 bp PCR product, while the heterozygous mice also produced the 390 bp PCR product (heterozygous animals still have one functional allele) as well as 290 and 220 bp PCR products.

The four genotypes (+/+ GHR without RZ, +/- GHR without RZ, +/+ GHR with RZ, and +/- GHR with RZ) were divided into two groups (Zn treated and control) to create 8 different groups of mice. Male and female mice were further divided to create 16 distinct groups of mice. The phenotypes that were measured were body weight (see figures 35-39) and GHR levels (see figure 40). All mice were weighed once a week on the same day. Weight measurements starting at weaning (4 weeks of age) and continued for 8 weeks. Statistical analysis of mouse weights revealed no significant change in weight between transgenic GHR-RZ mice and non-transgenic mice regardless of sex, "Knockout" genotype, or zinc treatment. Even when all groups were combined to create RZ transgenic and non-transgenic groups with n = 67 and n = 65, respectively, no significant difference in weights was observed (see figure 39). In addition, GHR western blot analysis of pooled male and female liver samples

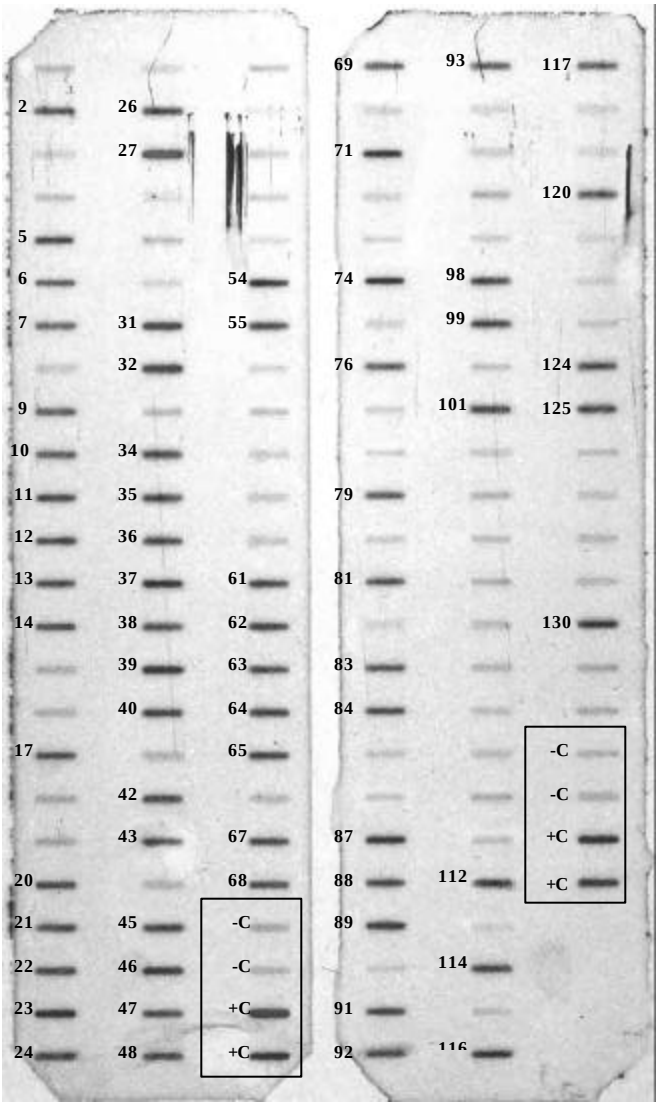

Figure 33. DNA slot blot analysis of tail DNA isolated from offspring of matings between founder 113 GHR-RZ mice and GHR heterozygous "knockout" mice. DNA slot blot analysis using a probe directed to the metallothionein-I transcriptional regulatory element was used to screen the mice. Of the 132 mice screened, 67 were DNA positive as indicated with animal number to the left of each corresponding blot. Two previously identified non-transgenic tail samples and two RZ transgenic tail samples were included as controls (boxed).

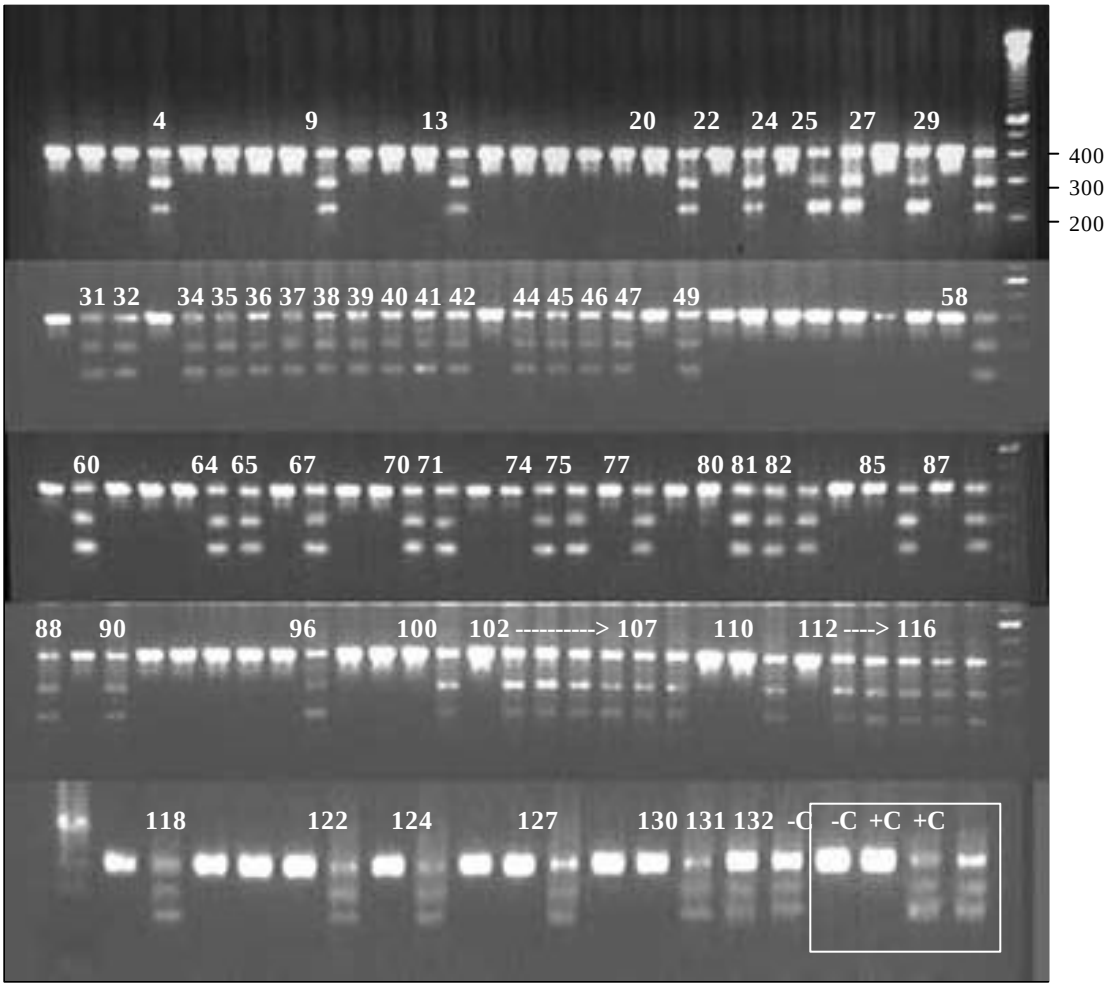

Figure 34. PCR screening of mouse tail DNA isolated from offspring of matings between founder 113 GHR-RZ mice and GHR heterozygous "knockout" mice. Of the 132 mice screened, 63 were DNA positive as indicated with animal number above each of the corresponding PCR products. Two previously identified wild type tail samples and two heterozygous "knockout" tail samples were included as controls (boxed). The 5'-primer was directed to sequence located in exon 3. Two 3'-primers were used to distinguish between the wild type GHR/BP gene and the disrupted gene. The first 3'-primer was directed to sequence located in exon 4. This sequence was present in both wild type and disrupted genes. The second 3'-primer was directed to a duplicated sequence located in the neomycin insert present only in disrupted genes. Wild type mice produced a single 390 bp PCR product, while the heterozygous mice also produced the 390 bp PCR product (heterozygous animals still have one functional allele) as well as 290 and 220 bp PRC products. A 100 bp DNA molecular weight standard is present in the top right lane. The 200, 300, and 400 bp bands are marked to the right of the bands.

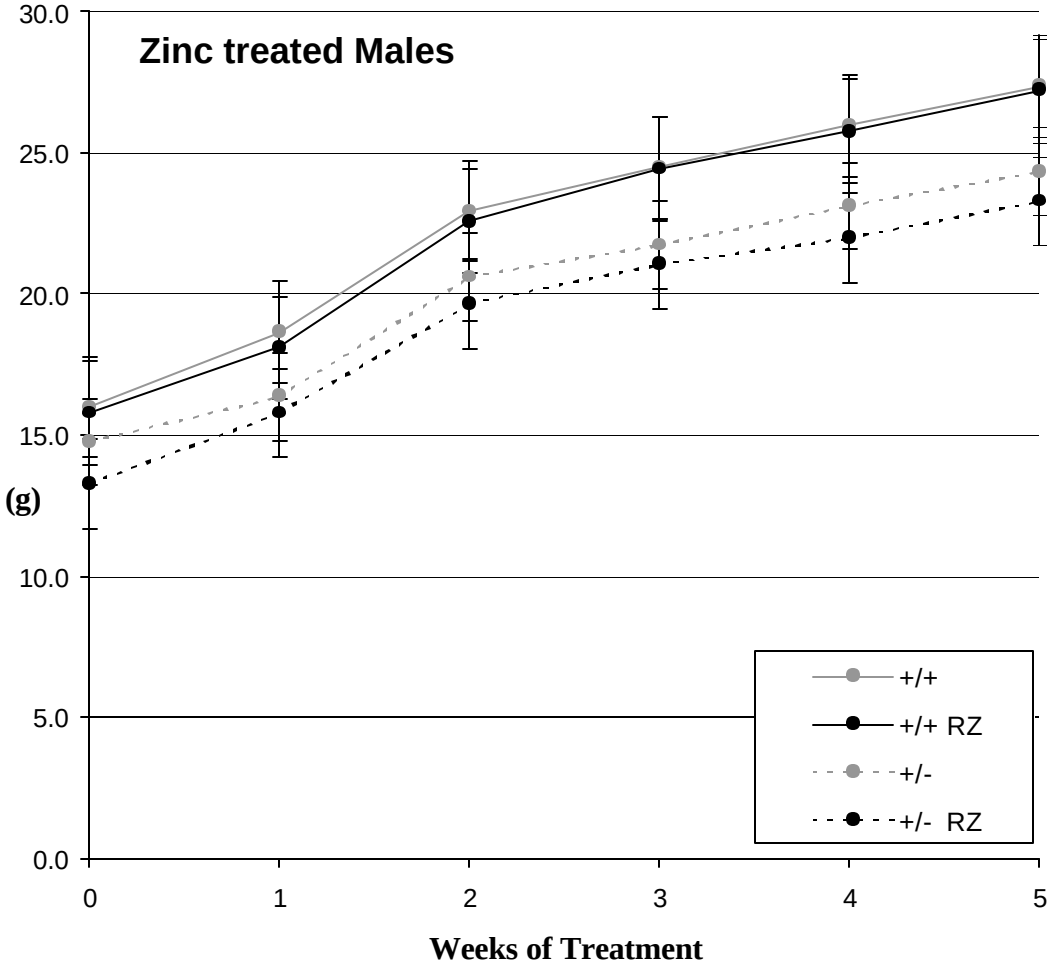

Figure 35. Mouse weights from zinc-treated male offspring of matings between GHR-RZ mice and GHR heterozygous "knockout" mice. Offspring were given 25 mM $ZnCl_2$ drinking water starting at one month of age. Weights were recorded at the start of treatment (1 month old) and continued for 5 weeks. Data points represent the average weights of groups with 6-9 individuals for each genotype. Four genotypes are represented for each group (+/+ = Wild type GHR, no RZ; +/+ RZ = Wild type GHR, RZ transgenic; +/- = Heterozygous GHR KO, no RZ; +/- RZ = Heterozygous GHR KO, RZ transgenic). Error bars represent standard error of the mean of each point.

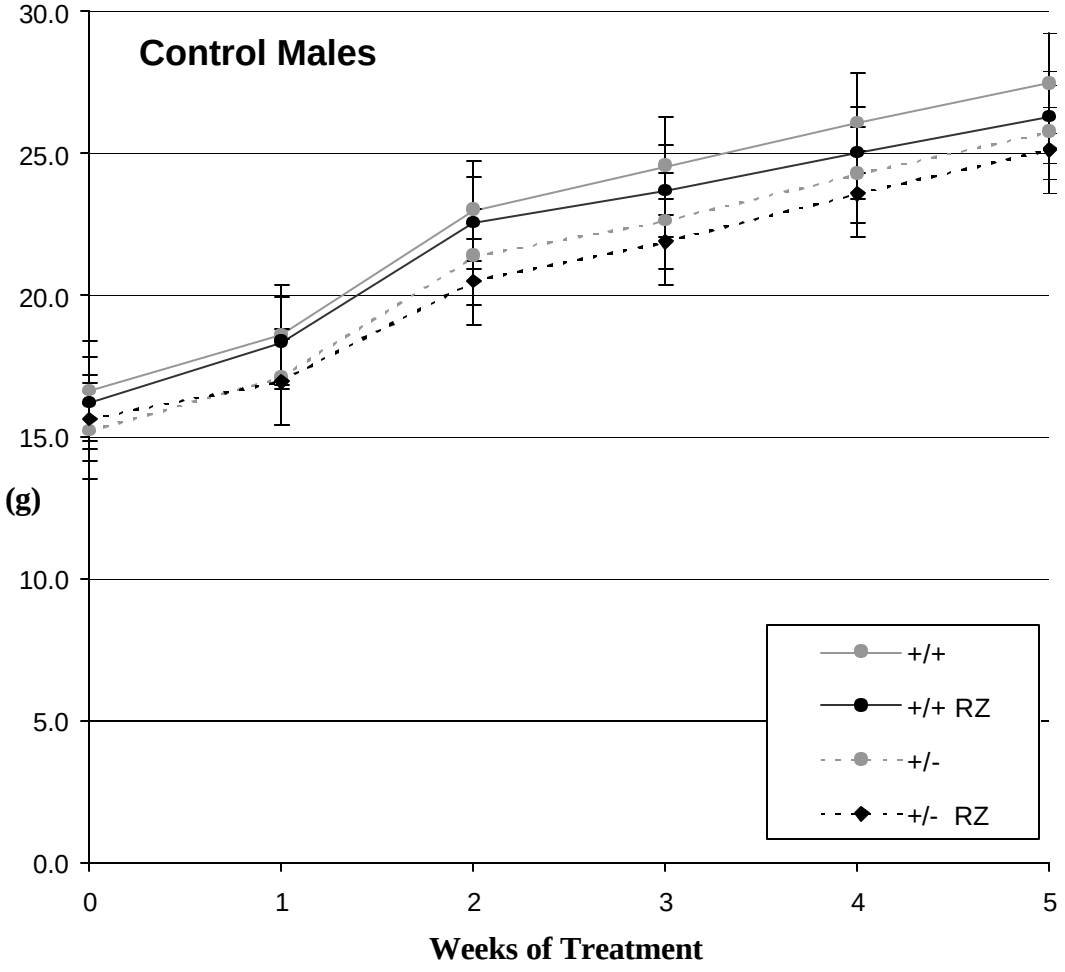

Figure 36. Mouse weights from non-treated male offspring of matings between GHR-RZ mice and GHR heterozygous "knockout" mice. Offspring were given distilled drinking water starting at one month of age. Weights were recorded starting at 1 month of age and continued for 5 weeks. Data points represent the average weights of groups with 6-9 individuals for each genotype. Four genotypes are represented for each group (+/+ = Wild type GHR, no RZ; +/+ RZ = Wild type GHR, RZ transgenic; +/- = Heterozygous GHR KO, no RZ; +/- RZ = Heterozygous GHR KO, RZ transgenic). Error bars represent standard error of the mean of each point.

Figure 37. Mouse weights from zinc-treated female offspring of matings between GHR-RZ mice and GHR heterozygous "knockout" mice. Offspring were given 25 mM $ZnCl_2$ drinking water starting at one month of age. Weights were recorded at the start of treatment (1 month old) and continued for 5 weeks. Data points represent the average weights of groups with 9-10 individuals for each genotype. Four genotypes are represented for each group (+/+ = Wild type GHR, no RZ; +/+ RZ = Wild type GHR, RZ transgenic; +/- = Heterozygous GHR KO, no RZ; +/- RZ = Heterozygous GHR KO, RZ transgenic). Error bars represent standard error of the mean of each point.

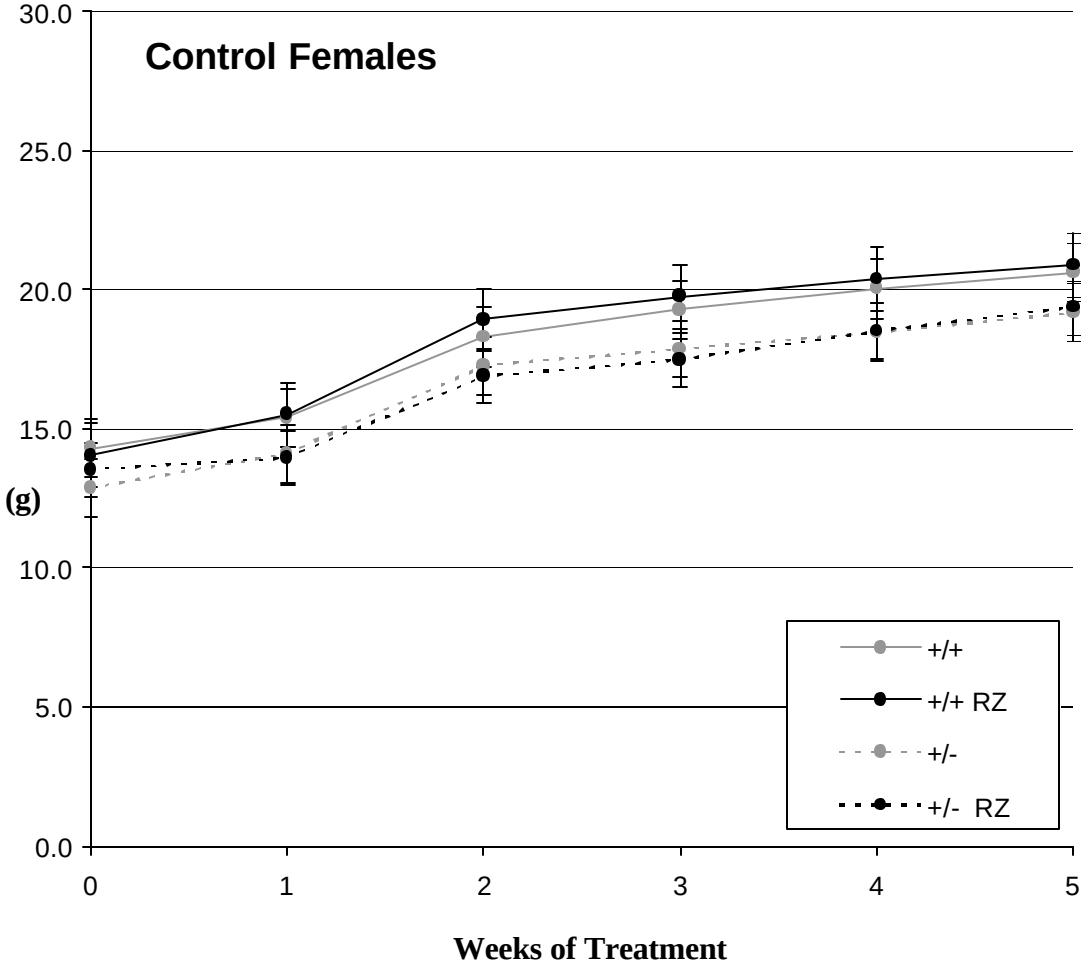

Figure 38. Mouse weights from non-treated female offspring of matings between GHR-RZ mice and GHR heterozygous "knockout" mice. Offspring were given distilled drinking water starting at one month of age. Weights were recorded starting at 1 month of age and continued for 5 weeks. Data points represent the average weights of groups with 9-10 individuals for each genotype. Four genotypes are represented for each group (+/+ = Wild type GHR, no RZ; +/+ RZ = Wild type GHR, RZ transgenic; +/- = Heterozygous GHR KO, no RZ; +/- RZ = Heterozygous GHR KO, RZ transgenic). Error bars represent standard error of the mean of each point.

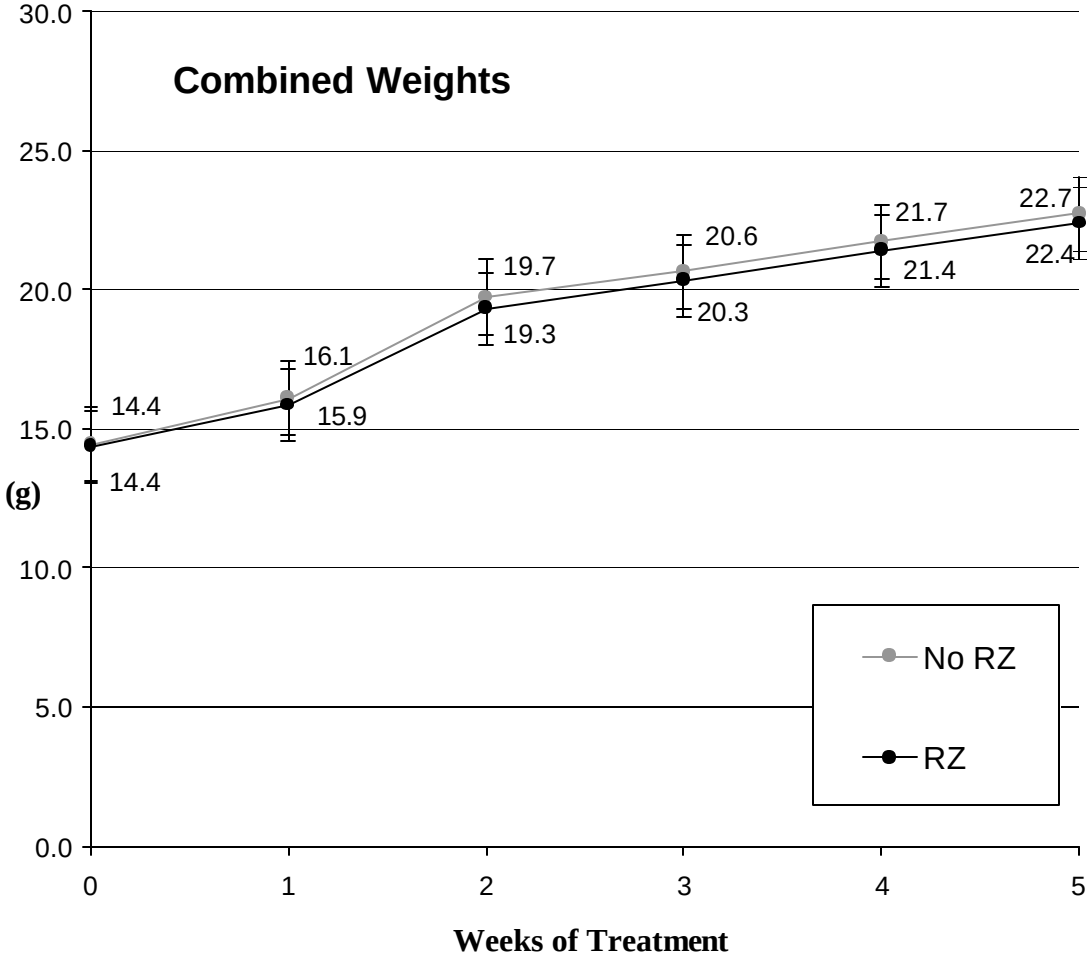

Figure 39. Mouse weights from all offspring of matings between GHR-RZ mice and GHR heterozygous "knockout" mice. To detect any effect the RZ had on animal weight, all genotypes (GHR +/+ and GHR +/-), sex, and zinc treatment groups of mice were combined into two main groups (RZ transgenic and non-transgenic). Data points for RZ transgenic mice represent the average weights from a group with 67 individuals, while data points for non-transgenic mice represent the average weights from a group with 65 individuals. Error bars represent standard error of the mean weight at each time point.

from each of the separate groups (except male and female samples) also showed no difference between GHR levels when GHR-RZ transgenic samples were compared to non-transgenic controls regardless of zinc treatment (see figure 40).

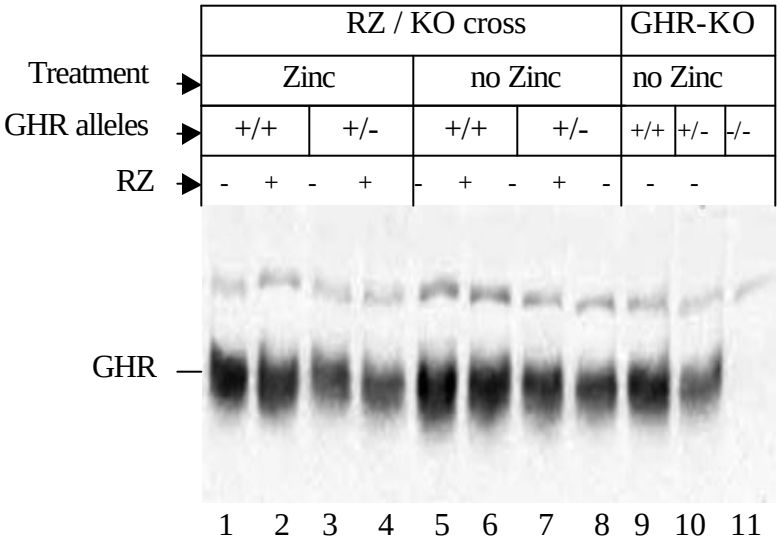

Figure 40. Western blot analysis of pooled mouse liver samples isolated from offspring of matings between founder line 113 GHR-RZ mice and GHR heterozygous "knockout" mice using a GHR antibody. All lanes contain pooled liver samples from 6 mice (3 male and 3 female) of the indicated genotype. Lanes 1-4 contained liver samples from the zinc treated mice with the genotypes indicated above the lanes. Lanes 5-8 contained liver samples from the mice not treated with zinc (genotypes are indicated above the lanes). Lanes 9-11 contained liver samples from the three genotypes of the non-zinc treated GHR "knockout" mice to serve as controls.

DISCUSSION

There are many factors to consider when designing an efficient hammerhead ribozyme for decreasing gene expression. First, an appropriate target sequence must be selected. While the target sequence can contain the nucleotides NUH, where N is any base and H can be A, U, or C, the triplet sequence GUC has been shown to have the highest cleavage potential (Shimayama et al., 1995). The second GTC following the ATG translational start site in exon 2 was selected as the target site for ribozyme cleavage. This site was selected based on several criteria reported to influence ribozyme activity. The specificity and efficiency of a RZ is proposed to be increased by increasing the number of adenosines (#As) in the ribozyme arms (Herschlag, 1991). Multiple repeats of a single nucleotide (m-Ns) are discouraged in primer prediction programs such as GeneWorks^{TM}. The strong binding associated with high (GC) content favors non-specific association with short stretches of sequence and is, therefore, discouraged (Herschlag, 1991). Ribozymes have been shown to degrade at a higher rate when UA and CA dinucleotides are present. These sites are specific targets for an unidentified endoribonuclease (Qiu et al., 1998). Using these criteria, the second GTC following the translational start site in exon 2 of the GHR was selected as the target site for ribozyme cleavage. This region was also selected because of its proximity to the 5' end of the message. The reasoning behind this strategy is to avoid the translation of a 5' cleavage product, as previously reported (Wang et al., 1999a). In this report, the 5' cleavage product of Apolipoprotien B mRNA was translated yielding a truncated protein with the predicted size. Potential GTC target sites located within the first exon of GHR representing the 5' untranslated

region of the message were not used due to presence of multiple 5' untranslated regions (Moffat et al., 1999). Similarly, the first GTC located in exon 2 was ruled out because the G in the GTC was the first nucleotide of the exon and any ribozyme designed to this region would have to span the splice junction from exon 1. The hammerhead ribozyme catalytic core was selected over other potential ribozymes due to its broad use and superior *in vitro* and *in vivo* catalytic activity when directly compared to the hairpin and HDV ribozymes (Chowrira et al., 1994). Flanking the hammerhead catalytic core were 12 nt 5' and 3' arms. Although this length was selected based mainly on other successful hammerhead ribozymes expressed in transgenic mice from the literature (Efrat et al., 1994; L'Huillier et al., 1996), this decision was more arbitrary than other design aspects of the ribozyme. The GC content and arrangement of each target site presented in the literature are unique and, therefore, each target sequence would most likely have its own "optimal length". With no steadfast number given for RZ arm length, several arguments in the literature were considered. The numbers of bases present in the antisense arms affects the specificity and turnover rate of the ribozyme. Longer antisense arms decrease the turnover rate, while increasing the specificity of the ribozyme to its designated target RNA. A greater G/C content also decreases the turnover rate because of the relative number of hydrogen bonds compared to A/U (three and two, respectively). It has been reported that the optimal K_{cat}/K_m at 37°C is achieved *in vitro* when helix I and III are a combined length of 12 nucleotides (Bertrand and Rossi, 1994). While this length may be optimal *in vitro*, it appears that longer lengths are required for target site

recognition *in vivo* (Gavin et al., 1997). In addition, the consequence of using a ribozyme that only recognizes 12 bases of a target mRNA would be an increase in non-specific mRNA cleavage. According to Alberts and his colleagues, there are an estimated 20,000 different mRNA species in a typical mammalian cell with an average length of 2000 bases (Alberts, 1994). If this estimation holds true, the sequence complexity would be $\sim 4 \times 10^7$. For a ribozyme to recognize a unique sequence, at least 13 bases are needed to produce a complexity of $\sim 7 \times 10^7$ or (4^{13}).

The final consideration affecting RZ performance was the type of mammalian expression plasmid. The expression plasmid used for RZ production in animal cells is an important consideration. High levels of RZ transcript are required for significant decreases in targeted gene products (Bertrand et al., 1997). The expression plasmid selected for RZ expression utilized the mouse metallothionein-I TRE and a bGH polyadenylation signal. The mouse metallothionein-I TRE coupled with the bGH polyadenylation signal has proven to be an effective combination in our and the laboratory of others (Kopchick et al., 1990; Miller et al., 1989; Naar et al., 1991; Sotelo et al., 1995). Even in the absence of metal ion treatment the mouse metallothionein-I TRE activates transcription at high levels in mouse cells. Moreover, the expression of metallothionein-I driven constructs is ubiquitous (Choudhuri et al., 1995; Leone, 1986; Pitt et al., 1992; Zelger et al., 1993). Therefore, this fusion gene was utilized for RZ expression in cultured cells and in mice.

Prior to expressing the RZ in cells, the ability of the RZ to specifically cleave GHR-RNA was tested. The incorporation of a core T7 promoter sequence into the

design of the 5' primer allowed the PCR product to serve as a template for run-off transcription by T7 DNA polymerase (Weier and Rosette, 1990). This strategy successfully allowed us to bypass an additional cloning step in which the GHR-RZ construct would have been sub-cloned into a T7 promoter containing plasmid for *in vitro* run-off transcription. PCR generated DNA templates of the GHR-RZ were designed to match the predicted size of the *in vivo* transcribed GHR-RZ. The beginning and ending of PCR amplification for the RZ DNA template was at the Met-I transcriptional start site and bGH poly A addition site, respectively. This allowed for the production of a PCR product that, when transcribed *in vitro* by T7 DNA polymerase run-off transcription, would produce RNA similar in size to the predicated RZ-mRNA transcribed *in vivo* with the exception of 5' and 3' end processing.

Initially, the same strategy that was used to create the full length RZ RNA was used to create GHR-DNA templates. Production of RNA from the full-length GHR-DNA templates (~2.1 kb) proved to be troublesome as low yields of *in vitro* transcribed GHR-RNA were obtained. The low yields from the *in vitro* transcription reactions are possibly due to the presence of sequences that resemble phage termination signals, or due to the longer length of template increasing the likelihood that the polymerase would fall off of the template prior to transcription of the full length RNA. Of the two possibilities, the latter appears to be more likely in that specific bands were not observed, only non-specific smears from the predicted size to ~500 bases were observed.

The second 3'-primer was designed to produce a truncated (618 bp) GHR-DNA template. The truncated GHR gave high yields of PCR generated full length DNA template, high yields of *in vitro* transcribed GHR-RNA, and the RNA was successfully resolved on polyacrylamide gels. Although a full length GHR-RNA substrate was more desirable in order to mimic the size of the cellular counterpart, even a full length *in vitro* transcribed GHR-RNA still would not represent the true cellular GHR-RNA. Events such as 5' and 3' processing not only change the size of the RNA but also allow for auxiliary RNA binding proteins to bind the RNA. This in addition to many other cellular factors that are not represented in test tube RNA reactions places less importance on obtaining a "full length" substrate RNA for *in vitro* cleavage reactions. Therefore, considering the statements above, the difficulty in obtaining and handling of full length substrate, and since the RZ cleavage site was located only 91 nts from the 5' end of the GHR transcript, the GHR truncated 618 nts after the transcriptional stat site was used for *in vitro* analysis.

Cleavage of the truncated GHR-RNA was observed in each RCA containing the GHR-RZ (with the exception of the RCAs performed at 0ºC, pHs below 7, and reaction performed without $MgCl_2$), while cleavage was not observed in similar reactions without RZ. This demonstrated that the GHR-RZ was catalytic. The production of *in vitro* synthesized RNA for the RZ cleavage assays also limited the possibility of proteinacious contaminates that could still be present if RNAs were isolated from cells or if RCAs were performed in cell lysates. The predicted 527nt 3' and 91nt 5' cleavage products observed in each of the reactions suggests that cleavage

had occurred at the engineered target site. No secondary cleavage bands were observed in any of the RCAs performed although non-specific smearing on the silver stained gels was observed to some degree for all of the RCAs performed. Examples of smearing are seen in figure 20 where the degree of smearing increased with incubation time. Since this smearing did not produce any discernable banding in the silver stained gels and because the smearing was similar to that observed in reactions without RZ, it appears that the degradation of the RNA was not related the RZ. The smearing was most likely due to RNase contamination (Bisbal, 1997; Goto and Mizuno, 1971; Hajnsdorf et al., 1994). With this said, one could argue that it is possible that a contaminating endo-RNase cleaved the GHR-RNA instead of the ribozyme still exists. However, since the smearing was observed in both RZ containing and non-RZ containing RCAs, and no specific band was observed in RCAs not containing RZ, it is highly unlikely that the contaminating RNases caused the specific cleavage observed only in RZ containing reactions. Another explanation for the nonspecific degradation of RNA was due to Mg^{2+} in the reactions. When Mg^{2+} concentrations were altered in the RCAs, non-specific smearing was also observed at higher concentrations of Mg^{2+} (see figure 17). This was not surprising since certain metal ions such as Mg^{2+} and Mn^{2+} are known to cause non-specific cleavage of RNA (Kuo and Herrin, 2000). Although Mg^{2+} probably contributed to the non-specific RNA degradation, the majority of the degradation was again most likely due to RNases because reactions performed in the absence of Mg^{2+} still exhibited degradation (figure 17).

Interestingly, the 5'-cleavage product was more protected from degradation than the 3'-cleavage product; uncleaved substrate RNA; and the RZ RNA as seen in figure 20. Following 24 hours of incubation, only the 5'-cleavage product remained clearly visible while the other RNAs were barley detectable. It is possible that the secondary structure formed in the 5'-cleavage product protected it from RNase degradation. While many RNases appear to be non-specific, some RNases have been shown to recognize certain RNA structures (Diwa et al., 2000). It is also possible that the small size of the 5'-cleavage product precluded it from RNase degradation. Certain RNA binding proteins such as poly A binding proteins (PABP) have been shown to require specific lengths of sequence, and once the sequence is reduced beyond this requirement, the PABPs no longer recognize the RNA and fall off (Beelman and Parker, 1995). While 91 nucleotides is much larger than the ~30 nucleotide requirement for PABP, it is possible that the particular RNases that are contaminating the *in vitro* RCAs have some sort of length requirement.

It must be noted that *in vitro* reactions were performed solely for the purposes of describing the enzymatic activity of the RZ *in vitro* and not as for the purpose of predicting success *in vivo.* This is important when considering the performance of the RZ under various conditions such as temperature. We see from the temperature optimization reactions that the RZ was most active at 59ºC (figure 19). If only *in vitro* results were considered when designing a RZ, then it would make sense to redesign the RZ with shorter antisense arms and/or lower GC content. But the complexity of the cell has made such predictions inappropriate as it has been shown previously that

no correlation exists between *in vitro* and *in vivo* RZ activity (Crisell et al., 1993; L'Huillier et al., 1992; Steinecke et al., 1994). Perhaps Crisell's experiments demonstrated this point most effectively by comparing the activities of 11 different hammerhead ribozymes *in vitro* and then *in vivo* for the ability to inhibit HIV. Crisell reported that ribozymes with high efficiency *in vitro* had failed to inhibit HIV in cells. In contrast, he also observed the inhibition of HIV by a ribozyme that did not show efficient catalytic activity *in vitro*. However, *in vitro* studies are valuable in that they demonstrate that a given RZ design possesses enzymatic activity. Detection of RZ cleavage *in vivo* is difficult due to rapid degradation of the unprotected cleavage products, therefore, performing in vitro cleavage assays are worthwhile.

Explanations for the lack of correlation when RZ are used *in vivo* can be attributed to reports that RZ activity can be enhanced or inhibited by associating with several types of molecules. RNA binding proteins such as nucleocapsid protein of HIV-1 (NCp7) and hnRNP A1 enhance the turnover rate of ribozymes by accelerating the attainment of the thermodynamically most stable species throughout the ribozyme catalytic cycle (Bertrand and Rossi, 1994; Herschlag et al., 1994; Tsuchihashi et al., 1993). In addition, NCp7 has been shown to resolve a misfolded ribozyme-substrate RNA complex that is otherwise long lived (Herschlag et al., 1994). Certain aminoglycosides can inhibit the activity of ribozymes (Earnshaw and Gait, 1998; Hermann and Westhof, 1998; Llano-Sotelo and Chow, 1999). Crystallography analysis has revealed structural complementarities between the charged amino groups on aminoglycosides and the metal binding sites within the catalytic pocket of

hammerhead ribozymes (Hermann and Westhof, 1998). This indicates the aminoglycosides actually compete with magnesium for the metal binding sites within the catalytic domain. In contrast, viomycin has been shown to enhance the interactions between RNA molecules, increasing the cleavage activity of ribozymes (Olive et al., 1995). Unlike aminoglycoside antibiotics, viomycin is a basic cyclic peptide antibiotic of the tuberactinomycin group. In the presence of viomycin, the required magnesium concentration is reported to be decreased by one order of magnitude. Oligonucleotide facilitators have also been shown to enhance or inhibit ribozyme activity (Jankowsky and Schwenzer, 1996; Jankowsky and Schwenzer, 1998). When short oligonucleotides directed to the substrate RNA immediately 5' and 3' of helix I and III formation were added to ribozyme cleavage reactions involving substrates of different lengths, it was shown that the presence of the facilitators enhanced ribozyme cleavage. It is proposed that the facilitators accelerate the association of the ribozyme and substrate by coaxial helix stacking. The effect of the facilitators may also cause a conformational change in the substrate RNA increasing accessibility to ribozyme binding. And while oligonucleotides do not exist in vivo, the presence of many RNA species could mimic this effect for certain targeted RNAs.

Following the *in vitro* confirmation that the GHR-RZ was catalytically active and specific for the engineered target site, the GHR-RZ was tested in cultured cells. Since the GHR-RZ was ultimately designed for expression in mice, a mouse cell line was chosen for cellular analysis. Although our laboratory already had mouse L cell lines stably transfected with GHR cDNA the cDNA was isolated from pig (Wang et

al., 1993b), analysis of the target site in the porcine GHR nucleotide sequence compared to that of the mouse revealed that 7 out of the 24 nucleotides represented in the RZ/GHR helices were mismatched. Therefore, to create a mouse line with high levels of mouse GHR, L cells were transfected with a mouse GHR/BP "mini-gene". The "mini-gene" contained mouse GHR cDNA from exon 2-10 with a section of genomic sequence from exon 7 through exon 8. Following confirmation by PCR of stable DNA incorporation, GHR expression was measured using GH binding assays. GHR expression was observed in 100% of 15 GHR/BP DNA positive lines isolated. This not only provided a cell line in which the GHR-RZ could be tested, it demonstrated that the mouse metallothionein TRE was active in these cells. One of the cell lines (E6) that demonstrated a relatively moderate level of GHR expression was selected for RZ analysis.

The GHR-RZ construct pMet-GHR-RZ was stably transfected into the E6 cell line. The stable integration of the pMet-GHR-RZ into the E6 cell genome was verified by PCR. The ability of the RZ to decrease GHR expression was verified by northern blot, western blot, and GH binding assays. All three methods used to measure GHR levels indicated a 50% decrease in GHR levels was achieved in two of the RZ transfected cell lines (6-4 and 6-5). Western blot analysis using a monoclonal antibody directed to the cytoplasmic region of the GHR revealed three separate bands (110 kDa, 66 kDa and 46 kDa) specific for the intracellular region of the GHR (see figure 24). While the predicted molecular mass of the GHR protein is 72.8 kDa, post-translational modifications such as glycosylation and ubiquitination produce a 110-120

kDa protein. While the presence of multiple bands is often described in GHR western blot analyses, the true identities of these bands remain unknown. Since the antibody used in this case was directed to the cytoplasmic domain of the GHR, the GHBP corresponding to the extracellular domain of the receptor can be ruled out. While it is tempting to suggest that the 110 kDa GHR yielded the 66 and 46 kDa bands, the specificity of the antibody to the cytoplasmic domain once again rules out this possibility. It is therefore likely that the bands represent two separate products of the cytoplasmic domain that differ in size but contain the same epitope to which the antibody recognized.

GHBP levels were also decreased in the RZ transfected cell lines 6-4 and 6-5 by 32 and 38%, respectively. While a decrease was expected in GHBP because the RZ targeted exonic sequence common to both GHR and GHBP mRNAs (exon 2), the decrease was not equal to that observed for the GHR (both ~50%). Analysis of the northern blot using a probe directed against exons 2-7 also demonstrated that more GHBP mRNA was present in RZ transfected cells as well as in non-RZ transfected cells (figure 23). This indicated that the parental E6 cells were producing more GHBP than GHR mRNA to begin with and that the RZ was not preferentially decreasing GHR message. The presence of introns flanking exon 8a in the pMet-GHR/BP "minigene" allowed for alternative splicing of the pre-mRNA GHR/BP transcript to GHBP and GHR mRNAs. The inclusion of exon 8a allows for the production of GHBP mRNA while skipping this exon allows for the production of GHR mRNA. Apparently a preference for the inclusion of exon 8a exists in this cell line with this

construct. Recently it has been suggested that the opposing effects of serine/arginine-rich proteins (SR) and heterogeneous nuclear ribonucleoprotein (hnRNP) A1 influence alternative splicing (Caceres et al., 1994; Ichida et al., 2000). Increased expression of SR activates proximal 5' splice sites, and promotes the exon inclusion, while increased expression of hnRNP A1 activates distal 5' splice sites and promotes exon skipping. Therefore, if this view of control during alternative splicing is correct, it would be interesting to see if SR is expressed to a greater extent than hnRNP A1 in these cells and if these cells favor exon inclusion for all pre-mRNAs.

Attempts to detect the RZ RNA were unsuccessful using northern blot analysis and RNase protection assays. Difficulties in detecting RZs expression with significant reductions in the targeted genes have been reported previously (Efrat et al., 1994; Heinrich et al., 1993; Sokol and Murray, 1996). Larsson and colleagues reported a 22-94% decrease in β2M mRNA levels from lung tissue of individual transgenic mice with no detection of RZ RNA by northern blot analysis, or by RNase protection assays (Larsson et al., 1994). Efrat and colleagues reported a 70% decrease in islet GK activity with no detection of RZ RNA by northern blot analysis, or by RNase protection assays (Efrat et al., 1994). The first ribozyme to be detected by Northern blot analysis in a transgenic mice was described by L'Huillier and colleges in 1996 (L'Huillier et al., 1996). Prior to this all other ribozymes were detected by RT-PCR. A possible reason for this may be due to differences in size. The RZ utilized here was predicted to be 161 nucleotides in length (not including the poly A tail). The RZ that was detected by northern was predicted to be 1150 bases after transcription and

splicing, not including polyadenylation. The large size of this ribozyme was due to the large 5' (transcription initiation was ~268 bases upstream of the ribozyme) and 3' (the poly (A) cleavage site was ~822 bases downstream of the ribozyme) untranslated regions. It is possible that the very nature of ribozymes with strong secondary structure, small size, and the formation of antisense recognition with target RNA, makes the detection of RZs difficult.

Following the successful reduction in GHR levels in the E6 cells transfected with RZ, we wanted to see if this reduction was sufficient to alter GH signaling through STAT-5 activation. The two RZ transfected cell lines (6-4 and 6-5) exhibited a distinct reduction in GH stimulated STAT-5 activation as determined by western blot analysis using anti-phosphotyrosine (PY-20) serum. The bands migrating at 95 kDa have been shown previously to be STAT-5 in three separate laboratories (Chow et al., 1996; Ram et al., 1996; Silva et al., 1996; Wang et al., 1994; Xu et al., 1996; Xu et al., 1995). The degree of reduction was greater than 50% for both of the RZ DNA positive cell lines. Therefore it appeared that a 50% reduction in GHR level was sufficient to decrease GH stimulated signal transduction through STAT-5 in E6 cells (see figure 25).

In an effort to better understand the relationship between GHR level and STAT-5 activation, the stable cell lines initially transfected with the GHR/BP "mini-gene" were further studied in greater detail. Utilizing the range of GHR expression observed in the 15 cell lines, 6 of the stable lines representing the highest, lowest, and 4 intermediate GHR expressers were selected to determine the effect of GHR level on

STAT-5 activation. GHR number in the 6 cell lines ranged from ~50,000 to ~240,000 GHR/cell. Analysis of cell surface receptor number plotted against STAT-5 activation in GH treated cells suggests that maximal activation was approached in cells expressing ~240,000 GHR/cell. Only a slight increase in STAT-5 activation was observed between the cell lines expressing ~160,000 GHR/cell and ~240,000 GHR/cell. In addition, a linear relationship was observed for cells expressing less than ~110,000 GHR/cell.

The RZ transfected clone 6-5 was also analyzed along side the 6 GHR expressing clones. The degree of STAT-5 activation in the RZ transfected cell line 6-5 was similar to that of the GHR expressing clone #8 which expressed ~80,000 GHR/cell. The number of GHRs/cell in the RZ transfected cell line was determined to be ~81,000, also similar to levels observed in clone #8. The similarities in receptor number and STAT-5 activation between these two clones (6-5 & 8) further verified the relationship in that two separate methods were used. For clone #8, 80,000 GHRs/cell were expressed in this cell line due to stable transfection of the GHR/BP "minigene". For clone 6-5, 81,000 GHRs/cell were expressed as the result of a stable RZ transfection into a cell line previously transfected with the GHR/BP "minigene". This was a 48% decrease in GHR number as compared to the parent E6 cells which expressed ~170,000GHR/cell. These results confirmed the previous findings that GHR levels were decreased in these cells by ~50%, and that this decrease was sufficient for a reduction in GH signaling through STAT-5. In addition, the ribozyme-associated reduction observed in clone 6-5 also helped to reinforce the relationship

described by the plot linking GHR number and the degree GH stimulated STAT-5 activation. The transfection of the RZ into clone E6 decreased both the number of GHRs and the degree of STAT-5 activation in a manner that obeyed the line describing the relationship between the two factors determined in the absence of RZ transfection. Simply stated, "the results from the RZ transfected cells were on the line of the results from the GHR transfected cells. "

The pMet-GHR-RZ mammalian expression plasmid was used to generate GHR-RZ transgenic mice. Three of the 127 mice screened by DNA slot blot analysis were DNA positive (mouse #93-female, #113-male, and #126-female). Intensity of the blots as compared to copy number controls indicated that the number of GHR-RZ "mini-genes" integrated in the genome of the positive mice ranged from ~5 to ~30 copies (~5 copies for founder #93, ~5 copies for founder #126, and ~30 copies for founder #113). The livers of sacrificed animals were used to perform GHR western blot analysis. Livers from GHR "knockout" mice were also obtained to serve as controls for the GHR westerns. Based on the intensity of bands following analysis of liver from individual mice, the conclusion drawn was that an insufficient number of samples due to large variations in GHR levels from animals in the same genotype. Determining GHR levels from individual mice was therefore difficult. Therefore, in an effort to increase the number of animals from a given genotype observed by western blot analysis, all 6 liver samples were pooled for each genotype analyzed. Analysis of immunoblots from three westerns revealed no change in GHR levels in transgenic mice from founder 93 and founder 126 when compared to non-transgenic

littermate controls. Only a slight change in GHR levels was observed in transgenic mice from founder 113 when compared to controls. Due to the variability observed in westerns performed on liver samples from individual mice it could not be concluded that a decrease in GHR had actually occurred in transgenic mice from founder 113. But, in the event that the observed slight decrease in GHR from the founder 113 mice was actually representative of a decrease in receptor levels, this line was further analyzed for decreased GHR levels.

Since it is known that heterozygous GHR (+/-) "knockout" mice have a decrease in GHR (only one functional allele) (Zhou 1997), and that these animals do not appear to exhibit any observed phenotypic change as a consequence, the founder 113 GHR-RZ mice were crossed with heterozygous "knockout" mice to produce GHR-RZ transgenic mice that have only one functional GHR allele. The reasoning for this cross was to create an observable phenotypic change in the heterozygous GHR (+/-) "knockout" mice. If a decrease in GHR levels had occurred in the founder 113 line of mice, this cross could possibly decrease the levels of GHR in the heterozygous GHR +/- mice to levels sufficient for phenotypic change. In a further attempted to create a phenotypic change in these mice by upregulating transcription of the metallothionein-I driven GHR-RZ "mini-gene", zinc was introduced to the mice. Treatment was continuous for 5 week. Supplementing the drinking water of a mouse with up to 25 mM $ZnSO_4$ has been shown to increase the rate of transcription of a metallothionein-I TRE containing transgene with no significant change in mortality rate (Eisen et al., 1998; Siewerdt et al., 2000). Mice receiving treatment had their

standard drinking water supplemented with 25 mM $ZnSO_4$ ad libitum starting at age weaning (28 days). Mice were selected at weaning through the next five weeks following weaning in an effort to catch the GH dependent phase of growth. The mice were not treated prior to this because it was not known exactly when the pups would begin drinking the water and if that transition was similar in timing for all mice studied. Therefore the time of regular weaning in the mouse colony was selected. Analysis of mouse growth curves in the GHR -/- mice indicate that the GH dependent growth in mice does not occur until approximately two weeks of age. This is evident in that GHR -/- animals do not show phenotypic differences from GHR +/+ littermates until ~2-3 weeks of age (Zhou 1997). Therefore, the growth in the five weeks following weaning appears to be effected to a great extent by GH. Additionally, because the weights of the mice were the phenotype that was measured, weights were not measured beyond this period as the effects of weight gain are influenced to a higher degree by body fat composition and to less of a degree by longitudinal growth as observed in younger mice. Analysis of mouse weights revealed no significant change between transgenic GHR-RZ mice and non-transgenic mice regardless of sex, "Knockout" genotype, or zinc treatment. In agreement, GHR western blot analysis of pooled male and female liver samples showed no difference in GHR levels when GHR-RZ transgenic samples were compared to non-transgenic controls. The GHR-RZ therefore was ineffective at decreasing GHR in mice.

The precise reason why the RZ failed is not known but several explanations are suggested in figure 41. The inability to detect RZ RNA suggests that the RZ was not

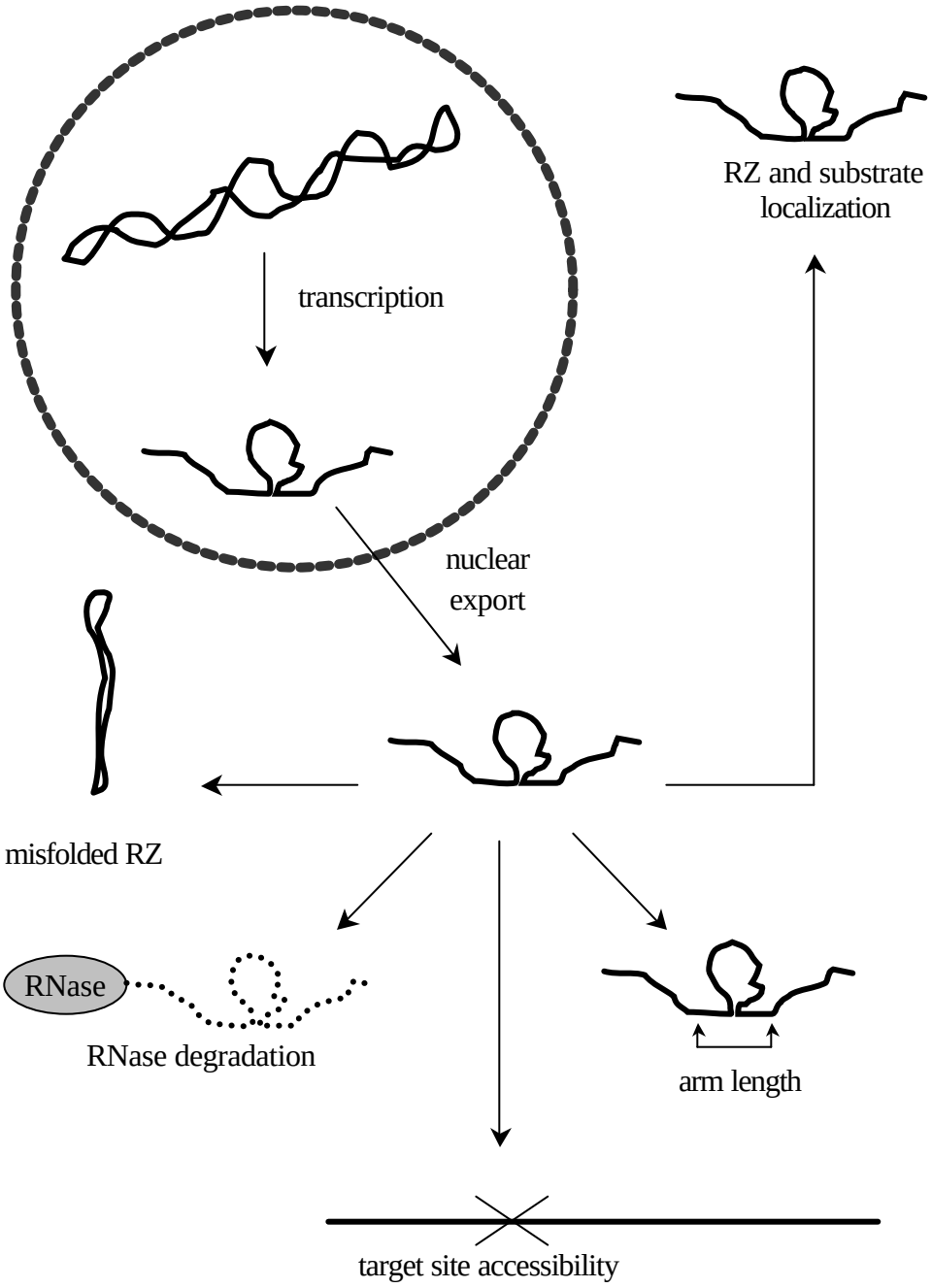

Figure 41. Several important factors that can influence the success of a ribozyme *in vivo*.

expressed. While this remains a likely scenario, the inability to detect RZ does not necessarily mean that it was not there. Reports of successful reductions in gene expression in the absence of RZ detection by northern blot and RNase protection assay suggests that unidentified factors can block RZ detection. The tight secondary structure of RZs and the presence of antisense arms may play a role in blocking detection. Since the RZ was specifically engineered to bind target RNA, it is possible that denaturing conditions during RNA analyses are not sufficient for separation.

If the RZ was not transcribed, a possible explanation might be due to the absence of an intron in the RZ construct. The inclusion of intronic sequence can allow for expression of cDNA in transgenic animals that are not transcribed or are transcribed at low levels in their absence (Brinster et al., 1988; Clark et al., 1993; Whitelaw et al., 1991). In addition, intron containing and non-intron containing constructs that have different transcription efficiencies in transgenic animals can be expressed in cell culture with no difference in transcription efficiency (Brinster et al., 1988; Whitelaw et al., 1991). It is thought that transcriptional enhancer sequences are located in certain introns and therefore inclusion of these introns increases transcription efficiency (Clark et al., 1993; Whitelaw et al., 1991). It is suggested that this effect on genes in animals differs from cultured cells in that cells in living organisms are exposed to more developmental influences (Brinster et al., 1988). In addition, the presence of splicing machinery is thought to increase transcription efficiency and assist in the export of mRNAs though the nuclear pores (Huang and Carmichael, 1996; Lewis and Izaurralde, 1997). Analysis of RZs that have been

shown to decrease target mRNA in transgenic mice previously suggest that the inclusion of an intron into the expression cassette allows for successful transcription of the RZ (Efrat et al., 1994; L'Huillier et al., 1996; Sokol et al., 1998). Although this requirement is not absolute in that a RZ not containing an intron has been reported to be expressed in transgenic mice with concomitant decrease in target RNA (Larsson et al., 1994). It is also possible that the RZ-DNA integrated into a location of the genome that silenced the gene (Clark et al., 1993). While this remains a possibility, it is less likely when we consider that all three separate lines of mice failed to decrease GHR levels. If this were the cause, it would have had to occur in all three mouse-lines. Other possible explanations for the failure of the RZ *in vivo* include: the presence of cellular inhibitors of RZ activity (Feig et al., 1998), misfolding of the RZ (Bassi et al., 1999), RNase degradation (Qiu et al., 1998), the inability of the RZ to be exported from the nucleus (Bertrand et al., 1997; Huang and Carmichael, 1996; Koseki et al., 1999), localization of the RZ to regions of cytoplasm that are distinct from the location of the GHR mRNA (Bertrand et al., 1997; Ding et al., 1993; Oleynikov and Singer, 1998), improper length of the annealing arms leading to decreased turnover for arms that are too long or non-specific recognition for arms that are too short (Gavin and Gupta, 1997; Sioud, 1997), an inaccessible target site due to secondary structure of the GHR mRNA and/or the presence of an RNA binding protein (Amarzguioui et al., 2000; Scherr and Rossi, 1998).

While the GHR-RZ did not decrease GHR levels in transgenic mice, the same RZ construct was successful at decreasing GHR levels by 50% in E6 cells. This

decrease was sufficient enough to alter GH signaling as observed by a concomitant decrease in GH stimulated STAT-5 activation. Therefore, GH resistance was created in the RZ transfected cells. A relationship between the level of GHR expression level and GH induced STAT-5 activation was established in the GHR/BP transfected cells. In RZ transfected cells, the decrease in GHR number and ability to activate STAT-5 conformed to this relationship. Whether a similar decrease in GHR levels in transgenic mice would result in a similar pattern remains unknown. Future experiments that may lead to the successful design of a RZ used for decreasing GHR gene expression to sufficient levels to elicit observable phenotypic changes involve the inclusion of an intron into the pMet-GHR-RZ plasmid and the use of highly active RNA polymerase III promoter driven tRNA-tethered RZs. Currently, tRNA-tethered RZs targeted to the GHR-mRNA have been constructed and preliminary results in cultured cells indicate that they are active (see appendix D). Whether or not these RZs will be active in transgenic mice remains unclear as results from cell culture analysis does not always represent results obtained in an organism.

The complete loss of functional gene expression is the cause of many inherited diseases. Animal models for these conditions can be created by homologous recombination resulting in a gene "knockout". While the complete loss of functional gene expression can account for many genetic disorders, certain diseases can arise from decreases in gene expression. For these conditions, gene disruption via homologous recombination is not always the best method for creating animal models. Ribozymes offer an alternative to conventional gene disruption by decreasing but not

eliminating functional gene expression as no ribozyme expressed *in vivo* has been reported to completely eliminate the gene expression of interest. Our laboratory has created mice that are completely unable to utilize GH (Zhou et al., 1997). This was accomplished using homologous recombination affectively disrupting the GHR gene resulting in GHR -/- mice. While these mice have proved to be a valuable tool for understanding the human condition termed Laron syndrome and have helped to elucidate GH action through studying its absence, we have not been able to study the effects of decreased GH action using these mice. The complete absence of GH action in these mice appears to have some very profound consequences. Aside from the more obvious decreases in growth parameters such body weight (Zhou et al., 1997), delayed sexual maturation (Chandrashekar et al., 1999; Zhou et al., 1997), and decreased bone mineral content (Sims et al., 2000; Sjögren et al., 2000), some beneficial changes such as protection from diabetic nephropathy (Bellush et al., 2000) and a significantly increased lifespan occur (Coschigano et al., 2000). Interestingly, the heterozygous GHR +/- littermates, which are reported to have a significant decrease in GHR expression, do not share any of these physiological "shortcomings" or benefits. With this in mind an important question arises: If the complete lack of GH causes such profound and beneficial effects and the heterozygous GHR +/- mice do not share any of these phenotypes, then at what level of GHR expression do we start to see changes in phenotype.

An answer to this question may also help in other areas of GH metabolism beyond Laron dwarfism. Starvation, sepsis, diabetes, surgery, and critical illness can

be associated with an increased catabolic rate that can prolong recovery and increase morbidity and mortality (Chiolero et al., 1997; Lewis et al., 1997; O'Leary et al., 2000; Thissen et al., 1999). These conditions are associated with GH resistance defined by normal levels of GH and with low levels of IGF-I. In a non-disease state serum IGF-I levels are positively regulated by serum GH, therefore normal to high levels of GH should produce normal to high levels of IGF-I. While complete GH insensitivity has been created in GHR -/- mice, no mouse model for GH resistance exists. Because the heterozygous GHR +/- mice are reported to have decreased GHR levels, it is logical to think that they could serve as a model for GH resistance. Unfortunately, as previously stated they do not exhibit any signs of GH resistance as no other phenotypic changes have been reported when these mice are compared to non-transgenic littermates. Apparently the extent to which GHR expression is decreased in the +/- mice is at a level that still allows for normal GH signaling. We see from the results obtained in cell culture that a 50% decrease in GHR number was sufficient to alter GH-stimulated STAT-5 activation. Moreover, we see that GH-stimulated STAT-5 activation was linear up to ~110,000 GHRs/cell. The relationship between GHR number and GH-stimulated STAT-5 activation began to approach a maximum beyond ~170,000 GHRs/cell as only a slight increase in STAT-5 activation was observed in cells expressing ~240,000 GHRs/cell. If these results obtained in cultured cells are representative of what was occurring *in vivo,* then it is possible that the level of GHRs in mice are above the linear range observed in cells. If this were true then the 50% decrease in GHR levels of the heterozygous male GHR "knockout" mice would only

slightly alter GH-stimulated STAT-5 activation. This phenomenon was observed between cell line 6 which expressed 170,000 GHR/cell and cell line 15 which expressed 240,000 GHRs/cell. The increase of 70,000 GHRs/cell between these two cell lines had little effect on GH-stimulated STAT-5 activation (~3% increase), while a smaller increase (~60,000 GHRs/cell) between cells expressing GHR levels in the linear range such as cell lines 12 (~50,000 GHRs/cell) and 10 (~110,000 GHRs/cell) resulted in a much greater effect on GH-stimulated STAT-5 activation (~69% increase).

BIBLIOGRAPHY

Abe, H., Molitch, M. E., Van Wyk, J. J. and Underwood, L. E. (1983). Human growth hormone and somatomedin C suppress the spontaneous release of growth hormone in unanesthetized rats. *Endocrinology* **113**, 1319-24.

Adam, S. A. (1999). Transport pathways of macromolecules between the nucleus and the cytoplasm. *Curr Opin Cell Biol* **11**, 402-6.

Adams, T. E., Baker, L., Fiddes, R. J. and Brandon, M. R. (1990). The sheep growth hormone receptor: molecular cloning and ontogeny of mRNA expression in the liver. *Mol Cell Endocrinol* **73**, 135-45.

Adams, T. E., Hansen, J. A., Starr, R., Nicola, N. A., Hilton, D. J. and Billestrup, N. (1998). Growth hormone preferentially induces the rapid, transient expression of SOCS-3, a novel inhibitor of cytokine receptor signaling. *J Biol Chem* **273**, 1285-7.

Adeniyi-Jones, S., Romeo, P. H. and Zasloff, M. (1984). Generation of long read-through transcripts in vivo and in vitro by deletion of 3' termination and processing sequences in the human tRNAimet gene. *Nucleic Acids Res* **12**, 1101-15.

Akaboshi, E., Guerrier-Takada, C. and Altman, S. (1980). Veal heart ribonuclease P has an essential RNA component. *Biochem Biophys Res Commun* **96**, 831-7.

Alberts, B. (1994). Molecular biology of the cell. In *Molecular biology of the cell*,, pp. 369. New York: Garland Publishing.

Albuquerque-Silva, J., Milican, F., Bollen, A. and Houard, S. (1999). Ribozyme-mediated decrease in mumps virus nucleocapsid mRNA level and progeny in infected vero cells [In Process Citation]. *Antisense Nucleic Acid Drug Dev* **9**, 279-88.

Allain, F. H. and Varani, G. (1995). Divalent metal ion binding to a conservedwobble pair defining the upstream site of cleavage of group I self-splicing introns. *Nucleic Acids Res* **23**, 341-50.

Allen, R. C., Graves, G. and Budowle, B. (1989). Polymerase chain reaction amplification products separated on rehydratable polyacrylamide gels and stained with silver. *Biotechniques* **7**, 736-44.

Amarzguioui, M., Brede, G., Babaie, E., Grotli, M., Sproat, B. and Prydz, H. (2000). Secondary structure prediction and in vitro accessibility of mRNA as tools in the selection of target sites for ribozymes. *Nucleic Acids Res* **28**, 4113-24.

Anazodo, M. I., Wainberg, M. A., Friesen, A. D. and Wright, J. A. (1995). Inhibition of human immunodeficiency virus type 1 (HIV) gag gene expression by an antisense oligodeoxynucleotide phosphorothioate. *Leukemia* **9 Suppl 1**, S86-8.

Anderson, N. G. (1992). Growth hormone activates mitogen-activated protein kinase and S6 kinase and promotes intracellular tyrosine phosphorylation in 3T3-F442A preadipocytes. *Biochem J* **284**, 649-52.

Andrews, G. K. and Adamson, E. D. (1987). Butyrate selectively activates the metallothionein gene in teratocarcinoma cells and induces hypersensitivity to metal induction. *Nucleic Acids Res* **15**, 5461-75.

Argetsinger, L. S., Campbell, G. S., Yang, X., Witthuhn, B. A., Silvennoinen, O., Ihle, J. N. and Carter-Su, C. (1993). Identification of JAK2 as a growth hormone receptor-associated tyrosine kinase. *Cell* **74**, 237-44.

Argetsinger, L. S., Hsu, G. W., Myers, M. G., Jr., Billestrup, N., White, M. F. and Carter-Su, C. (1995). Growth hormone, interferon-gamma, and leukemia inhibitory factor promoted tyrosyl phosphorylation of insulin receptor substrate-1. *J Biol Chem* **270**, 14685-92.

Argetsinger, L. S., Norstedt, G., Billestrup, N., White, M. F. and Carter-Su, C. (1996). Growth hormone, interferon-gamma, and leukemia inhibitory factor utilize insulin receptor substrate-2 in intracellular signaling. *J Biol Chem* **271**, 29415-21.

Arts, G. J., Kuersten, S., Romby, P., Ehresmann, B. and Mattaj, I. W. (1998). The role of exportin-t in selective nuclear export of mature tRNAs. *Embo J* **17**, 7430-41.

Asakawa, A., Inui, A., Kaga, T., Yuzuriha, H., Nagata, T., Ueno, N., Makino, S., Fujimiya, M., Niijima, A., Fujino, M. A. et al. (2001). Ghrelin is an appetite-stimulatory signal from stomach with structural resemblance to motilin. *Gastroenterology* **120**, 337-45.

Bai, C. and Tolias, P. P. (1996). Cleavage of RNA hairpins mediated by a developmentally regulated CCCH zinc finger protein. *Mol Cell Biol* **16**, 6661-7.

Baka, I. D., Ninkina, N. N., Pinon, L. G., Adu, J., Davies, A. M., Georgiev, G. P. and Buchman, V. L. (1996). Intracellular compartmentalization of two differentially spliced s- rex/NSP mRNAs in neurons. *Mol Cell Neurosci* **7**, 289-303.

Banerjee, A. K. (1980). 5'-terminal cap structure in eucaryotic messenger ribonucleic acids. *Microbiol Rev* **44**, 175-205.

Barinaga, M., Yamonoto, G., Rivier, C., Vale, W., Evans, R. and Rosenfeld, M. G. (1983). Transcriptional regulation of growth hormone gene expression by growth hormone-releasing factor. *Nature* **306**, 84-5.

Barsh, G. S., Seeburg, P. H. and Gelinas, R. E. (1983). The human growth hormone gene family: structure and evolution of the chromosomal locus. *Nucleic Acids Res* **11**, 3939-58.

Bartke, A., Brown-Borg, H. M., Bode, A. M., Carlson, J., Hunter, W. S. and Bronson, R. T. (1998). Does growth hormone prevent or accelerate aging? *Exp Gerontol* **33**, 675-87.

Bassi, G. S., Mollegaard, N. E., Murchie, A. I. and Lilley, D. M. (1999). RNA folding and misfolding of the hammerhead ribozyme. *Biochemistry* **38**, 3345-54.

Baumbach, W. R., Horner, D. L. and Logan, J. S. (1989). The growth hormone-binding protein in rat serum is an alternatively spliced form of the rat growth hormone receptor. *Genes Dev* **3**, 1199-205.

Beck, J. C., McGarry, E. E., Dyrenfuth, I. and Venning, E. H. (1957). Metabolic effects of human and monkey growth hormone in man. *Science* **125**, 884-5.

Beelman, C. A. and Parker, R. (1995). Degradation of mRNA in eukaryotes. *Cell* **81**, 179-83.

Bellush, L. L., Doublier, S., Holland, A. N., Striker, L. J., Striker, G. E. and Kopchick, J. J. (2000). Protection against diabetes-induced nephropathy in growth hormone receptor/binding protein gene-disrupted mice
0010614635. *Endocrinology* **141**, 163-8.

Berelowitz, M., Firestone, S. L. and Frohman, L. A. (1981a). Effects of growth hormone excess and deficiency on hypothalamic somatostatin content and release and on tissue somatostatin distribution. *Endocrinology* **109**, 714-9.

Berelowitz, M., Szabo, M., Frohman, L. A., Firestone, S., Chu, L. and Hintz, R. L. (1981b). Somatomedin-C mediates growth hormone negative feedback by effects on both the hypothalamus and the pituitary. *Science* **212**, 1279-81.

Bertrand, E., Castanotto, D., Zhou, C., Carbonnelle, C., Lee, N. S., Good, P., Chatterjee, S., Grange, T., Pictet, R., Kohn, D. et al. (1997). The expression cassette determines the functional activity of ribozymes in mammalian cells by controlling their intracellular localization. *Rna* **3**, 75-88.

Bertrand, E. L. and Rossi, J. J. (1994). Facilitation of hammerhead ribozyme catalysis by the nucleocapsid protein of HIV-1 and the heterogeneous nuclear ribonucleoprotein A1. *Embo J* **13**, 2904-12.

Berzal-Herranz, A., Joseph, S. and Burke, J. M. (1992). In vitro selection of active hairpin ribozymes by sequential RNA- catalyzed cleavage and ligation reactions. *Genes Dev* **6**, 129-34.

Birren, B. W. and Herschman, H. R. (1986). Regulation of the rat metallothionein-I gene by sodium butyrate. *Nucleic Acids Res* **14**, 853-67.

Bisbal, C. (1997). RNase L: effector nuclease of an activatable RNA degradation system in mammals. *Prog Mol Subcell Biol* **18**, 19-34.

Bjorbaek, C., Elmquist, J. K., Frantz, J. D., Shoelson, S. E. and Flier, J. S. (1998). Identification of SOCS-3 as a potential mediator of central leptin resistance. *Mol Cell* **1**, 619-25.

Borneman, J., Tritz, R., Hampel, A. and Altschuler, M. (1995). Detection of cleavage products from an in vivo transcribed cis hairpin ribozyme in turnips using the CaMV plant virus. *Gene* **159**, 137-42.

Bouloy, M., Plotch, S. J. and Krug, R. M. (1980). Both the 7-methyl and the 2'-O-methyl groups in the cap of mRNA strongly influence its ability to act as primer for influenza virus RNA transcription. *Proc Natl Acad Sci U S A* **77**, 3952-6.

Bradford, M. M. (1976). A Rapid and Sensitive Method for the Quantitation of Microgram Quantities of Protein Utilizing the Principle of Protein-Dye Binding. *Anal Biochem* **72**, 248-254.

Bramlage, B., Alefelder, S., Marschall, P. and Eckstein, F. (1999). Inhibition of luciferase expression by synthetic hammerhead ribozymes and their cellular uptake. *Nucleic Acids Res* **27**, 3159-67.

Brinster, R. L., Allen, J. M., Behringer, R. R., Gelinas, R. E. and Palmiter, R. D. (1988). Introns increase transcriptional efficiency in transgenic mice. *Proc Natl Acad Sci U S A* **85**, 836-40.

Brower, V., Chahine, K., Dorey, E., Dove, A., Francisco, M., Hodgson, J., Michael, A. and Marshall, A. (1998). All clear for HIV-targeting ribozyme in phase II [news]. *Nat Biotechnol* **16**, 123.

Brown-Borg, H. M., Bode, A. M. and Bartke, A. (1999). Antioxidative mechanisms and plasma growth hormone levels: potential relationship in the aging process 0010668640. *Endocrine* **11**, 41-8.

Buzayan, J. M., Garlach, W. L. and Bruening, G. (1986a). Non-enzymatic cleavage and ligation of RNAs complementary to a plant virus satellite RNA. *Nature* **323**, 349-53.

Buzayan, J. M., Hampel, A. and Bruening, G. (1986b). Nucleotide sequence and newly formed phosphodiester bond of spontaneously ligated satellite tobacco ringspot virus RNA. *Nucleic Acids Res* **14**, 9729-43.

Caceres, J. F., Stamm, S., Helfman, D. M. and Krainer, A. R. (1994). Regulation of alternative splicing in vivo by overexpression of antagonistic splicing factors. *Science* **265**, 1706-9.

Campbell, G. S., Meyer, D. J., Raz, R., Levy, D. E., Schwartz, J. and Carter-Su, C. (1995). Activation of acute phase response factor (APRF)/Stat3 transcription factor by growth hormone. *J Biol Chem* **270**, 3974-9.

Campbell, G. S., Pang, L., Miyasaka, T., Saltiel, A. R. and Carter-Su, C. (1992). Stimulation by growth hormone of MAP kinase activity in 3T3-F442A fibroblasts. *J Biol Chem* **267**, 6074-80.

Carter-Su, C., Rozsa, F. W., Wang, X. and Stubbart, J. R. (1988). Rapid and transitory stimulation of 3-O-methylglucose transport by growth hormone. *Am J Physiol* **255**, E723-9.

Carter-Su, C., Schwartz, J. and Smit, L. S. (1996). Molecular mechanism of growth hormone action. *Annu Rev Physiol* **58**, 187-207.

Carter-Su, C. and Smit, L. S. (1998). Signaling via JAK tyrosine kinases: growth hormone receptor as a model system. *Recent Prog Horm Res* **53**, 61-82.

Cataldo, L. (2001). Characterization of growth hormone induced signal transduction intermediates in liver, kidney and fat of "dwarf" and "giant" mice. Dissertation In *Department of Chemistry*, Athens: Ohio University.

Cech, T. R., Zaug, A. J. and Grabowski, P. J. (1981). In vitro splicing of the ribosomal RNA precursor of Tetrahymena: involvement of a guanosine nucleotide in the excision of the intervening sequence. *Cell* **27**, 487-96.

Cepero, E., Hnatyszyn, H. J., Kraus, G. and Lichtenheld, M. G. (1998). Potent inhibition of CTLA-4 expression by an anti-CTLA-4 ribozyme. *Biochem Biophys Res Commun* **247**, 838-43.

Chandrashekar, V., Bartke, A., Coschigano, K. T. and Kopchick, J. J. (1999). Pituitary and testicular function in growth hormone receptor gene knockout mice. *Endocrinology* **140**, 1082-8.

Chapman, K. B. and Szostak, J. W. (1995). Isolation of a ribozyme with 5'-5' ligase activity. *Chem Biol* **2**, 325-33.

Chen, C. J., Banerjea, A. C., Haglund, K., Harmison, G. G. and Schubert, M. (1992). Inhibition of HIV-1 replication by novel multitarget ribozymes. *Ann N Y Acad Sci* **660**, 271-3.

Chen, S., Song, C. S., Lavrovsky, Y., Bi, B., Vellanoweth, R., Chatterjee, B. and Roy, A. K. (1998). Catalytic cleavage of the androgen receptor messenger RNA and functional inhibition of androgen receptor activity by a hammerhead ribozyme. *Mol Endocrinol* **12**, 1558-66.

Chen, Z., Kamath, P., Zhang, S., Weil, M. M. and Shillitoe, E. J. (1995). Effectiveness of three ribozymes for cleavage of an RNA transcript from human papillomavirus type 18. *Cancer Gene Ther* **2**, 263-71.

Chiolero, R., Revelly, J. P. and Tappy, L. (1997). Energy metabolism in sepsis and injury. *Nutrition* **13**, 45S-51S.

Choudhuri, S., Kramer, K. K., Berman, N. E., Dalton, T. P., Andrews, G. K. and Klaassen, C. D. (1995). Constitutive expression of metallothionein genes in mouse brain. *Toxicol Appl Pharmacol* **131**, 144-54.

Chow, J. C., Ling, P. R., Qu, Z., Laviola, L., Ciccarone, A., Bistrian, B. R. and Smith, R. J. (1996). Growth hormone stimulates tyrosine phosphorylation of JAK2 and STAT5, but not insulin receptor substrate-1 or SHC proteins in liver and skeletal muscle of normal rats in vivo. *Endocrinology* **137**, 2880-6.

Chowrira, B. M., Berzal-Herranz, A., Keller, C. F. and Burke, J. M. (1993). Four ribose 2'-hydroxyl groups essential for catalytic function of the hairpin ribozyme. *J Biol Chem* **268**, 19458-62.

Chowrira, B. M., Pavco, P. A. and McSwiggen, J. A. (1994). In vitro and in vivo comparison of hammerhead, hairpin, and hepatitis delta virus self-processing ribozyme cassettes. *J Biol Chem* **269**, 25856-64.

Cioffi, J. A., Wang, X. and Kopchick, J. J. (1990). Porcine growth hormone receptor cDNA sequence. *Nucleic Acids Res* **18**, 6451.

Clark, A. J., Archibald, A. L., McClenaghan, M., Simons, J. P., Wallace, R. and Whitelaw, C. B. (1993). Enhancing the efficiency of transgene expression. *Philos Trans R Soc Lond B Biol Sci* **339**, 225-32.

Clark, R. G., Jansson, J. O., Isaksson, O. and Robinson, I. C. (1985). Intravenous growth hormone: growth responses to patterned infusions in hypophysectomized rats. *J Endocrinol* **104**, 53-61.

Cobb, M. H. and Goldsmith, E. J. (1995). How MAP kinases are regulated. *J Biol Chem* **270**, 14843-6.

Colosi, P., Wong, K., Leong, S. R. and Wood, W. I. (1993). Mutational analysis of the intracellular domain of the human growth hormone receptor. *J Biol Chem* **268**, 12617-23.

Cooke, C. and Alwine, J. C. (1996). The cap and the 3' splice site similarly affect polyadenylation efficiency. *Mol Cell Biol* **16**, 2579-84.

Cooke, N. E., Coit, D., Shine, J., Baxter, J. D. and Martial, J. A. (1981). Human prolactin. cDNA structural analysis and evolutionary comparisons. *J Biol Chem* **256**, 4007-16.

Cooke, N. E., Ray, J., Emery, J. G. and Liebhaber, S. A. (1988). Two distinct species of human growth hormone-variant mRNA in the human placenta predict the expression of novel growth hormone proteins. *J Biol Chem* **263**, 9001-6.

Cornelissen, M. (1989). Nuclear and cytoplasmic sites for anti-sense control. *Nucleic Acids Res* **17**, 7203-9.

Coschigano, K. T., Clemmons, D., Bellush, L. L. and Kopchick, J. J. (2000). Assessment of growth parameters and life span of GHR/BP gene-disrupted mice. *Endocrinology* **141**, 2608-13.

Coschigano, K. T., Riders, M. E., Bellush, L. L. and Kopchick, J. J. (1999). Glucose metabolism in growth hormone receptor/binding protein gene disrupted mice. *81st Annual Meeting of the Endocrine Society* **Abstract P3-537**, 553.

Cote, C. A., Gautreau, D., Denegre, J. M., Kress, T. L., Terry, N. A. and Mowry, K. L. (1999). A Xenopus protein related to hnRNP I has a role in cytoplasmic RNA localization. *Mol Cell* **4**, 431-7.

Crick, F. H. (1968). The origin of the genetic code. *J Mol Biol* **38**, 367-79.

Crisell, P., Thompson, S. and James, W. (1993). Inhibition of HIV-1 replication by ribozymes that show poor activity in vitro. *Nucleic Acids Res* **21**, 5251-5.

Cunningham, B. C., Ultsch, M., De Vos, A. M., Mulkerrin, M. G., Clauser, K. R. and Wells, J. A. (1991). Dimerization of the extracellular domain of the human growth hormone receptor by a single hormone molecule. *Science* **254**, 821-5.

Dai, X., De Mesmaeker, A. and Joyce, G. F. (1995). Cleavage of an amide bond by a ribozyme [published erratum appears in Science 1996 Apr 5;272(5258):18-9]. *Science* **267**, 237-40.

Danilovich, N., Wernsing, D., Coschigano, K. T., Kopchick, J. J. and Bartke, A. (1999). Deficits in female reproductive function in GH-R-KO mice; role of IGF-I. *Endocrinology* **140**, 2637-40.

David, M., Chen, H. E., Goelz, S., Larner, A. C. and Neel, B. G. (1995). Differential regulation of the alpha/beta interferon-stimulated Jak/Stat pathway by the SH2 domain-containing tyrosine phosphatase SHPTP1. *Mol Cell Biol* **15**, 7050-8.

Davidson, M. B. (1987). Effect of growth hormone on carbohydrate and lipid metabolism. *Endocr Rev* **8**, 115-31.

de la Hoya, M., Vila, V., Jimenez, O. and Castrillo, J. L. (1998). Anterior pituitary development and Pit-1/GHF-1 transcription factor. *Cell Mol Life Sci* **54**, 1059-66.

Delihas, N., Rokita, S. E. and Zheng, P. (1997). Natural antisense RNA/target RNA interactions: possible models for antisense oligonucleotide drug design. *Nat Biotechnol* **15**, 751-3.

Denman, R. B. (1993). Using RNAFOLD to predict the activity of small catalytic RNAs. *Biotechniques* **15**, 1090-5.

Denman, R. B. (1999). Hairpin ribozyme specificity in vivo: a case of promiscuous cleavage. *Biochem Biophys Res Commun* **257**, 356-60.

Denman, R. B., Smedman, M., Ju, W., Rubenstein, R., Potempska, A. and Miller, D. L. (1994). Ribozyme mediated degradation of beta-amyloid peptide precursor mRNA in COS-7 cells. *Nucleic Acids Res* **22**, 2375-82.

DeNoto, F. M., Moore, D. D. and Goodman, H. M. (1981). Human growth hormone DNA sequence and mRNA structure: possible alternative splicing. *Nucleic Acids Res* **9**, 3719-30.

Desai, L. S., Lazarus, H., Li, C. H. and Foley, G. E. (1973). Human leukemic cells. Effect of human growth hormone. *Exp Cell Res* **81**, 330-2.

Desjardins, J. P., Sproat, B. S., Beijer, B., Blaschke, M., Dunkel, M., Gerdes, W., Ludwig, J., Reither, V., Rupp, T. and Iversen, P. L. (1996). Pharmacokinetics of a synthetic, chemically modified hammerhead ribozyme against the rat cytochrome P-450 3A2 mRNA after single intravenous injections. *J Pharmacol Exp Ther* **278**, 1419-27.

DeYoung, M. B., Siwkowski, A. and Hampel, A. (1997). Determination of catalytic parameters for hairpin ribozymes. *Methods Mol Biol* **74**, 209-20.

Diener, T. O. (1971). Potato spindle tuber "virus". IV. A replicating, low molecular weight RNA. *Virology* **45**, 411-28.

Diener, T. O. (1989). Circular RNAs: relics of precellular evolution? *Proc Natl Acad Sci U S A* **86**, 9370-4.

Ding, D., Parkhurst, S. M. and Lipshitz, H. D. (1993). Different genetic requirements for anterior RNA localization revealed by the distribution of Adducin-like transcripts during Drosophila oogenesis. *Proc Natl Acad Sci U S A* **90**, 2512-6.

Diwa, A., Bricker, A. L., Jain, C. and Belasco, J. G. (2000). An evolutionarily conserved RNA stem-loop functions as a sensor that directs feedback regulation of RNase E gene expression. *Genes Dev* **14**, 1249-60.

Dominici, F. P., Arostegui Diaz, G., Bartke, A., Kopchick, J. J. and Turyn, D. (2000). Compensatory alterations of insulin signal transduction in liver of growth hormone receptor knockout mice. *J Endocrinol* **166**, 579-90.

Du, Z., Ricordi, C., Podack, E. and Pastori, R. L. (1996). A hammerhead ribozyme that cleaves perforin and fas-ligand RNAs in vitro. *Biochem Biophys Res Commun* **226**, 595-600.

Earnshaw, D. J. and Gait, M. J. (1998). Hairpin ribozyme cleavage catalyzed by aminoglycoside antibiotics and the polyamine spermine in the absence of metal ions. *Nucleic Acids Res* **26**, 5551-61.

Eckner, R., Ellmeier, W. and Birnstiel, M. L. (1991). Mature mRNA 3' end formation stimulates RNA export from the nucleus. *Embo J* **10**, 3513-22.

Edens, A., Southard, J. N. and Talamantes, F. (1994). Mouse growth hormone-binding protein and growth hormone receptor transcripts are produced from a single gene by alternative splicing. *Endocrinology* **135**, 2802-5.

Efrat, S., Leiser, M., Wu, Y. J., Fusco-DeMane, D., Emran, O. A., Surana, M., Jetton, T. L., Magnuson, M. A., Weir, G. and Fleischer, N. (1994). Ribozyme-mediated attenuation of pancreatic beta-cell glucokinase expression in transgenic mice results in impaired glucose-induced insulin secretion. *Proc Natl Acad Sci U S A* **91**, 2051-5.

Eisen, E. J., Peterson, C. B., Parker, I. J. and Murray, J. D. (1998). Effects of zinc ion concentration on growth, fat content and reproduction in oMT1a-oGH transgenic mice. *Growth Dev Aging* **62**, 173-86.

Ekland, E. H. and Bartel, D. P. (1996). RNA-catalysed RNA polymerization using nucleoside triphosphates. *Nature* **383**, 192.

Elisha, Z., Havin, L., Ringel, I. and Yisraeli, J. K. (1995). Vg1 RNA binding protein mediates the association of Vg1 RNA with microtubules in Xenopus oocytes. *Embo J* **14**, 5109-14.

Endo, T. A., Masuhara, M., Yokouchi, M., Suzuki, R., Sakamoto, H., Mitsui, K., Matsumoto, A., Tanimura, S., Ohtsubo, M., Misawa, H. et al. (1997). A new protein containing an SH2 domain that inhibits JAK kinases. *Nature* **387**, 921-4.

Epstein, L. M. and Gall, J. G. (1987). Self-cleaving transcripts of satellite DNA from the newt. *Cell* **48**, 535-43.

Fain, J. N., Kovacev, V. P. and Scow, R. O. (1965). Effect of growth hormone and dexamethasone on lipolysis and metabolism in isolated fat cells of the rat. *J Biol Chem* **240**, 3522-9.

Favre, H., Benhamou, A., Finidori, J., Kelly, P. A. and Edery, M. (1999). Dual effects of suppressor of cytokine signaling (SOCS-2) on growth hormone signal transduction. *FEBS Lett* **453**, 63-6.

Feig, A. L., Scott, W. G. and Uhlenbeck, O. C. (1998). Inhibition of the hammerhead ribozyme cleavage reaction by site- specific binding of Tb. *Science* **279**, 81-4.

Ferbeyre, G., Smith, J. M. and Cedergren, R. (1998). Schistosome satellite DNA encodes active hammerhead ribozymes. *Mol Cell Biol* **18**, 3880-8.

Ferrandon, D., Elphick, L., Nusslein-Volhard, C. and St Johnston, D. (1994). Staufen protein associates with the 3'UTR of bicoid mRNA to form particles that move in a microtubule-dependent manner. *Cell* **79**, 1221-32.

Forsdyke, D. R. (1995). Sense in antisense? *J Mol Evol* **41**, 582-6.
Forster, A. C. and Symons, R. H. (1987). Self-cleavage of plus and minus RNAs of a virusoid and a structural model for the active sites. *Cell* **49**, 211-20.

Frank, B. L. and Goodchild, J. (1997). Selection of accessible sites for ribozymes on large RNA transcripts. *Methods Mol Biol* **74**, 37-43.

Frankenne, F., Closset, J., Gomez, F., Scippo, M. L., Smal, J. and Hennen, G. (1988). The physiology of growth hormones (GHs) in pregnant women and partial characterization of the placental GH variant. *J Clin Endocrinol Metab* **66**, 1171-80.

Frankenne, F., Rentier-Delrue, F., Scippo, M. L., Martial, J. and Hennen, G. (1987). Expression of the growth hormone variant gene in human placenta. *J Clin Endocrinol Metab* **64**, 635-7.

Frohman, L. A., MacGillivray, M. H. and Aceto, T., Jr. (1967). Acute effects of human growth hormone on insulin secretion and glucose utilization in normal and growth hormone deficient subjects. *J Clin Endocrinol Metab* **27**, 561-7.

Funato, T., Shitara, T., Tone, T., Jiao, L., Kashani-Sabet, M. and Scanlon, K. J. (1994). Suppression of H-ras-mediated transformation in NIH3T3 cells by a ras ribozyme. *Biochem Pharmacol* **48**, 1471-5.

Gamblin, S. J. and Smerdon, S. J. (1999). Nuclear transport: what a kary-on! *Structure Fold Des* **7**, R199-R204.

Garcia-Aragon, J., Lobie, P. E., Muscat, G. E., Gobius, K. S., Norstedt, G. and Waters, M. J. (1992). Prenatal expression of the growth hormone (GH) receptor/binding protein in the rat: a role for GH in embryonic and fetal development? *Development* **114**, 869-76.

Gardiner, K. and Pace, N. R. (1980). RNase P of Bacillus subtilis has a RNA component. *J Biol Chem* **255**, 7507-9.

Gavin, D. K. and Gupta, K. C. (1997). Efficient hammerhead ribozymes targeted to the polycistronic Sendai virus P/C mRNA. Structure-function relationships. *J Biol Chem* **272**, 1461-72.

Gebert, C. A., Park, S. H. and Waxman, D. J. (1997). Regulation of signal transducer and activator of transcription (STAT) 5b activation by the temporal pattern of growth hormone stimulation. *Mol Endocrinol* **11**, 400-14.

Gerhartz, C., Heesel, B., Sasse, J., Hemmann, U., Landgraf, C., Schneider-Mergener, J., Horn, F., Heinrich, P. C. and Graeve, L. (1996). Differential activation of acute phase response factor/STAT3 and STAT1 via the cytoplasmic domain of the interleukin 6 signal transducer gp130. I. Definition of a novel phosphotyrosine motif mediating STAT1 activation. *J Biol Chem* **271**, 12991-8.

Gerich, J. E., Lorenzi, M., Bier, D. M., Tsalikian, E., Schneider, V., Karam, J. H. and Forsham, P. H. (1976). Effects of physiologic levels of glucagon and growth hormone on human carbohydrate and lipid metabolism. Studies involving administration of exogenous hormone during suppression of endogenous hormone secretion with somatostatin. *J Clin Invest* **57**, 875-84.

Gervaix, A., Li, X., Kraus, G. and Wong-Staal, F. (1997). Multigene antiviral vectors inhibit diverse human immunodeficiency virus type 1 clades. *J Virol* **71**, 3048-53.

Geyer, C. R. and Sen, D. (1998). Lanthanide probes for a phosphodiester-cleaving, lead-dependent, DNAzyme. *J Mol Biol* **275**, 483-9.

Giannini, C. D., Roth, W. K., Piiper, A. and Zeuzem, S. (1999). Enzymatic and antisense effects of a specific anti-Ki-ras ribozyme in vitro and in cell culture. *Nucleic Acids Res* **27**, 2737-44.

Gilbert, W. (1986). Evolution of antibodies. The road not taken [news]. *Nature* **320**, 485-6.

Gilman, M. (1997). Preparation and analysis of RNA. In *Current protocols in molecular biology*, vol. Supplement 37 (ed. K. R. E.), pp. 4.0.1: John Wiley and Sons, Inc.

Gilmartin, G. M., Fleming, E. S., Oetjen, J. and Graveley, B. R. (1995). CPSF recognition of an HIV-1 mRNA 3'-processing enhancer: multiple sequence contacts involved in poly(A) site definition. *Genes Dev* **9**, 72-83.

Golde, D. W., Bersch, N. and Li, C. H. (1977). Growth hormone: species-specific stimulation of erythropoiesis in vitro. *Science* **196**, 1112-3.

Golden, B. L., Gooding, A. R., Podell, E. R. and Cech, T. R. (1998). A preorganized active site in the crystal structure of the Tetrahymena ribozyme [see comments]. *Science* **282**, 259-64.

Goodchild, J. (1992). Enhancement of ribozyme catalytic activity by a contiguous oligodeoxynucleotide (facilitator) and by 2'-O-methylation. *Nucleic Acids Res* **20**, 4607-12.

Goodman, H. M. (1968). Multiple effects of growth hormone on lipolysis. *Endocrinology* **83**, 300-8.

Goto, S. and Mizuno, D. (1971). Degradation of RNA in rat reticulocytes. I. Purification and properties of rat reticulocyte RNase. *Arch Biochem Biophys* **145**, 64-70.

Greenlund, A. C., Farrar, M. A., Viviano, B. L. and Schreiber, R. D. (1994). Ligand-induced IFN gamma receptor tyrosine phosphorylation couples the receptor to its signal transduction system (p91). *Embo J* **13**, 1591-600.

Griffin, E. E. and Miller, L. L. (1974). Effects of hypophysectomy of liver donor on net synthesis of specific plasma proteins by the isolated perfused rat liver. Modulation of synthesis of albumin, fibrinogen, alpha 1-acid glycoprotein, alpha 2- (acute phase)-globulin, and haptoglobin by insulin, cortisol, triiodothyronine, and growth hormone. *J Biol Chem* **249**, 5062-9.

Gronowski, A. M. and Rotwein, P. (1994). Rapid changes in nuclear protein tyrosine phosphorylation after growth hormone treatment in vivo. Identification of phosphorylated mitogen- activated protein kinase and STAT91. *J Biol Chem* **269**, 7874-8.

Gronowski, A. M., Zhong, Z., Wen, Z., Thomas, M. J., Darnell, J. E., Jr. and Rotwein, P. (1995). In vivo growth hormone treatment rapidly stimulates the tyrosine phosphorylation and activation of Stat3. *Mol Endocrinol* **9**, 171-7.

Guerrier-Takada, C., Gardiner, K., Marsh, T., Pace, N. and Altman, S. (1983). The RNA moiety of ribonuclease P is the catalytic subunit of the enzyme. *Cell* **35**, 849-57.

Ha, J. and Kim, K. H. (1994). Inhibition of fatty acid synthesis by expression of an acetyl-CoA carboxylase-specific ribozyme gene. *Proc Natl Acad Sci U S A* **91**, 9951-5.

Hackett, R. H., Wang, Y. D., Sweitzer, S., Feldman, G., Wood, W. I. and Larner, A. C. (1997). Mapping of a cytoplasmic domain of the human growth hormone receptor that regulates rates of inactivation of Jak2 and Stat proteins. *J Biol Chem* **272**, 11128-32.

Hager, A. J. and Szostak, J. W. (1997). Isolation of novel ribozymes that ligate AMP-activated RNA substrates. *Chem Biol* **4**, 607-17.

Hajnsdorf, E., Steier, O., Coscoy, L., Teysset, L. and Regnier, P. (1994). Roles of RNase E, RNase II and PNPase in the degradation of the rpsO transcripts of Escherichia coli: stabilizing function of RNase II and evidence for efficient degradation in an ams pnp rnb mutant. *Embo J* **13**, 3368-77.

Hansen, L. H., Wang, X., Kopchick, J. J., Bouchelouche, P., Nielsen, J. H., Galsgaard, E. D. and Billestrup, N. (1996). Identification of tyrosine residues in the intracellular domain of the growth hormone receptor required for transcriptional signaling and Stat5 activation. *J Biol Chem* **271**, 12669-73.

Harding, P. A., Wang, X. Z. and Kopchick, J. J. (1995). Growth hormone (GH)-induced tyrosine-phosphorylated proteins in cells that express GH receptors. *Receptor* **5**, 81-92.

Hardt, W. D., Schlegl, J., Erdmann, V. A. and Hartmann, R. K. (1995). Kinetics and thermodynamics of the RNase P RNA cleavage reaction: analysis of tRNA 3'-end variants. *J Mol Biol* **247**, 161-72.

Harris, A. G. (1996). Acromegaly and its management. Philadelphia: Lippincott-Raven Publishers.

Haseloff, J. and Gerlach, W. L. (1988). Simple RNA enzymes with new and highly specific endoribonuclease activities. *Nature* **334**, 585-91.

Hauser, S. D., McGrath, M. F., Collier, R. J. and Krivi, G. G. (1990). Cloning and in vivo expression of bovine growth hormone receptor mRNA. *Mol Cell Endocrinol* **72**, 187-200.

Hauser-Kronberger, C. (1998). Highly sensitive DNA, RNA and antigen detection methods: streptavidin- Nanogold-silver staining. *Cell Vis* **5**, 83.

Heidenreich, O. and Eckstein, F. (1992). Hammerhead ribozyme-mediated cleavage of the long terminal repeat RNA of human immunodeficiency virus type 1. *J Biol Chem* **267**, 1904-9.

Heinrich, J. C., Tabler, M. and Louis, C. (1993). Attenuation of white gene expression in transgenic Drosophila melanogaster: possible role of a catalytic antisense RNA. *Dev Genet* **14**, 258-65.

Heinrich, J. C., Tabler, M. and Louis, C. (1995). Influence of chromosomal position and copy number of a white-directed ribozyme gene on the suppression of eye pigmentation in Drosophila melanogaster. *Antisense Res Dev* **5**, 155-60.

Henco, K., Riesner, D. and Sanger, H. L. (1977). Conformation of viroids. *Nucleic Acids Res* **4**, 177-94.

Hermann, T. and Westhof, E. (1998). Aminoglycoside binding to the hammerhead ribozyme: a general model for the interaction of cationic antibiotics with RNA. *J Mol Biol* **276**, 903-12.

Herschlag, D. (1991). Implications of ribozyme kinetics for targeting the cleavage of specific RNA molecules in vivo: more isn't always better. *Proc Natl Acad Sci U S A* **88**, 6921-5.

Herschlag, D. and Cech, T. R. (1990). Catalysis of RNA cleavage by the Tetrahymena thermophila ribozyme. 2. Kinetic description of the reaction of an RNA substrate that forms a mismatch at the active site. *Biochemistry* **29**, 10172-80.

Herschlag, D., Khosla, M., Tsuchihashi, Z. and Karpel, R. L. (1994). An RNA chaperone activity of non-specific RNA binding proteins in hammerhead ribozyme catalysis [published erratum appears in EMBO J 1994 Aug 15;13(16):3926]. *Embo J* **13**, 2913-24.

Hillig, R. C., Renault, L., Vetter, I. R., Drell, T. t., Wittinghofer, A. and Becker, J. (1999). The crystal structure of rna1p: a new fold for a GTPase-activating protein. *Mol Cell* **3**, 781-91.

Hjalmarson, A., Isaksson, O. and Ahren, K. (1969). Effects of growth hormone and insulin on amino acid transport in perfused rat heart. *Am J Physiol* **217**, 1795-802.

Holl, R. W., Thorner, M. O. and Leong, D. A. (1988). Intracellular calcium concentration and growth hormone secretion in individual somatotropes: effects of growth hormone-releasing factor and somatostatin. *Endocrinology* **122**, 2927-32.

Howard, A. D., Feighner, S. D., Cully, D. F., Arena, J. P., Liberator, P. A., Rosenblum, C. I., Hamelin, M., Hreniuk, D. L., Palyha, O. C., Anderson, J. et al. (1996). A receptor in pituitary and hypothalamus that functions in growth hormone release. *Science* **273**, 974-7.

Hua, J. and Muschel, R. J. (1996). Inhibition of matrix metalloproteinase 9 expression by a ribozyme blocks metastasis in a rat sarcoma model system. *Cancer Res* **56**, 5279-84.

Huang, Y. and Carmichael, G. C. (1996). Role of polyadenylation in nucleocytoplasmic transport of mRNA. *Mol Cell Biol* **16**, 1534-42.

Hutchins, C. J., Rathjen, P. D., Forster, A. C. and Symons, R. H. (1986). Self-cleavage of plus and minus RNA transcripts of avocado sunblotch viroid. *Nucleic Acids Res* **14**, 3627-40.

Ichida, M., Hakamata, Y., Hayakawa, M., Ueno, E., Ikeda, U., Shimada, K., Hamamoto, T., Kagawa, Y. and Endo, H. (2000). Differential regulation of exonic regulatory elements for muscle- specific alternative splicing during myogenesis and cardiogenesis. *J Biol Chem* **275**, 15992-6001.

Isgaard, J., Carlsson, L., Isaksson, O. G. and Jansson, J. O. (1988). Pulsatile intravenous growth hormone (GH) infusion to hypophysectomized rats increases insulin-like growth factor I messenger ribonucleic acid in skeletal tissues more effectively than continuous GH infusion. *Endocrinology* **123**, 2605-10.

Izaurralde, E., Lewis, J., McGuigan, C., Jankowska, M., Darzynkiewicz, E. and Mattaj, I. W. (1994). A nuclear cap binding protein complex involved in pre-mRNA splicing. *Cell* **78**, 657-68.

Izaurralde, E. and Mattaj, I. W. (1992). Transport of RNA between nucleus and cytoplasm. *Semin Cell Biol* **3**, 279-88.

Jacobson, A. and Peltz, S. W. (1996). Interrelationships of the pathways of mRNA decay and translation in eukaryotic cells. *Annu Rev Biochem* **65**, 693-739.

Jacquier, A. and Michel, F. (1987). Multiple exon-binding sites in class II self-splicing introns. *Cell* **50**, 17-29.

James, W. and Cowe, E. (1997). Computational approaches to the identification of ribozyme target sites. *Methods Mol Biol* **74**, 17-26.

Jan, Y. N. and Jan, L. Y. (1998). Asymmetric cell division. *Nature* **392**, 775-8.

Jankowsky, E. and Schwenzer, B. (1996). Efficient improvement of hammerhead ribozyme mediated cleavage of long substrates by oligonucleotide facilitators. *Biochemistry* **35**, 15313-21.

Jankowsky, E. and Schwenzer, B. (1998). Oligonucleotide facilitators enable a hammerhead ribozyme to cleave long RNA substrates with multiple-turnover activity. *Eur J Biochem* **254**, 129-34.

Jansen, R. P., Dowzer, C., Michaelis, C., Galova, M. and Nasmyth, K. (1996). Mother cell-specific HO expression in budding yeast depends on the unconventional myosin myo4p and other cytoplasmic proteins. *Cell* **84**, 687-97.

Jefferson, L. S. and Korner, A. (1967). A direct effect of growth hormone on the incorporation of precursors into proteins and nucleic acids of perfused rat liver. *Biochem J* **104**, 826-32.

Joyce, G. F. (1989). RNA evolution and the origins of life. *Nature* **338**, 217-24.

Junn, E. and Kang, C. (1996). Detection of hammerhead ribozyme-mediated cleavage and reduced expression of LacZ' mRNA in E. coli. *Genet Anal* **13**, 1-7.

Kanazawa, Y., Ohkawa, K., Ueda, K., Mita, E., Takehara, T., Sasaki, Y., Kasahara, A. and Hayashi, N. (1996). Hammerhead ribozyme-mediated inhibition of telomerase activity in extracts of human hepatocellular carcinoma cells. *Biochem Biophys Res Commun* **225**, 570-6.

Kawakami, J., Yuda, K., Suh, Y. A., Kumar, P. K., Nishikawa, F., Maeda, H., Taira, K., Ohtsuka, E. and Nishikawa, S. (1996). Constructing an efficient trans-acting genomic HDV ribozyme. *FEBS Lett* **394**, 132-6.

Kim, S. K. and Wold, B. J. (1985). Stable reduction of thymidine kinase activity in cells expressing high levels of anti-sense RNA. *Cell* **42**, 129-38.

Kobayashi, H., Dorai, T., Holland, J. F. and Ohnuma, T. (1994). Reversal of drug sensitivity in multidrug-resistant tumor cells by an MDR1 (PGY1) ribozyme. *Cancer Res* **54**, 1271-5.

Koizumi, M., Iwai, S. and Ohtsuka, E. (1988). Construction of a series of several self-cleaving RNA duplexes using synthetic 21-mers. *FEBS Lett* **228**, 228-30.

Koizumi, M. and Ohtsuka, E. (1991). Effects of phosphorothioate and 2-amino groups in hammerhead ribozymes on cleavage rates and Mg2+ binding [published erratum appears in Biochemistry 1992 Apr 28;31(16):4156]. *Biochemistry* **30**, 5145-50.

Kojima, M., Hosoda, H., Date, Y., Nakazato, M., Matsuo, H. and Kangawa, K. (1999). Ghrelin is a growth-hormone-releasing acylated peptide from stomach. *Nature* **402**, 656-60.

Kole, R., Baer, M. F., Stark, B. C. and Altman, S. (1980). E. coli RNAase P has a required RNA component. *Cell* **19**, 881-7.

Kopchick, J. J. and Laron, Z. (1999). Is the Laron mouse an accurate model of Laron syndrome? *Mol Genet Metab* **68**, 232-6.

Kopchick, J. J., McAndrew, S. J., Shafer, A., Blue, W. T., Yun, J. S., Wagner, T. E. and Chen, W. Y. (1990). In-vitro mutagenesis of the bovine growth hormone gene. *J Reprod Fertil Suppl* **41**, 25-35.

Koseki, S., Tanabe, T., Tani, K., Asano, S., Shioda, T., Nagai, Y., Shimada, T., Ohkawa, J. and Taira, K. (1999). Factors governing the activity in vivo of ribozymes transcribed by RNA polymerase III. *J Virol* **73**, 1868-77.

Kruger, K., Grabowski, P. J., Zaug, A. J., Sands, J., Gottschling, D. E. and Cech, T. R. (1982). Self-splicing RNA: autoexcision and autocyclization of the ribosomal RNA intervening sequence of Tetrahymena. *Cell* **31**, 147-57.

Kuo, T. C. and Herrin, D. L. (2000). Quantitative studies of Mn(2+)-promoted specific and non-specific cleavages of a large RNA: Mn(2+)-GAAA ribozymes and the evolution of small ribozymes. *Nucleic Acids Res* **28**, 4197-206.

Kuwabara, T., Warashina, M., Nakayama, A., Ohkawa, J. and Taira, K. (1999). tRNAVal-heterodimeric maxizymes with high potential as geneinactivating agents: simultaneous cleavage at two sites in HIV-1 Tat mRNA in cultured cells. *Proc Natl Acad Sci U S A* **96**, 1886-91.

Kuwabara, T., Warashina, M., Orita, M., Koseki, S., Ohkawa, J. and Taira, K. (1998). Formation of a catalytically active dimer by tRNA(Val)-driven short ribozymes. *Nat Biotechnol* **16**, 961-5.

Lacy, E., Costantini, F., Beddington, R. and Hogan, B. (1994). Manipulating the mouse embryo: A laboratory manual. New York: Cold Springs Harbor Laboratory Press.

Lahav, N. (1993). The RNA-world and co-evolution hypotheses and the origin of life: implications, research strategies and perspectives. *Orig Life Evol Biosph* **23**, 329-44.

Landry, M. and Hokfelt, T. (1998). Subcellular localization of preprogalanin messenger RNA in perikarya and axons of hypothalamo-posthypophyseal magnocellular neurons: an in situ hybridization study. *Neuroscience* **84**, 897-912.

Larsson, S., Hotchkiss, G., Andang, M., Nyholm, T., Inzunza, J., Jansson, I. and Ahrlund-Richter, L. (1994). Reduced beta 2-microglobulin mRNA levels in transgenic mice expressing a designed hammerhead ribozyme. *Nucleic Acids Res* **22**, 2242-8.

Lee, M. O. and Schaffer, N. K. (1934). Anterior pituitary growth hormone and the composition of growth. *J Nutr* **7**, 337-63.

Leone, A. (1986). Metallothionein gene regulation in Menkes' disease. *Horiz Biochem Biophys* **8**, 207-56.

Leung, D. W., Spencer, S. A., Cachianes, G., Hammonds, R. G., Collins, C., Henzel, W. J., Barnard, R., Waters, M. J. and Wood, W. I. (1987). Growth hormone receptor and serum binding protein: purification, cloning and expression. *Nature* **330**, 537-43.

Lewis, J. D. and Izaurralde, E. (1997). The role of the cap structure in RNA processing and nuclear export. *Eur J Biochem* **247**, 461-9.

Lewis, M. I., LoRusso, T. J. and Fournier, M. (1997). Effect of insulin-like growth factor I and/or growth hormone on diaphragm of malnourished adolescent rats. *J Appl Physiol* **82**, 1064-70.

L'Huillier, P. J., Davis, S. R. and Bellamy, A. R (1992). Cytoplasmic delivery of ribozymes leads to efficient reduction in alpha- lactalbumin mRNA levels in C127I mouse cells. *Embo J* **11**, 4411-8.

L'Huillier, P. J., Soulier, S., Stinnakre, M. G., Lepourry, L., Davis, S. R., Mercier, J. C. and Vilotte, J. L. (1996). Efficient and specific ribozyme-mediated reduction of bovine alpha- lactalbumin expression in double transgenic mice. *Proc Natl Acad Sci U S A* **93**, 6698-703.

Li, Y. and Breaker, R. R. (1999). Deoxyribozymes: new players in the ancient game of biocatalysis. *Curr Opin Struct Biol* **9**, 315-23.

Lieber, A., He, C. Y., Polyak, S. J., Gretch, D. R., Barr, D. and Kay, M. A. (1996). Elimination of hepatitis C virus RNA in infected human hepatocytes by adenovirus-mediated expression of ribozymes. *J Virol* **70**, 8782-91.

Lieber, A., Rohde, M. and Strauss, M. (1997). Selection of efficient ribozyme cleavage sites in target RNAs. *Methods Mol Biol* **74**, 45-50.

Lieber, A. and Strauss, M. (1995). Selection of efficient cleavage sites in target RNAs by using a ribozyme expression library. *Mol Cell Biol* **15**, 540-51.

List, E. O. (1994). In vitro characterization of hammerhead ribozymes directed against bone morphogenetic protein receptor kinase 3 (BRK-3) mRNA. Thesis In *Department of Biological Sciences*, pp. 162. Athens: Ohio University.

Llano-Sotelo, B. and Chow, C. S. (1999). RNA-aminoglycoside antibiotic interactions: fluorescence detection of binding and conformational change. *Bioorg Med Chem Lett* **9**, 213-6.

Macdonald, P. M. and Kerr, K. (1997). Redundant RNA recognition events in bicoid mRNA localization. *Rna* **3**, 1413-20.

MacKay, S. L., Tannahill, C. L., Auffenberg, T., Ksontini, R., Copeland, E. M., 3rd and Moldawer, L. L. (1999). Characterization in vitro and in vivo of hammerhead ribozymes directed against murine tumor necrosis factoralpha. *Biochem Biophys Res Commun* **260**, 390-7.

Madsen, K., Makower, A. M., Friberg, U., Eden, S. and Isaksson, O. (1985). Effect of human growth hormone on proteoglycan synthesis in cultured rat chondrocytes. *Acta Endocrinol (Copenh)* **108**, 338-42.

Maiter, D., Underwood, L. E., Maes, M., Davenport, M. L. and Ketelslegers, J. M. (1988). Different effects of intermittent and continuous growth hormone (GH) administration on serum somatomedin-C/insulin-like growth factor I and liver GH receptors in hypophysectomized rats. *Endocrinology* **123**, 1053-9.

Maniatis, T., Fritch, E. F. and Sambrook, J. (1982). Molecular cloning: A laboratory manual. Cold Springs Harbor: Cold Springs Harbor Laboratory.

Martini, J. F., Pezet, A., Guezennec, C. Y., Edery, M., Postel-Vinay, M. C. and Kelly, P. A. (1997). Monkey growth hormone (GH) receptor gene expression. Evidence for two mechanisms for the generation of the GH binding protein. *J Biol Chem* **272**, 18951-8.

Mathews, D. H., Sabina, J., Zuker, M. and Turner, D. H. (1999). Expanded sequence dependence of thermodynamic parameters improves prediction of RNA secondary structure. *J Mol Biol* **288**, 911-40.

Mathews, L. S., Enberg, B. and Norstedt, G. (1989). Regulation of rat growth hormone receptor gene expression. *J Biol Chem* **264**, 9905-10.

Matsuhisa, A., Kishi, Y. and Shiba, K. (1994). A simple staining method for dna and rna blotted on a membrane using a polyethyleneimine-enzyme conjugate. *J Biochem (Tokyo)* **116**, 478-81.

Matysiak, M., Wrzesinski, J. and Ciesiolka, J. (1999). Sequential folding of the genomic ribozyme of the hepatitis delta virus: structural analysis of RNA transcription intermediates [In Process Citation]. *J Mol Biol* **291**, 283-94.

McCall, M. J., Hendry, P. and Jennings, P. A. (1992). Minimal sequence requirements for ribozyme activity. *Proc Natl Acad Sci U S A* **89**, 5710-4.

McConaghey, P. and Sledge, C. B. (1970). Production of "sulphation factor" by the perfused liver. *Nature* **225**, 1249-50.

McKee, K. K., Palyha, O. C., Feighner, S. D., Hreniuk, D. L., Tan, C. P., Phillips, M. S., Smith, R. G., Van der Ploeg, L. H. and Howard, A. D. (1997). Molecular analysis of rat pituitary and hypothalamic growth hormone secretagogue receptors. *Mol Endocrinol* **11**, 415-23.

McSwiggen, J. A. and Cech, T. R. (1989). Stereochemistry of RNA cleavage by the Tetrahymena ribozyme and evidence that the chemical step is not rate-limiting. *Science* **244**, 679-83.

Mei, H., Karret, T. W. and Bruice, T. C. (1989). Computational approach to the mechanism of self-cleavage of hammerhead ribozymes. *Proc Natl Acad Sci USA* **86**, 9727-31.

Mellado, M., Rodriguez-Frade, J. M., Kremer, L., von Kobbe, C., de Ana, A. M., Merida, I. and Martinez, A. C. (1997). Conformational changes required in the human growth hormone receptor for growth hormone signaling. *J Biol Chem* **272**, 9189-96.

Menger, M., Tuschl, T., Eckstein, F. and Porschke, D. (1996). Mg(2+)-dependent conformational changes in the hammerhead ribozyme. *Biochemistry* **35**, 14710-6.

Metcalfe, P., Johnston, D. G., Nosadini, R., Orksov, H. and Alberti, K. G. (1981). Metabolic effects of acute and prolonged growth hormone excess in normal and insulin-deficient man. *Diabetologia* **20**, 123-8.

Meyer, D. J., Campbell, G. S., Cochran, B. H., Argetsinger, L. S., Larner, A. C., Finbloom, D. S., Carter-Su, C. and Schwartz, J. (1994). Growth hormone induces a DNA binding factor related to the interferon- stimulated 91-kDa transcription factor. *J Biol Chem* **269**, 4701-4.

Michienzi, A., Prislei, S. and Bozzoni, I. (1996). U1 small nuclear RNA chimeric ribozymes with substrate specificity for the Rev pre-mRNA of human immunodeficiency virus. *Proc Natl Acad Sci U S A* **93**, 7219-24.

Miller, K. F., Bolt, D. J., Pursel, V. G., Hammer, R. E., Pinkert, C. A., Palmiter, R. D. and Brinster, R. L. (1989). Expression of human or bovine growth hormone gene with a mouse metallothionein-1 promoter in transgenic swine alters the secretion of porcine growth hormone and insulin-like growth factor-I. *J Endocrinol* **120**, 481-8.

Minvielle-Sabastia, L. and Keller, W. (1999). mRNA polyadenylation and its coupling to other processing reactions and to transcription. *Curr Opin Cell Biol* **11**, 352-7.

Moffat, J. G., Edens, A. and Talamantes, F. (1999). Structure and expression of the mouse growth hormone receptor/growth hormone binding protein gene. *J Mol Endocrinol* **23**, 33-44.

Mori, K., Yoshimoto, A., Takaya, K., Hosoda, K., Ariyasu, H., Yahata, K., Mukoyama, M., Sugawara, A., Hosoda, H., Kojima, M. et al. (2000). Kidney produces a novel acylated peptide, ghrelin. *FEBS Lett* **486**, 213-6.

Moutoussamy, S., Renaudie, F., Lago, F., Kelly, P. A. and Finidori, J. (1998). Grb10 identified as a potential regulator of growth hormone (GH) signaling by cloning of GH receptor target proteins. *J Biol Chem* **273**, 15906-12.

Muccioli, G., Papotti, M., Locatelli, V., Ghigo, E. and Deghenghi, R. (2001). Binding of 125I-labeled ghrelin to membranes from human hypothalamus and pituitary gland. *J Endocrinol Invest* **24**, RC7-9.

Mukhopadhyay, T. and Roth, J. A. (1994). Visualization of RNA in gel by shortwave UV epi-illumination without staining. *Biotechniques* **17**, 619-20.

Munro, T. P., Magee, R. J., Kidd, G. J., Carson, J. H., Barbarese, E., Smith, L. M. and Smith, R. (1999). Mutational analysis of a heterogeneous nuclear

ribonucleoprotein A2 response element for RNA trafficking. *J Biol Chem* **274**, 34389-95.

Murray, J. B., Terwey, D. P., Maloney, L., Karpeisky, A., Usman, N., Beigelman, L. and Scott, W. G. (1998). The structural basis of hammerhead ribozyme self-cleavage. *Cell* **92**, 665-73.

Murthy, K. G. and Manley, J. L. (1992). Characterization of the multisubunit cleavage-polyadenylation specificity factor from calf thymus. *J Biol Chem* **267**, 14804-11.

Naar, E. M., Bartke, A., Majumdar, S. S., Buonomo, F. C., Yun, J. S. and Wagner, T. E. (1991). Fertility of transgenic female mice expressing bovine growth hormone or human growth hormone variant genes. *Biol Reprod* **45**, 178-87.

Naka, T., Narazaki, M., Hirata, M., Matsumoto, T., Minamoto, S., Aono, A., Nishimoto, N., Kajita, T., Taga, T., Yoshizaki, K. et al. (1997). Structure and function of a new STAT-induced STAT inhibitor. *Nature* **387**, 924-9.

Nakamaye, K. L. and Eckstein, F. (1994). AUA-cleaving hammerhead ribozymes: attempted selection for improved cleavage. *Biochemistry* **33**, 1271-7.

Nakazato, M., Murakami, N., Date, Y., Kojima, M., Matsuo, H., Kangawa, K. and Matsukura, S. (2001). A role for ghrelin in the central regulation of feeding. *Nature* **409**, 194-8.

Narazaki, M., Fujimoto, M., Matsumoto, T., Morita, Y., Saito, H., Kajita, T., Yoshizaki, K., Naka, T. and Kishimoto, T. (1998). Three distinct domains of SSI-1/SOCS-1/JAB protein are required for its suppression of interleukin 6 signaling. *Proc Natl Acad Sci U S A* **95**, 13130-4.

Niall, H. D., Hogan, M. L., Sauer, R., Rosenblum, I. Y. and Greenwood, F. C. (1971). Sequences of pituitary and placental lactogenic and growth hormones: evolution from a primordial peptide by gene reduplication. *Proc Natl Acad Sci U S A* **68**, 866-70.

Nilsson, A., Swolin, D., Enerback, S. and Ohlsson, C. (1995). Expression of functional growth hormone receptors in cultured human osteoblast-like cells 0008530587. *J Clin Endocrinol Metab* **80**, 3483-8.

Ohlsson, C., Isgaard, J., Tornell, J., Nilsson, A., Isaksson, O. G. and Lindahl, A. (1993a). Endocrine regulation of longitudinal bone growth 0008219475. *Acta Paediatr Suppl* **82 Suppl 391**, 33-40; discussion 41.

Ohlsson, C., Lovstedt, K., Holmes, P. V., Nilsson, A., Carlsson, L. and Tornell, J. (1993b). Embryonic stem cells express growth hormone receptors: regulation by retinoic acid. *Endocrinology* **133**, 2897-903.

Ohta, Y., Kijima, H., Kashani-Sabet, M. and Scanlon, K. J. (1996a). Suppression of the malignant phenotype of melanoma cells by anti- oncogene ribozymes. *J Invest Dermatol* **106**, 275-80.

Ohta, Y., Kijima, H., Ohkawa, T., Kashani-Sabet, M. and Scanlon, K. J. (1996b). Tissue-specific expression of an anti-ras ribozyme inhibits proliferation of human malignant melanoma cells. *Nucleic Acids Res* **24**, 938-42.

Ojwang, J. O., Hampel, A., Looney, D. J., Wong-Staal, F. and Rappaport, J. (1992). Inhibition of human immunodeficiency virus type 1 expression by a hairpin ribozyme. *Proc Natl Acad Sci U S A* **89**, 10802-6.

O'Leary, M. J., Quinton, N., Ferguson, C. N., Preedy, V. R., Ross, R. J. and Hinds, C. J. (2000). In rats with sepsis, the acute fall in IGF-I is associated with an increase in circulating growth hormone-binding protein levels. *Intensive Care Med* **26**, 1547-52.

Oleynikov, Y. and Singer, R. H. (1998). RNA localization: different zipcodes, same postman? *Trends Cell Biol* **8**, 381-3.

Olive, J. E., De Abreu, D. M., Rastogi, T., Andersen, A. A., Mittermaier, A. K., Beattie, T. L. and Collins, R. A. (1995). Enhancement of Neurospora VS ribozyme cleavage by tuberactinomycin antibiotics. *Embo J* **14**, 3247-51.

Orgel, L. E. (1968). Evolution of the genetic apparatus. *J Mol Biol* **38**, 381-93.

Orgel, L. E. and Crick, F. H. (1993). Anticipating an RNA world. Some past speculations on the origin of life: where are they today? *Faseb J* **7**, 238-9.

Orita, M., Vinayak, R., Andrus, A., Warashina, M., Chiba, A., Kaniwa, H., Nishikawa, F., Nishikawa, S. and Taira, K. (1996). Magnesium-mediated conversion of an inactive form of a hammerhead ribozyme to an active complex with its substrate. An investigation by NMR spectroscopy. *J Biol Chem* **271**, 9447-54.

Ortigao, J. F., Rosch, H., Selter, H., Frohlich, A., Lorenz, A., Montenarh, M. and Seliger, H. (1992). Antisense effect of oligodeoxynucleotides with inverted terminal internucleotidic linkages: a minimal modification protecting against nucleolytic degradation. *Antisense Res Dev* **2**, 129-46.

Palfner, K., Kneba, M., Hiddemann, W. and Bertram, J. (1995). Short technical reports. Quantification of ribozyme-mediated RNA cleavage using silver-stained polyacrylamide gels. *Biotechniques* **19**, 926-9.

Paolella, G., Sproat, B. S. and Lamond, A. I. (1992). Nuclease resistant ribozymes with high catalytic activity. *Embo J* **11**, 1913-9.

Parr, T. (1996). Insulin exposure controls the rate of mammalian aging. *Mech Ageing Dev* **88**, 75-82.

Parr, T. (1997). Insulin exposure and aging theory. *Gerontology* **43**, 182-200.

Peino, R., Baldelli, R., Rodriguez-Garcia, J., Rodriguez-Segade, S., Kojima, M., Kangawa, K., Arvat, E., Ghigo, E., Dieguez, C. and Casanueva, F. F. (2000). Ghrelin-induced growth hormone secretion in humans. *Eur J Endocrinol* **143**, R11-4.

Peracchi, A., Beigelman, L., Scott, E. C., Uhlenbeck, O. C. and Herschlag, D. (1997). Involvement of a specific metal ion in the transition of the hammerhead ribozyme to its catalytic conformation. *J Biol Chem* **272**, 26822-6.

Perriman, R., Delves, A. and Gerlach, W. L. (1992). Extended target-site specificity for a hammerhead ribozyme. *Gene* **113**, 157-63.

Pitt, B. R., Brookens, M. A., Steve, A. R., Atlas, A. B., Davies, P., Kuo, S. M. and Lazo, J. S. (1992). Expression of pulmonary metallothionein genes in late gestational lambs. *Pediatr Res* **32**, 424-30.

Pley, H. W., Flaherty, K. M. and McKay, D. B. (1994). Three-dimensional structure of a hammerhead ribozyme [see comments]. *Nature* **372**, 68-74.

Pontius, B. W., Lott, W. B. and von Hippel, P. H. (1997). Observations on catalysis by hammerhead ribozymes are consistent with a two-divalent-metal-ion mechanism. *Proc Natl Acad Sci U S A* **94**, 2290-4.

Qin, P. Z. and Pyle, A. M. (1999). Antagonistic substrate binding by a group II intron ribozyme. *J Mol Biol* **291**, 15-27.

Qiu, L., Moreira, A., Kaplan, G., Levitz, R., Wang, J. Y., Xu, C. and Drlica, K. (1998). Degradation of hammerhead ribozymes by human ribonucleases. *Mol Gen Genet* **258**, 352-62.

Raben, M. S. (1958). Human growth hormone. *J Clin Endocrinol Metab* **18**, 71-115.

Raben, M. S. (1959). Treatment of a pituitary dwarf with human growth hormone. *Recent Prog Horm Res* **15**, 901-3.

Raillard, S. A. and Joyce, G. F. (1996). Targeting sites within HIV-1 cDNA with a DNA-cleaving ribozyme. *Biochemistry* **35**, 11693-701.

Rajagopal, J., Doudna, J. A. and Szostak, J. W. (1989). Stereochemical course of catalysis by the Tetrahymena ribozyme. *Science* **244**, 692-4.

Ram, P. A., Park, S. H., Choi, H. K. and Waxman, D. J. (1996). Growth hormone activation of Stat 1, Stat 3, and Stat 5 in rat liver. Differential kinetics of hormone desensitization and growth hormone stimulation of both tyrosine phosphorylation and serine/threonine phosphorylation. *J Biol Chem* **271**, 5929-40.

Ram, P. A. and Waxman, D. J. (1997). Interaction of growth hormone-activated STATs with SH2-containing phosphotyrosine phosphatase SHP-1 and nuclear JAK2 tyrosine kinase. *J Biol Chem* **272**, 17694-702.

Renault, L., Nassar, N., Vetter, I., Becker, J., Klebe, C., Roth, M. and Wittinghofer, A. (1998). The 1.7 A crystal structure of the regulator of chromosome condensation (RCC1) reveals a seven-bladed propeller. *Nature* **392**, 97-101.

Robinson-Benion, C. and Holt, J. T. (1995). Antisense techniques. *Methods Enzymol* **254**, 363-75.

Rosen, C. A. and Pavlakis, G. N. (1990). Tat and Rev: positive regulators of HIV gene expression [published erratum appears in AIDS 1990 Aug;4(8):following A48]. *Aids* **4**, 499-509.

Ross, A. F., Oleynikov, Y., Kislauskis, E. H., Taneja, K. L. and Singer, R. H. (1997). Characterization of a beta-actin mRNA zipcode-binding protein. *Mol Cell Biol* **17**, 2158-65.

Ross, J. (1996). Control of messenger RNA stability in higher eukaryotes. *Trends Genet* **12**, 171-5.

Rowe, P. M. (1996). Ribozymes enter clinical trials for HIV-1 treatment [news]. *Lancet* **348**, 1302.

Ruffner, D. E., Stormo, G. D. and Uhlenbeck, O. C. (1990). Sequence requirements of the hammerhead RNA self-cleavage reaction. *Biochemistry* **29**, 10695-702.

Rui, L., Mathews, L. S., Hotta, K., Gustafson, T. A. and Carter-Su, C. (1997). Identification of SH2-Bbeta as a substrate of the tyrosine kinase JAK2 involved in growth hormone signaling. *Mol Cell Biol* **17**, 6633-44.

Sakamoto, T., Kim, M. H., Kurihara, Y., Sasaki, N., Noguchi, T., Katahira, M. and Uesugi, S. (1997). Properties of a hammerhead ribozyme with deletion of stem II. *J Biochem (Tokyo)* **121**, 288-94.

Saldanha, R., Mohr, G., Belfort, M. and Lambowitz, A. M. (1993). Group I and group II introns. *Faseb J* **7**, 15-24.

Scanlon, K. J., Jiao, L., Funato, T., Wang, W., Tone, T., Rossi, J. J. and Kashani-Sabet, M. (1991). Ribozyme-mediated cleavage of c-fos mRNA reduces gene expression of DNA synthesis enzymes and metallothionein. *Proc Natl Acad Sci U S A* **88**, 10591-5.

Scanlon, K. J., Ohta, Y., Ishida, H., Kijima, H., Ohkawa, T., Kaminski, A., Tsai, J., Horng, G. and Kashani-Sabet, M. (1995). Oligonucleotide-mediated modulation of mammalian gene expression. *Faseb J* **9**, 1288-96.

Scheithauer, B. W., Sano, T., Kovacs, K. T., Young, W. F., Jr., Ryan, N. and Randall, R. V. (1990). The pituitary gland in pregnancy: a clinicopathologic and immunohistochemical study of 69 cases. *Mayo Clin Proc* **65**, 461-74.

Scherr, M., Grez, M., Ganser, A. and Engels, J. W. (1997). Specific hammerhead ribozyme-mediated cleavage of mutant N-ras mRNA in vitro and ex vivo. Oligoribonucleotides as therapeutic agents. *J Biol Chem* **272**, 14304-13.

Scherr, M. and Rossi, J. J. (1998). Rapid determination and quantitation of the accessibility to native RNAs by antisense oligodeoxynucleotides in murine cell extracts. *Nucleic Acids Res* **26**, 5079-85.

Schon, A. (1999). Ribonuclease P: the diversity of a ubiquitous RNA processing enzyme. *FEMS Microbiol Rev* **23**, 391-406.

Scott, W. G., Finch, J. T. and Klug, A. (1995). The crystal structure of an all-RNA hammerhead ribozyme: a proposed mechanism for RNA catalytic cleavage. *Cell* **81**, 991-1002.

Scott, W. G., Murray, J. B., Arnold, J. R. P., Stoddard, B. L. and Klug, A. (1996). Capturing the structure of a catalytic RNA intermediate: the hammerhead ribozyme. *Science* **274**, 2065-9.

Sczakiel, G. and Tabler, M. (1997). Computer-aided calculation of the local folding potential of target RNA and its use for ribozyme design. *Methods Mol Biol* **74**, 11-5.

Sen, D. and Geyer, C. R. (1998). DNA enzymes. *Curr Opin Chem Biol* **2**, 680-7.

Seoane, L. M., Tovar, S., Baldelli, R., Arvat, E., Ghigo, E., Casanueva, F. F. and Dieguez, C. (2000). Ghrelin elicits a marked stimulatory effect on GH secretion in freely- moving rats. *Eur J Endocrinol* **143**, R7-9.

Shea, B. T., Hammer, R. E. and Brinster, R. L. (1987). Growth allometry of the organs in giant transgenic mice. *Endocrinology* **121**, 1924-30.

Shen, Y., Li, R. and Shiosaki, K. (1997). Inhibition of p75 tumor necrosis factor receptor by antisense oligonucleotides increases hypoxic injury and beta-amyloid toxicity in human neuronal cell line. *J Biol Chem* **272**, 3550-3.

Shimayama, T., Nishikawa, S. and Taira, K. (1995). Generality of the NUX rule: kinetic analysis of the results of systematic mutations in the trinucleotide at the cleavage site of hammerhead ribozymes. *Biochemistry* **34**, 3649-54.

Siewerdt, F., Eisen, E. J., Murray, J. D. and Parker, I. J. (2000). Response to 13 generations of selection for increased 8-week body weight in lines of mice carrying a sheep growth hormone-based transgene. *J Anim Sci* **78**, 832-45.

Sil, A. and Herskowitz, I. (1996). Identification of asymmetrically localized determinant, Ash1p, required for lineage-specific transcription of the yeast HO gene. *Cell* **84**, 711-22.

Silva, C. M., Isgaard, J. and Thorner, M. O. (1999). Cytokines in endocrine function. *Adv Protein Chem* **52**, 199-221.

Silva, C. M., Lu, H. and Day, R. N. (1996). Characterization and cloning of STAT5 from IM-9 cells and its activation by growth hormone. *Mol Endocrinol* **10**, 508-18.

Silva, C. M., Lu, H., Weber, M. J. and Thorner, M. O. (1994). Differential tyrosine phosphorylation of JAK1, JAK2, and STAT1 by growth hormone and interferon-gamma in IM-9 cells. *J Biol Chem* **269**, 27532-9.

Sims, N. A., Clement-Lacroix, P., Da Ponte, F., Bouali, Y., Binart, N., Moriggl, R., Goffin, V., Coschigano, K., Gaillard-Kelly, M., Kopchick, J. et al. (2000). Bone homeostasis in growth hormone receptor-null mice is restored by IGF-I but independent of stat5 [In Process Citation]. *J Clin Invest* **106**, 1095-103.

Sioud, M. (1997). Effects of variations in length of hammerhead ribozyme antisense arms upon the cleavage of longer RNA substrates. *Nucleic Acids Res* **25**, 333-8.

Sioud, M., Natvig, J. B. and Forre, O. (1992). Preformed ribozyme destroys tumour necrosis factor mRNA in human cells. *J Mol Biol* **223**, 831-5.

Sjögren, K., Bohlooly, Y. M., Olsson, B., Coschigano, K., Törnell, J., Mohan, S., Isaksson, O. G., Baumann, G., Kopchick, J. and Ohlsson, C. (2000). Disproportional skeletal growth and markedly decreased bone mineral content in growth hormone receptor -/- mice. *Biochem Biophys Res Commun* **267**, 603-8.

Slim, G. and Gait, M. J. (1991). Configurationally defined phosphorothioate-containing oligoribonucleotides in the study of the mechanism of cleavage of hammerhead ribozymes. *Nucleic Acids Res* **19**, 1183-8.

Smit, L. S., Meyer, D. J., Billestrup, N., Norstedt, G., Schwartz, J. and Carter-Su, C. (1996). The role of the growth hormone (GH) receptor and JAK1 and JAK2 kinases in the activation of Stats 1, 3, and 5 by GH. *Mol Endocrinol* **10**, 519-33.

Smith, W. C., Kuniyoshi, J. and Talamantes, F. (1989). Mouse serum growth hormone (GH) binding protein has GH receptor extracellular and substituted transmembrane domains. *Mol Endocrinol* **3**, 984-90.

Snyder, D. S., Wu, Y., Wang, J. L., Rossi, J. J., Swiderski, P., Kaplan, B. E. and Forman, S. J. (1993). Ribozyme-mediated inhibition of bcr-abl gene expression in a Philadelphia chromosome-positive cell line. *Blood* **82**, 600-5.

Sokol, D. L. and Murray, J. D. (1996). Antisense and ribozyme constructs in transgenic animals. *Transgenic Res* **5**, 363-71.

Sokol, D. L., Passey, R. J., MacKinlay, A. G. and Murray, J. D. (1998). Regulation of CAT protein by ribozyme and antisense mRNA in transgenic mice. *Transgenic Res* **7**, 41-50.

Sorrentino, S. and Libonati, M. (1997). Structure-function relationships in human ribonucleases: main distinctive features of the major RNase types. *FEBS Lett* **404**, 1-5.

Sotelo, A. I., Dominici, F. P., Engbers, C., Bartke, A., Talamantes, F. and Turyn, D. (1995). Growth hormone-binding protein in normal mice and in transgenic mice expressing bovine growth hormone gene. *Am J Physiol* **268**, E745-51.

Sotiropoulos, A., Goujon, L., Simonin, G., Kelly, P. A., Postel-Vinay, M. C. and Finidori, J. (1993). Evidence for generation of the growth hormone-binding protein

through proteolysis of the growth hormone membrane receptor. *Endocrinology* **132**, 1863-5.

St Johnston, D., Beuchle, D. and Nusslein-Volhard, C. (1991). Staufen, a gene required to localize maternal RNAs in the Drosophila egg. *Cell* **66**, 51-63.

Stahl, N., Farruggella, T. J., Boulton, T. G., Zhong, Z., Darnell, J. E., Jr. and Yancopoulos, G. D. (1995). Choice of STATs and other substrates specified by modular tyrosine- based motifs in cytokine receptors. *Science* **267**, 1349-53.

Stark, B. C., Kole, R., Bowman, E. J. and Altman, S. (1977). Ribonuclease P: an enzyme with an essential RNA component. *Proc Nat Acad Sci USA* **75**, 3719-21.

Starr, R. and Hilton, D. J. (1998). SOCS: suppressors of cytokine signalling. *Int J Biochem Cell Biol* **30**, 1081-5.

Starr, R., Metcalf, D., Elefanty, A. G., Brysha, M., Willson, T. A., Nicola, N. A., Hilton, D. J. and Alexander, W. S. (1998). Liver degeneration and lymphoid deficiencies in mice lacking suppressor of cytokine signaling-1. *Proc Natl Acad Sci U S A* **95**, 14395-9.

Starr, R., Willson, T. A., Viney, E. M., Murray, L. J., Rayner, J. R., Jenkins, B. J., Gonda, T. J., Alexander, W. S., Metcalf, D., Nicola, N. A. et al. (1997). A family of cytokine-inducible inhibitors of signalling. *Nature* **387**, 917-21.

Steinecke, P., Steger, G. and Schreier, P. H. (1994). A stable hammerhead structure is not required for endonucleolytic activity of a ribozyme in vivo. *Gene* **149**, 47-54.

Strickland, S., Huarte, J., Belin, D., Vassalli, A., Rickles, R. J. and Vassalli, J. D. (1988). Antisense RNA directed against the 3' noncoding region prevents dormant mRNA activation in mouse oocytes. *Science* **241**, 680-4.

Sun, L. Q., Wang, L., Gerlach, W. L. and Symonds, G. (1995). Target sequence-specific inhibition of HIV-1 replication by ribozymes directed to tat RNA. *Nucleic Acids Res* **23**, 2909-13.

Sun, L. Q., Warrilow, D., Wang, L., Witherington, C., Macpherson, J. and Symonds, G. (1994). Ribozyme-mediated suppression of Moloney murine leukemia virus and human immunodeficiency virus type I replication in permissive cell lines. *Proc Natl Acad Sci U S A* **91**, 9715-9.

Szathmary, E. (1997). Origins of life. The first two billion years [news]. *Nature* **387**, 662-3.

Tabler, M., Homann, M., Tzortzakaki, S. and Sczakiel, G. (1994). A three-nucleotide helix I is sufficient for full activity of a hammerhead ribozyme: advantages of an asymmetric design. *Nucleic Acids Res* **22**, 3958-65.

Takebe, Y., Seiki, M., Fujisawa, J., Hoy, P., Yokota, K., Arai, K., Yoshida, M. and Arai, N. (1988). SR alpha promoter: an efficient and versatile mammalian cDNA expression system composed of the simian virus 40 early promoter and the R-U5 segment of human T-cell leukemia virus type 1 long terminal repeat. *Mol Cell Biol* **8**, 466-72.

Tanner, J. W., Leingang, K. A., Mueckler, M. M. and Glenn, K. C. (1992). Cellular mechanism of the insulin-like effect of growth hormone in adipocytes. Rapid translocation of the HepG2-type and adipocyte/muscle glucose transporters. *Biochem J* **282**, 99-106.

Tanner, M. A. and Cech, T. R. (1997). Joining the two domains of a group I ribozyme to form the catalytic core. *Science* **275**, 847-9.

Tarasow, T. M., Tarasow, S. L. and Eaton, B. E. (1997). RNA-catalysed carbon-carbon bond formation. *Nature* **389**, 54-7.

Taylor, N. R., Kaplan, B. E., Swiderski, P., Li, H. and Rossi, J. J. (1992). Chimeric DNA-RNA hammerhead ribozymes have enhanced in vitro catalytic efficiency and increased stability in vivo. *Nucleic Acids Res* **20**, 4559-65.

Thissen, J. P., Underwood, L. E. and Ketelslegers, J. M. (1999). Regulation of insulin-like growth factor-I in starvation and injury. *Nutr Rev* **57**, 167-76.

Thomas, D. J., Angle, C. R., Swanson, S. A. and Caffrey, T. C. (1991). Effect of sodium butyrate on metallothionein induction and cadmium cytotoxicity in ROS 17/2.8 cells. *Toxicology* **66**, 35-46.

Thompson, J. D., Ayers, D. F., Malmstrom, T. A., McKenzie, T. L., Ganousis, L., Chowrira, B. M., Couture, L. and Stinchcomb, D. T. (1995). Improved accumulation and activity of ribozymes expressed from a tRNA- based RNA polymerase III promoter. *Nucleic Acids Res* **23**, 2259-68.

Tokumoto, Y. and Saigo, K. (1992). RNA-RNA and RNA-DNA ligation with the sTobRV(+) hammerhead ribozyme. *Nucleic Acids Symp Ser* **27**, 21-2.

Traboni, C., Ciliberto, G. and Cortese, R. (1984). Mutations in Box B of the promoter of a eucaryotic tRNAPro gene affect rate of transcription, processing, and stability of the transcripts. *Cell* **36**, 179-87.

Trivedi, B. and Daughaday, W. H. (1988). Release of growth hormone binding protein from IM-9 lymphocytes by endopeptidase is dependent on sulfhydryl group inactivation. *Endocrinology* **123**, 2201-6.

Tsuchihashi, Z., Khosla, M. and Herschlag, D. (1993). Protein enhancement of hammerhead ribozyme catalysis. *Science* **262**, 99-102.

Tsuji, H., Iehara, N., Masegi, T., Imura, M., Ohkawa, J., Arai, H., Ishii, K., Kita, T. and Doi, T. (1998). Ribozyme targeting of receptor for advanced glycation end products in mouse mesangial cells. *Biochem Biophys Res Commun* **245**, 583-8.

Uchimaru, T., Tanabe, K., Shimayama, T., Uebayasi, M. and Taira, K. (1993). Theoretical analyses on the role of metal cations in RNA cleavage processes. *Nucleic Acids Symp Ser* **29**, 179-80.

Ueno, H., Sasaki, K., Miyagawa, K., Honda, H., Mitani, K., Yazaki, Y. and Hirai, H. (1997). Antisense repression of proto-oncogene c-Cbl enhances activation of the JAK-STAT pathway but not the ras pathway in epidermal growth factor receptor signaling. *J Biol Chem* **272**, 8739-43.

Uhlenbeck, O. C. (1987). A small catalytic oligoribonucleotide. *Nature* **328**, 596-600.

Umesono, K., Giguere, V., Glass, C. K., Rosenfeld, M. G. and Evans, R. M. (1988). Retinoic acid and thyroid hormone induce gene expression through a common responsive element. *Nature* **336**, 262-5.

van Tol, H., Buzayan, J. M., Feldstein, P. A., Eckstein, F. and Bruening, G. (1990). Two autolytic processing reactions of a satellite RNA proceed with inversion of configuration. *Nucleic Acids Res* **18**, 1971-5.

VanderKuur, J., Allevato, G., Billestrup, N., Norstedt, G. and Carter-Su, C. (1995a). Growth hormone-promoted tyrosyl phosphorylation of SHC proteins and SHC association with Grb2. *J Biol Chem* **270**, 7587-93.

Vanderkuur, J. A., Butch, E. R., Waters, S. B., Pessin, J. E., Guan, K. L. and Carter-Su, C. (1997). Signaling molecules involved in coupling growth hormone receptor to mitogen-activated protein kinase activation. *Endocrinology* **138**, 4301-7.

VanderKuur, J. A., Wang, X., Zhang, L., Allevato, G., Billestrup, N. and Carter-Su, C. (1995b). Growth hormone-dependent phosphorylation of tyrosine 333 and/or 338 of the growth hormone receptor. *J Biol Chem* **270**, 21738-44.

VanderKuur, J. A., Wang, X., Zhang, L., Campbell, G. S., Allevato, G., Billestrup, N., Norstedt, G. and Carter-Su, C. (1994). Domains of the growth hormone receptor required for association and activation of JAK2 tyrosine kinase. *J Biol Chem* **269**, 21709-17.

Wahle, E. and Ruegsegger, U. (1999). 3'-End processing of pre-mRNA in eukaryotes. *FEMS Microbiol Rev* **23**, 277-95.

Waldrop, M. M. (1992). Finding RNA makes proteins gives 'RNA world' a big boost [news; comment]. *Science* **256**, 1396-7.

Wang, J. F., Downs, W. D. and Cech, T. R. (1993a). Movement of the guide sequence during RNA catalysis by a group I ribozyme. *Science* **260**, 504-8.

Wang, J. P., Enjoji, M., Tiebel, M., Ochsner, S., Chan, L. and Teng, B. B. (1999a). Hammerhead ribozyme cleavage of apolipoprotein B mRNA generates a truncated protein. *J Biol Chem* **274**, 24161-70.

Wang, Q., Mullah, B., Hansen, C., Asundi, J. and Robishaw, J. D. (1997). Ribozyme-mediated suppression of the G protein gamma7 subunit suggests a role in hormone regulation of adenylylcyclase activity. *J Biol Chem* **272**, 26040-8.

Wang, Q., Mullah, B. K. and Robishaw, J. D. (1999b). Ribozyme approach identifies a functional association between the G protein beta1gamma7 subunits in the beta-adrenergic receptor signaling pathway. *J Biol Chem* **274**, 17365-71.

Wang, X., Cioffi, J. A, Kelder, B., Harding, P. A., Chen, W. Y. and Kopchick, J. J. (1993b). Expression of a functional porcine growth hormone receptor cDNA in mouse L cells. *Mol Cell Endocrinol* **94**, 89-96.

Wang, X., Darus, C. J., Xu, B. C. and Kopchick, J. J. (1996). Identification of growth hormone receptor (GHR) tyrosine residues required for GHR phosphorylation and JAK2 and STAT5 activation. *Mol Endocrinol* **10**, 1249-60.

Wang, X., Moller, C., Norstedt, G. and Carter-Su, C. (1993c). Growth hormone-promoted tyrosyl phosphorylation of a 121-kDa growth hormone receptor-associated protein. *J Biol Chem* **268**, 3573-9.

Wang, X., Souza, S. C., Kelder, B., Cioffi, J. A. and Kopchick, J. J. (1995). A 40-amino acid segment of the growth hormone receptor cytoplasmic domain is essential for GH-induced tyrosine-phosphorylated cytosolic proteins. *J Biol Chem* **270**, 6261-6.

Wang, X., Xu, B., Souza, S. C. and Kopchick, J. J. (1994). Growth hormone (GH) induces tyrosine-phosphorylated proteins in mouse L cells that express recombinant GH receptors. *Proc Natl Acad Sci U S A* **91**, 1391-5.

Waxman, D. J., Ram, P. A., Park, S. H. and Choi, H. K. (1995). Intermittent plasma growth hormone triggers tyrosine phosphorylation and nuclear translocation of a liver-expressed, Stat 5-related DNA binding protein. Proposed role as an intracellular regulator of male- specific liver gene transcription. *J Biol Chem* **270**, 13262-70.

Weerasinghe, M., Liem, S. E., Asad, S., Read, S. E. and Joshi, S. (1991). Resistance to human immunodeficiency virus type 1 (HIV-1) infection in human CD4+ lymphocyte-derived cell lines conferred by using retroviral vectors expressing an HIV-1 RNA-specific ribozyme. *J Virol* **65**, 5531-4.

Wehrenberg, W. B., Baird, A. and Ling, N. (1983). Potent interaction between glucocorticoids and growth hormone-releasing factor in vivo. *Science* **221**, 556-8.

Weier, H. U. and Rosette, C. (1990). Generation of clonal DNA templates for in vitro transcription without plasmid purification. *Biotechniques* **8**, 252-7.

Welch, P. J., Yei, S. and Barber, J. R. (1998). Ribozyme gene therapy for hepatitis C virus infection. *Clin Diagn Virol* **10**, 163-71.

Wells, J. A. and de Vos, A. M. (1996). Hematopoietic receptor complexes. *Annu Rev Biochem* **65**, 609-34.

Werther, G. A., Haynes, K. M., Barnard, R. and Waters, M. J. (1990). Visual demonstration of growth hormone receptors on human growth plate chondrocytes. *J Clin Endocrinol Metab* **70**, 1725-31.

Westhof, E. and Michel, F. (1998). Ribozyme architectural diversity made visible [comment]. *Science* **282**, 251-2.

Whitelaw, C. B., Archibald, A. L., Harris, S., McClenaghan, M., Simons, J. P. and Clark, A. J. (1991). Targeting expression to the mammary gland: intronic sequences can enhance the efficiency of gene expression in transgenic mice. *Transgenic Res* **1**, 3-13.

Whitfield, J. F., MacManus, J. P. and Rixon, R. H. (1971). Stimulation by growth hormone of deoxyribonucleic acid synthesis and proliferation of rat thymic lymphocytes. *Horm Metab Res* **3**, 28-33.

Wilson, G. M. and Brewer, G. (1999). The search for trans-acting factors controlling messenger RNA decay. *Prog Nucleic Acid Res Mol Biol* **62**, 257-91.

Wilson, J. D. and Foster, D. W. (1998). Williams textbook of endocrinology. **9th Edition**, 249-340.

Windahl, S. H., Vidal, O., Andersson, G., Gustafsson, J. A. and Ohlsson, C. (1999). Increased cortical bone mineral content but unchanged trabecular bone mineral density in female ERbeta(-/-) mice. *J Clin Invest* **104**, 895-901.

Winston, L. A. and Bertics, P. J. (1992). Growth hormone stimulates the tyrosine phosphorylation of 42- and 45- kDa ERK-related proteins. *J Biol Chem* **267**, 4747-51.

Wolin, S. L. and Matera, A. G. (1999). The trials and travels of tRNA. *Genes Dev* **13**, 1-10.

Wong-Staal, F., Poeschla, E. M. and Looney, D. J. (1998). A controlled, Phase 1 clinical trial to evaluate the safety and effects in HIV-1 infected humans of autologous lymphocytes transduced with a ribozyme that cleaves HIV-1 RNA. *Hum Gene Ther* **9**, 2407-25.

Wood, T. J., Sliva, D., Lobie, P. E., Pircher, T. J., Gouilleux, F., Wakao, H., Gustafsson, J. A., Groner, B., Norstedt, G. and Haldosen, L. A. (1995). Mediation of growth hormone-dependent transcriptional activation by mammary gland factor/Stat 5. *J Biol Chem* **270**, 9448-53.

Xu, B. C., Wang, X., Darus, C. J. and Kopchick, J. J. (1996). Growth hormone promotes the association of transcription factor STAT5 with the growth hormone receptor. *J Biol Chem* **271**, 19768-73.

Xu, B. C., Wang, X., James, C. and Kopchick, J. J. (1995). Characterization of growth hormone-induced tyrosine-phosphorylated proteins in mouse cells that express GH receptors. *Receptor* **5**, 105-16.

Xu, Z. D., Oey, L., Mohan, S., Kawachi, M. H., Lee, N. S., Rossi, J. J. and Fujita-Yamaguchi, Y. (1999). Hammerhead ribozyme-mediated cleavage of the human insulin-like growth factor-II ribonucleic acid in vitro and in prostate cancer cells. *Endocrinology* **140**, 2134-44.

Yamamoto, H., Irie, A., Fukushima, Y., Ohnishi, T., Arita, N., Hayakawa, T. and Sekiguchi, K. (1996). Abrogation of lung metastasis of human fibrosarcoma cells by ribozyme- mediated suppression of integrin alpha6 subunit expression. *Int J Cancer* **65**, 519-24.

Yeivin, A., Tang, D. C. and Taylor, M. W. (1992). Sodium butyrate selectively induces transcription of promoters adjacent to the MoMSV viral enhancer. *Gene* **116**, 159-64.

Yokoyama, Y., Takahashi, Y., Shinohara, A., Lian, Z., Wan, X., Niwa, K. and Tamaya, T. (1998). Attenuation of telomerase activity by a hammerhead ribozyme targeting the template region of telomerase RNA in endometrial carcinoma cells. *Cancer Res* **58**, 5406-10.

Yoshimura, A., Ohkubo, T., Kiguchi, T., Jenkins, N. A., Gilbert, D. J., Copeland, N. G., Hara, T. and Miyajima, A. (1995). A novel cytokine-inducible gene CIS encodes an SH2-containing protein that binds to tyrosine-phosphorylated interleukin 3 and erythropoietin receptors. *Embo J* **14**, 2816-26.

Yu, M., Poeschla, E., Yamada, O., Degrandis, P., Leavitt, M. C., Heusch, M., Yees, J. K., Wong-Staal, F. and Hampel, A. (1995). In vitro and in vivo characterization of a second functional hairpin ribozyme against HIV-1. *Virology* **206**, 381-6.

Yu, Q., Pecchia, D. B., Kingsley, S. L., Heckman, J. E. and Burke, J. M. (1998). Cleavage of highly structured viral RNA molecules by combinatorial libraries of hairpin ribozymes. The most effective ribozymes are not predicted by substrate selection rules. *J Biol Chem* **273**, 23524-33.

Zamecnik, P. C. and Stephenson, M. L. (1978). Inhibition of Rous sarcoma virus replication and cell transformation by a specific oligodeoxynucleotide. *Proc Natl Acad Sci U S A* **75**, 280-4.

Zelger, B., Hittmair, A., Schir, M., Ofner, C., Ofner, D., Fritsch, P. O., Bocker, W., Jasani, B. and Schmid, K. W. (1993). Immunohistochemically demonstrated metallothionein expression in malignant melanoma. *Histopathology* **23**, 257-63.

Zhang, B. and Cech, T. R. (1997). Peptide bond formation by in vitro selected ribozymes. *Nature* **390**, 96-100.

Zhang, B. and Cech, T. R. (1998). Peptidyl-transferase ribozymes: trans reactions, structural characterization and ribosomal RNA-like features. *Chem Biol* **5**, 539-53.

Zhao, J. J. and Pick, L. (1993). Generating loss-of-function phenotypes of the fushi tarazu gene with a targeted ribozyme in Drosophila. *Nature* **365**, 448-51.

Zhou, C., Bahner, I., Rossi, J. J. and Kohn, D. B. (1996). Expression of hammerhead ribozymes by retroviral vectors to inhibit HIV- 1 replication: comparison of RNA levels and viral inhibition. *Antisense Nucleic Acid Drug Dev* **6**, 17-24.

Zhou, Y., He, L. and Kopchick, J. J. (1994). An exon encoding the mouse growth hormone binding protein (mGHBP) carboxy terminus is located between exon 7 and 8 of the mouse growth hormone receptor gene. *Receptor* **4**, 223-7.

Zhou, Y., Xu, B. C., Maheshwari, H. G., He, L., Reed, M., Lozykowski, M., Okada, S., Cataldo, L., Coschigamo, K., Wagner, T. E. et al. (1997). A mammalian model for Laron syndrome produced by targeted disruption of the mouse growth hormone receptor/binding protein gene (the Laron mouse). *Proc Natl Acad Sci U S A* **94**, 13215-20.

Zimmerly, S., Guo, H., Eskes, R., Yang, J., Perlman, P. S. and Lambowitz, A. M. (1995a). A group II intron RNA is a catalytic component of a DNA endonuclease involved in intron mobility. *Cell* **83**, 529-38.

Zimmerly, S., Guo, H., Perlman, P. S. and Lambowitz, A. M. (1995b). Group II intron mobility occurs by target DNA-primed reverse transcription. *Cell* **82**, 545-54.

Zipf, W. B., Payne, A. H. and Kelch, R. P. (1978). Prolactin, growth hormone, and luteinizing hormone in the maintenance of testicular luteinizing hormone receptors. *Endocrinology* **103**, 595-600.

Zoumadakis, M. and Tabler, M. (1995). Comparative analysis of cleavage rates after systematic permutation of the NUX consensus target motif for hammerhead ribozymes. *Nucleic Acids Res* **23**, 1192-6.

Zuker, M., Jaeger, J. A. and Turner, D. H. (1991). A comparison of optimal and suboptimal RNA secondary structures predicted by free energy minimization with structures determined by phylogenetic comparison. *Nucleic Acids Res* **19**, 2707-14.

Zuker, M., Mathews, D. H. and Turner, D. H. (1999). Algorithms and Thermodynamics for RNA Secondary Structure Prediction: A Practical Guide
In RNA Biochemistry and Biotechnology. In *NATO ASI Series*, (ed. J. Barciszewski and B. F. C. Clark), pp. 11-43: Kluwer Academic Publishers.

APPENDIX A

pMSV-GHR-RZ

Summary of experiments

In an effort to create a cell line that expresses GHR-RZ in an inducible manner, the sodium butyrate inducible (Yeivin et al., 1992) Maloney murine sarcoma virus long terminal repeat (MSV-LTR) was cloned 5' of the GHR-RZ. An MSV containing expression cassette (pMSV-bGH-c) was first created. Sequencing analysis confirmed the proper cloning of the construct. The MSV-driven RZ expression vector (pMSV-GHR-RZ) was then cloned and sequenced. To analyze the GHR-RZ in cells, mouse L cells stably transfected with a GHR/BP "mini-gene" (E6 cells) were stably transfected with pMSV-GHR-RZ. Following treatment with sodium butyrate, we expected the MSV-driven GHR-RZ to decrease the level of GHR compared to non-sodium butyrate treated cells. Unexpectedly, GHR levels actually increased in the sodium butyrate treated cells as compared to the non-treated cells (as determined by GHR binding assays). Therefore, it appears that the metallothionein-I transcriptional regulatory element is also inducible by sodium butyrate treatment in agreement with previous reports (Andrews and Adamson, 1987; Birren and Herschman, 1986; Thomas et al., 1991).

Creation of pMSV-bGH-c expression cassette

The plasmid pMSV-GHR-RZ containing a MSV-LTR was used as an expression vector for the GHR ribozyme. First an expression cassette was constructed

from two other expression cassettes, pCMVie-bGH and pMSV-Δ29 (see figure 42). The plasmid pCMVie-bGH was prepared for ligation by digestion with *Pvu*II and *Nde*I to produce four fragments 798nt, 881nt, 1224nt, and 2330nt in size. The plasmid pMSV-Δ29 was prepared by digestion with *BamH*I to produce two fragments 1000nt and 7500nt in size. The 5' overhangs resulting from the *BamH*I digestion were then filled in with Klenow enzyme. The "blunt ended" fragments from pMSV-Δ29 were then digested with *Nde*I to produce four fragments 996nt, 1000nt, 2500nt, and 4000nt in size. The fragments from both plasmids were separated by electrophoresis. The ~2330nt fragment from pCMVie-bGH containing the bGH poly A signal sequence, ampicillin resistance gene and the origin of replication was removed with a scalpel and retained for purification. The ~966nt fragment from pMSV-Δ29 containing the MSV transcriptional regulator element was removed with a scalpel and retained for purification. The two fragments were placed into dialysis tubing containing TAE and isolated using dialysis tubing and Elutip-d^{TM} ion-exchange columns as described previously in the method section of this dissertation. The isolated DNA fragments were resusended in deionized H_2O and ligated using T4 DNA polymerase. DNA mini-preparations were performed and positive clones were sequenced (see figure 43) to verify proper sub-cloning.

Creation of pMSV-GHR-RZ expression vector

Using the pMSV-bGH-c expression cassette, the GHR-RZ was sub-cloned in

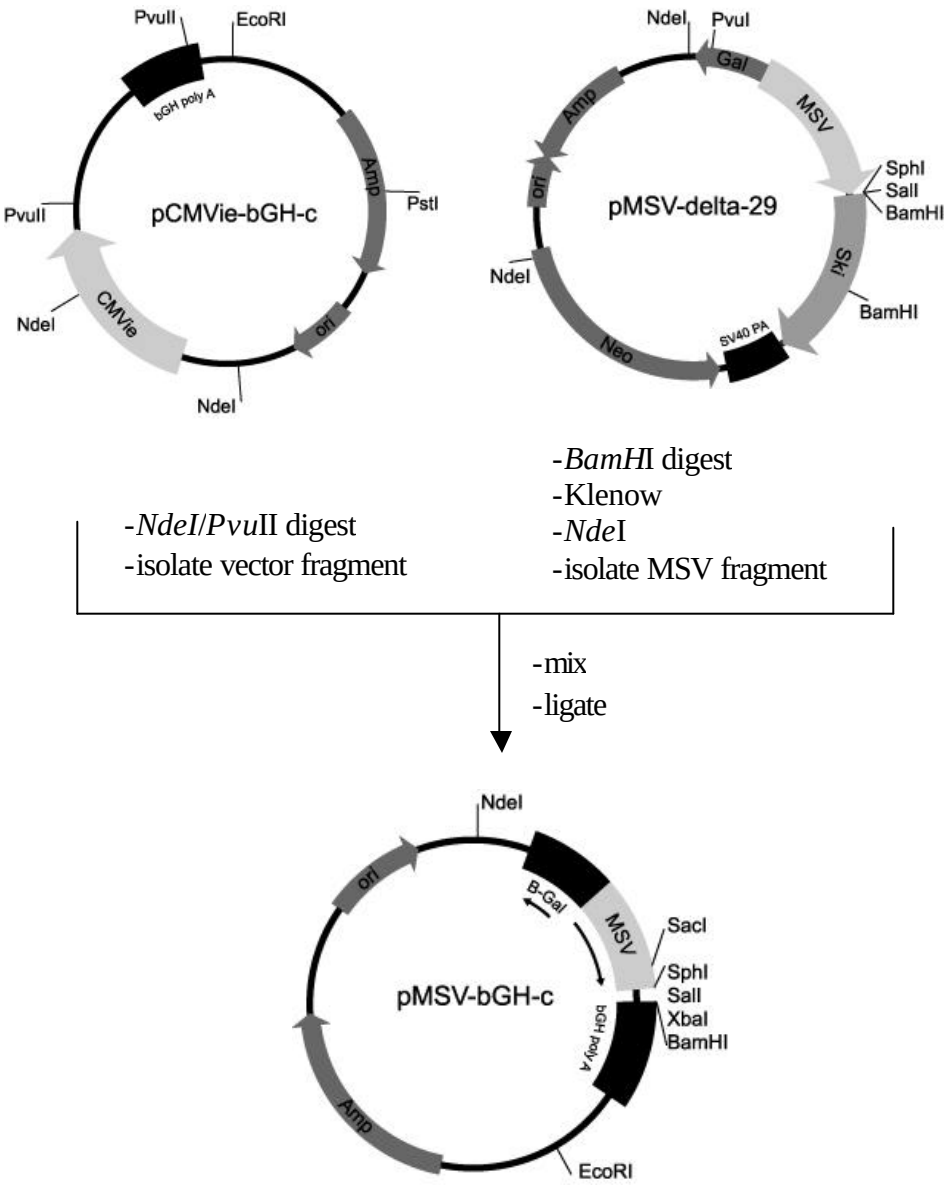

Figure 42. Construction of the plasmid pMSV-bGH-c. The plasmids pCMVie-bGH-c and pMSV-delta 29 were used to sub-clone the sodium inducible expression cassette pMSV-bGH-c. Following digestion with NdeI and PvuII, a ~2330nt fragment from pCMVie-bGH containing the bGH poly A signal sequence, ampicillin resistance gene and the origin of replication was isolated. Following a digestion with *BamH*I, "blunt end" reaction with Klenow, and a second digestion with *Nde*I, a ~966nt fragment from pMSV-Δ29 containing the MSV transcriptional regulator element was isolated. The two fragments were ligated, and the positive clones were sequenced.

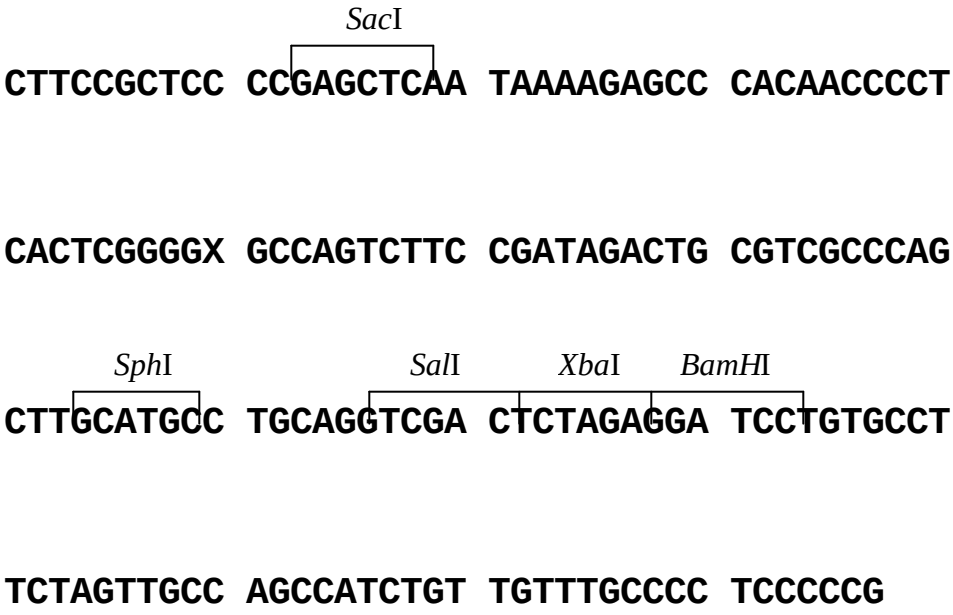

Figure 43. Sequence of pMSV-bGH-c. DNA sequencing results confirmed the proper integration of RZ-DNA into the expression plasmid. The 157 nucleotides span the poly linker region containing four restriction sites (SphI, *Sal*I, *Xba*I, and *BamH*I). The region 5' of the poly linker contains sequence from the 3' end of MSV-LTR, while the region 3' of the poly linker contains sequence from the 5' end of the bGH poly A addition sequence.

to create the pMSV-GHR-RZ expression vector (see figure 44). The plasmid pMSV-bGH-c was prepared for ligation by digestion with *BamH*I to linearize the vector. The 5' overhangs of the linearized vector were then filled in with Klenow enzyme. The previously annealed double stranded RZ DNA fragments were also "blunt ended" with Klenow enzyme. Both fragments were gel purified and placed into dialysis tubing containing TAE and isolated using dialysis tubing and Elutip-d^{TM} ion-exchange columns as described previously in the method section of this dissertation. The isolated DNA fragments were resusended in deionized H_2O and ligated using T4 DNA polymerase. DNA mini-preparations were performed and positive clones were sequenced (see figure 45) to verify proper sub-cloning.

Stable transfection of E6 cells with a GHR-RZ

E6 cells, which express GHR (Mouse L cells stably transfected with GHR/BP DNA), were used for pMSV-GHR-RZ transfections. pGHR-RZ transfections were performed according to the general procedure for stable transfection of adherent cells with LipofectAMINE^{TM} outlined by the manufacturer's protocol (Gibco BRL) and is outlined in the method section of this dissertation for the stable transfection of E6 cells with GHR-RZ.

PCR screening of GHR-RZ transfected E6 cells

PCR was performed on 10 stable cell lines to verify the presence of the transfected GHR-RZ DNA. The method of screening used was similar to method

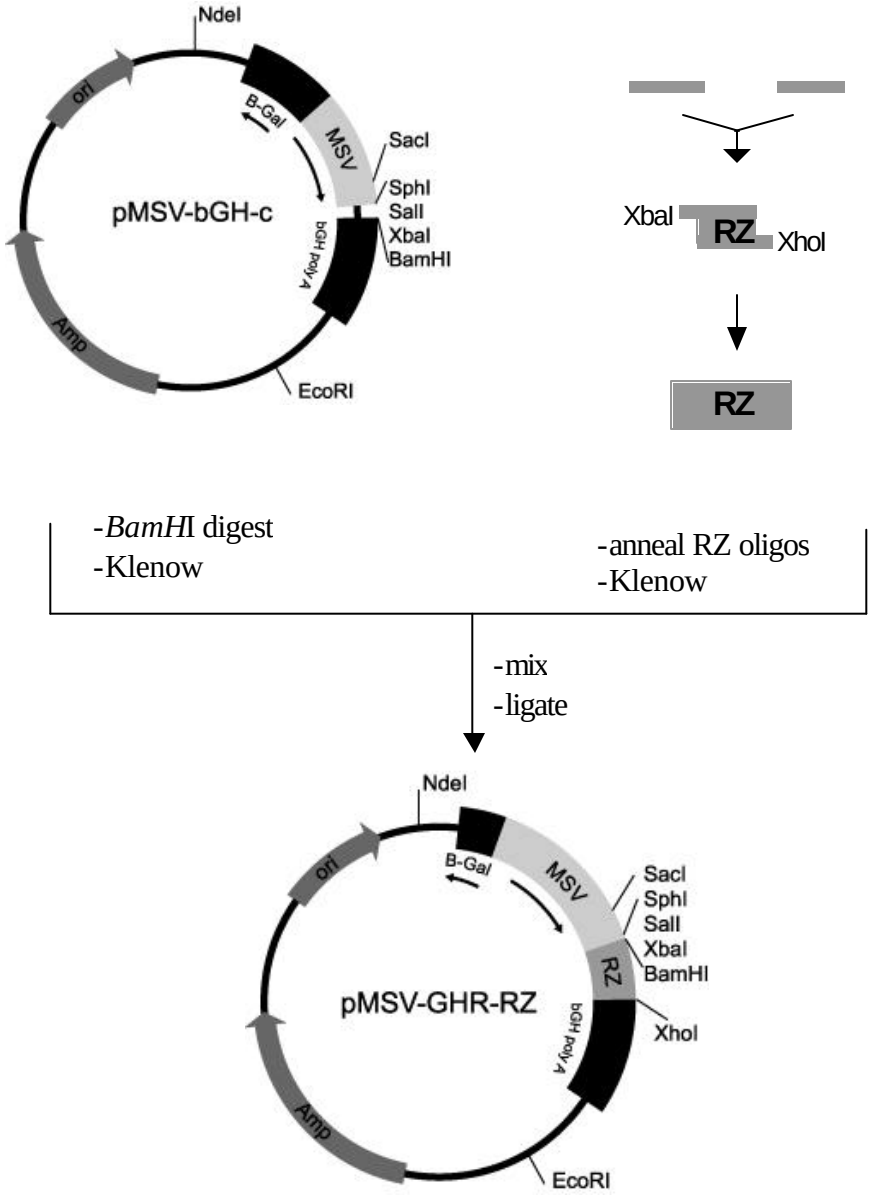

Figure 44. Construction of plasmid pMSV-GHR-RZ. The plasmid pMSV-bGH-c containing the ampicillin resistance gene, a bovine growth hormone poly adenylation signal sequence, and an MSV-LTR was used as an expression vector for the GHR ribozyme. The plasmid was prepared for ligation by digestion at a unique *BamH*I site followed by a "blunt end" reaction with Klenow. Oligonucleotides encoding the sense and antisense sequences of the GHR-RZ were annealed and the *Xba*I/*Xbo*I overhangs were "blunt ended" by Klenow prior to ligation.

*Sac*I

CTTCCGCTCC CCGAGCTCAA TAAAAGAGCC CACAACCCCT

CACTCGGGGX GCCAGTCTTC CGATAGACTG CGTCGCCCAG

*Sph*I *Sal*I *Xba*I *BamH*I

CTTGCATGCC TGCAGGTCGA CTCTAGAGGA TCCTAGACAA

GGTTAAGAAC TGATGAGTCC GTGAGGACGA AACCTGACAA

AGACTCGAGA TCCTGTGCCT TCTAGTTGCC AGCCATCTGT

TGTTTGCCCC TCCCCCG

Figure 45. Sequence of the plasmid pMSV-GHR-RZ. DNA sequencing results confirmed the proper integration of RZ-DNA into the expression plasmid. The shaded sequence represents the ribozyme insert with the 12 nt 5' and 3' arms boxed. The restriction sites are indicated with brackets.

described earlier for PCR screening of pMet-GHR-RZ transfected cells with the following exception: While the same 3' primer was used for detecting the RZ "mini-gene", **CTACAAATAGCATGACTGCTAGTCC** (directed to the poly adenylation signal sequence located in the bGH sequence 3' of the RZ), a different 5' primer **CCAGTCTTCCGATAGACTGC** (directed to a sequence in the MSV transcriptional regulatory element) was used.

Screening cells for functional GHR expression

The stably transfected GHR/BP DNA positive L cells as well as double transfected pMSV-GHR-RZ cells were screened for GHR expression using GHR binding assays. In 6-well tissue culture plates monolayers of the stable cells were propagated to 100% confluence (~$1x10^6$ cells/well). In half the wells, 5mM sodium butyrate was added to the culture media 24 hours prior to depletion. The cells were depleted in serum free DMEM medium for 2 hours at 37°C. Sodium butyrate treated cells were depleted in serum free DMEM medium with 5 mM sodium butyrate for 2 hours at 37°C. Binding assays were performed as previously described in the methods section for the screening of functional GHR expression with the exception of sodium butyrate treatment.

APPENDIX B

GHBP specific ribozyme

Summary of experiments

The GHR and GHBP mRNAs are alternatively spliced from the same pre-mRNA. The GHBP transcript contains exons 1-7 and 8a while GHR contains exons 1-10 but not 8a. The inclusion of exon 8a determines whether or not the GHBP transcript is the spliced message. Since sequences in exon 8a are the only sequence unique to the GHBP transcript, targeting a RZ to this exon should be a GHBP specific gene "knockdown". Therefore, in an attempt to specifically "knockdown" GHBP and not GHR, a RZ was designed to target a GTC located in exon 8a of the mouse GHBP mRNA. The amount of GHBP produced was measured in GHBP-RZ DNA positive clones as well as in the parent E6 cells. The samples were then sent to Dr. Gerhard Baumann at Northwestern University where GHBP levels were determined using GH affinity columns. None of the GHBP-RZ DNA positive cells had a statistically significant decrease in GHBP levels as compared to levels of GHBP in the parent E6 cells. While the reason for the failure of the GHBP-RZ is not known, it is possible that spanning the splice site may have provided some unknown complication. If transcription of the GHBP-RZ occurred (as no data for the presence of RZ-RNA was obtained), then it is possible that the different sequence in the arms (as compared to the GHR-RZ) of the GHBP-RZ could have rendered the transcript unstable leading to rapid degradation of RZ.

Selection of the GHBP ribozyme target site

The cDNA sequence of the mouse GHR/BP (see figure 46) was used to identify a GTC triplet sequence in exon 8a. From the GTC target sequence, twelve base pair helices flanking the cytosine of the GTC target were identified. Since 12 nucleotide arms were used and the cytosine of the GTC was only 9 bases from the 5' end of exon 8a, 3 of the nucleotide in the 3' endo of exon 7 were also required for complete RZ recognition. These helices, representing helix I and III of a hammerhead ribozyme / target RNA interaction, were analyzed using criteria reported in the literature to be important for ribozyme design. A general rating scheme represented in figure 46 was created based on these factors.

GHBP-RZ plasmid construction

The plasmid pMTK-bGH-c containing the ampicillin resistance gene, a bovine growth hormone poly adenylation signal sequence, and a mouse metallothionine-I transcriptional regulatory element was used as an expression vector for the GHBP ribozyme (see figure 47). The plasmid was prepared for ligation by digestion with *Bgl*II and *Pvu*II. The fragments were separated by electrophoresis and the ~4000 bp band corresponding to the pMTK-bGH-c expression vector alone, minus the thymidine kinase gene (TK), was removed with a scalpel. The fragment was then gel purified and placed into dialysis tubing containing TAE and isolated using dialysis tubing and Elutip-d^{TM} ion-exchange columns as described previously in the method section of this dissertation. The isolated DNA fragment was resusended in deionized

A.

Exon 7

atgggccctatatggttaacatactgtccagtgtactcattgagaatggataaagaacatgaagtgcgggtgagatccagaca
acggagctttgaaaagtacagcgagttcagcgaagtcctccgtgtaatatttcctcagacgaacatattggaagcatgtgaag
aag

Exon 8a

gaaccaa**GTC**caattctcagcacccacatcaagagattgacaaccacctgtatcaccagcttcagaggatccgccatcc
ctagccttgtgggcacctgcattcatatgcacatacatgcatacgcataattcaaaataataaaa

B.

		#As	m-Ns	GC	CA/UA
Exon 8a:	aaggaaccaaGTCcaattctcagca uuccuugguuca guuaagagucgu	**10**	**1**	**10**	**2**

Figure 46. Target sequence of the GHBP-RZ. A. The full-length sequence of exons 7 and 8a of mouse GHR are represented. The GTC hammerhead ribozyme target sequence is represented in bold print. The 12 nucleotides (shaded boxes) flanking the cytosine of the GTC represent helices I and III of the ribozyme-GHBP mRNA recognition complex. This sequence runs into the last three nucleotides of exon 7. B. The GTC target site from exon 8a. The numbers to the right of the sequences represent criteria reported to be important for ribozyme design. The greater the number of adenosines (#As) present in the ribozyme arms the better (Herschlag, 1991). Multiple repeats of a single nucleotide (m-Ns) is discouraged in primer prediction programs such as GeneWorks™. The strong binding associated with high (GC) content favors non-specific association with short stretches of sequence and is discouraged (Herschlag, 1991). Ribozymes have been shown to degrade at a higher rate when UA and CA dinucleotides or present. These sites are specific targets for an unidentified endoribonuclease (Qiu et al., 1998). Key: **(bold underlined = optimal; bold = good;** regular text = indifferent; *italic = sub optimal*)

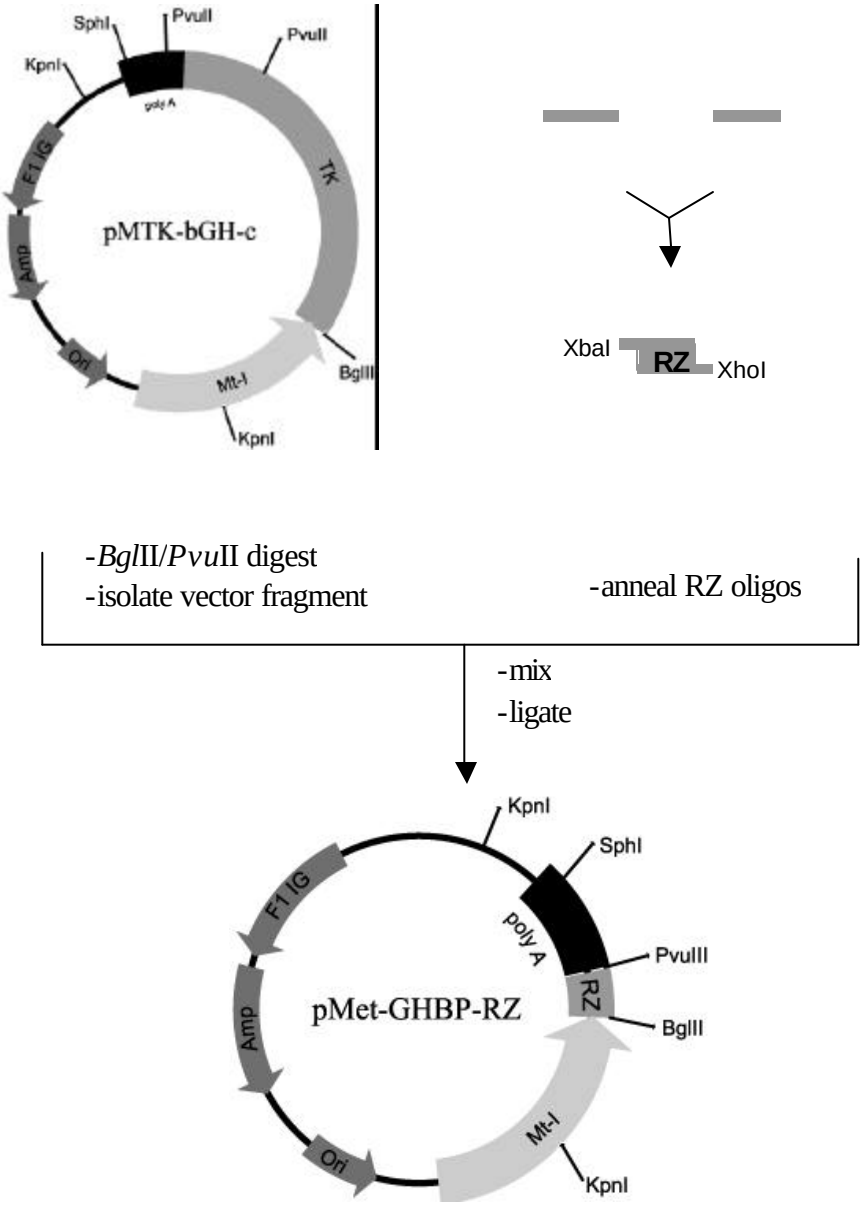

Figure 47. Construction of pMet-GHBP-RZ. The plasmid pMTK-bGH-c containing the ampicillin resistance gene, a bovine growth hormone poly adenylation signal sequence, and a mouse metallothionine-I transcriptional regulatory element was used as an expression vector for the GHR ribozyme. The plasmid was prepared for ligation by digestion at unique *Bgl*II and *Pvu*II sites. Oligonucleotides encoding the sense and antisense sequences of the GHR-RZ were annealed creating a *Bgl*II overhang and a blunt end at the 5' and 3' ends, respectively.

H_2O. The GHBP DNA was prepared by annealing 10 ug of sense, and 10 ug of antisense oligonucleotides in T4 DNA ligase buffer from Promega as described for the cloning of the GHR-RZ in the methods section. The DNA fragments were ligated using T4 DNA polymerase. DNA mini-preparations were performed and positive clones were sequenced to verify proper sub-cloning.

Stable transfection of E6 cells with a GHR-RZ

E6 cells, which express GHR and GHBP (Mouse L cells stably transfected with GHR/BP DNA), were used for pMet-GHBP-RZ transfections. pMet-GHBP-RZ transfections were performed according to the general procedure for stable transfection of adherent cells with LipofectAMINE^{TM} outlined by the manufacturer's protocol (Gibco BRL) and is outlined in the method section of this dissertation for the stable transfection of E6 cells with GHR-RZ.

PCR screening of GHR-RZ transfected E6 cells

PCR was performed on 25 stable cell lines to verify the presence of the transfected GHBP-RZ DNA. The method of screening used was similar to method described earlier for PCR screening of pMet-GHR-RZ transfected cells with the use of the same 5'-Met primer (**GTCACCACGACTTCAACGTCC)** and 3'-bGH primer (**CTACAAATAGCATGACTGCTAGTCC),** respectively.

No Decrease in GHBP or GHR levels in GHBP-RZ transfected cells

The amount of GHBP produced was measured in GHBP-RZ DNA positive clones as well as in the parent E6 cells. Using 75 cm^2 flasks, cells were allowed to grow to 100% confluence (approximately $9x10^7$ cells). Upon reaching confluence, the cells were washed and covered with 15 ml DMEM without serum. The media were collected after 24 hours of incubation and filtered using 0.45 µm-vacuum filters and placed on dry ice. The samples were then sent to Dr. Gerhard Baumann at Northwestern University where GHBP levels were determined using GH affinity columns. None of the GHBP-RZ DNA positive cells had a statistically significant decrease in GHBP levels as compared levels of GHBP in the parent E6 cells. Binding assays were also performed as previously described in the methods section for the screening of functional GHR expression. Once again, no decrease in GHR levels was detected.

APPENDIX C

Subcloning a targeting vector for GHBP specific gene disruption

Summary of experiments

Attempts to "knockout" the GH binding protein (GHBP) specifically while leaving its alternatively spliced gene product partner, the GHR, intact were unsuccessful following two years of attempts in our laboratory. The gene-disruption targeting vector used was pGHBPKO/97, which had lox P sequences flanking thymidine kinase (TK) and neomycin (Neo) resistance genes. The targeting vector contained GHR/BP genomic sequence from the 3'-most *Xba*I site of the intron before exon 7 to the *Sal*I site in exon 10. To prevent alternative splicing involving inclusion of exon 8a (which results in production of the GHBP transcript) the genomic sequence in the targeting vector had a fused (in frame) exon 7/8. The lox P TK/Neo sequence was positioned in the targeting vector such that it interrupted a region of GHR/BP genomic sequence at the *Not*I site in the intron between exon 8 and 9. The position of the lox P TK/Neo sequence resulted in ~5 kb of genomic sequence available for homologous recombination at the 3' end of the construct while only ~600 bases of genomic sequence was available at the 5' end. It was likely that the ~600 bases of genomic sequence in the targeting vector was insufficient for homologous recombination leading to the two year failure of the project. In an attempt to extend the 5' region of genomic sequence, the a new targeting vector was sub-cloned from 3 plasmids containing fragments of genomic GHR/BP sequence (pGB2/B, pGB1/H, and pGB/HR-7/8) and 1 plasmid containing the lox P TK/Neo sequences (pNTL).

First, clone pGB2/B containing GHR sequence from the first *Kpn*I site of intron 6/7 to the *Sal*I site at the end of exon 8a was digested with *Kpn*I and re-ligated to form the plasmid pGB2/BK (see figure 48). This step effectively removed a ~2500 nucleotide portion of intron 6/7 leaving ~1000 bases of the intron sequence immediately 5' of exon 7 for what will ultimately serve as the 5' extension in the new targeting vector. Second, pGB2/BK and pGB 1/H were each digested with *Sal*I and *Xba*I (see figure 49). The fragment containing the pUC-19 backbone and ~770 bases of intron 6/7 stopping at *Xba*I was gel purified from the pGB2/BK digest, while a fragment containing sequences from the *Xba*I site of intron 8/9 to the *Sal*I of 10 was purified from the pGB 1/H digest. The two gel purified fragments were ligated to yield the plasmid p2BK-1/H which lacked the sequence from the *Xba*I of intron 6/7 to the *Xba*I of intron 8/9. This sequence was added by ligating the *Xba*I to *Xba*I fragment from pGB/HR-7/8 into p2BK-1/H linearized at *Xba*I (see figure 50). The *Xba*I to *Xba*I fragment from pGB/HR-7/8 contained a short portion of intron 6/7, exon 7 directly fussed to exon 8, and a short portion of intron 8/9. Therefore, the resulting plasmid p2BK-1/H-7/8 contained sequences from the *Kpn*I site in intron 6/7, a fussed exon 7/8, intron 8/9, exon 9, intron 9/10, and exon 10 to the *Sal*I site. To this plasmid the lox-TK-neo-lox sequence was isolated from pNTL at *Bst*XI / ClaI unique restriction sites, blunt ended with T4 DNA polymerase and ligated into p2BK-l/H-7/8 at a unique (T4 DNA polymerase blunt ended) *Not*I site present in intron 8/9 (see figure 51). The resulting plasmid pBPKO/99 was similar to the older pBPKO/97 targeting vector with the exception of an extra ~800 base added to the 5' genomic sequence.

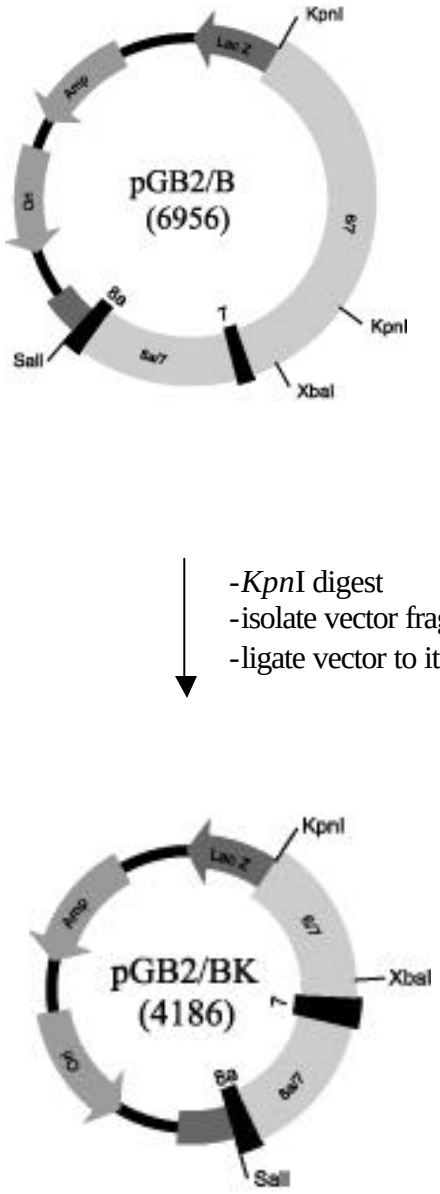

Figure 48. Construction of the plasmid pGB2/BK. Clone pGB2/B (containing GHR sequence from the first KpnI I site of intron 6/7 to the *Sal*I site at the end of exon 8a) was digested with *Kpn*I and re-ligated to form the plasmid pGB2/BK. This step effectively removed a ~2500 nucleotide portion of intron 6/7 leaving ~1000 bases of the intron sequence immediately 5' of exon 7 for what will ultimately serve as the 5' extension in the new targeting vector.

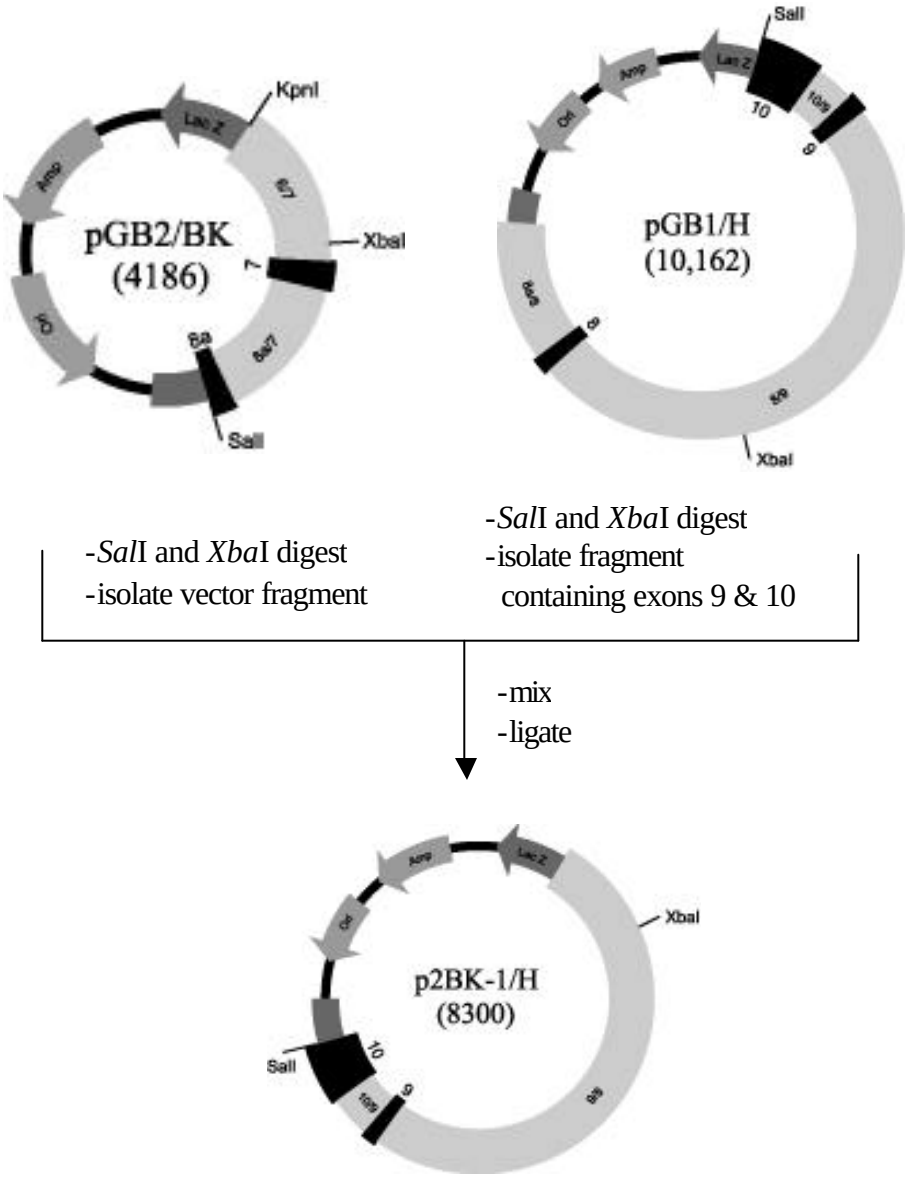

Figure 49. Construction of plasmid p2BK-1/H. The plasmids pGB2/BK and pGB 1/H were each digested with *Sal*I and *Xba*I. The fragment containing the pUC-19 backbone and ~770 bases of intron 6/7 stopping at *Xba*I was gel purified from the pGB2/BK digest, while a fragment containing sequences from the *Xba*I site of intron 8/9 to the *Sal*I of 10 was purified from the pGB 1/H digest. The two gel purified fragments were ligated to yield the plasmid p2BK-1/H.

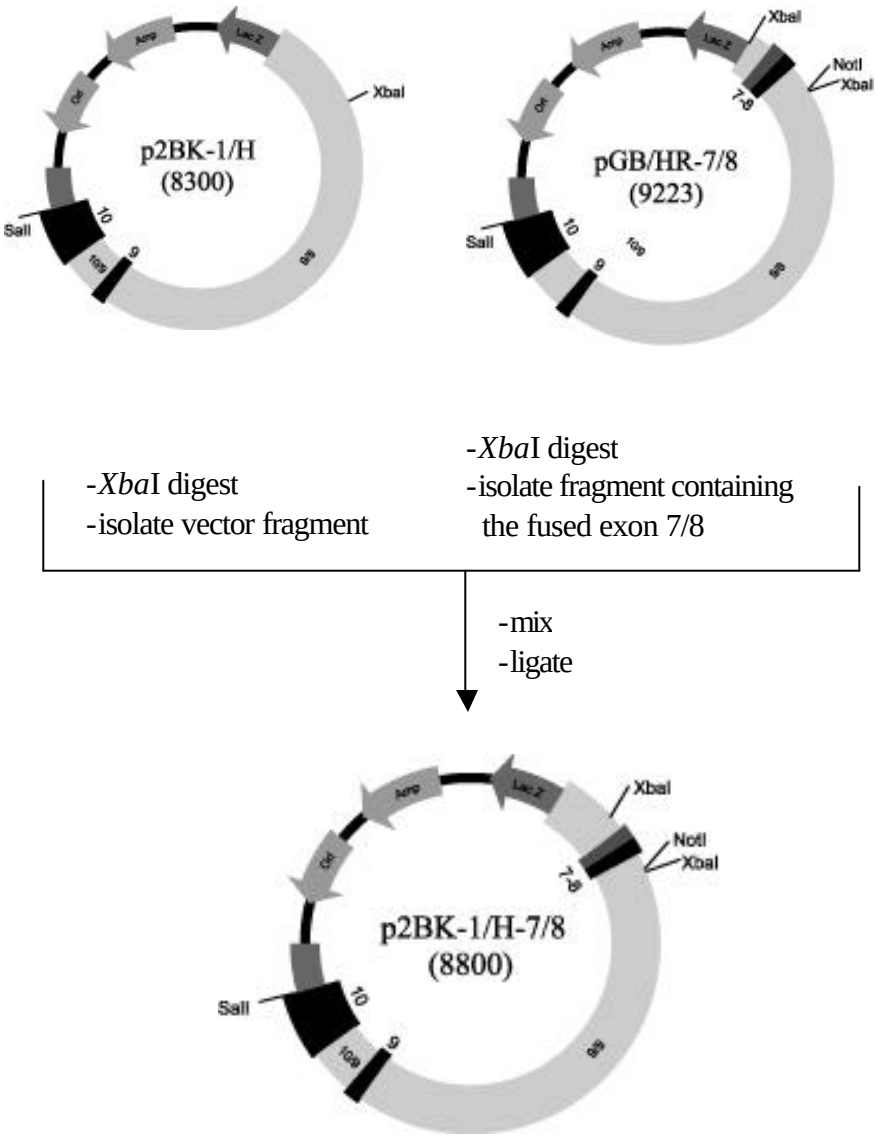

Figure 50. Construction of the plasmid p2BK-1/H 7/8. The sequence from the *Xba*I of intron 6/7 to the *Xba*I of intron 8/9 was added to the plasmid p2BK-1/H by ligating the *Xba*I to *Xba*I fragment from pGB/HR-7/8 into p2BK-1/H linearized at *Xba*I. The *Xba*I to *Xba*I fragment from pGB/HR-7/8 contained a short portion of intron 6/7, exon 7 directly fussed to exon 8, and a short portion of intron 8/9. The resulting plasmid p2BK-1/H-7/8 contained sequences from the *Kpn*I site in intron 6/7, a fussed exon 7/8, intron 8/9, exon 9, intron 9/10, and exon 10 to the *Sal*I site.

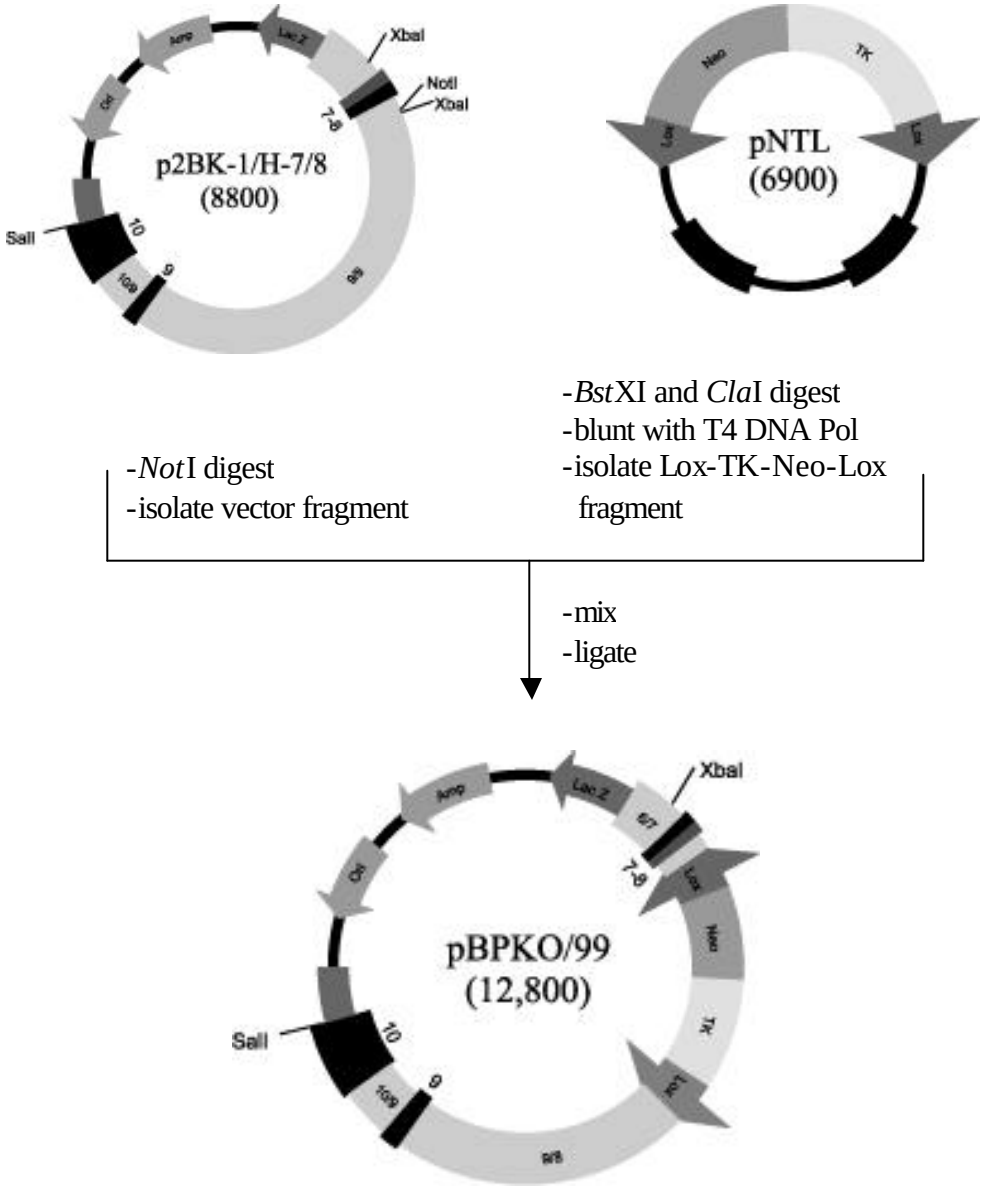

Figure 51. Construction of targeting vector pBPKO99. To the *Not*I linearized plasmid p2BK-1/H-7/8, the lox-TK-neo-lox sequence was isolated from pNTL at *Bst*XI / ClaI unique restriction sites, blunt ended with T4 DNA polymerase and ligated into p2BK-l/H-7/8 at a unique (T4 DNA polymerase blunt ended) *Not*I site present in intron 8/9. The resulting plasmid pBPKO/99 was similar to the older pBPKO/97 targeting vector with the exception of an extra ~800 base added to the 5' genomic sequence.

The pBPKO/99 targeting vector was used by our laboratory to create successful homologous recombination of the GHR/BP gene in embryonic stem cells. The embryonic stem cells were successfully implanted into mouse blastocysts to create chimeric animals. At the time this dissertation was written, the chimeric mice were in the process of breeding to create heterozygous offspring. Therefore, with the failure of the first targeting vector (pBPKO/97) containing only ~600 bases of genomic sequence at the 5' end and the success of the second targeting vector (pBPKO/99) containing ~1400 bases of genomic sequence at the 5' end, it appears (in our hands at least) that the limitations of genomic sequence length for a given "arm" in reasonably achieving homologous recombination lies somewhere between 600 and 1400 bases of genomic sequence.

APPENDIX D

tRNA-tethered GHR-RZs

Summary of experiments

The use of tRNA derived promoters to improve the transcription of recombinant RNAs have been reported with >100 fold increases in accumulation of transcripts compared to pol II systems (Thompson et al., 1995). Due to the high expression levels of pol III driven transcripts, ribozyme constructs tethered to tRNAs have been successfully used to drive ribozyme expression (Koseki et al., 1999; Kuwabara et al., 1999; Kuwabara et al., 1998; Thompson et al., 1995). To avoid 3' end processing of tRNAs, which would cleave the tethered ribozyme sequence, the last seven bases of the mature tRNA-Val can be removed without effecting transcription (Koseki et al., 1999). The altered 3' seven bases of the tRNA-Val construct reported by Koseki et al has been used with at least 12 separate ribozymes, all of which were found in the cytoplasm after transcription suggesting that this sequence is not involved in exportin/RanGTP binding (Koseki et al., 1999). The efficiency of the tRNA-Val/ribozyme tethered system developed by Koseki et al was demonstrated in cells stably transfected with the tRNA-Val/ribozyme by a 97% decrease in targeted U5 HIV RNA gene product and a ~99% inhibition of HIV replication in HIV challenged cells. Therefore, in an effort to use the same highly efficient construct developed by Koseki, the pUC19dt plasmid containing the tRNA-Val sequence was requested and received from Dr. Kazunari Taira (University of Tsukuba, Japan).

tRNA-RZ design

The 8 nt RZ arms along with the tRNA-tethered ribozymes were designed around the 8 nt target site sequences outlined in figure 52. The most stable secondary structure at 37°C for the tRNA-tethered ribozymes were predicted (see figures 53 & 54) using a computer program mfold 3.1 provided by Michael Zuker (Professor of Mathematical Science, Rensselaer Polytechnic Institute, Troy, NY) (Mathews et al., 1999; Zuker et al., 1999). Selection of tRNA-RZ from secondary structure analysis was based primarily on the formation of a proper tRNA structure. Other criteria that were considered were the number and GC content of nucleotides in the RZ arms that were bound and therefore not available for target recognition. In addition, the total number and GC content of bound RNA in the entire tRNA-RZs was considered. In theory, a more "open" tRNA-RZ should be more accessible to the target sequence as long as the "open" region of the tRNA-RZ includes the arms. In contrast, a more open tRNA-RZ might also be more accessible to RNases, leading to a short half-life and less effective RZ. Therefore, the four tRNA-RZ selected (2A, 2C, 5a, and 5full) ranged from "open" to "closed".

Cloning the RZs into the tRNA-Val containing plasmid

A similar strategy was used for cloning RZ sequence into pUC19dt that was used by Koseki (Koseki et al., 1999). Prior to cloning, the pUC19dt plasmid containing tRNA-Val was sequenced to confirm the reported sequence (Koseki et al., 1999) of the plasmid. Sequence analysis revealed the TTT reported by Koseki in a

	site	m-Ns GC CA/UA
Exon 2:	**A:**	**atctttGTCaggtcttc****
		uagaaaca uccagaag
	B:	tgtcagGTCttcttaac
		acagucca aagaauug
	C:	**ctggcaGTCaccagcag****
		gaccguca uggucguc
Exon 4:		ccaagtGTCgttcccct
		gguucaca caagggga
Exon 5:		**gattatGTCtctgctgg******
		cuaauaca agacgacc
Exon 7:	A:	catactGTCcagtgtac
		guaugaca gucacaug
	B:	agcgaaGTCctccgtgt
		ucgauuca gaggcaca
Exon 8a:		aaccaaGTCcaattctc
		uugguuca guuaagag
Exon 9:		cccccaGTCccagttcc
		ggggguca ggucaagg

Figure 52. Potential tRNA-Val-RZ target sites from exons 2-9. The corresponding 8 nucleotide antisense arms that represent helices I and III of ribozyme-GHR mRNA recognition are included. (******) These sites were selected for targeting based on secondary structure analysis of tRNA-tethered RZs designed against the target sequences. (****) Two tRNA-RZs were designed against this single target site. Different linker sequences between these two RZs and the tRNAs altered their secondary structures.

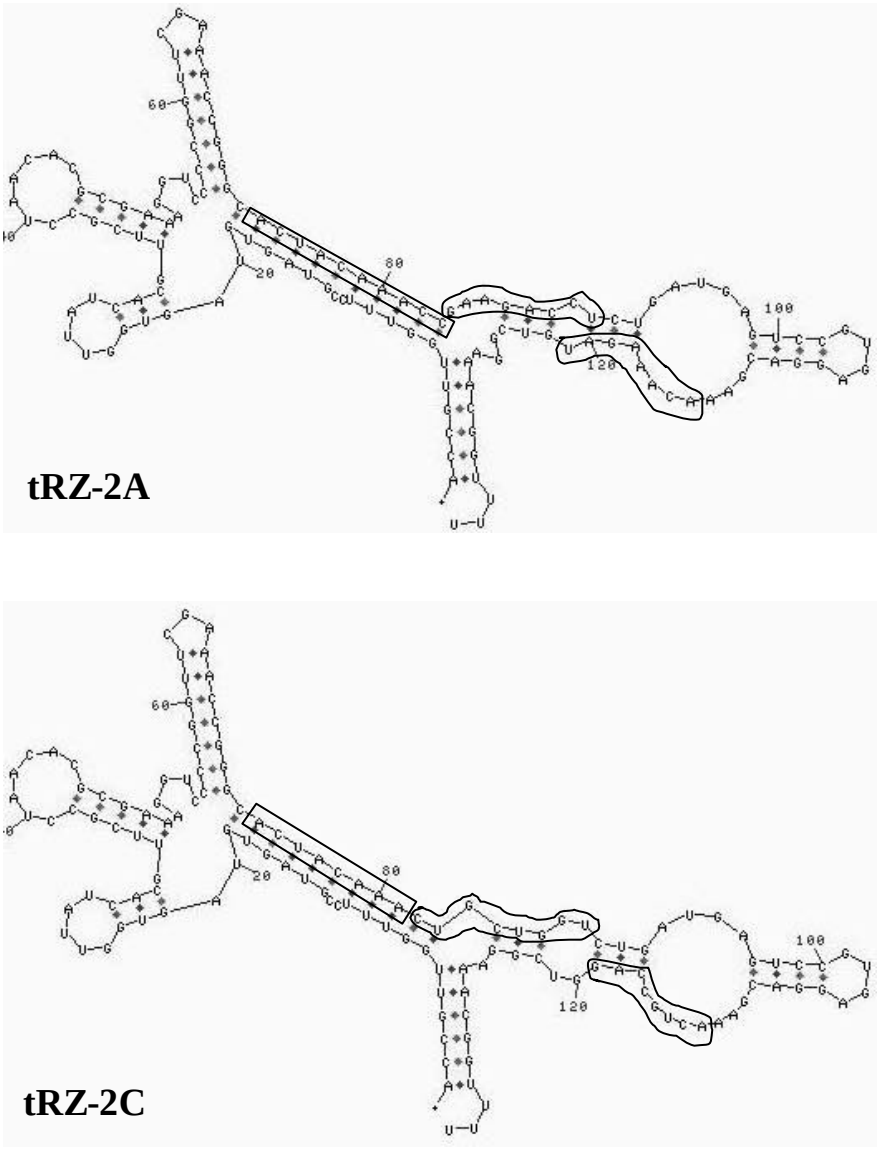

Figure 53. Predicted secondary structures of tRZ-2A and tRZ-2C. tRZ-2A and tRZ-2C are directed to separate target sequences in exon 2. The linker sequences are boxed and the RZ arms are circled. 6 of the 16 nts in the arms of tRZ-2A were predicted to be bound, with 3 of the 6 bound nts in G:C interactions. 8 of the 16 nts in the arms of tRZ-2C were predicted to be bound with 5 of the 8 bound nts in G:C interactions. Thus, the structure of tRZ-2A is slightly more "open" than the structure of tRZ-2A.

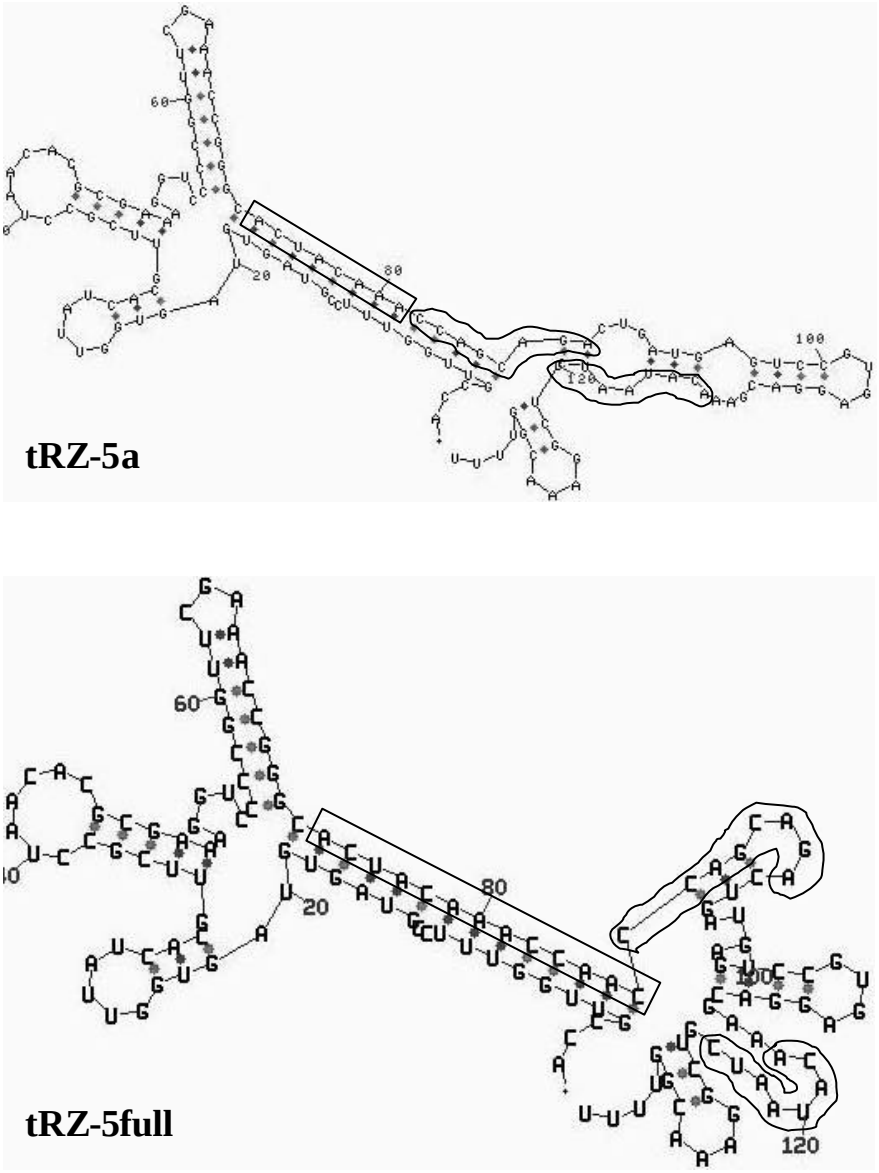

Figure 54. Predicted secondary structures of tRZ-5a and tRZ-5full. tRZ-5a and tRZ-5full are targeted to the same target sequence, have the same exact arm, RZ, and tRNA sequences. The only difference between the two is the presence of a longer linker sequence in tRZ-5full. The linker sequences are boxed and the RZ arms are circled. This difference in linker size was designed to convert the relatively "closed" structure of tRZ-5a (10 of the 16 nts in the arms were predicted to be bound, with 5 of the 10 bound nts in G:C interactions) to a relatively "open" structure of tRZ-5full (only 3 of the 16 nts in the arms were predicted to be bound with only 2 G:C interactions) as predicted by secondary structure analysis.

sequence to which a primer was used for cloning in the RZ sequences was incorrect. The actual sequence was TTTT. This TTTT was also in agreement with the NCBI database published sequence for human tRNA-Val. Using the sequencing information (see figure 55), a 5'-primer was designed 352 bases downstream of an arbitrary number 1 designated position in the plasmid. The primer was therefore designated 5'-352. The transcriptional start site of the tRNA sequence was 440 bases from the arbitrary number 1 site in the plasmid therefore the 5'-352 primer was 88 bases from the start site of the tRNA. The 3'-primers used for cloning contained long stretches of antisense at the 5' and 3' ends of the primer that were directed to tRNA sequence in the plasmid. In the center of each 3'-primer was the RZ and linker sequences, which were unique to each of the four RZs generated. PCR amplification was performed using the same 5'-352 primer and a unique 3'-primer for each of the four sets of reactions. The PCR products were digested with *EcoR*I and *Sal*I and gel purified, placed into dialysis tubing containing TAE and isolated using electro-elution and Elutip-d^{TM} ion-exchange columns as described previously in the method section of this dissertation. The pUC19dt plasmid was prepared for cloning by digestion with *EcoR*I and *Sal*I and isolated in the same manner as the PCR products. The fragments were ligated using T4 DNA Pol, transfected into DH5-a cells, screened by mini-preparations, and sequenced using method previously described in the methods section of this dissertation.

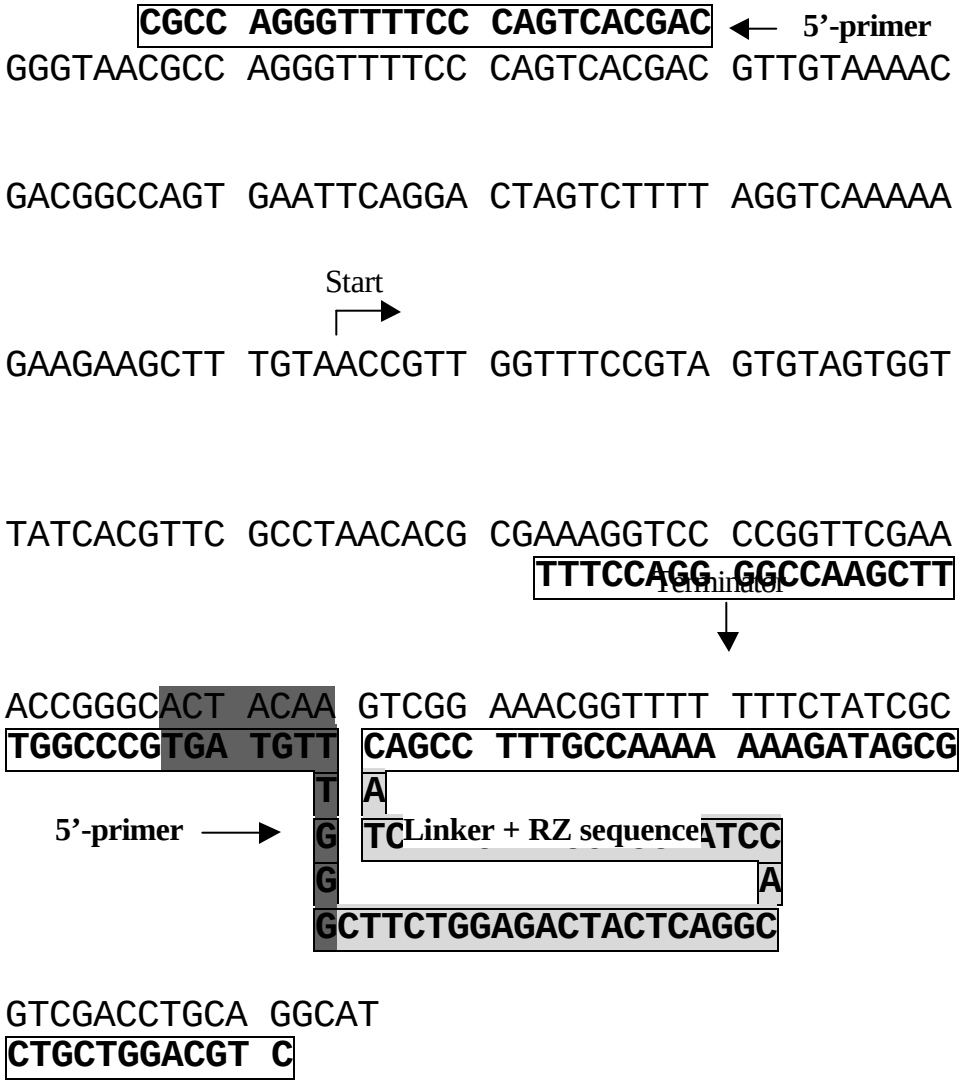

Figure 55. PCR primers for cloning the RZ and linker sequences into the 3' end of tRNA-Val. The 3'-primers used for cloning contained long stretches of antisense sequences at the 5' and 3' ends of the primer that were directed to tRNA sequence in the plasmid. In the center of each 3'-primer was the RZ and linker sequences, which were unique to each of the four RZs generated. PCR amplification was performed using the same 5'-352 primer and a unique 3'-primer for each of the four sets of reactions. DNA sequencing results confirmed the proper sequence for human tRNA-Val was correct. The plasmid sequence is represented by the non-bolded print. The primer sequences are boxed and in bold print. The RZ sequence contained in a bulge of the 3'-primer is shaded light gray. A portion of the linker sequence (shaded dark gray) is located in the plasmid. Any additional linker sequence can also be added to

the bulge of the 3'-primer. The location of tRNA transcriptional start site and the terminator site are indicated.

Transient transfections/binding assays

All four clones ptRZ-2A, ptRZ-2C, ptRZ-5a, ptRZ-5full as well as the non-RZ containing parent plasmid pUC19dt (to serve as a control) were transiently transfected using LipofectAMINE (Gibco BRL) into E6 cells according to manufacture's protocol for transient transfection of adherent cells. E6 cells were maintained in HAT medium at 37°C in a humidified atmosphere of 5% CO_2. Cells were cultured in a 75-cm^2 flask to a confluence of approximately 50% (~$5x10^6$ cells). 1 ml of solution A (20 ug tRZ plasmid, 200 ng pRSV-neo, DMEM to a total volume of 1 ml) and 1 ml of solution B (600 ul LipofectAMINE^{TM}, DMEM to a total volume of 1 ml) were prepared in polystyrene tubes. The two solutions were mixed gently together and incubated for 30 minutes at room temperature. During the incubation, the cells were washed with DMEM and 10 ml HT media without serum (DMEM with only 15 ug/ml hypoxanthine, and 5.15 ug/ml thymidine added) was added back to the flask. Following the 30-minute incubation, the A/B mixture, was gently added to the flask. 5 hours after the start of the transfection, 10 ml of HT media with 20% serum was added to the flask and incubated for 20 hours. Following the 20-hour incubation, the transfection medium was removed and fresh HAT medium was added back to the cells. 48 hours after the start of the transfection, the cells were transferred to 6-well plates with HAT media. 72 hours after the start of transfection, the cells were screened by GHR binding assays using the same protocol outlined in the methods section of this dissertation. Results of the binding assays indicate that the two tRNA-

RZ targeted to the same site on exon 5 demonstrated the greatest ability to decrease GHR (75% decrease for both clone tRZ-5a and tRZ5full) (see table 7). The other two tRNA-RZs also demonstrated an ability to decrease GHR levels as clone tRZ-2A and tRZ-2C demonstrated a 63% and a 69% decrease in GHR levels, respectively. A slight decrease was observed in the GHR levels of cells transfected with tRNA alone as a 10% decrease was observed in these cells. While the specific reasons why tRNA would cause such a decrease is not known, it may be caused by using up the cells machinery (such as RNA polymerase III) on the transfected tRNA leaving less for native tRNA synthesis.

Both tRZ-5a and tRZ-5full are targeted to the same target sequence, have the same exact arm, RZ, and tRNA sequences. The only difference was a longer linker sequence in tRZ-5full. This difference in linker size was designed to convert the relatively "closed" structure of tRZ-5a (10 of the 16 nts in the arms were predicted to be bound, with 5 of the 10 bound nts in G:C interactions) to a relatively "open" structure of tRZ-5full (only 3 of the 16 nts in the arms were predicted to be bound with only 2 G:C interactions) as predicted by secondary structure analysis. Therefore the availability of the RZ arms did not appear to influence the activity of the RZ in these experiments. Moreover, the relative success of all four ribozymes, which were predicted to form an intact tRNA structure, suggests that this may be an important indicator of a successful tRNA-RZ. Secondary structure analysis of the three tRNA-RZs in Koseki's agrees with this (see figure 56). When the secondary structures of the

three tRNA-RZ were calculated using the mfold program, the only tRNA-RZ that that did not form a tRNA structure was not active in cultured cells (Koseki et al., 1999).

Table 7. GHR expression in E6 cells transiently transfected with tRNA-RZs: Specific binding of ^{125}I-labled hGH.

RZ	Specific Binding (SB)	SB / E6 SB	SB / tRNA SB
E6	21,305	-	-
tRNA	19,108	0.90	-
2A	8,219	0.37	0.43
2C	6,917	0.31	0.36
5A	5,568	0.25	0.29
5F	5,520	0.25	0.29
GHR-RZ	5906	0.28	0.31

In 6-well tissue culture plates monolayers of the stable cells were propagated to ~1x10^6 cells/well. 160,000 cpm of ^{125}I-hGH at a concentration 1 nM in 2 ml of 1x PBS with 0.1% BSA was added to each well with or without 100 nM non-radioactive bGH. The cells were incubated for 2 hours at room temperature. The cells were lyses by the addition of 1 ml of 0.1 N NaOH + 1% SDS to each well. Cell lysates were then transferred to vials and the number of counts was measured using a scintillation counter.

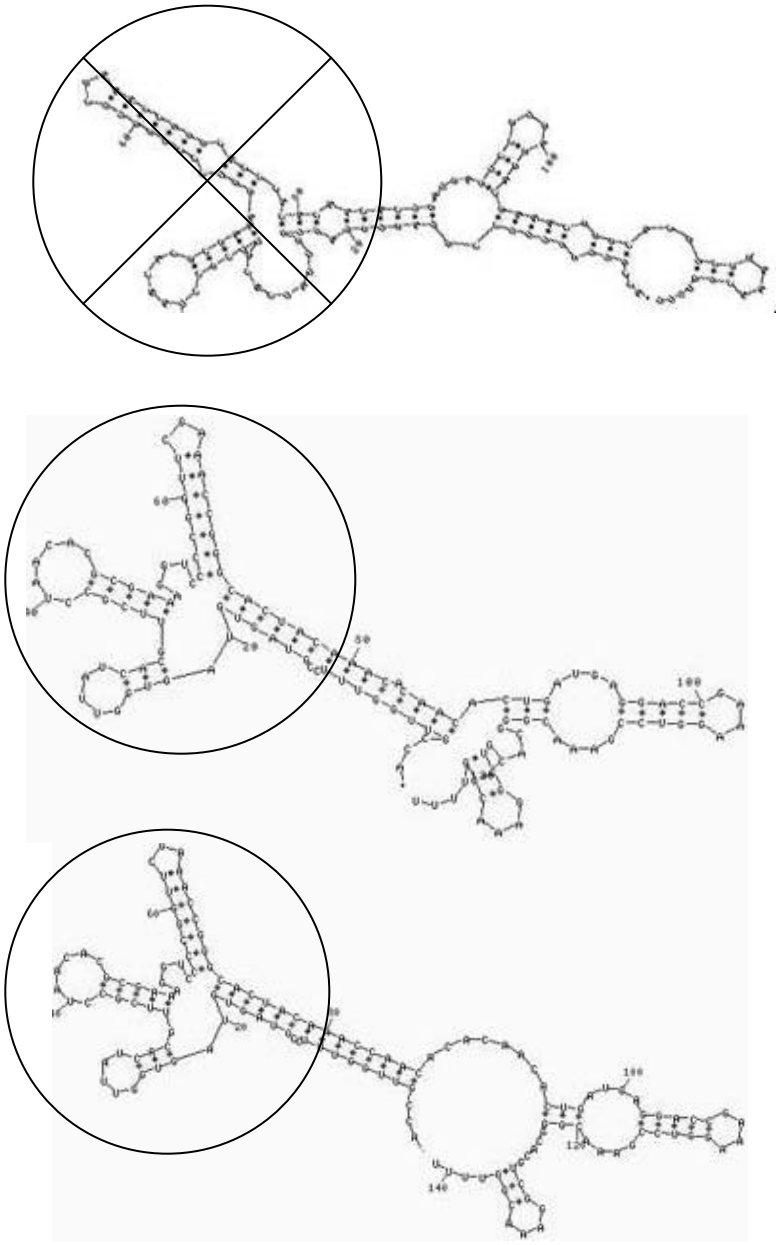

Figure 56. Secondary structure analysis of Koseki's three tRNA-RZs using mfold program. While both tRZ-2 and tRZ-3 formed proper tRNA secondary structures using the mfold program, tRZ-1 did not as indicated. Analysis of RZ activity in cultured cells revealed that RZ-2 and RZ-3 had the ability to decrease message while RZ-1 was almost completely inactive (Koseki et al., 1999).

The pMet-GHR-RZ plasmid was also transiently transfected along with the tRNA-tethered RZs. This transfection was performed in order to roughly compare the conventional GHR-RZ (referred to as GHR-RZ in table 7) to the tRNA-tethered RZs. Surprisingly the conventional GHR-RZ demonstrated a 72% decrease in GHR. This decrease approached that achieved by tRZ-5a and tRZ-5full (75% for both). While these preliminary results suggest that the best of the tRZ constructs were only slightly superior to the conventional GHR-RZ, it is important to remember that the ability of the tRNA-tethered RZs to decrease GHR in stably transfected cells as well as in transgenic mice was not tested. Therefore, whether or not the tRNA-tethered RZs could outperform the conventional GHR-RZ as stable transgenes in the genome of an animal and or cultured cells remains unknown.